# Retrospective Assessment of Human Exposures to Low Dose Ionizing Radiation Using Electron Paramagnetic Resonance (EPR) Dosimetry with Tooth Enamel

by

Lekhnath Ghimire

A thesis submitted to the School of Graduate and Postdoctoral Studies in partial fulfillment of the requirements for the degree of

**Doctor of Philosophy**

**in**

**Nuclear Engineering**

Faculty of Energy Systems and Nuclear Science

University of Ontario Institute of Technology

(Ontario Tech University)

Oshawa, Ontario, Canada

April 2022

## THESIS EXAMINATION INFORMATION

Submitted by: **Lekhnath Ghimire**

**Doctor of Philosophy in Nuclear Engineering**

Thesis title: **Retrospective Assessment of Human Exposures to Low Dose Ionizing Radiation Using Electron Paramagnetic Resonance (EPR) Dosimetry with Tooth Enamel**

An oral defense of this thesis took place on April 27, 2022, in front of the following examining committee:

**Examining Committee:**

| | |
|---|---|
| Chair of Examining Committee | Dr. Jennifer McKellar |
| Research Supervisor | Dr. Edward Waller |
| Examining Committee Member | Dr. Anthony Waker |
| Examining Committee Member | Dr. Hélène LeBlanc |
| University Examiner | Dr. Sean Forrester, Faculty of Science |
| External Examiner | Dr. Carmel Mothersill, McMaster University |

The above committee determined that the thesis is acceptable in form and content and that a satisfactory knowledge of the field covered by the thesis was demonstrated by the candidate during an oral examination. A signed copy of the Certificate of Approval is available from the School of Graduate and Postdoctoral Studies.

**ABSTRACT**

This study collected the extracted teeth from people of different ages in the Durham region and analyzed them using the X-band CW EPR spectroscopy. The total dose rate from the natural and anthropogenic sources was 1.9721 mSv/year. The anthropogenic dose rate from the various sources was 0.6341 mSv/year, about 47.39% of the natural background dose (1.338 mSv/year) in Durham Region, Ontario. The combined anthropogenic doses from these sources were lower than the local background dose in Durham Region, Ontario, and lower than the regulatory annual effective dose limit of 1 mSv/year in Canada. These data demonstrated that the background doses to the public are lower than the regulatory limit. There is a minimal risk to the public from the anthropogenic doses in Durham Region populations. The dose contribution of the nuclear generating stations is small in Durham Region, Ontario. So, the excess anthropogenic doses could be from diagnostic radiology, nuclear medicines, radiation therapy, and other industrial uses of radiation or radioactive materials, but further study would be needed for conclusions about this region's situation. At the same time, there are more chances of providing deciduous teeth for the low dose (10 - 100 mGy) reconstruction in the actual radiation accidents or chronic exposures. To this end, this study used the dose spiking technique in alanine, where a low dose down to 20 mGy was measured with reasonable precision and accuracy. The same method was used in deciduous teeth for measuring low doses, which was challenging to measure precisely using the conventional EPR methods. The measurement accuracy and reproducibility in the deciduous teeth enamel were significantly higher in that dose range than the conventional methods. Thus, this method can solve the measurement problems associated with low doses and is helpful for retrospective and accident dosimetry. Finally, this study concluded that the total anthropogenic doses in the teeth of Durham

Region residents were lower than the regulatory limits. The dose spiking technique can be used to measure low doses in tooth enamel for retrospective and accident dosimetry.

**Keywords:** X-band CW EPR spectroscopy; EPR dosimetry with tooth enamel; ionizing radiation; free radicals; low doses; retrospective and accident dosimetry; deciduous tooth enamel; dose spiking techniques

**AUTHOR'S DECLARATION**

I hereby declare that this thesis consists of original work of which I have authored. This is a true copy of the thesis, including any required final revisions, as accepted by my examiners.

I authorize the University of Ontario Institute of Technology (Ontario Tech University) to lend this thesis to other institutions or individuals for the purpose of scholarly research. I further authorize University of Ontario Institute of Technology (Ontario Tech University) to reproduce this thesis by photocopying or by other means, in total or in part, at the request of other institutions or individuals for the purpose of scholarly research. I understand that my thesis will be made electronically available to the public.

The research work in this thesis was performed in compliance with the Research Ethics Board/Animal Care Committee regulations under **REB Certificate number 14870.**

Lekhnath Ghimire

LEKHNATH GHIMIRE

## STATEMENT OF CONTRIBUTIONS

This project reveals the total background doses in the local population from various anthropogenic sources.

- Part of the work described in Chapter 4 will be submitted for publication as Ghimire, L., Waller, E., 2022. EPR measurements of background doses in teeth of Durham Region residents, Ontario. Health Phys. (under preparation).
- Part of the work described in Chapter 5 has been presented in the UNENE R & D workshop on December 16, 2019 (Toronto).
- Chapter 5 has been submitted for publication as Ghimire, L., Waller, E., 2022. Application of the dose spiking method for the quantitative measurements of low doses in EPR alanine dosimetry. J. Nucl. Eng. Radiat. Sci. (under review).
- For the work described in Chapter 6, the Canadian Radiation Protection Association (CRPA) nominated me for the Young Scientists and Professionals Award in the IRPA 2022 North American Regional Congress, St. Louis, Missouri, USA, from February 20-24, 2022.
- The work described in Chapter 6 has been presented at the 2022 IRPA North American Regional Congress, St. Louis, Missouri, from February 20-24, 2022.
- Part of the work described in Chapter 6 will be submitted for publication as Ghimire, L., Waller, E., 2022. The dose spiking technique for measuring low doses in deciduous teeth enamel using EPR spectroscopy for retrospective and accident dosimetry (under preparation).

I hereby certify that I am the sole author of this thesis. I have used standard referencing practices to acknowledge ideas, research techniques, or other materials that belong to others. Furthermore, I hereby certify that I am the sole source of the creative works and/or inventive knowledge described in this thesis.

## ACKNOWLEDGMENTS

I am eternally grateful to my supervisor, Dr. Edward Waller, for his guidance and continuous support throughout my PhD research activities. I would like to thank my supervisory committee members, Dr. Anthony Waker and Dr. Hélène LeBlanc, for their suggestions to improve my thesis. Also, I would like to thank Dr. Nicholas Priest for his suggestion and encouragement for this project. I would like to acknowledge the Natural Science and Engineering Research Council of Canada (NSERC) and the CANDU Owners Group (COG) for providing financial support for the projects. Also, I would like to acknowledge the Ontario Graduate Scholarship (OGS) provided by the Ministry of Colleges and Universities (Ontario) and the Dean Graduate Scholarship provided by the Faculty of Energy Systems and Nuclear Science, Ontario Tech University.

I would also like to thank my colleagues and friends at the Faculty of Energy Systems and Nuclear Science (FESNS) for the wonderful atmosphere, several fruitful discussions, and continuous support, making graduate studies a memorable experience. Many thanks to those who provided extracted teeth for the study; without their help, this project would not have succeeded. Finally, I would like to thank my family for their unwavering support and encouragement throughout my study. Without their support over the past few years, it would be impossible to complete my study. I would like to dedicate this thesis to my mother, who was my source of inspiration for higher studies, scientific research, and lifelong learning.

*“Nothing in life is to be feared, it is only to be understood”.*

- Marie Curie

**TABLE OF CONTENTS**

**LIST OF TABLES**

**CHAPTER 1**



**CHAPTER 2**



**CHAPTER 3**

**CHAPTER 4**



**CHAPTER 5**



**CHAPTER 6**

**LIST OF CONTENT**

**CHAPTER 1**



**CHAPTER 2**

**CHAPTER 3**

## CHAPTER 4

**CHAPTER 5**

**CHAPTER 6**

**CHAPTER 7**



**LIST OF ABBREVIATIONS AND SYMBOLS**

**Abbreviations or Acronyms**

a.u.: Arbitrary Units

ADC: Analog to Digital Converter

AFC: Automatic frequency control

ALARA: As Low As Reasonably Achievable

BDAP: 1,3-bisdiphenylene-2-phenylallyl

BGS: Background Signal

BWR: Boiling Water Reactors

CALA: Canadian Association for Laboratory Accreditation

CNL: Canadian Nuclear Laboratories

CNSC: Canadian Nuclear Safety Commission

CT: Computed tomography

COHERE: Organization on Health Effects from Radiation Exposure

CW EPR: Continuous Wave Electron Paramagnetic Resonance

$D_{medical}$ : medical dose

DOE: The US Department of Energy

DPPH: α, α'-diphenyl-β-picryl hydrazyl

DRLs: Derived Release Limits

ENDOR: Electron-Nuclear Double Resonance

EPR: Electron Paramagnetic Resonance

ERC: Energy Research Center

ESR: Electron Spin Resonance

HPLC: High-performance liquid chromatography

h: hour

IAEA: International Atomic Energy Agency

ICRP: The International Commission on Radiological Protection

ICRU: The International Commission on Radiation Units and Measurements

IEMP: Independent Environmental Monitoring Program

ISO: The International Organization for Standardization

KERMA: Kinetic Energy Release Per Unit Mass or Kinetic Energy Released in Matter

LDIR: Low Dose Ionizing Radiation

LDRR: Low Dose Radiation Research Program

LET: Linear Energy Transfer

LNT: Linear Non-Threshold

LWR: Light Water Reactors

NGS: Nuclear Generating Station

OD: Outer Diameter

OPG: Ontario Power Generation

OSL: Optically Stimulated Luminescence

P2P: Peak-to-Peak

PWR: Pressurized Water Reactors

R: P2P Amplitude Height

REB: Research Ethics Board

REMP: Radiological Environmental Monitoring Program

RIS: Radiation Induced Signal

RSD: Relative Standard Deviation

SARs: Stable Alanine Radicals

SNR: Signal to Noise Ratio

TL: Thermoluminescence

TEC DOC: Technical Documents

UNEP: United Nations Environment Program

UNSCEAR: United Nations Scientific Committee on the Effects of Atomic Radiation

QA: Quality Assurance

QC: Quality Control

**Symbols and Units**

$B_0$: magnetic field

$B_{mod}$: field modulation amplitude

$B_{res}$: resonance

C: carbon

Ci: Curie (1 Ci = $3.7\times10^{10}$ Bq = 37 GBq)

$CH_2O$: formalin

$CH_3COOH$: acetic acid

dB: microwave attenuation

$D_X$: total dose, [J/kg]

$D_{BG}$: background dose

kg: kilogram

J: Joule, [kg $m^2/s^2$]

m: meter

e: electron charge [$1.602\times10^{-19}$ C]

$EDTANa_2$: ethylenediaminetetraacetic acid disodium salt

eV: electron Volt [$1.602176634\times10^{-19}$ J]

G: gauss

g: Lande´ factor or spectroscopic splitting factor or simply the g factor ($g_e$ = 2.002319)

$g_{\parallel}$: component of g factor parallel to the magnetic field

$g_{\perp}$: component of g factor perpendicular to the magnetic field

GHz: gigahertz

Gy: Grey, absorbed dose,[J/kg]

h: Plank's Constant [$6.626 \times 10^{-34}$ Js]

H: hydrogen

$H_3PO_4$: phosphoric acid

HA: hydroxyapatite

I: nuclear spin quantum number

$k_\beta$: Boltzmann constant [1.3806 $\times 10^{-23}$ J $K^{-1}$]

kBq: kilobecquerel [$10^3$ Bq]

keV: kilo Electron Volt (1,000103 eV)

KOH: potassium hydroxide

kHz: kilohertz

MeV: megaelectron Volt ($10^6$ eV)

mT: millitesla

mW: milliwatt,  microwave power

n: neutron

N: nitrogen

NaOCl: sodium hypochlorite

$N_\alpha$: occupancy numbers of the upper level

$N_\beta$: occupancy numbers of the lower levels

$m_s$: spin quantum number

O: oxygen

R: peak to peak amplitude or intensity

Sv: Sievert, unit of equivalent dose

T: absolute temperature, [K]

UV: ultraviolet

*ν:* radiation frequency

α: alpha particle

β: beta particles

γ: gamma rays

ΔB: peak-to-peak linewidth

μ: magnetic moment of the electron

$\mu_B$: Bohr magneton

μM: micro molar

*η:* filling factor

Q: Q-factor

$V_{res}$:  cavity's resonant frequency

# Chapter 1

# Introduction

## 1.1 Retrospective and accident dosimetry techniques

There are three main techniques for solid-state retrospective radiation dosimetry, also called physical dosimetry techniques: (1) Thermoluminescence (TL) dosimetry using brick, porcelain, and dental ceramics (Bailiff, 1997; Maruyama et al., 2005; Sato et al., 2002; Nagatomo et al., 1995); (2) Optically Stimulated Luminescence (OSL) dosimetry with tooth enamel (Sholom et al., 2011; Sholom and Desrosiers, 2014; Godfrey-Smith, 2008; Yukihara et al., 2007); and (3) Electron Paramagnetic Resonance (EPR) also called Electron Spin Resonance (ESR) dosimetry with tooth enamel (Jacob et al., 2002, IAEA, 2002; ICRU, 2002; Fattibene and Callens, 2010; Desrosiers and Schauer, 2001). These techniques can be used to measure a wide variety of samples for retrospective and accident dose assessment of exposures to ionizing radiation (ICRU, 2002). However, the most frequently used dosimeter is TL due to the availability of samples and instruments for the dose measurements. The basic principles of all three dosimetric techniques are the same: measuring the relative number of unpaired electrons or radical anions trapped in a crystal lattice during irradiation, as shown in Figure 1.1a. However, in TL, the dosimetric signals are read out destructively (i.e., thermally). The OSL read-out process is not destructive, dosimeters can be read repeatedly, but the signal depletion per reading is 0.036% (Wesolowska et al., 2017). On the other hand, EPR spectroscopy measures the number of unpaired electrons or radical anions, often called paramagnetic centers, without altering their positions. So, it is a nondestructive process (except for a dose additive method). The sample can be measured indefinitely or verified

independently in other laboratories for accuracy and reproducibility (Fattibene and Callens, 2010; Desrosiers and Schauer, 2001; ICRU, 2002).

However, there are some samples whose signals may fade by a certain percentage based on the storage conditions, temperature, and humidity (IAEA, 2002; ICRU, 2002; Hayes, 1999). Various materials such as tooth enamel, bones, shells, nails, brick, quartz, glass, porcelain, etc., can be used for the EPR retrospective dosimetry. Thus, EPR is a versatile technique for retrospective and accident radiation dosimetry (IAEA, 2002; ICRU, 2002; Hayes, 1999). Among these materials, human teeth, often called 'biological dosimeters, have been known as ionizing radiation detectors for external (mainly gamma) exposures for more than four decades (Brady et al., 1968; Swartz et al., 2007; Wieser et al., 1996). In terms of stability of the radiation-induced signal and its ability to retain its memory of radiation damage for millions of years, the human tooth enamel is regarded as the essential material for the EPR retrospective and accident dosimetry (Hennig et al., 1981; IAEA, 2002; ICRU, 2002). Additionally, it is commonly used for dose reconstruction and has become an important tool for retrospective and accident dosimetry, where dosimetric information is incomplete or unknown for individuals, groups, or populations (IAEA, 2002; Desrosiers and Schauer, 2001; Schauer et al., 2007; Ivannikov et al., 2002).

### 1.1.1 Human tooth as a 'biological dosimeter'

Human tooth enamel is about 97% hydroxyapatite [$Ca_{10}(PO_4)_6(OH)_2$], and the rest are organic and inorganic (i.e., trace elements) materials. Carbonate ions ($CO_3^{2-}$) are incorporated into the carbonated hydroxyapatite as an impurity during the hydroxyapatite crystals formation in a tooth, as described in Chapter 2 (Section 2.2). When teeth are exposed to ionizing radiation (i.e., gamma rays, X-rays, etc.) due to chronic exposures or radiological accidents, the carbonate ions

($CO_3^{2-}$) and carbon dioxide molecules ($CO_2$) on the hydroxyapatite crystals (mineral matrix) absorb electrons formed by ionizing radiation (i.e., secondary thermalized electrons) and produce mainly the $^{\bullet}CO_2^-$ radical anions as depicted in Figures 1.2, 2.4 and Equations 2.1 and 2.2 (Chapter 2). The concentration of radiation-induced $^{\bullet}CO_2^-$ radical anions can be determined using EPR spectroscopy in the form of an EPR spectrum, as depicted in Figure 1.1b. The amplitude height of the spectrum (R) is proportional to the absorbed dose, as shown in Figure 1.1b (Jacob et al., 2002, Fattibene and Callens, 2010). ICRU report 68 (ICRU, 2002) and the IAEA technical documents 1331 (TEC DOC 1331) provided detailed procedures and results of retrospective dose assessment using the conventional X-band (9-10 GHz) CW EPR spectroscopy (IAEA, 2002). Four international intercomparisons have been conducted in the last 20 years and the results demonstrated that EPR dosimetry was a reliable technique for retrospective dose assessment (Wieser et al., 2000; Wieser et al., 2005; Wieser et al., 2006; Fattibene et al., 2011). The International Organization for Standardization (ISO) has published the international standard for EPR dosimetry (i.e., ISO protocol 13304-1 for EPR retrospective dosimetry) (ISO, 2013), which has helped to make the dose assessment technique widely available, consistent, and provided recommendations about the sample collection and dose reporting (ISO, 2013).

**(a)**

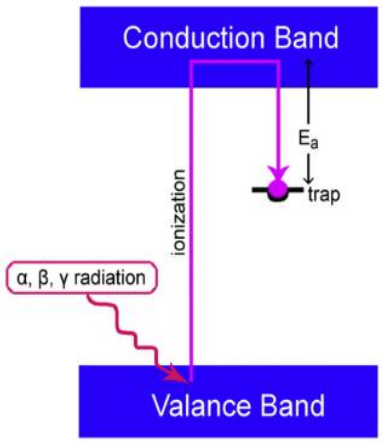

**(b)**

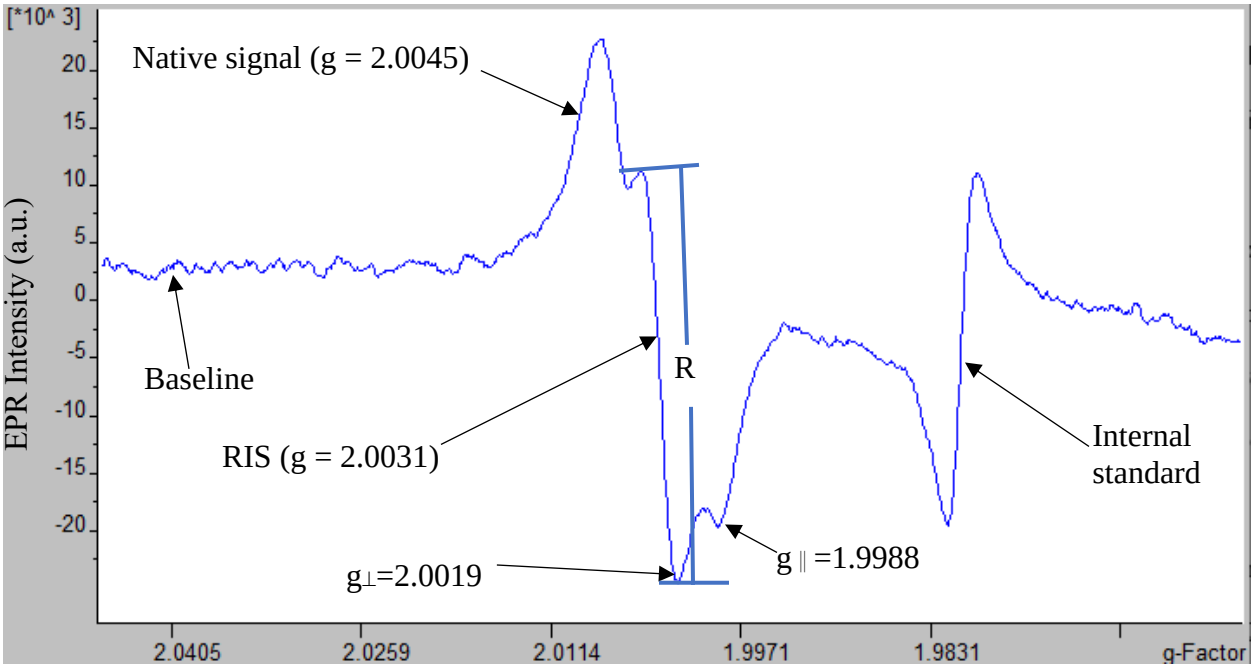


**Figure 1.1: (a)** Upon exposure to ionizing radiation, the excited electron jumps to the conduction band. Although most of the electrons return to the ground state, a few electrons trapped in the charge site defects have specific energy above the ground state. In the case of EPR, the trapped electrons with unpaired spins (S = 1/2) result in a radiation-induced signal (i.e., EPR spectrum). **(b)** An EPR spectrum of tooth enamel exposed to an absorbed dose of 600 mGy (gamma rays) from the Hopewell G-10 ($^{137}$Cs gamma source) shows the radiation-induced and native EPR signals. R is the peak-to-peak (P2P) amplitude height of the RIS, distinct from the native or background signals. The RIS and native signals are separated based on their characteristics g-values ($g_{\perp}$=2.0019, $g_{\parallel}$=1.9988, maximum g = 2.0031), and the signal width ($\Delta$pp) = 0.508 mT.

However, in an EPR spectrum, the RIS is intertwined with the native signal arising from the organic matter and other impurities in tooth enamel at low doses, which makes the low dose (<100 mGy) measurement extremely challenging using EPR (IAEA, 2002; ICRU, 2002; Jacob et al., 2002). Many techniques have been used to separate the RIS from the BGS for low dose measurements, such as spectrum deconvolution methods (Ivannikov et al., 2002; Zhumadilov et al., 2005; Zhumadilov et al., 2006; Wieser and El-Faramawy, 2002), empty tube and background subtraction (Hayes et al., 1998), and the signal selective microwave saturation (Ignatiev et al., 1996). However, there were more than 20% measurement errors in the dose range of 30 - 500 mGy from these techniques. Therefore, from these results and the results from the international intercomparisons (Wieser et al., 2000; Wieser et al., 2005; Wieser et al., 2006), it is clear that the precise low dose estimation using the conventional tooth enamel EPR dosimetry is challenging. These studies concluded that future standardization is required for EPR tooth enamel dosimetry dose calibration. To this end, measurement accuracy and reproducibility can be significantly increased by removing impurities (dentin) from the tooth enamel (by using both chemical and mechanical methods as described in Chapter 3 (Section 3.1.4), using highly sensitive EPR resonators as described in Section 3.2.3 (Chapter 3), background subtraction, etc. Most importantly, unlike many modern instruments, EPR spectrometers are designed and built in a tradition of use primarily by specialists and are not designed to be foolproof. So, a highly skillful EPR technician is needed to get the full benefits of this technique (Barr et al., 2008).

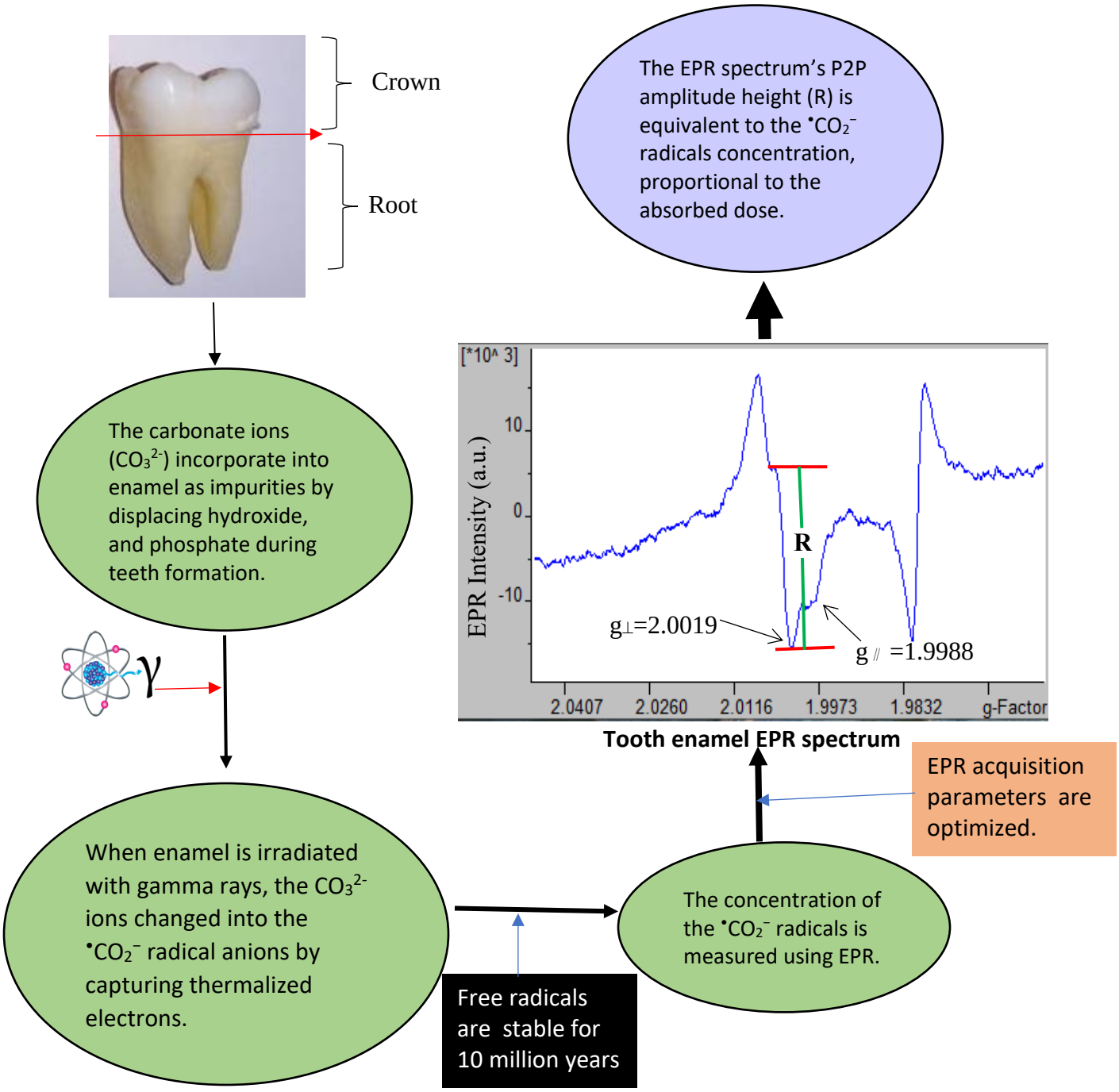


**Figure 1.2:** Schematic illustration of human tooth enamel as an EPR dosimeter material for retrospective and accident dosimetry. R is the P2P amplitude height of the RIS in human permanent molar tooth enamel exposed to the absorbed dose of 0.3 Gy from the $^{137}$Cs source (G-10) gamma rays. The amplitude height (P2P) of the spectrum is measured using the WIN-EPR software, proportional to the absorbed dose in enamel.

### 1.1.2 International intercomparisons and the ISO standards in tooth enamel EPR dosimetry

There must be consistency in the data obtained in different laboratories before using EPR dosimetry for radio-epidemiology. To that end, four international inter-comparisons have been arranged since 1996: (1) to check whether the results produced by different laboratories are consistent and accurate; and (2) to work towards establishing a *standardized technique (harmonization of the method)* for EPR dosimetry or regulate the practical applications of EPR dosimetry with tooth enamel (Chumak et al., 1996; Romanyukha and Schauer, 2002). In most of these comparisons except the most recent one (i.e., fourth intercomparison), blind tests were performed (i.e., results from the different laboratories were compared) to check the accuracy and consistency of their results. In their second intercomparison, eighteen participants were provided tooth enamel samples irradiated from 0-1000 mGy. Six out of eighteen participants could reconstruct all applied doses within ±25% and ±100 mGy below 400 mGy (Wieser et al., 2000).

Based on all participants' results, they concluded that besides EPR parameters and lab conditions, the quality of the EPR spectrometer used highly influenced the data obtained for dose reconstruction (Wieser et al., 2000). In their third international intercomparison, fourteen international laboratories participated in the program; the participants' laboratories performed tooth enamel dosimetry in the range of 79-704 mGy. As shown in Figure 1.3, the results of different labs were inconsistent, and the mean dose was 22 mGy lower than the applied dose of 176 mGy with a standard deviation of ± 51 mGy. However, the mean dose was 8 mGy lower than the applied dose of 79 mGy with a standard deviation of ± 19 mGy, as shown in Figure 1.3. In all these methods, the *relative standard deviation* was better than 27% for the applied doses in the range of 79-704 mGy (Wieser et al., 2005).

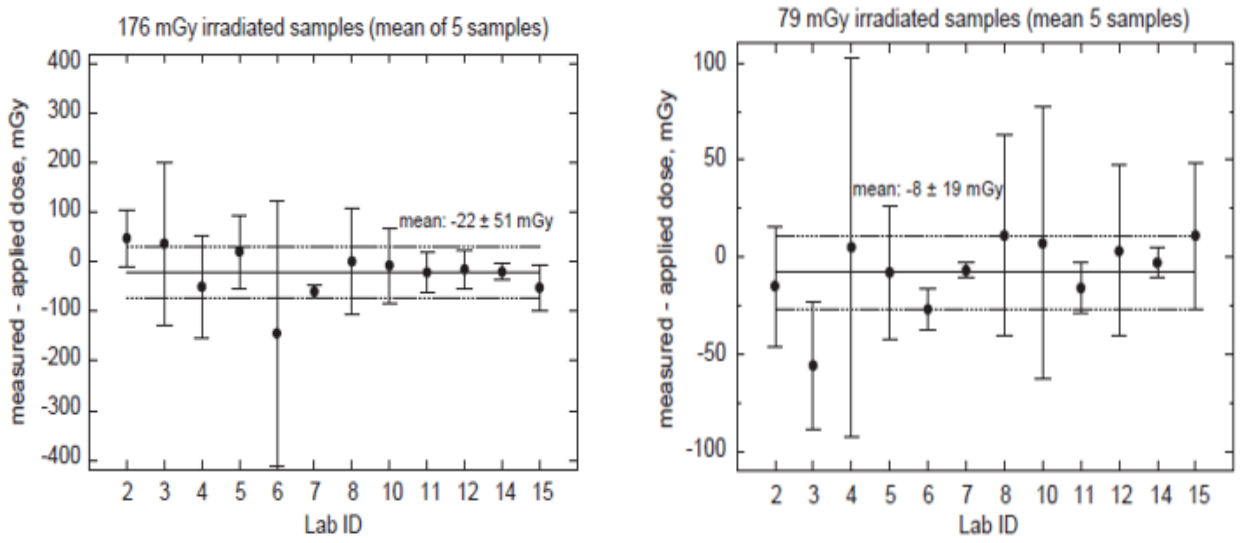


**Figure 1.3:** Dose measurements variation among the participating laboratories in the 3rd international intercomparison for the tooth samples irradiated to 176 mGy and 76 mGy. From Wieser et al. (2005).

From their first to third international intercomparisons, the test samples were used. In the fourth international intercomparison, the actual samples were used to evaluate the detection limit in EPR tooth enamel dosimetry leading to the harmonization of the method rather than correctness. It was demonstrated that the precision of calibration and the accuracy of dose determination were increased by using the improved spectrum processing procedure (Ivannikov et al., 2007). Five out of six samples were irradiated at 0.1, 0.2, 0.5, 1.0, and 1.5 Gy air kerma inside a Plexiglas phantom box with 5-mm-thick walls on all sides with the dose rate of 0.05 Gy/min, and the unirradiated samples were kept as a control—Fatibene et al. (2011) mean value of the detection limit was 205 mGy (ranging from 56-649 mGy) using the specific calibration curve and measurement conditions. The organizer calculated the critical dose (i.e., a minimum significant estimated dose distinguished from the background noises). The organizer calculated the detection limit (i.e., minimum measurable dose) based on the calibration curve parameters obtained from every participating

laboratory. They also calculated the detection limit (DL) and critical level (CL) (or critical dose) using EPR intensities obtained from the irradiated and unirradiated samples (i.e., natural background radiation), respectively. Using the homoscedastic approach (i.e., the standard uncertainties of the signal intensity from non-exposed and exposed samples are assumed to be equal), the detection limit of the dose is twice the critical level ($D_{DL} = 2D_{CL}$). The ratio of dose detection limit to critical dose level ($D_{DL}/D_{CL}$) was calculated. The average ratios were lower than 2 (1.994 ± 0.002, 1.987 ± 0.007, and 1.971 ± 0.020) for almost all participating laboratories. However, this technique significantly decreased the measurement uncertainty (Fattibene et al., 2011). Details of their calculations and methods (algorithms) were given in the Fattibene et al. (2011) (The 4th international comparison on EPR dosimetry with tooth enamel Part 1: Report on the results). Such international intercomparisons made it easier to select the best dose evaluation procedures and identify the weaknesses in the EPR dose reconstruction processes. However, further efforts are required to decrease the measurement errors and establish a widely accepted protocol to regulate the practical applications of EPR dosimetry (Romanyukha and Schauer, 2002).

Based on all these different international intercomparisons and developments in the EPR retrospective tooth enamel dosimetry, an ISO standard for EPR tooth enamel dosimetry was published entitled Minimum criteria for EPR spectroscopy for retrospective dosimetry of ionizing radiation – Part 1: General principles (ISO protocol 13304-1 for EPR retrospective dosimetry) (ISO, 2013). The main aims of the ISO standard were: (1) to make this technique widely available and to provide the minimum acceptable criteria for tooth enamel EPR retrospective dosimetry; and (2) to facilitate the comparison of absorbed doses obtained at different laboratories for the data consistency and accuracy (ISO, 2013). These comparisons and the ISO standard have demonstrated that EPR dosimetry with tooth enamel is a mature and well-developed method for

retrospective dosimetry (Fattibene et al., 2011; ISO, 2013). This thesis followed the internationally validated standardized techniques published by ISO and the dose spiking technique to check the accuracy and consistency of the method for the low dose measurements using EPR (ISO, 2013; Toyoda, 2019).

### 1.1.3 Retrospective and accident dose assessment using deciduous teeth

Permanent teeth are the first choice for EPR dosimetrists to reconstruct retrospective and accident doses due to their many years of dose accumulation and enough sample (i.e., enamel) available for the EPR analysis using the X-band CW EPR spectrometer (IAEA, 2002, ICRU, 2002; Wieser et al., 2000; Wieser et al., 2005; Wieser et al., 2006; Desrosiers and Schauer, 2001). However, dose estimation using EPR dosimetry with deciduous teeth is vital as children are more vulnerable to potentially harmful effects from radiation exposure than adults (ICRP, 2007). One of the most practical advantages of using deciduous teeth is that they fall out naturally at age 6-12 and are readily available for EPR measurements. However, their enamel content may be less (i.e., 50 mg) than permanent teeth and, in such situation, the whole tooth crown has been proposed for analysis without preliminary sample preparation (Haskell et al., 1999; Wieser and El-Faramawy, 2002; El-Faramawy and Wieser, 2006). Different studies have found that deciduous teeth and permanent teeth radiation sensitivities and dosimetric signals were similar. However, their native signals were slightly different (i.e., native signal P2P linewidth was narrower, about 0.65 mT vs. 0.8 mT) (Wieser and El-Faramawy, 2002).

Nonetheless, the different native signals do not affect a dose reconstruction process as they are radiation insensitive and do not determine the absorbed dose in deciduous teeth. Also, Skaleric et al. (1982) found a weaker EPR signal anisotropy in deciduous teeth than in permanent teeth,

which could be due to shorter enamel formation and mineralization time, leading to a different degree of microcrystal arrangement in the enamel of deciduous teeth. Despite their different microcrystal arrangement, deciduous teeth' radiation sensitivities and radiation detection thresholds are comparable to permanent teeth and extremely useful for retrospective and accident dose assessment (Fattibene and Callens, 2010).

## 1.2 Low doses measurement challenges in EPR dosimetry with tooth enamel

### 1.2.1 Standard EPR techniques for low dose measurements

Two techniques have been used in low-dose EPR tooth enamel dosimetry to reconstruct radiation doses: (1) the calibration curve method (also called the dose-response curve); and (2) the dose additive method, as shown in Figures 1.4a and 1.4b. The first method is non-destructive; however, a statistically valid number of teeth are required to construct the calibration curve. Once the curve is constructed, the same curve can be used to determine the absorbed doses in tooth enamel. However, the main drawback of this technique is to get a statistically valid number of samples, which is sometimes difficult and time-consuming (Fattibene and Callens, 2010). On the other hand, the dose additive method does not need a statistically valid number of samples (i.e., even a dose of a single sample can be determined). However, the same sample is irradiated multiple times to back extrapolate the line to determine the retrospective or accident doses, as shown in Figure 1.4a. The multiple irradiations of the same sample may introduce errors at each irradiation step which could be the reason behind approximately 39% of errors (Fattibene and Callens, 2010; IAEA, 2002; ICRU, 2002) in low dose measurements using this technique. Therefore, the measurement accuracy and reproducibility at low doses using this method are not high enough for low-dose retrospective dosimetry.

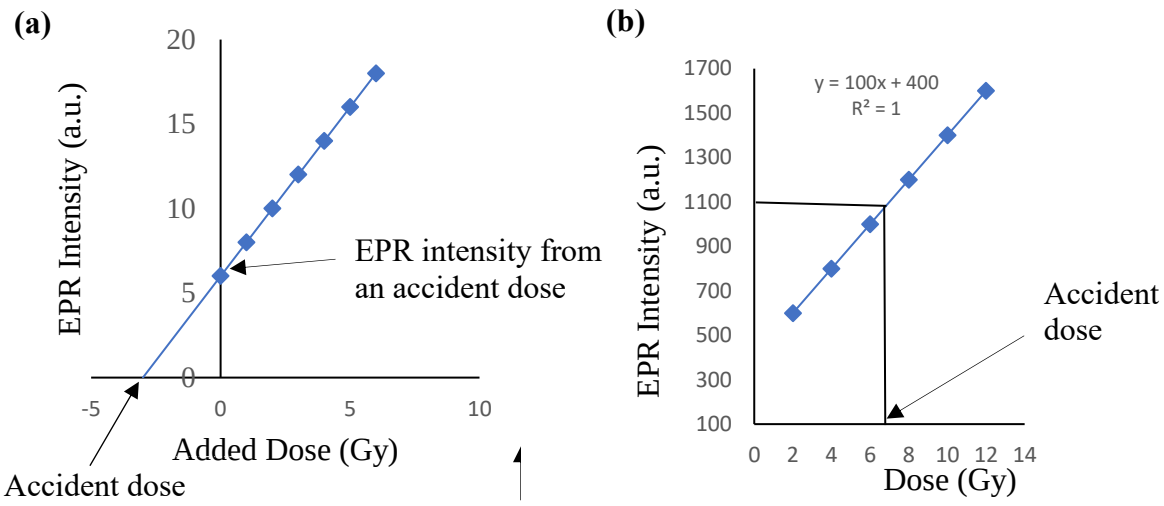


**Figure 1.4: (a)** The conventional EPR dose reconstruction technique using the additive dose method. **(b)** The calibration curve method. The dose additive is destructive; however, the calibration curve method is non-destructive, which means the same sample can be reused to assess the doses in the future.

Moreover, due to multiple irradiations, this technique is destructive. The same sample cannot be used to reassess the dose in the future if one needs to re-evaluate the absorbed doses (i.e., replicate analysis is not possible by another laboratory for re-measurement in the future) (Fattibene and Callens, 2010; ICRU, 2002). Since EPR dosimetry with tooth enamel is a well-established technique for radiation dose reconstruction as described in Section 1.1.2, this study's priority is to apply the standardized EPR technique prepared by the international intercomparisons, and the ISO standard described in Section 1.1.2 and depicted in Figure 1.5. However, the dosimetric signals are intertwined with the native signals at low doses. So, the dosimetric signals cannot be separated and measured precisely, which over or underestimates the low measured doses in tooth enamel. In this situation, as an alternative method, this study will explore the feasibility

of using the dose spiking EPR technique to measure low doses, especially in the dose range of 10-100 mGy.

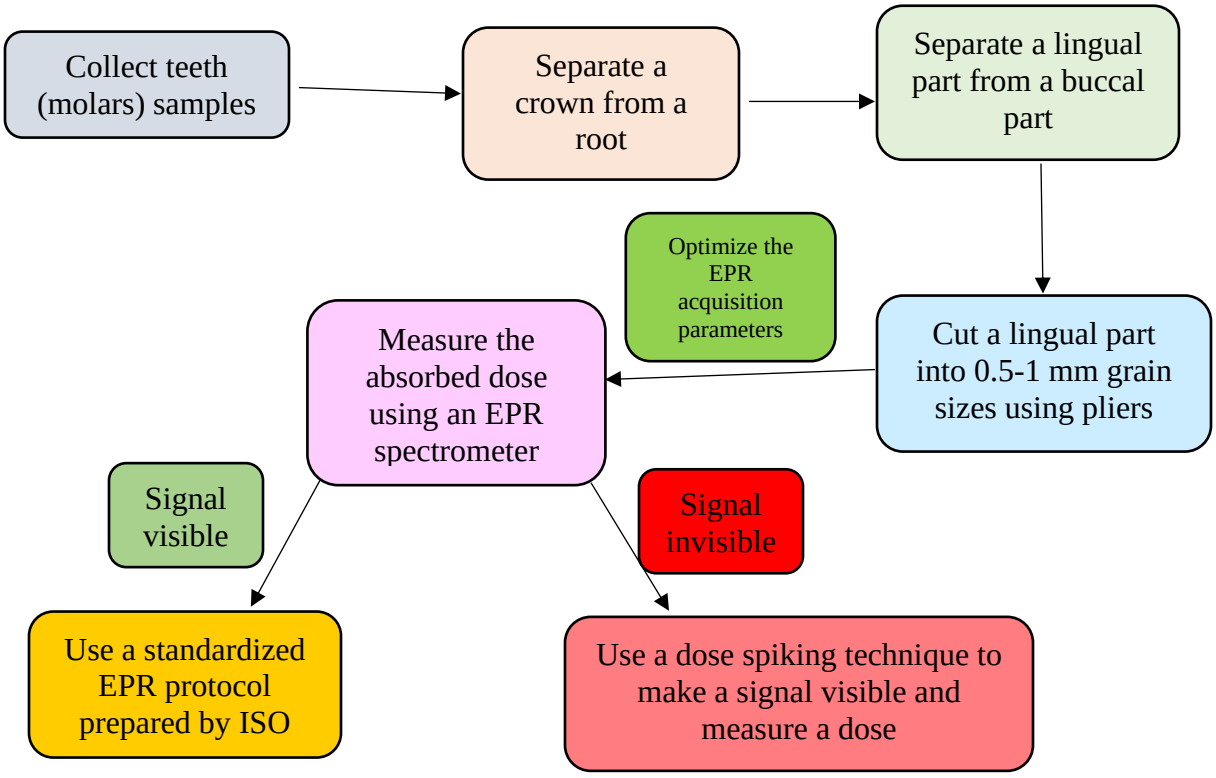


**Figure 1.5:** A conceptual model of an EPR analysis plan for a low dose measurement for retrospective and accident dosimetry.

### 1.2.2 The dose spiking EPR technique

At low doses (10-100 mGy) and small sample sizes (<100 mg), the intensity of a radiation-induced signal is minimal. Therefore, the EPR intensity is too small to be visible and measurable in an EPR measurement using the X-band CW EPR spectroscopy. Additionally, the dosimetric signals are overshadowed by the native or background signals, complicating the actual dosimetric signal measurements and radiation dose reconstruction. The dose additive (or additive dose) method has been used to estimate the low dose using the X-band CW EPR spectrometer

(Desrosiers and Schauer, 2001; Schauer et al., 2007; Ivannikov et al., 2002). In this method, an aliquot of tooth enamel (>100 mg) was irradiated in different doses multiple times and extrapolated the graph as shown in Section 1.2.1 (Figure 1.4a) to determine the low dose (or an accident dose). However, as described in Section 1.2.1, the same tooth enamel sample was irradiated multiple times to extrapolate the graph because it is almost impossible to make seven or eight aliquots of a >100 mg sample from a single human molar tooth, which may contribute a huge error in low dose measurements. So, a low dose may not be measured precisely using this technique (Harvey, 2000; Geso et al., 2018). To overcome these challenges, the dose spiking technique was used as described in chapters 5 and 6 (Harvey, 2000; Geso et al., 2018), where the sample was irradiated only at a single time and subtracted from the spike dose as described in Section 5.2.3 (Chapter 5). First, the dose spiking technique was used in analytical chemistry to measure an analyte's extremely low concentrations (i.e., micromolar level). The idea behind this technique was that the measurement errors were always lower in the high dose (>4Gy) measurements (i.e., less than 5%) than in the low dose using X-band CW EPR spectrometers. However, the measurement accuracy at high doses also depends on the laboratory protocol, EPR technician, sample preparation, storage, and the purity of the samples.

### 1.2.3 Health effects of low dose radiation

At lower doses of radiation (below the doses at which the immediate effects of radiation such as injury and death due to cell-killing), an exposed population may show an increased rate of incidence of certain types of cancer, years or decades later, compared with the populations that were not exposed to the radiation. So, ionizing radiation is a carcinogen similar to cigarette smoke, and the incidence of cancer in a population increases with radiation exposures (UNSCEAR, n.d.). However, we do not know enough about low-dose radiation risks (Brenner, 2011; UNSCEAR,

2012) due to the lack of data to verify the effects. So, the magnitude of the risks from the low doses and the dose rates (i.e., below 100 mSv and/or 0.1 mSv $min^{-1}$) remains controversial due to a lack of direct human evidence (UNSCEAR, 2006; Pernot et al., 2012). The health effects produced would be minor, but there may be adverse (e.g., the bystander effect) or even beneficial (e.g., threshold or hermetic) health effects that could be produced when the exposures are chronic and occur gradually over time, as shown in Figure 1.6 (UNSCEAR, 2012; Azzam et al., 2016). It is, therefore, essential to determine the chronic low dose radiation level received by the local population to understand its possible long-term health impacts. This is particularly important since some residents living near nuclear-generating stations (NGSs) have expressed concern about their possible exposures (Priest, 2018). Epidemiological studies for low-dose radiation exposures have been paramount in allaying public fears of nuclear technology.

**Table 1.1:** Bands of radiation dose as per the United Nations Scientific Committee on the Effects of Atomic Radiation (UNSCEAR) 2012 Report.

| **Dose bands** | **Range of low dose for low LET radiation** | **Scenarios** |
|---|---|---|
| High | <1 Gy | Whole-body or partial after severe radiation accident or from radiotherapy |
| Moderate | About 100 mGy to 1Gy | Doses to about 100,000 recovery workers after the Chernobyl accident |
| **Low** | **About 10 mGy to 100 mGy** | **Doses to an individual from multiple whole-body CT scans** |
| Very low | <10 mGy | Doses to an individual from conventional radiology (without CT scans) |

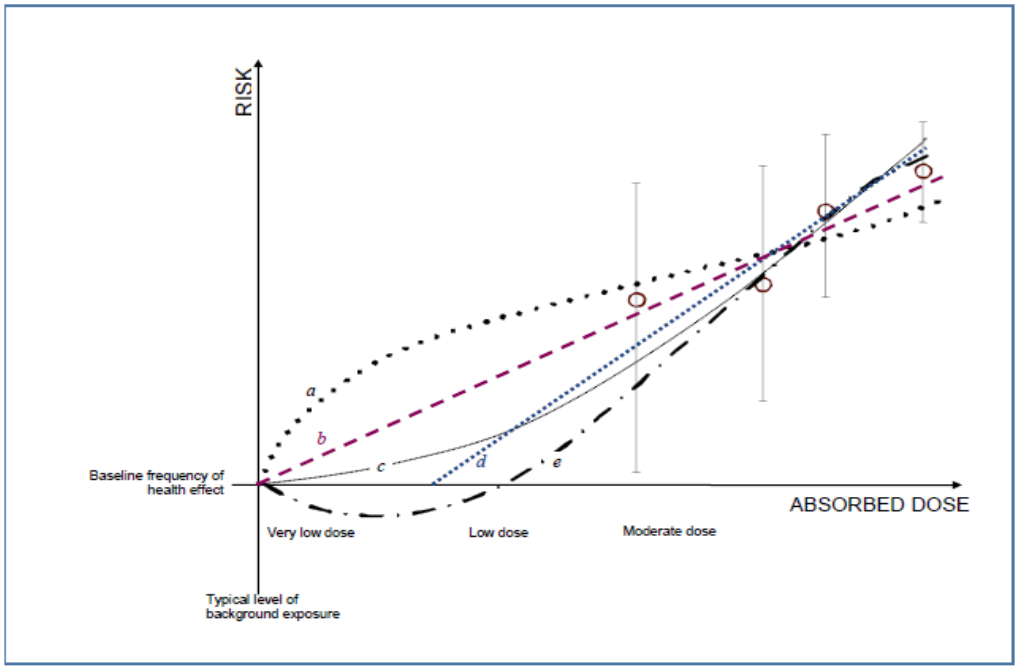


**Figure 1.6:** Schematic presentation of plausible dose-response relationships for cancer risk in very low, low, and moderate doses. The various lines represent the following plausible dose-response relationships for inferred risk of cancer for exposures in the ranges of low and very low doses: **(a)** supralinear due to bystander effect); **(b)** linear non-threshold (LNT); **(c)** linear–quadratic; **(d)** threshold; and **(e)** hermetic. From UNSCEAR (2012).

Interestingly, the data from the atomic bomb survivors (Hiroshima and Nagasaki) demonstrated that there is no significant risk of death from cancers (both solid cancers and leukemia) for a single dose below 100 mSv (Allison, 2006; Sutou, 2018). On the contrary, the atomic bomb survivors' lifespan was longer than the un-irradiated populations (Sutou, 2018). To further understand the health effects of low dose radiation, the low dose and its epidemiology is getting international priority. As such, Canada has a Federal low dose radiation research program (LDRR): the Canadian Organization on Health Effects from Radiation Exposure (COHERE), a joint initiative between Health Canada and the Canadian Nuclear Safety Commission (CNSC), has

been established to improve understanding of the potential health effects from exposure to low dose radiation. Likewise, Canadian Nuclear Laboratories (CNL) has a low-dose radiobiology program. Similarly, the US Department of Energy (DOE) also has a low-dose radiation research program under the Low-Dose Radiation Research Act of 2019 (National Academies of Sciences, Engineering, and Medicine, 2019). The UK, EU, Japan, and France have low-dose radiation research programs.

There are two main challenges in low-dose radio-epidemiology: (1) precise low dose measurements (Table 1.1) are extremely challenging due to the weak measurement signals in EPR and other techniques such as TL and OSL. In addition, impurities in the samples produce the background noises/signals, which sometimes mask the dosimetric signals at low doses (<100 mGy) (IAEA, 2002, ICRU, 2002; Bailiff et al., 2016; Fattibene and Callens, 2010); and (2) the health effects from the low dose may be slow or small, so, it is complicated and challenging to monitor in individuals, groups, or populations (Pernot et al., 2012). Also, there are no biomarkers presently available to distinguish whether cancers have been caused by radiation exposure or not. To quantify risks from low-dose exposures, we need to determine one or more early molecular markers for radiation-induced cancers (UNSCEAR, 2012). At the same time, a robust method is required to accurately measure the low doses from external exposures to overcome measurement challenges, which will be instrumental in determining the radio-epidemiology of populations. To this end, besides conventional methods described in Section 1.2.1, this research also explored the feasibility of measuring low doses in alanine using the dose spiking EPR technique. It measured the low doses (down to 20 mGy) in alanine with ±10% error as described in Chapter 5. Furthermore, since different samples' measurement techniques are the same, this technique was used in deciduous teeth to determine its applicability in tooth enamel EPR dosimetry.

### 1.3 Motivation of thesis

First, there are growing concerns about the health risks from exposure to low levels of ionizing radiation. Therefore, the present study aims to measure the low doses in tooth enamel for the retrospective assessment of exposure to ionizing radiation from external exposures in Durham Region populations. Since the background doses in Durham Region residents, Ontario, are not available, the chronic low dose radiation received by the local population from the nearby NGSs, and other anthropogenic sources is unknown. The local dose from the nearby NGSs was determined using environmental measurements and modeling (OPG, 2020). However, they are not direct indicators of the doses in humans. Therefore, it is vital to determine the direct total anthropogenic low doses in public from the various sources (including NGSs) to determine the health effects of chronic exposures and radio-epidemiology of the region. In previous studies (IAEA, 2002; ICRU, 2002), human tooth enamel was used successfully to estimate the acute and chronic exposures in individuals, groups, or populations. Therefore, this study focuses on determining the total doses in tooth enamel to determine the chronic exposures from the various sources in Durham Region populations and study retrospective dosimetry using the EPR dose reconstruction for external ionizing radiation exposures.

Second, tooth enamel's low-dose (10-100 mGy) measurements are highly challenging due to the weak EPR signals or intensities, and impurities present in the sample. Therefore, as an alternative to the calibration curve and dose additive methods, this study uses the dose spiking EPR technique in alanine to check the accuracy and consistency of the method. The accuracy obtained in this method is higher than the conventional methods for that dose range. That is why this method is used to measure the low doses in deciduous teeth. Because given their availability, there is a high probability of obtaining teeth from children (deciduous) for dose reconstruction in

the actual radiation accidents like Fukushima Daiichi Nuclear Power Plants (Murahashi et al., 2017). Furthermore, it is vital to determine the accident doses in children because children are more susceptible than adults to ionizing radiation due to their higher radiation risk per dose (ICRP, 2007; Wiser and El-Faramawy, 2002).

### 1.4 Objective of thesis

This thesis aims to measure the total doses in tooth enamel from Durham Region populations, Ontario, for retrospective dosimetry using the technique verified through four international intercomparisons and the ISO protocol for the EPR tooth enamel dosimetry (ISO, 2013). Also, it explores the feasibility of using the dose spiking EPR technique in alanine. Then the same technique is applied to measure the low doses in deciduous tooth enamel to determine its accuracy and consistency for reconstructing chronic or accident doses in deciduous tooth enamel.

More specifically:

- Determine the total ionizing radiation doses in human tooth enamel in Durham Region residents using EPR dosimetry.
- Study retrospective dosimetry using the EPR dose reconstruction of low doses to Durham Region populations.
- To systematically investigate the feasibility of using the dose spiking EPR technique to measure low doses in alanine.
- Study the feasibility of using deciduous teeth for retrospective and accident dosimetry using the conventional EPR techniques and the dose spiking EPR technique.

## 1.5 **Novelty and contribution**

The magnitude of low doses from various sources in Durham Region populations is uncertain. The low doses around nuclear facilities have been determined using environmental samples and modeling (OPG, 2020). However, environmental samples and modeling may not provide the actual or total doses (i.e., background doses) that the local people are getting from the various sources, including two NGSs in Durham Region, Ontario. Human teeth, often called a 'biological dosimeter,' can record radiation doses throughout our life and has a high radiation dose stability rate. Thus, the human tooth enamel was used to measure the low doses using EPR dosimetry which provided the actual doses that the local populations in Durham Region are getting from the various sources with reliable precision and accuracy. The total background doses can be used to understand the total radiation exposure to the local populations and radiation epidemiology.

Moreover, EPR dosimetry with tooth enamel is a widely used technique to determine the external dose exposures both in radiation accidents and chronic exposures, as described in Section 1.1.2. However, a low dose measurement with high precision and accuracy is highly challenging due to the weak EPR signals and background noises, as described in Chapters 5 and 6. To overcome these challenges, this study successfully uses the dose spiking EPR technique to measure the low doses in alanine with ±10% measurement accuracy, as described in Chapter 5. The impurities present in the sample greatly influence the measurement precision in EPR dosimetry. The powder alanine is a 99% pure substance, whereas tooth enamel may contain more significant amounts of impurities than alanine. That is why one cannot directly extrapolate the results from alanine to tooth enamel to determine the low doses in tooth enamel using EPR. As a result, the dose spiking EPR technique was used to determine its applicability to measure the low doses in deciduous tooth enamel, as described in Chapter 6. Both permanent and deciduous teeth' radiation

sensitivity is almost the same. However, given the availability of deciduous teeth, which naturally fall out from children aged 6 to 13, there is a high probability of providing deciduous teeth for retrospective and accident dosimetry. So, this study estimated the low doses in deciduous teeth with high accuracy and precision, as described in Chapter 6, which demonstrated that these teeth could also be used in place of the permanent teeth for dose reconstruction.

### 1.6 Approach

Research ethics approval was obtained from the University Research Ethics Board (REB) to collect the extracted teeth in Durham Region, Ontario. The extracted tooth samples have been collected from Durham Region with the help of the local dentists/dental clinics and residents. The sample preparation and analysis have been done at Ontario Tech University (Aerosol and Radiation Research laboratory, ERC 3092). The low doses in tooth enamel have been determined at Ontario Tech (Aerosol and Radiation Research laboratory, ERC 3092) using the X-band CW EPR spectrometer. While one of the main objectives of this research is to determine the low dose radiation in human tooth enamel, the dose spiking EPR technique has been used in deciduous tooth enamel to decrease the detection limit in low dose measurements.

### 1.7 Outline of the thesis

This thesis consists of an introduction that describes the scope of the work, a brief description of the tooth enamel EPR retrospective and accident dosimetry, international intercomparisons, and the ISO standard in EPR tooth enamel dosimetry and research objectives. Chapter 2 provides an extensive literature review of the X- and Q-band EPR retrospective and accident dosimetry. Chapter 3 provides details about the low dose measurement technique – sampling, EPR parameters optimization, acquisition, dose estimation, data precision, and

accuracy. Chapter 4 focuses on the total doses in tooth enamel from Durham Region residents and the retrospective dose reconstruction processes. Chapter 5 presents the low dose measurement in powder alanine using the dose spiking EPR technique. Chapter 6 focuses on the low dose measurement in deciduous tooth enamel using the dose spiking technique. The thesis ends with the conclusion, recommendations, future work, a list of references (Chapter 7), and appendices.

### 1.8 References


Azzam, E.I., Colangelo, N.W., Domogauer, J.D., Sharma, N., de Toledo, S. M., 2016. Is ionizing radiation harmful at any exposure? An echo that continues to vibrate. Health Phys. 110.

Bailiff, I.K., 1997. Retrospective dosimetry with ceramics. Radiat. Meas. 27, 923-941.

Bailiff, I.K., Sholom, S., McKeever, S.W.S., 2016. Retrospective and emergency dosimetry in response to radiological incidents and nuclear mass-casualty events: A review. Radiat. Meas. 94, 83-139.

Barr, D., Eaton, S.S., Eaton, G.R., 2008. Workshop on quantitative EPR. At the 31st annual international EPR symposium, Breckenridge, Colorado.

Brenner, D.J., 2011. We don't know enough about low-dose radiation risk. Nature News published online Apr. 5.

Chumak, V., Bailiff, I., Baran, N., Bugap, A., Dubovsky, S., Fedesov, I., et al., 1996. The first international intercomparison of EPR-dosimetry with teeth: first results. Appl. Radiat. Isot. 47, 1281-1286.

De, T., Romanyukha, A., Trompier, F., Pass, B., Misra, P., 2013. Feasibility of Q-Band EPR Dosimetry in Biopsy Samples of Dental Enamel, Dentine and Bone. Appl. Magn. Reson. 44, 375–387.

Desrosiers, M., Schauer, D.A., 2001. Electron paramagnetic resonance (EPR) biodosimetry. Nucl. Instr. and Meth. in Phys. Res. B. 184, 219-228.

El-Faramawy, N., Wieser, A., 2006. The use of deciduous molars in EPR dose reconstruction. Radiat. Environ. Biophys. 44, 273–277.

Fattibene, P., Callens, F., 2010. EPR dosimetry with tooth enamel: A review. Appl. Radiat. Isot. 68, 2033-2116.

Fattibene, P., Wieser, A., Adolfsson, E., Benevides, L.A., Brai, M., Callens, F., et al., 2011. The 4th international comparison on EPR dosimetry with tooth enamel. Part 1: report on the results. Radiat. Meas. 46, 765–771.

Godfrey-Smith, D.I., 2008. Towards in vivo OSL dosimetry of human tooth enamel. Radiat. Meas. 45, 854-858.

Geso, M., Ackerly, T., Lim, S.A., Best, S.P., Gagliardi, F., Smith, C., 2018. Application of the 'Spiking' method to the measurement of low dose radiation (≤ 1Gy) using alanine dosimeters. Appl. Radiat. Isot. 133, 111-116.

Harvey, D., 2000. Modern analytical chemistry. McGraw Hill, New York.

Haskell, E.D., Hayes, R.B., Kenner, G.H., 1999. An EPR dosimetry method for rapid scanning of children following a radiation accident using deciduous teeth. Health Phys.76,137–144.

Hayes, R.B., Haskell, E.H., Romanyukha, A.A., Kenner, G.H., 1998. Technique for increasing reproducibility in EPR dosimetry of tooth enamel. Meas. Sci. Technol. 9, 1994–2006.

Hayes, R B., 1999. Electron paramagnetic resonance dosimetry: Methodology and material characterization. (Doctoral dissertation). Available from ProQuest Dissertations & Theses Global database. (UMI No. 9937601).

Hennig, G.J., Herr, W., Weber, E., Xirotiris, N.I., 1981. ESR-dating of the fossil hominid cranium from Petralona Cave, Greece. Nature. 292: 533-536.

ICRP, 2007. ICRP Publication 103: The 2007 recommendations of the international commission on radiological protection. Ann. ICRP 37 (2–4), 1–332.

ICRU, 2002. Retrospective Assessment of Exposures to Ionising Radiation. International Commission on Radiation Units and Measurements. International Commission on Radiation Units and Measurements, Bethesda, USA. ICRU Report 68.

ISO, 2013. Radiological protection – Minimum criteria for electron paramagnetic resonance (EPR) spectroscopy for retrospective dosimetry of ionizing radiation – Part 1: General principles, International Standard, ISO 13304-1.

IAEA, 2002. Use of the Electron Paramagnetic Resonance Dosimetry with Tooth Enamel for Retrospective Dose Assessment. IAEA-TECDOC-1331.International Atomic Energy Agency, Vienna, Austria, 57pp.

Ignatiev, E.A, Romanyukha, A., Koshta, A.A., Wieser, A., 1996. Selective saturation method for EPR dosimetry with tooth enamel. Appl. Radiat. Isotop. 47, 333–7.

Ivannikov, A.I., Zhumadilov, Zh, Gusev, B.I., Miyazawa, Ch, Jiao, L., Skvortsov, V.G., et al., 2002. Individual dose reconstruction among residents living in the vicinity of the Semipalatinsk Nuclear Test Site using EPR spectroscopy of tooth enamel. Health Phys. 83, 183-196.

Ivannikov, A., Toyoda, S., Hoshi, M., Zhumadilov, K., Fukumura, A., Apsalikov, K., et al., 2007. Inter laboratory comparison on tooth enamel dosimetry on Semipalatinsk region: Part 2, effects of spectra processing. Radiat. Meas. 42, 1015–1020.

Jacob, P., Goksu, Y., Meckbach, R., Wieser, A., 2002. Retrospective dosimetry for external exposures. International Congress Series. 1225, 141-148.

Murahashi, M., Toyoda, S., Hoshi, M., Ohtaki, M., Endo, S., Tanaka, K., Yamada, Y., 2017. The sensitivity variation of the radiation induced signal in deciduous teeth to be used in ESR tooth enamel dosimetry. Radiat Meas. 106, 450–4.

Maruyama, T., Cullings, H.M., Hoshi, M., Nagatomo, T., Kumamoto, Y., Kerr, G. D., 2005. Thermoluminescence dosimetry for gamma rays, Chap. 7 Part B. In: Young, R.W., Kerr, G.D. (Eds.), Reassessment of the Atomic Bomb Radiation Dosimetry for Hiroshima and Nagasaki dosimetry System 2002 (DS02), vol. 1. Radiation Effects Research Foundation, Hiroshima, Japan, pp. 362-394.

Nagatomo, T., Hoshi, M., Ichikawa, Y., 1995. Thermoluminescence dosimetry of the Hiroshima atomic-bomb gamma-rays between 1.59 km and 1.63 km from the hypocentre. Health Phys. 69, 556-559.

National Academies of Sciences, Engineering, and Medicine, 2019. The Future of Low Dose Radiation Research in the United States: Proceedings of a Symposium. Washington, DC: The National Academies Press. https://doi.org/10.17226/25578.

Ontario Power Generation (OPG), 2020. Results of environmental monitoring programs. N-REP-03443-10026. Retrieved October 10, 2021, from https://www.opg.com/documents/environmental-monitoring-program-2020-report/

Pernot, E., Hall, J., Baatout, S., Benotmane, M.A., Blanchardon, E., Bouffler, S., et al., 2012. Ionizing radiation biomarkers for potential use in epidemiological studies. Mutat. Res. 751 (2), 258–286.

Priest, N., 2018. Roadmap: Addressing public concerns about their exposure to low doses of anthropogenic radiation. CANDU Owner Group Inc. Saskatoon Meeting, University of Saskatchewan, SK, Canada.

Romanyukha, A.A., Schauer, D.A., 2002. EPR dose reconstruction in teeth: Fundamentals, applications, problems, and perspectives. In: Kawamori, A., Yamauchi, J., Ohta, H. (Eds.), EPR in the 21" Century: Basics and applications to material, life and earth sciences. Elsevier Science B.V., pp. 603-612.

Sato, H., Takatsuji, T., Takada, J., Endo, S., Hoshi, M., Sharifov, V.F., et al., 2002. Measuring the external exposure dose in the contaminated area near the Chernobyl nuclear power station using the thermoluminescence of quartz in bricks. Health Phys. 83, 227-236.

Scientific Committee on the Effects of Atomic Radiation, UNSCEAR, 2006. Effects of Ionizing Radiation, Volume I, United Nations.

Scientific Committee on the Effects of Atomic Radiation, UNSCEAR, 2012. Sources, Effects and Risks of Ionizing Radiation, Scientific Annexes A and B, United Nations.

Scientific Committee on the Effects of Atomic Radiation, UNSCEAR, n.d. Answers to Frequently Asked Questions (FAQs). Retrieved October 10, 2021, from https://www.unscear.org/unscear/en/faq.html

Schauer, D.A., Iwasaki, A., Romanyukha, A.A., Swartz, H.M., Onori, S., 2007. Electron paramagnetic resonance (EPR) in medical dosimetry. Radiat. Meas. 41, 117-123.

Skaleric, U., Ravnik, C., Cevc, P., Schara, M., 1982. Microcrystal arrangement in human deciduous dental enamel studied by electron paramagnetic resonance. Caries Res. 16, 47–50.

Sholom, S., Desrosiers, M.F., 2014. EPR and OSL emergency dosimetry with teeth: a direct comparison of two techniques. Radiat. Meas. 71, 494-497.

Sholom, S., DeWitt, R., Simon, S.L., Bouville, A., McKeever, S.W.S., 2011. Emergency dose estimation using optically stimulated luminescence from human tooth enamel. Radiat. Meas. 46, 778-782.

Sutou, S., 2018. Low-dose radiation from A-bombs elongated lifespan and reduced cancer mortality relative to un-irradiated individuals. Genes Environ. 40, 26, 1-14. https://doi.org/10.1186/s41021-018-0114-3

Swartz, H.M., Burke, G., Coey, M., Demidenko, E., Dong, R., Grinberg, O., et al., 2007. In vivo EPR for dosimetry. Radiat. Meas. 42, 1075-1084.

Toyoda, S., 2019. Recent Issues in X-Band ESR Tooth Enamel Dosimetry. In: Shukla A. K. (Eds.), Electron Spin Resonance Spectroscopy in Medicine. Springer Nature Singapore, pp. 135-151. Pte Ltd. https://doi.org/10.1007/978-981-13-2230-3.

Wesolowska P.E., Cole A., Santos T., Bokulic T., Kazantsev P., Izewska J., 2017. Characterization of three solid state dosimetry systems for use in high energy photon dosimetry audits in radiotherapy. Radiat Meas. 106: 556-562.

Wieser, A., El-Faramawy, N., 2002. Dose reconstruction with electron paramagnetic resonance spectroscopy of deciduous teeth. Radiat. Prot. Dosim. 101 (1–4), 545–548.

Wieser, A., Romanyukha, A., Degteva, M., Kozheurov, V., Petzoldt, G., 1996. Tooth enamel as a natural beta dosimeter for bone seeking radionuclides. Radiat. Prot. Dosim. 65, 413–416.

Wieser, A., Mehta, K., Amira, S., Aragno, D., Bercea, S., Brik, A., et al., 2000. The 2nd international intercomparison on EPR tooth dosimetry. Radiat. Meas. 32, 549-557.

Wieser, A., Debuyst, R., Fattibene, P., Meghzifene, A., Onori, S., Bayankin, S.N., et al., 2005. The 3rd international intercomparison on EPR tooth dosimetry: Part 1, general analysis. Appl. Radiat. Isot. 62, 163-171.

Wieser, A., Debuyst, R., Fattibene, P., Meghzifene, A., Onori, S., Bayankin, S.N., et al., 2006. The 3rd international intercomparison on EPR tooth dosimetry: part 2, final analysis. Radiat. Prot. Dosim. 120, 176-183.

Yukihara, E.G., Mittani, J., McKeever, S.W.S., Simon, S.L., 2007. Optically stimulated luminescence (OSL) of dental enamel for retrospective assessment of radiation exposure. Radiat. Meas. 42, 1256 – 1260.

Zhumadilov, K., Ivannikov, A., Skvortsov, V., Stepanenko, V., Zhumadilov, Z., Endo, S., et al., 2005. Tooth enamel EPR dosimetry: optimization of EPR spectra recording parameters and effect of sample mass on spectral sensitivity. J. Radiat. Res. (Tokyo) 46(4), 435–442.

Zhumadilov, K., Ivannikov, A., Apsalikov, K.N., Zhumadilov, Zh., Toyoda, S., Zharlyganova, D., et al., 2006. Radiation dose estimation by tooth enamel EPR dosimetry for residents of Dolon and Bodene. J. Radiat. Res. 47, A47-A53.

# Chapter 2

# Literature Review

### 2.1 EPR Dosimetry with tooth enamel

Gordy et al. (1955) were the first to report radiation-induced EPR signals in an X-ray irradiated skull bone at 9 and 23 GHz. A few years later, Cole and Silver (1963) and Brady et al. (1968) reported several EPR signals in tooth enamel, which formally started the EPR tooth enamel dosimetry to ionizing radiation, retrospective, and accident dosimetry. The motivation for further development and application of EPR dosimetry with tooth enamel resulted from the Chernobyl accident in 1986 (Chumak et al., 1999; Chumak et al., 1998; Romanyukha and Schauer, 2002). Since that time, tooth enamel and bone EPR dosimetry have been used for retrospective and emergency dosimetry for broad radio-epidemiological studies on health effects of ionizing radiation (Desrosiers and Schauer, 2001; Schauer et al., 2007; Ivannikov et al., 2002). The EPR spectra of bones and dental enamel have the radiation-induced signals (RISs), which provide information about the total doses that the tooth enamel or bones absorbs from external exposures, whereas the BGSs are due to contamination and caused by environmental exposures, as shown in Figure 2.1 (Krefft et al., 2014; Bailiff et al., 2016).

However, in bones and teeth, the teeth are highly desirable to reconstruct retrospective or accident doses because the hydroxyapatite of teeth enamel does not change over time, which means the recorded doses become highly stable for a very long time. On the other hand, the hydroxyapatite of bones changes due to growth or demineralization, which means the recorded doses may fade or decrease over time. However, if a tooth is unavailable, a bone can also provide

helpful information about the absorbed doses for retrospective or accident dosimetry (Baffa et al., 2002).

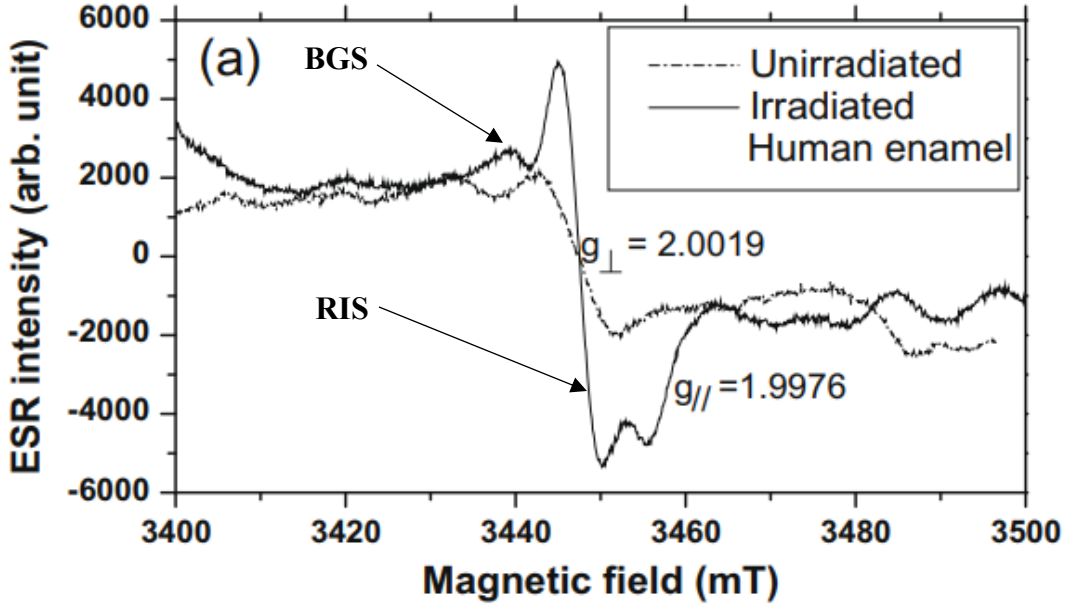


**Figure 2.1:** EPR spectra from the irradiated (γ-rays dose of 5 Gy from 60Co ) and unirradiated tooth enamel. The dosimetric signal is clear in the irradiated tooth enamel, but it is not visible in unirradiated tooth enamel. From Hassan et al. (2010).

This technology was limited to determining external exposures on tooth enamel using the X-band CW EPR technique. However, many recent studies have demonstrated that the lower band EPR technique, such as the L-band (1.2 GHz) EPR is equally effective and convenient for measuring radiation doses in vivo (Demidenko et al., 2007; Salikhov et al., 2003; Zdravkova et al., 2003a). This type of a low band EPR spectrometer does not influence much by the presence of moisture in biological materials and suitable in vivo measurements (Godfrey-Smith, 2008; Demidenko et al., 2007; Salikhov et al., 2003; Zdravkova et al., 2003). However, the *in vivo* L-band EPR dosimetry with tooth enamel was less sensitive than the X-band, and the resolution of the radiation-induced signal at low doses was also worse. It can only measure the absorbed dose

below 10 Gy (Zdravkova et al., 2003). However, in the case of nuclear or radiation accidents, the radiation dose of concern is 100 mGy to 1000 mGy and higher (UNSCEAR, 2012), where the L-band is not a suitable technique. Likewise, the higher frequency Q-band (34 GHz) EPR spectrometer has been used to determine not only the lower doses (i.e., <5 Gy) but also to measure the small sample size (<70 mg) with a high degree of precision and accuracy due to its increased signal-to-noise ratio (SNR). The Q-band is 20 times more sensitive than the X-band CW EPR. Due to its significantly high sensitivity, the tooth enamel does not need a chemical treatment or other enamel purification processes for sample preparation. Consequently, the EPR spectrum will be free from the background or native signals from chemical impurities present in the samples. So the Q-band EPR techniques would be highly effective for the low dose retrospective and accidental dosimetry studies (De et al., 2013; Romanyukha et al., 2014; Romanyukha et al., 2007; Guilarte et al., 2016).

Besides human tooth enamel (Desrosiers and Schauer, 2001), cows and goats (Jiao et al., 2014), camels (El-Faramawy et al., 2018), and a wild boar (Harshman and Johnson, 2019) tooth enamel was also used to reconstruct doses for retrospective and environmental dose assessment. Additionally, these animals' teeth can easily be used to determine the external exposures in accident-stricken areas in the absence of human tooth enamel (Hassan et al., 2010: Jiao et al., 2014). As shown in Figure 2.2, the radiation sensitivity of cow tooth enamel was found to be very similar to human tooth enamel (Hassan et al., 2010; Toyoda et al., 2003). However, the mouse teeth were about 25% lower radiation sensitivity than the human teeth (Khan, 2003; Toyoda et al., 2003). Hayes et al. (1998) analyzed the Pacific Walrus check teeth, and their minimum detectable dose was 350 mGy. The animal tooth enamel with less background noises, high radiation sensitivity, and the ability to detect the lowest doses would be vital for their applicability in the

EPR dose measurements and retrospective dose reconstruction (Hassan et al., 2010; Toyoda et al., 2003; Jiao et al., 2014; Harshman and Johnson, 2019). Additionally, animal teeth enamel dosimetry is vital for estimating environmental doses in case of nuclear or radiological accidents, which eventually helps to protect non-human species from radiation exposures (ICRP, 2003). Also, the dose determined in these animals can be used to deduce doses in humans by comparing their radiation sensitivities.

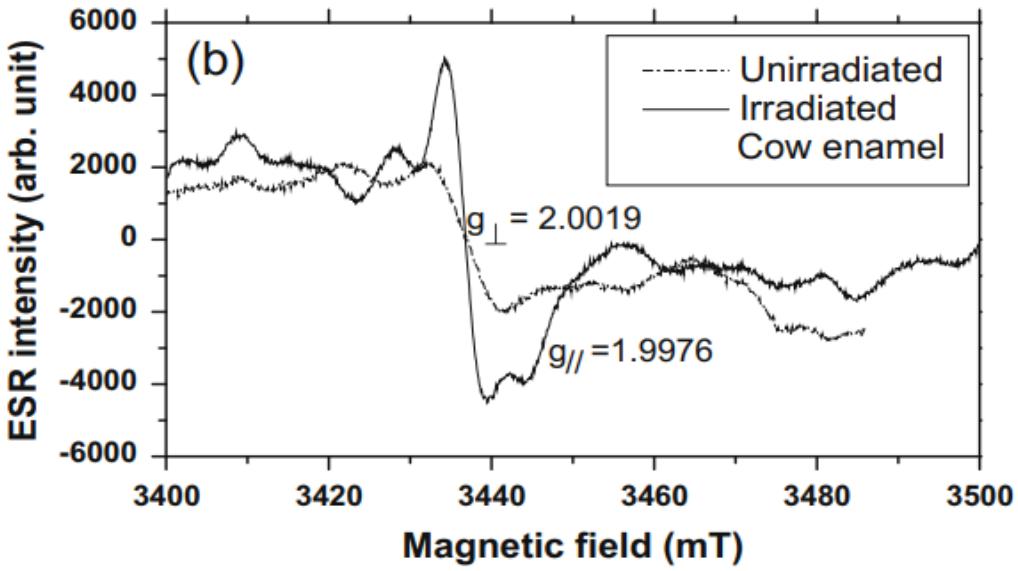


**Figure 2.2:** EPR spectra of cow teeth enamel before and after irradiation to γ-rays dose of 5 Gy from $^{60}$Co. From Hassan et al. (2010).

## 2.2 **Fundamentals of EPR dose reconstruction in tooth enamel**

The tooth's outer surface is made entirely from enamel, white, semitransparent material that varies in thickness from 0.01 mm to about 2.5 mm in the grinding part of molars (Mitchell, 2004). A molar tooth or pre-molar contains about 1,000 mg of enamel; however, an animal tooth contains slightly more enamel. Enamel contains almost exclusively (~97%) of the mineral hydroxyapatite [$Ca_{10}(PO_4)_6(OH)_2$], the main mineral component of the calcified tissues such as

teeth and bones, which contains the carbonate ions as impurities as $Ca_{10}[(PO_4)_{6-x}(CO_3)_x][(OH)_{2-y}(CO_3)_y]$, as shown in Figure 2.4, where x is about 0.039, and y is about 0.01 (Jacob et al., 2002). The remaining content (about 3%) is mainly organic materials and other trace elements, as shown in Tables 2.1 and 2.2. Carbonate impurities in the hydroxyapatite make tooth enamel highly sensitive to ionizing radiation (Desrosiers and Schauer, 2001; Jiao et al., 2014; Hassan et al., 2010). The EPR dosimetry with tooth enamel is based on the measurement of the radiation-induced $^{\bullet}CO_2^-$ radical anions in the hydroxyapatite $Ca_{10}[(PO_4)_{6-x}(CO_3)_x][(OH)_{2-y}(CO_3)_y]$ crystals, which is highly stable for a long time and can be used in radiation dosimetry, dating, detection of irradiated foodstuffs, etc. (Jacob et al., 2002; Romanyukha and Schauer, 2002). The EPR and Electron Nuclear Double Resonance (ENDOR) study of the carbonated hydroxyapatite crystals have revealed that the EPR radiation induced signal is a composite of different paramagnetic species ($^{\bullet}CO_2^-$, $^{\bullet}CO_3^{3-}$,$^{\bullet}CO_3^-$, $O^-$, $O_3^-$) in the locations such as hydroxyl (A site), phosphate (B-site) or the surface site location. However, among these paramagnetic species, the most important and highly stable radiation-induced radical anions ($^{\bullet}CO_2^-$) are located in the hydroxyapatite's A and B sites and on the surface. Which can be used as a probe for determining the personal accident doses or retrospective doses in the case of low dose exposures (Romanyukha and Schauer, 2002; IAEA, 2002).

The hydroxyapatite crystal has a hexagonal crystalline structure (a = b = 9.432 Å, c = 6.881 Å) as shown in Figures 2.4a and 2.4b, the $^{\bullet}CO_2^-$ radical anion has its O-O axis along the pseudo-hexagonal c-axis of the peptide structure around which it is rapidly rotating, as shown in Figure 2.3 (Callens et al., 2002). As it can be seen in Figure 2.3, the O atoms of the $^{\bullet}CO_2^-$ radical anion are in the same plane (i.e., parallel to the applied magnetic field, g∥), which rotates upon absorbance of gamma rays. However, carbon (C) is on a different plane (i.e., perpendicular to the

applied magnetic field, g⊥). Due to this molecular structure of the $^{\bullet}CO_2^-$ radical anions in irradiated enamel, we can observe the sample and EPR spectrum anisotropy in the EPR measurements (Wieser and El-Faramawy, 2002), with an anisotropic g-factor shape (g⊥=2.0027, g‖ =1.9970) as depicted in Figure 2.3.

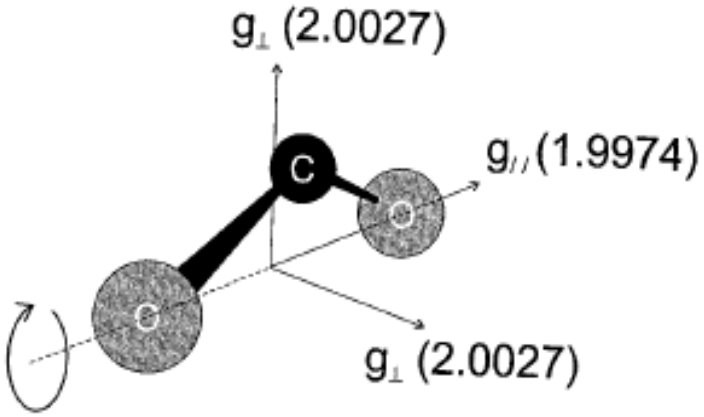


**Figure 2.3:** Model for $^{\bullet}CO_2^-$ in the hydroxyapatite crystal lattice, which gives an asymmetric EPR spectrum with two different g-values (g⊥=2.0027, g‖ =1.9970). From Callens et al. (2002).

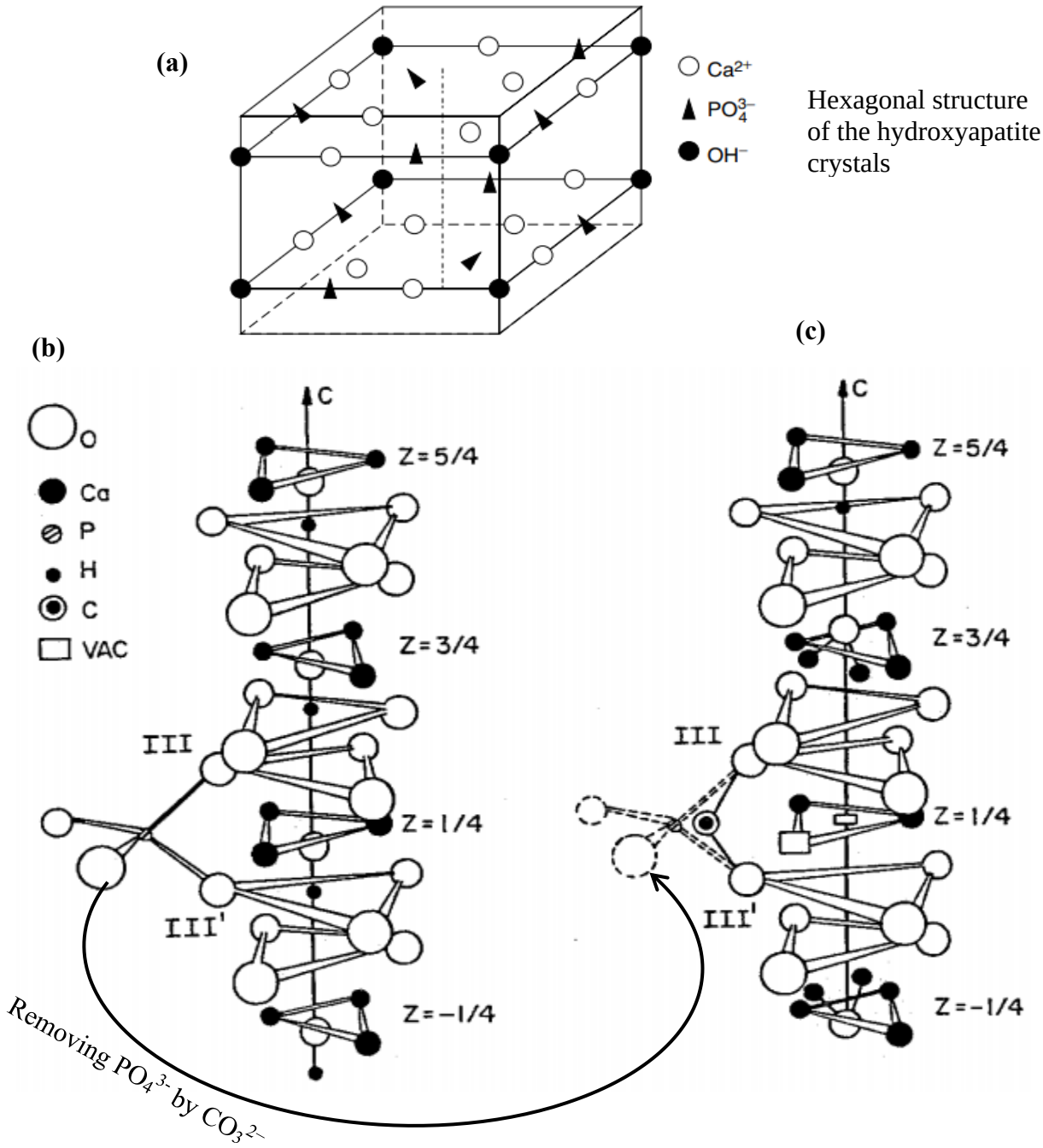


**Figure 2.4: (a)** Hexagonal crystal structure of the hydroxyapatite crystals with $Ca^{2+}$ and $PO_4^{3-}$ (unit cell perspective). From Mitchell (2004). **(b)** The crystallographic structure of the hydroxyapatite crystals closes to the hexagonal c-axis, where $PO_4^{3-}$ is removed by $CO_3^{2-}$ ions . **(c)** Carbonate groups substitute the phosphate from the B site of the hydroxyapatite crystal lattice and the proposed $^{\bullet}CO_2^{-}$ radical anions site in the hydroxyapatite structure. From Vugman et al. (1995).

The size of these hydroxyapatite crystals varies in different calcified tissues from approximately 200 to 400 Å in dentin and bones to 7000 to 8000 Å in tooth enamel. These hydroxyapatite crystals are bound to the aqueous organic matrix (60% water and 40% organic component), contributing to the native or background signals in the X-band CW EPR measurements at a g-value of 2.0045 (Romanyukha and Schauer, 2002; Romanyukha et al., 1994). The biological hydroxyapatite contains about 2-3% of $CO_3^{2-}$ ions, major and minor constituents (i.e., trace elements), as shown in Tables 2.1 and 2.2 (Elliott, 1994; Fattibene and Callens, 2010; Driessens and Verbeeck, 1990, p. 107). These major and minor constituents are incorporated during teeth formation; some are paramagnetic and contribute parasitic signals in EPR measurements.

**Table 2.1:** Major and minor constituents in tooth enamel in % dry weight. From Driessens and Verbeeck (1990, p. 107).

| Constituents | Average concentration (dry weight %) |
|---|---|
| Ca | 36.6 |
| P | 17.7 |
| $CO_3^{2-}$ | 3.2 |
| Na | 0.67 |
| Mg | 0.35 |
| Cl | 0.35 |
| K | 0.04 |

**Table 2.2:** Trace element concentrations in tooth enamel (μg/g, dry weight). From Driessens and Verbeeck (1990, p. 107).

| Constituents | Mean concentration (μg/g, dry weight) |
|---|---|
| Zn | 179 |
| Sr | 156 |
| Si | 136 |
| F | 120 |
| S | 59 |
| Al | 51 |
| Fe | 33 |

The free electrons originate from impurities in the hydroxyapatite crystals by ionizing radiation or temperature when tooth enamel is exposed to ionizing radiation (Rudko et al., 2010). Therefore, when the hydroxyapatite crystals absorb ionizing radiation, the carbonate ion ($CO_3^{2-}$) located in hydroxyl (A site) and phosphate (B site) of the hydroxyapatite lattice and the neutral $CO_2$ molecule on the surface of crystallites absorbs the free electrons originate from the ionization of impurities (i.e., secondary thermalized electrons) in the hydroxyapatite and form the $^{\bullet}CO_2^-$ radical anions as shown in equations 2.1 and 2.2. In this process, two types of paramagnetic centers (mainly $^{\bullet}CO_2^-$) are formed: (1) the axial paramagnetic center ($a = b \neq c$); and (2) the orthorhombic paramagnetic center ($a \neq b \neq c$) (Rudko et al., 2010).

$$CO_2 + e^- \text{ (secondary thermalized electrons)} \rightarrow {}^{\bullet}CO_2^- \quad (2.1)$$

Their ratios depend on the photon energy and quality of materials (i.e., defectiveness in tooth enamel). However, Rudko et al. (2010) found that in biological hydroxyapatite crystals, the axial $^{\bullet}CO_2^-$ radical anions are predominantly formed as a result of spontaneous decay of short-lived (intermediate) $CO_3^{2-}$ anions as follows:

$$CO_3^{2-} + e^- \text{ (secondary thermalized electrons)} \rightarrow \underset{\text{(Short-lived radical)}}{CO_3^{3-}} \rightarrow \underset{\text{(Stable free radical anion)}}{^{\bullet}CO_2^-} \quad (2.2)$$

The main contribution to the dosimetric EPR signal is due to the axial-symmetric $^{\bullet}CO_2^-$ radical anion ($a = b \neq c$) at $g_{\perp}=2.0027$, $g_{\parallel} =1.9970$, as shown in Figure 2.3.

**2.3 g-anisotropy in a tooth enamel EPR spectrum**

The g-anisotropy can be observed in many powder samples with crystalline properties; however, it depends on the crystal structure of materials and the external magnetic field direction with respect to the crystal axis (i.e., g-value changes in a crystalline material depending on the external magnetic field direction). The shape of the solid-state spectrum depends on the different orientations of the free radical species with respect to the applied magnetic field ($B_0$). Therefore, the spectrum symmetry (e.g., cubic, axial, and rhombic symmetry) will reflect on the final spectrum of EPR measurements, as depicted in Figure 2.6b. For instance, if the crystal has a high symmetry like in cubic, anisotropy in a spectrum is absent because all axes are equal, and there will be no difference in a resonance field when the $B_0$ is aligned in the XY plane perpendicular to the applied field, and parallel to the Z-axis. However, in the case of the axial symmetry ($a = b \neq c$), the anisotropy will be observed in the XY plane perpendicular to the applied field and parallel to the Z-axis as depicted in Figures 2.5a, 2.5b, and 2.6a. In other words, the g-anisotropy will be observed in the perpendicular and parallel orientations of the magnetic field with respect to the XY plane and Z-axis. In the third case, rhombic symmetry ($a \neq b \neq c$), all crystal axes are unequal, so the resonance field will differ when the $B_0$ is aligned in three different axes, as depicted in Figure 2.6b (d). (Duin, 2013; Brustolon and Giamello, 2009). However, axial symmetry is the most common crystal symmetry in the tooth enamel hydroxyapatite crystals (i.e., orthorhombic crystal). The $^{\bullet}CO_2^-$ radical anions in the axial symmetry remain in the XY plane of the crystal

axes, perpendicular to the applied magnetic field ($B_0$), and parallel to the Z-axis as shown in Figures 2.5a and 2.5b. Since there are a large number of $^{\bullet}CO_2^-$ radical anions in the XY plane than in the Z-axis, the intensity of a spectrum is stronger around g⊥ than g‖ ( g⊥=2.0027, g‖ =1.9970) as depicted in Figures 2.6a and 2.3 (Lund et al., 2011; Duin, 2013; Callens et al., 2002). The errors from the g-anisotropy can be reduced by rotating samples and averaging the resulting spectra during the EPR measurements, as described in Chapter 4 (Section 4.3.2) and Chapter 5 (Section 5.3.3). However, a high-frequency EPR spectrometer may be needed for the complete resolution of g-anisotropy.

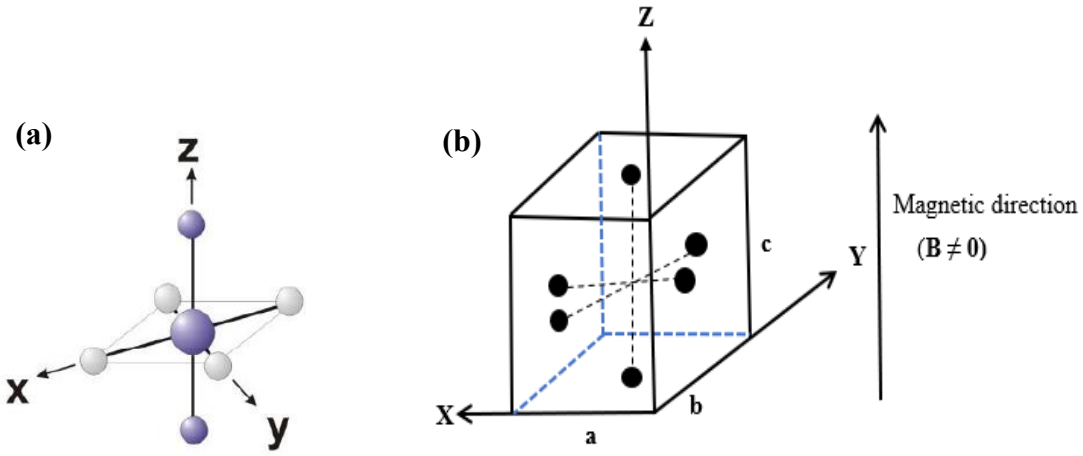


**Figure 2.5: (a)** An axial g-tensor (g-value) dependence on the different orientations of molecules in the magnetic field (laboratory axes). **(b)** The axial symmetry (a = b ≠ c) with the direction of the magnetic field ($B_0$). From Brustolon and Giamello (2009); Duin (2013).

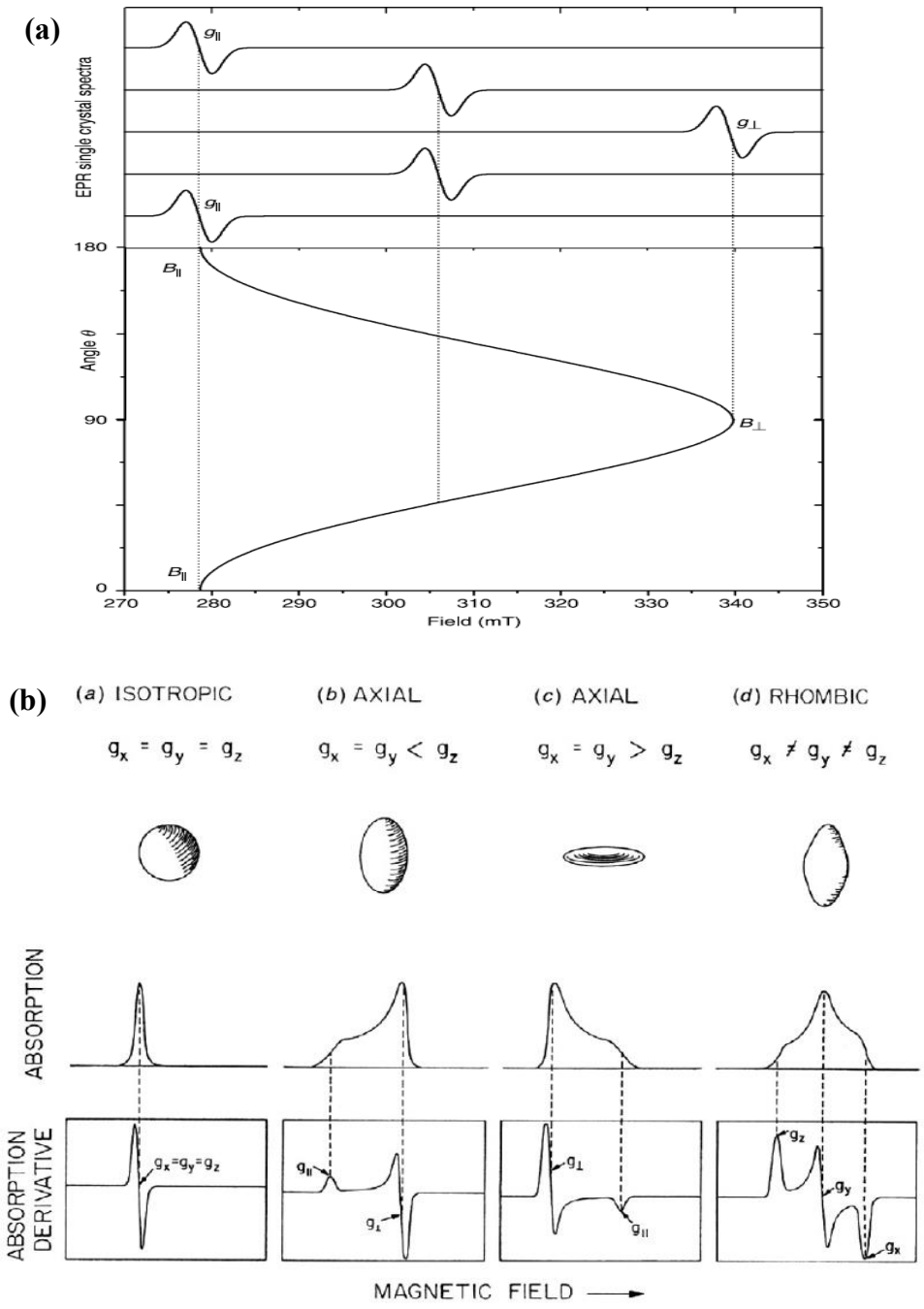


**Figure 2.6: (a)** Powder X-band CW EPR spectra of a single crystal showing the axial g-anisotropy. As a sample rotates from θ = 0 to 180˚ within the field, the peak position is changed from the XY plane perpendicular to the parallel Z-axis. **(b)** The g-values of an isotropic spectrum ($g_x = g_y = g_z$), an axial symmetry spectrum ($g_x + g_y = g\perp$ and $g_z = g\parallel$, and a rhombic symmetry spectrum ($g_x \neq g_y \neq g_z$). From Duin (2013).

## 2.4 Applications of tooth enamel in EPR dose reconstruction

As explained in Section 2.2, the greater abundance of the hydroxyapatite crystals in tooth enamel and its high degree of crystallinity makes it the ideal material for retrospective dosimetry (Desrosiers and Schauer, 2001; Jacob et al., 2002). However, the radiation-induced signal must be separated to reconstruct the absorbed doses in tooth enamel, as shown in Figure 2.7. Additionally, it is one of the most important tissues in our body to reconstruct the absorbed doses and fulfills the EPR dosimetry criteria: (1) it has a high free-radical yield; (2) it has short relaxation times so that high microwave power can be applied; (3) it has a linear dose-response from about 30 mGy to above 10 kGy, a significant range for the reconstruction of accidental doses (Ikeya, 1993; Romanyukha and Schauer, 2002); (4) it has high stability of the radiation-induced free radicals so that the dosimeter can be kept as a document of the radiation doses; and (5) it is a non-destructive read-out dosimeter, which means the dose accumulation at repeated exposures can be monitored (Romanyukha and Schauer, 2002) using EPR spectroscopy.

The potential of EPR tooth enamel dosimetry for dose reconstruction has been used since the mid-1960 (Swartz, 1965). It has already been successfully used to reconstruct doses in many major nuclear accidents, nuclear bomb test sites and to assess the occupational radiation exposure (Ikeya et al., 1984; Nakamura et al., 1998; Young and Kerr, 2005; Romanyukha et al., 2000; Romanyukha et al., 1994). Essentially, this technique is typically helpful for measuring relatively low dose exposures where conventional dosimeters are not available in the case of nuclear accidents or other chronic exposures (IAEA, 2002). The main advantages of the techniques are:
(1) The tooth enamel has long-term signal stability, a period longer than a human lifespan, which is the main advantage of dose reconstruction methods (IAEA, 2002; Desrosiers and Schauer,

2001). As a result, the measurement of a radiation dose in tooth enamel would provide doses that individuals get throughout his/her life;

(2) As the hydroxyapatite crystal's composition is the same in different teeth, it has lower variability of the radiation sensitivity among different teeth if they are exposed to the same amount of ionizing radiation (Desrosiers and Schauer, 2001; Schauer et al., 2007; Bailiff et al., 2016; IAEA, 2002; Fattibene and Callens, 2010). Sholom and Chumak (2005) study found ± 4% variability among different teeth in the Ukrainian population and ±7% variability in teeth from different parts. Thus, EPR tooth enamel dosimetry is extremely important for reconstructing a total lifetime dose in individuals (Bhat, 2005).

However, it is not always possible to get the extracted teeth for dose reconstruction from all individuals in this kind of study (Romanyukha et al., 2001; Wieser et al., 1996; IAEA, 2002). A city close to NGSs can establish a local tooth bank collaborating with the dentists/ dental clinics and dental hospitals, which would provide extracted teeth for periodic monitoring of the background doses in populations.

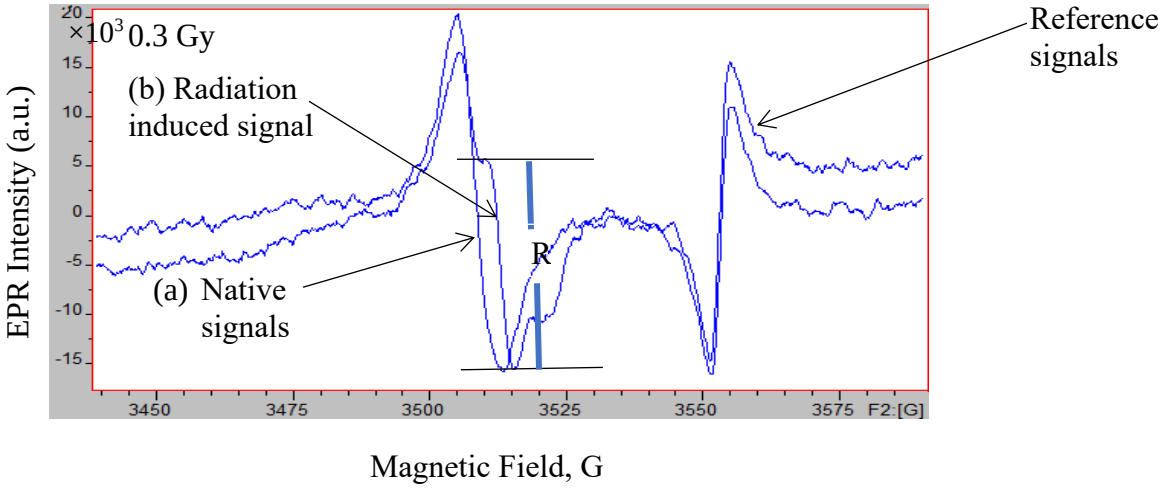


**Figure 2.7: (a)** An EPR spectrum from the unirradiated tooth enamel only contains the background or native signal (g = 2.0045). **(b)** An EPR spectrum from a tooth enamel sample irradiated to 0.3

Gy (gamma). The native and RISs were separated at this dose in tooth enamel. R is the P2P amplitude height used for EPR dose reconstruction.

### 2.5 Low dose measurements in EPR tooth enamel dosimetry

Tooth enamel is the only human tissue that can record the radiation dose throughout life and measure the low doses using the X-band CW EPR spectrometers. The minimum detection limit found in tooth enamel using EPR dosimetry (X-band) as per the literature is <100 mGy (down to 30 mGy) (Hayes et al., 1998; Shishkina et al., 2016). However, the actual detection limit depends on how experiments are conducted. Some sensitive parameters include:

1. Complete removal of impurities from enamel using both mechanical and chemical methods;
2. Using a goniometer for rotating samples to eliminate the measurement errors from the sample anisotropy;
3. Using an internal standard (i.e., marker accessory) to calibrate the g-factor;
4. Making an accurate calibration curve using a pure and statistically valid number of samples;
5. The EPR instrument's routine calibration check;
6. System performance tests (i.e., a signal to noise ratio (S/N);
7. Cavity background signal tests (Hayes et al., 1998).

At the same time, the EPR spectral acquisition processes are vital for data accuracy, precision, and measuring the low doses in tooth enamel (Bailiff et al., 2016; Ivannikov et al., 2000; Ivannikov et al., 2001; Ivannikov et al., 2002). Relevant papers that measured the radiation dose level from 30 - 649 mGy using the X-band CW EPR spectrometer are presented in Table 2.3.

**Table 2.3:** The type of EPR spectrometers and the minimum detection limit reported in the literature.

| EPR type | Minimum detection limit (mGy) | Reference |
|---|---|---|
| EPR (X-band CW) | 30 mGy | Hayes et al. (1998) |
| EPR (X-band CW) | 30 mGy | Shishkina et al. (2016) |
| EPR (X-band CW) | <100 mGy | Egersdorfer et al. (1996) |
| EPR (X-band CW) | <100 mGy | Wieser et al. (2006) |
| EPR (X-band CW) | 101–552 and 67–561 mGy | Wieser et al. (2008) |
| EPR (X-band CW) | 205 mGy, ranging from 56 to 649 mGy | Fattibene et al. (2011) |
| EPR (X-band CW) | 100 mGy to 1100 mGy | Haskell et al. (1999b) |
| EPR (X-band CW) | 200 mGy | Haskell et al. (1997) |

Thus, the EPR tooth enamel dosimetry is one of the most vital tools for determining the low dose exposures to the local population and environment from the various sources (Romanyukha et al., 2000; Ainsbury et al., 2011). EPR dosimetry with tooth enamel has been using the X-band CW EPR for the assessment of absorbed doses from ionizing radiation; however, the X-band has a lower signal to noise ratio (SNR) in a dose below 0.5 Gy, lower sensitivity, and requires a large sample size (i.e., ~100 mg enamel) for radiation dose estimation (De et al., 2013; Romanyukha et al., 2007). Still, the X-band CW EPR spectrometer is the most widely used for the retrospective dose assessment because of its availability, moderate sensitivity, and reasonable price, and it does not influence as much by water content (or moisture) as other higher frequency bands of EPR spectrometers (IAEA, 2002; Schauer et al., 2007).

## 2.6 Retrospective and accident dosimetry

The estimation of a radiation dose received by an individual recently (i.e., within the last few weeks or only a few hours ago), historically (in the past), or chronically (over many years) using methods other than the conventional dosimeters is called the retrospective dosimetry (Ainsbury et al., 2011; ISO, 2013; Bailiff et al., 2016; ICRU, 2002). However, the immediate evaluation of radiation dose (i.e., external exposures) to individuals after a nuclear or radiological accident or attack is called the accident or emergency dosimetry (Bailiff et al., 2016). EPR dosimetry with tooth enamel is the most advanced and widely accepted method for the retrospective dose assessment for individuals and groups or populations (Ainsbury et al., 2011; IAEA, 2002; Fattibene and Callens, 2010). Additionally, retrospective dosimetry is one of the essential tools for assessing past radiation exposures where no helpful information can be obtained from radiation monitoring instruments (Mesterhazy et al., 2011; Takahashi et al., 2002). Also, the main applications of retrospective dosimetry are (1) to supply the dosimetric information for epidemiological studies; (2) to evaluate the historical and chronic exposures; and (3) to support the judgment about the induction of cancer in employees due to past occupational exposures (ICRU, 2002).

Several EPR tooth enamel retrospective dose assessments have been conducted to assess the acute and chronic radiation exposures: (1) the atomic bomb survivors in Hiroshima and Nagasaki (Ikeya et al., 1984; Nakamura et al., 1998; Young and Kerr, 2005); (2) Chernobyl accident (Chumak et al., 1999; Chumak et al., 1996; Ishii et al., 1990; Chumak et al., 1998; Gualtieri et al., 2001; Tatsumi-Miyajima and Okajima, 1991); (3) Techa River (Shishkina et al., 2011; Degteva et al., 2015); (4) Semipalatinsk nuclear test site (Ivannikov et al., 2002; Pivovarov et al., 2002; Zhumadilov et al., 2007; Zhumadilov et al., 2013; Bailiff et al., 2004); (5) the nuclear

weapons test sites in the former Soviet Union (Dolon and Bodene) (Zhumadilov et al., 2006); and (6) Russian nuclear workers (Romanyukha et al., 2000; Romanyukha et al., 1994). In all these studies, human tooth enamel was used successfully to estimate acute and chronic exposures (i.e., doses received by populations due to several accidents and occupational exposures) in individuals, groups, or populations. Thus, it was suggested that the results obtained from the EPR tooth enamel dosimetry were essential for the individual dose reconstruction and assessment of the health effects of radiation in populations (Ivannikov et al., 2002; IAEA, 2002).

### 2.6.1 Retrospective dosimetry

#### 2.6.1.1 Physical and biological retrospective dosimetry

There are mainly two types of retrospective dosimetry techniques: (1) biological dosimetry, which uses a chromosome aberration analysis in human lymphocytes and somatic-mutation assays to detect and quantify radiation exposures; and (2) physical dosimetry, which uses humans extracted teeth, nails, and bones for determining the radiation exposure to individual persons using EPR methods (Ainsbury et al., 2011; ICRU, 2002). The most appropriate method of retrospective dosimetry depends on the type of study and the number of years' data we need (ICRU, 2002). The absorbed dose is stable for a short period in biological samples such as blood and muscle. In contrast, the free radicals in tooth enamel which are directly related to the absorbed dose are stable for a very long period (i.e., longer than the human lifespan) in normal conditions (Desrosiers and Schauer, 2001; ICRU, 2002; Kleinerman et al., 2006; Ainsbury et al., 2011). Therefore, if we need to determine the radiation exposure to evaluate a past radiation event, then the physical dosimetry with tooth enamel would be the best option due to its very long dose stability rate (Desrosiers and Schauer, 2001; ICRU, 2002; IAEA, 2002; Fattibene and Callens, 2010). Additionally, the EPR tooth enamel dosimetry can provide a cumulative environmental exposure and the accident dose.

It is a gold standard for retrospective dosimetry and reconstructing individuals' total lifetime accumulated radiation doses (Shishkina et al., 2003; Bhat, 2005). EPR tooth enamel dosimetry, in conjunction with epidemiology, can be reliably used to assess the radiation risk to individuals and populations. However, the method used must be well established and validated by the international intercomparisons (Chumak et al., 1996; Wieser et al., 2000; Wieser et al., 2005; Wieser et al., 2006; Fattibene et al., 2011).

Nevertheless, there is no equally suitable technique to reconstruct absorbed doses in all situations. The dose reconstruction depends on the availability of the sample and the dose range that we need to determine for a particular situation. For instance, as shown in Figure 2.8, FISH (Fluorescent in Situ Hybridization) biodosimetry could be used in any situation (i.e., both accident and retrospective dosimetry) as a small blood sample would be sufficient for the complete dose analysis. However, the lowest detection limit of this technique is 300 mGy, so this technique is not suitable if we need to determine the accident dose lower than 300 mGy. On the other hand, EPR dosimetry with teeth has a lower dose detection limit (about 50 mGy), which is in a reasonable radiation dose range. However, its application is limited by the availability of samples for analysis, as a whole molar tooth sample is needed for the complete analysis of the absorbed dose using X-band CW EPR spectroscopy (Chumak, 2013).

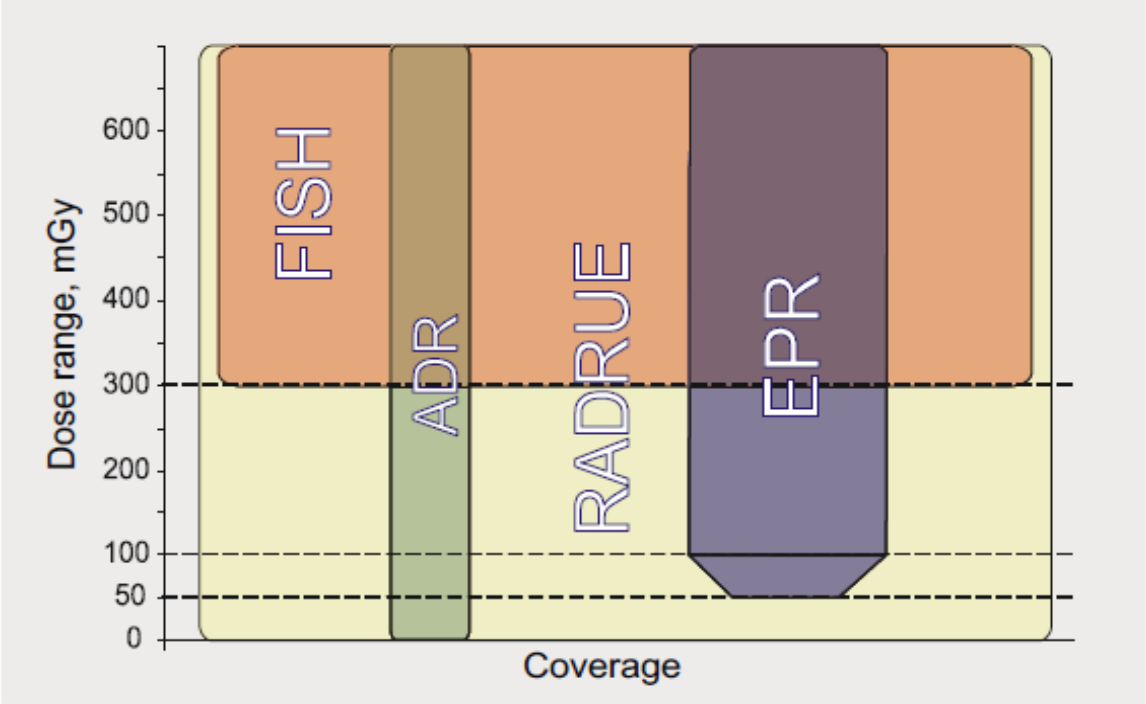


**Figure 2.8:** The plausible methodologies for the retrospective reconstruction of individual doses after nuclear or radiological accidents. From Chumak (2013).

To overcome these shortcomings from the FISH biodosimetry and EPR dosimetry with tooth enamel, a highly sensitive technique that requires about 2 mg sample for the complete dose reconstruction has been developed for accident and retrospective dosimetry. Since samples can be obtained through a mini-biopsy procedure, there is no need to extract teeth or wait for teeth samples until extraction for analysis. This emerging technology can make EPR tooth enamel dosimetry a versatile technique useful for accident and retrospective dosimetry (Romanyukha et al., 2007).

### 2.6.2 Accident or emergency dosimetry using EPR with tooth enamel

Tooth enamel EPR dosimetry has been applied to assess the accident doses in victims of the Chernobyl accident (Chumak et al., 1999; Chumak et al., 1996) and also assessed the radiation doses in children living in an area about 30–60 km from the Chernobyl reactor, in the Gomel State (Belarus) (Gualtieri et al., 2001). Furthermore, Krefft et al. (2014) used bones obtained from the

oncology patients to determine the absorbed dose during radiotherapy. In their study, the absorbed dose determined using EPR dosimetry in bones extracted within six months of radiotherapy was consistent with the delivered doses during the treatment. However, the doses determined 6 years after the treatment was 14% lower than the delivered doses. Also, this technique has been used to assess the radiation doses received in case of accidental overexposures at the Regional Cancer Center in Gdynia (Poland), as described by Trompier et al. (2007), where the authors estimated the absorbed dose due to an accidental overexposure in breast cancer patients using EPR dosimetry in rib bones. The doses determined in bones using EPR (i.e., by a dose additive method) were as high as 60-80 Gy, which means the patients were severely overexposed during the treatment due to a piece of defective equipment.

Similarly, on 11 December 1991, an accelerator operator at an industrial facility in Maryland (USA) was overexposed to radiation (3 MeV electron beam). An operator placed his hands, head, and feet in the radiation beam. After three months of the accident, four digits of the victim's right hand and most of the four digits of his left hand were amputated. EPR spectroscopy was used to determine the radiation dose in the victim's extremities, and the estimated doses ranged from 55.0 ± 4.7 Gy to 108 ± 24.1 Gy (Schauer et al., 1996). In another accident, a 42-y-old mechanics technician (at the time of the accident in 1995), who was untrained to handle a radiation source, accidentally touched the $^{60}$Co radiotherapy source, as shown in Figures 2.9a and 2.9b, with his right hand in November 1995. The activity of the source at the time of the accident was 55.5 TBq, and the estimated dose rate was 300 Gy min$^{-1}$ at 1 cm from the source. The victim was exposed for about 2 seconds. Four years after exposure (i.e., in 1999), the middle finger was amputated, and bones were obtained for a dose assessment from the middle finger. Their estimated dose using EPR was 6.4 ± 0.5 Gy; however, the dose estimation using biological dosimetry (i.e.,

Fluorescence in Situ Hybridization Method) was 20 ± 3 Gy. The considerable variability between the physical and biological dosimetry was not determined properly (Kinoshita et al., 2003). These studies concluded that the EPR dosimetry with tooth enamel and bones is an essential tool to assess the accident doses in radiological incidents and nuclear mass-casualty events.

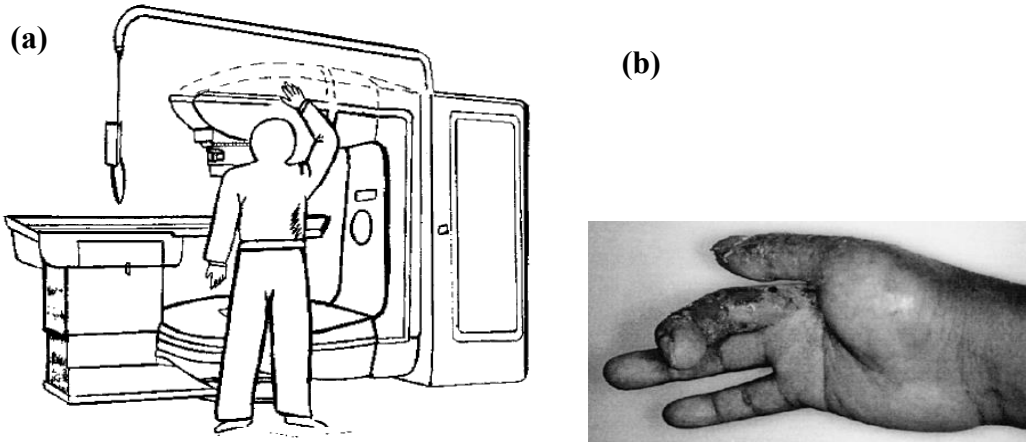


**Figure 2.9: (a)** The $^{60}$Co radiotherapy source and the accidental exposure to the right hand. **(b)** The victim's right-hand middle finger was amputated. From Kinoshita et al. (2003).

**2.7 EPR dosimetry using deciduous molar teeth**

Only a few studies have been conducted to estimate the retrospective and accident doses using deciduous molar teeth (El-Faramawy et al., 2006; Wieser and El-Faramawy, 2002; Haskell et al., 1999a; Skaleric et al., 1982; El-Faramawy, 2005). The typical EPR spectra obtained from deciduous tooth enamel exposed to gamma rays of 0.1, 0.5, 1, and 10 Gy are shown in Figure 2.11. The radiation-induced signals are identified using characteristic g-values ($g_{\perp}$=2.0019, $g_{\parallel}$ = 1.9973) of the $^{\bullet}CO_2^-$ radical anions generated by gamma rays in tooth enamel (El-Faramawy, 2005). The minimum absorbed dose measured in deciduous teeth using the X-band CW EPR was 100 mGy based on a limited number of incisors from one child (El-Faramawy and Wieser, 2006). However, many incisors from different children are needed to determine the detection thresholds

and dosimetric signals fading in deciduous teeth with proper sample storage (El-Faramawy and Wieser, 2006). To determine the dosimetric signal stability in deciduous molar teeth, El-Faramawy and Wieser (2006) estimated the absorbed doses in molar deciduous teeth using EPR. They did not find any signal variation within the first 40 days of sample irradiation (or fading before and after the irradiation process), as depicted in Figure 2.10. However, a decay of background signal within two weeks of irradiation was found, as shown in Figure 2.10. These results demonstrated that the EPR dosimetry with deciduous teeth is suitable for retrospective and accident dosimetry, the same as permanent teeth. Their lowest detection limit was 198 and 21 mGy using spectrum deconvolution software. Based on their results, two factors determined the detection limit in EPR dosimetry with deciduous tooth enamel: (1) complete removal of organic materials (i.e., dentin and other impurities); and (2) sample analysis after two weeks of sample preparation using chemical and mechanical separation techniques and the irradiation process.

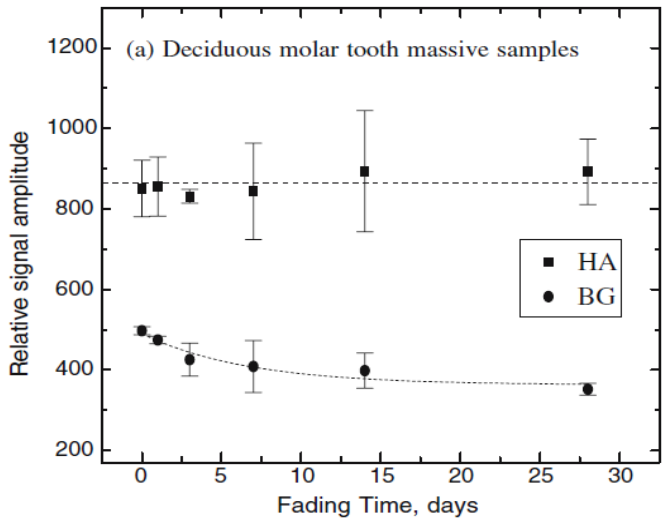


**Figure 2.10:** Dose stability in the deciduous molar teeth hydroxyapatite (HA) crystals (*squares*) and a decay of BGS (*circles*) within 2 weeks of irradiation. From El-Faramawy and Wieser (2006).

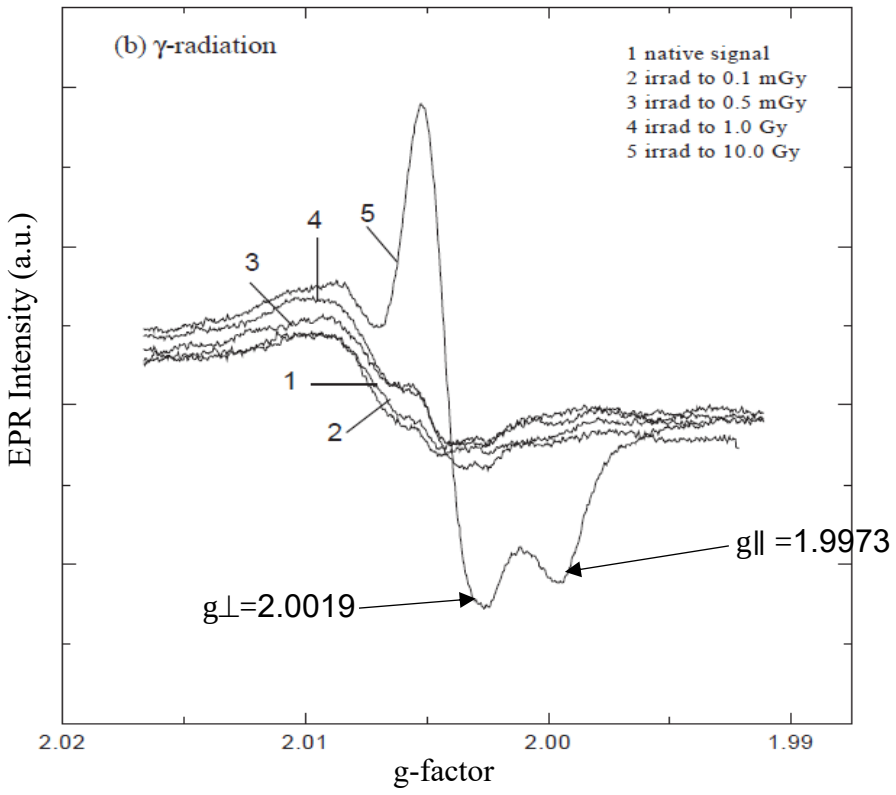


**Figure 2.11:** EPR spectra of deciduous teeth enamel irradiated at different doses (0.1 Gy, 0.5 Gy, 1 Gy, and 10 Gy. From El-Faramawy (2005).

**2.8 The Q-band EPR tooth enamel dosimetry**

As depicted in Figure 2.14, both X- and Q-bands CW EPR spectroscopy effectively measure retrospective or accident doses in tooth enamel. However, the application of these techniques depends on the availability of the sample, exposure scenarios, and the instruments. Several studies have demonstrated that the high-frequency Q-band EPR (34 GHz) in tooth enamel EPR dosimetry provided accurate measurements of radiation doses lower than 0.5 Gy using smaller samples or micro samples (~2 mg) (i.e., this is less than 0.5% of the total amount of tooth enamel in one molar tooth) because of their increased signal-to-noise ratios (SNRs) (Romanyukha et al., 2007; Guilarte et al., 2016; Romanyukha et al., 2014). However, the X-band requires much larger samples (~70-110 mg enamel) and can only measure precisely higher than 0.5 Gy. Because

below 0.5 Gy, the X-band cannot separate the radiation-induced EPR signal (RIS) from the background or native signals due to lower spectral resolution in conventional measurements. Therefore, the EPR tooth enamel dosimetry with the Q-band is ideal for environmental low-dose radiation research. The advantage of small sample sizes (~2mg) is very important for measuring the low doses in EPR dosimetry because the collected tooth samples which are extracted for medical reasons may be severely damaged by caries and other dental diseases and may have insufficient sound enamel for the X-band measurements (Romanyukha et al., 2007). Other materials, such as corals, mollusks, fish, etc., may also be benefitted from the small sample size, higher spectral resolution, and sensitivity offered by the Q-band resonators (Romanyukha et al., 2007; Guilarte et al., 2016).

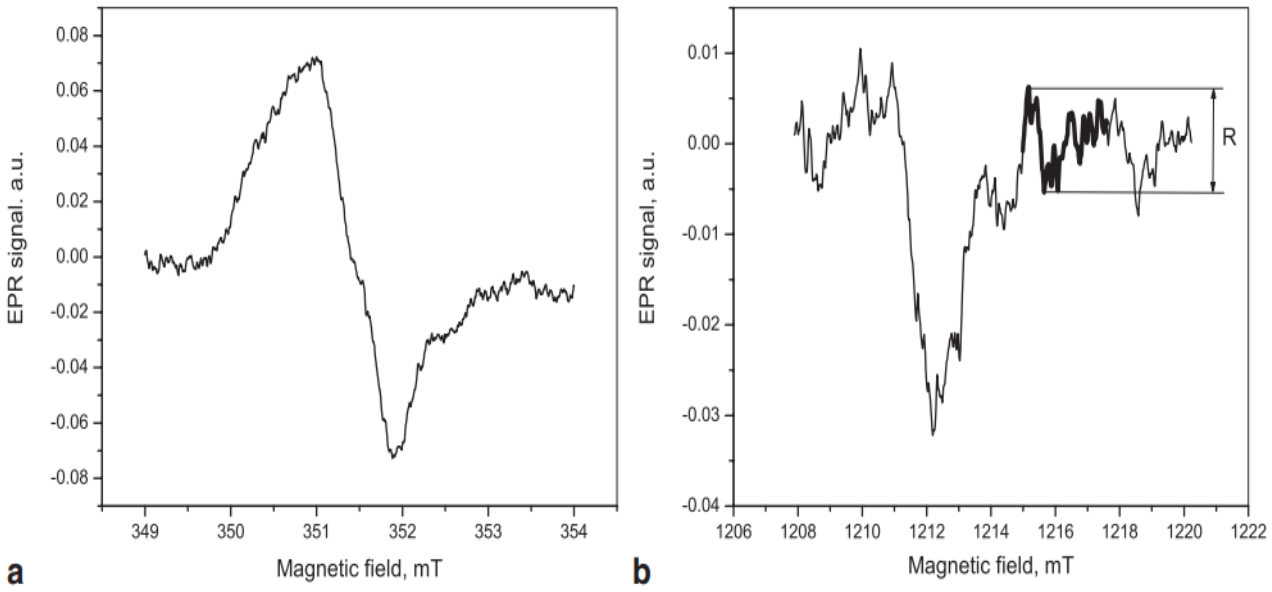


**Figure 2.12:** EPR spectra from a tooth enamel sample irradiated to 0.2 Gy measured in the X-band (a) and the Q-band EPR (b). The spectrum obtained from the Q-band is distinct (bold line) and clear; however, at the X-band EPR, the RIS is not distinct and measurable. R is the P2P amplitude height used to reconstruct the absorbed dose. From Romanyukha et al. (2007).

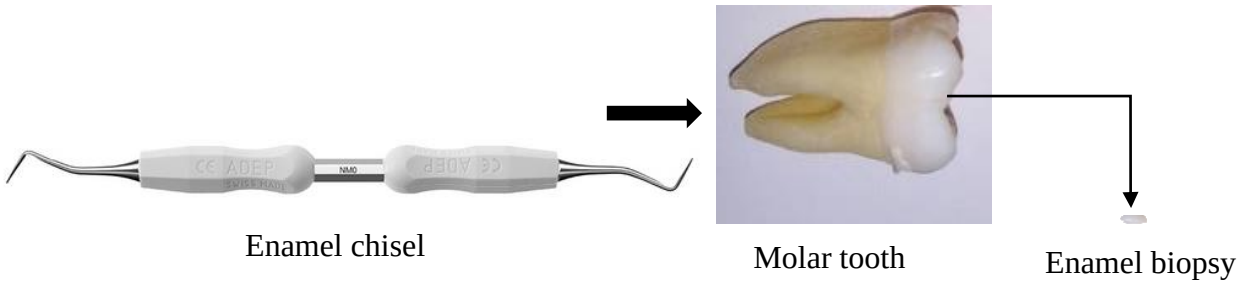


**Figure 2.13:** About 2 mg tooth enamel biopsy from a molar tooth using an enamel chisel.

The other essential advantages of Q-band EPR dosimetry for the low dose research (<100mGy) are: (1) It provides full resolution of the RISs from the native or background signals inherent to tooth enamel for doses below 0.5 Gy. As shown in Figure 2.12, the signal separation in the Q-band measurement makes dose-response measurements much easier than the conventional X-band EPR measurements, where EPR signals (i.e., dosimetric and native) overlap. Thus, the separation of the RIS in the Q-band spectra for doses below 0.5 Gy from other spectral components of tooth enamel makes dose-response measurements much easier and more precise than the conventional X-band measurements. As a result, the Q-band (34 GHz) EPR provides accurate measurements of low doses in tooth enamel and other samples (Romanyukha et al., 2007); (2) Additionally, the Q-band EPR requires tiny amounts of samples (~2mg), which can be easily obtained through biopsy, as depicted in Figure 2.13 in case of a nuclear accident or radiological accident (Romanyukha et al., 2014); (3) the Q-band offers a significant improvement in terms of sensitivity (~20 times), the minimum detection limit is about six times higher than the X-band CW EPR dosimetry (Romanyukha et al., 2014; Romanyukha et al., 2007; De et al., 2013; Guilarte et al., 2016); and (4) Tooth samples require time-consuming and labor-intensive chemical preparation for the X-band CW EPR measurements. However, the Q-band EPR has superior spectral resolution and sensitivity and does not require chemical treatments to purify samples. The use of untreated samples in the Q-band dosimetry of tooth enamel reduces the sample's impurities

and background signals in measurements, which improves the accuracy of dose measurements. Therefore, the Q-band EPR can be better suited for low-dose radiation dosimetry for emergency dosimetry and dose reconstruction for all targeted individuals in acute and chronic exposures or radiological accidents (De et al., 2013)

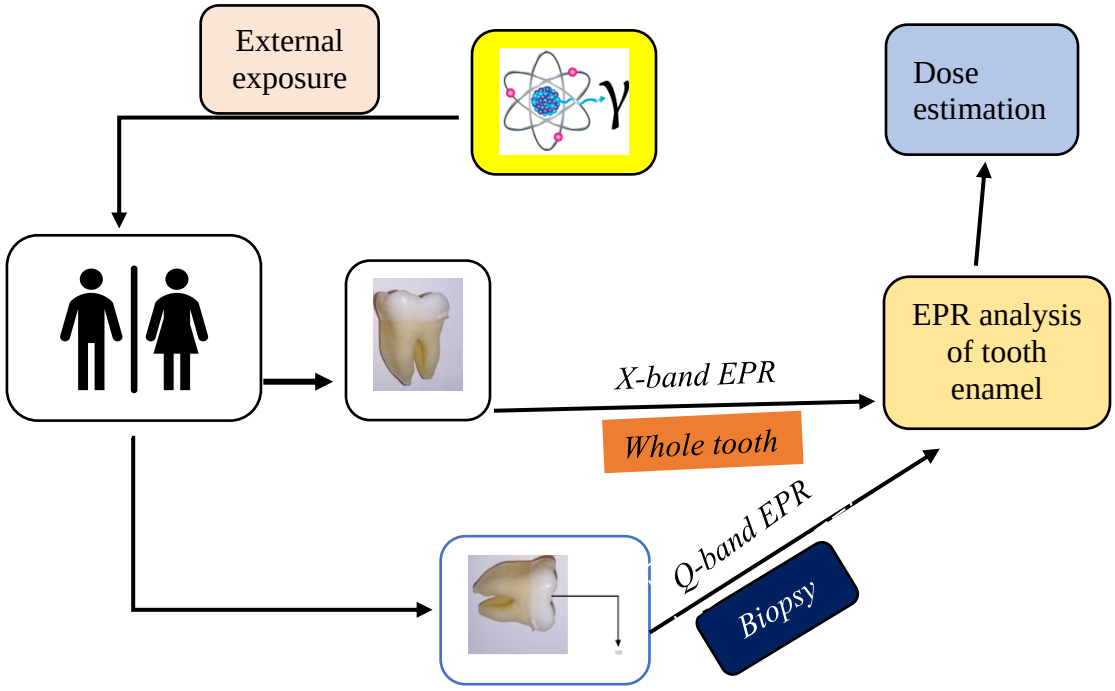


**Figure 2.14:** A conceptual model of EPR dose reconstruction from the external exposures using human tooth enamel or mini-biopsy enamel from a victim of radiation accidents.

However, the Q-band EPR has some disadvantages:

(1) A Q-band EPR spectrometer is very expensive, and it is only available in limited labs around the world;

(2) The Q-band is highly influenced by moisture or water content in a tooth enamel sample than the X-band CW EPR, which may decrease the inherent precision of EPR intensity measurements by the Q-band EPR. The sample moisture must be removed entirely from the sample to take the

benefit of the Q-band EPR high resolution and sensitivity for low dose retrospective and accident dosimetry.

**2.9 EPR dosimetry with tooth enamel in a mixed radiation field**

In case of a nuclear reactor accident or any other nuclear or radiological accident, external alpha (α) and beta (β) particles (rays) can not contribute to the absorbed dose in tooth enamel due to their low penetration depth, as depicted in Figure 2.15. Therefore, these radiations can not be measured for external exposures using tooth enamel. On the other hand, neutrons penetrate the tooth enamel and generate the $^{\bullet}CO_2^-$ radical anions that are the same as the photons (i.e., gamma rays) but with much less efficiency than gamma rays. These radicals ($^{\bullet}CO_2^-$) generate the same EPR spectrum with the same g-values ($g_{/\!/}$ = 1.9973, $g_{\perp}$ = 2.0023,) and the linewidths (0.4 mT, 0.3 mT) in EPR measurements. So, only by using the X-band CW EPR, it is almost impossible to estimate the neutron dose separately (Khan, 2003; Trompier et al., 2006). Additionally, since neutrons' interaction with matter is different from photons (gamma rays), the mechanism or tendency of the $^{\bullet}CO_2^-$ radical anions formation in tooth enamel by neutrons may be different. For example, if the neutron travels through tooth enamel, strikes with impurities, and initiates an (n, α) reaction, the emitted α particle will release its energy within an extremely short distance (i.e., a few microns). If the carbonate ions are not at that distance or on a path of the α particles, the energy released from the α particles may not produce the $^{\bullet}CO_2^-$ radical anions needed for the EPR signals. The neutron energy per unit surface area of tooth enamel greatly influences the neutron sensitivity of tooth enamel (Fattibene et al., 2010). Also, the impurities with a low or high cross-section to neutrons significantly change the response of dosimeters. Due to these reasons, different studies have found a relatively low neutron sensitivity of tooth enamel than photons (Khan, 2003; Fattibene et al., 2003; Fattibene et al., 2004a; Fattibene et al., 2004b; Zdravkova et al., 2003b).

Also, tooth enamel response to the high-LET radiation was lower than the X-rays and γ-rays. This was demonstrated by an EPR measurement of irradiated tooth enamel by carbon ions from medical irradiators (Yamaguchi et al., 2016).

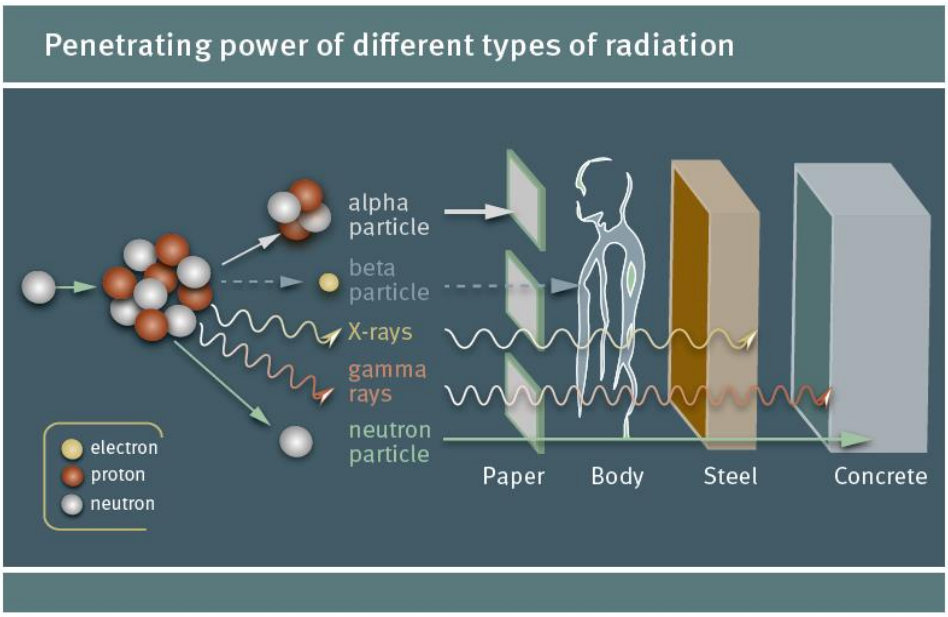


**Figure 2.15:** Different radiations have a different penetrating power. Alpha particles are highly ionizing and transfer more energy than beta and gamma but can be stopped by a sheet of paper. Beta particles can go through a centimeter or two of living tissues. Gamma rays and X-rays are highly penetrating and can go through a human body and a thick slab of steel. Neutrons are electrically neutral and the most penetrating of all the radiation. A material can absorb it with lots of hydrogen-like water, plastics, paraffin wax, etc. From UNEP (2016).

To provide a standardized protocol to evaluate the separate absorbed dose of neutrons and photons in tooth enamel retrospective dosimetry, ICRU published a report called the ICRU report 26 (ICRU, 1977). In the ICRU report 26 protocols, the tooth enamel and dentin sensitivities to photons and neutrons were investigated to differentiate the neutrons and photons components (i.e., mixed field). The estimated tooth enamel and dentin relative sensitivities were at 0.03± 0.02 and

0.14 ± 0.10 for fission neutrons (1keV–1MeV). Based on these results, the neutrons and photons doses were calculated in the nuclear reactor or radiological accidents with reasonable accuracy (Trompier et al., 2006).

## 2.10 **Conclusions**

The high stability of the radiation-induced radical anions ($^{\bullet}CO_2^-$) in enamel and its capacity to retain the memory of radiation doses for a long time without any disturbance makes tooth enamel an ideal material for retrospective and accident dosimetry studies (Hennig et al., 1981; IAEA, 2002; ICRU, 2002). The EPR dosimetric techniques are well developed and widely used by the dosimetry research community around the world for retrospective and accident dose assessment (IAEA, 2002; ICRU, 2002; Desrosiers and Schauer, 2001; Jacob et al., 2002; Bailiff et al., 2016; Fattibene and Callens, 2010). The reliability and validity of the EPR experimental protocols (i.e., sample preparation, instrumentation, dose determination and interpretation, uncertainty analysis, etc.) for the retrospective dosimetry and dose reconstruction have been verified through different international intercomparisons (Wieser et al., 2000; Wieser et al., 2005; Wieser et al., 2006). The ISO has published a sampling and data acquisition protocol to make this technique widely available, provide minimum acceptable criteria for retrospective dose reconstruction using EPR tooth enamel dosimetry, and facilitate the international intercomparisons of absorbed doses obtained at different laboratories for data accuracy, consistency, and reproducibility (ISO, 2013). Human teeth are the only tissue that can retain radiation doses for a long time and be measured at a low dose down to 30 mGy with high precision and accuracy using X-band CW EPR spectrometers.

However, besides the radiation of concern (e.g., gamma rays from an accident or nuclear power plant), human teeth may be exposed to radiation such as UV and medical X-rays, which

also contribute to the EPR spectrum, same as gamma photons. The EPR spectrum from other sources over or underestimates the absorbed dose in tooth enamel. For data precision and measurement accuracy, the dose contribution to tooth enamel from the UV, natural background, etc., needs to be removed as described in Chapter 3, Section 3.10.3 to determine the anthropogenic doses. Despite these advantages in EPR dosimetry with tooth enamel, one of the main problems of using the X-band CW EPR for dosimetry is to get the extracted tooth samples for reconstructing doses. The Q-band (34 GHz) EPR can be used to avoid these challenges. It requires minimal amounts of samples (~2 mg), which we can quickly obtain through a small biopsy of a tooth in case of a nuclear accident or radiological emergency. So, these techniques would make dose reconstruction much easier and faster for emergency dosimetry for all targeted individuals in both acute and chronic exposures. Thus, the Q-band EPR technique would be viable for low dose emergency and retrospective dosimetry (Romanyukha et al., 2007; Guilarte et al., 2016; Romanyukha et al., 2014; De et al., 2013). Still, both X- and Q-bands EPR retrospective and accident dosimetry techniques are equally important for dose reconstruction. They can be used based on the situations (i.e., availability of a whole tooth or small biopsy samples and instruments). Besides human teeth, animal teeth also can be a viable option for retrospective dosimetry and radiation protection of non-human species (Hassan et al., 2010; Toyoda et al., 2003; Jiao et al., 2014; Harshman and Johnson, 2019).

## 2.11 References

Ainsbury, E.A., Bakhanova, E., Barquinero, J.F., Brai, M., Chumak, V., Correcher, V. et al., 2011. Review of retrospective dosimetry techniques for external ionising radiation exposures. Radiat. Prot. Dosim. 147 (4), 573-592.

Baffa, O., Kinoshita, A., Chen Abregoa, F., Silva, N.A., 2002. ESR and NMR dosimetry. In: Kawamori, A., Yamauchi, J., Ohta, H. (Eds.), EPR in the 21" Century: Basics and applications to material, life and earth sciences. Elsevier Science B.V., pp. 614-623.

Bailiff, I.K., Sholom, S., McKeever, S.W.S., 2016. Retrospective and emergency dosimetry in response to radiological incidents and nuclear mass-casualty events: A review. Radiat. Meas. 94, 83-139.

Bailiff, I.K., Stepanenko, V.F., Goksu, H.Y., Jungner, H., Balmukhanov, S.B., Balmukhanov, et al., 2004. The application of retrospective dosimetry in areas affected by fallout from the Semipalatinsk Nuclear Test Site: an evaluation of potential. Health Phys. 87, 625-641.

Bhat, M., 2005. EPR tooth enamel as a tool for validation of retrospective doses: an end-user perspective. Appl. Radiat. Isot. 62,155-161.

Brady, J.M., Aarestad, N.O., Swartz, H.M., 1968. In vivo dosimetry by electron spin resonance spectroscopy. Med. Phys. 15, 43 - 47.

Brustolon, M., Giamello, E., (Eds.). 2009. Electron paramagnetic resonance, a practitioner's toolkit. John Wiley & Sons, Inc., Hoboken, New Jersey.

Callens, F., Vanhaelewyn, G., Matthys, P., 2002. Some recent multi-frequency electron paramagnetic resonance results on systems relevant for dosimetry and dating. Spectrochim. Acta Part A 58, 1321–1328.

Chumak, V., Likhtarev I., Sholom S., Meckbach R., Krjuchkov V., 1998. Chernobyl experience in field of retrospective dosimetry: reconstruction of doses to the population and liquidators involved in the accident. Radiat. Prot. Dos. 77, 91–95.

Chumak, V., Sholom, S., Pasalkaya, L., 1999. Application of high precision EPR dosimetry with teeth for reconstruction of doses to Chernobyl populations. Radiat. Prot. Dosim. 84, 515–520.

Chumak, V.V., Sholom, S.V., Likhtarev, I.A., 1996. Some results of retrospective dose reconstruction for selected groups of exposed population in Ukraine. In: The Radiological Consequences of the Chernobyl Accident. Report EUR 16544 EN, European Commission, Brussels, 1059–1062.

Chumak, V.V., 2013. Retrospective dosimetry of populations exposed to reactor accident: Chernobyl example, lesson for Fukushima. Radiat. Meas. 55, 3-11.

Cole, T., Silver, A.H., 1963. Production of hydrogen atom in teeth by X-ray irradiation. Nature 20022: 700-701.

De, T., Romanyukha, A., Trompier, F., Pass, B., Misra, P., 2013. Feasibility of Q-Band EPR Dosimetry in Biopsy Samples of Dental Enamel, Dentine and Bone. Appl. Magn. Reson. 44, 375–387.

Degteva, M.O., Shagina, N.B., Shishkina, E.A., Vozilova, A.V., Volchkova, A.Y., Vorobiova, et al., 2015. Analysis of EPR and FISH studies of radiation doses in persons who lived in the upper reaches of the Techa River. Radiat. Environ. Biophys. 54 (4), 433-444.

Desrosiers, M., Schauer, D.A., 2001. Electron paramagnetic resonance (EPR) biodosimetry. Nucl. Instr. and Meth. in Phys. Res. B. 184, 219-228.

Demidenko, E., Williams, B.B., Sucheta, A., Dong, R., Swartz, H.M., 2007. Radiation dose reconstruction from L-band in vivo EPR spectroscopy of intact teeth: comparison of methods. Radiat. Meas. 42 (6–7), 1089–1093.

Driessens, F.C.M., Verbeeck, R.M.H., 1990. Biominerals. CRC Press, Boca Raton, ISBN: 0-8493-5280-0, 428 pp.

Duin, E., 2013. Electron Paramagnetic Resonance Theory. Chemistry. Assessed at http://webhome.auburn.edu/~duinedu/epr/1_theory.pdf

Egersdorfer, S., Wieser, A., Muller, A., 1996. Tooth enamel as a detector material for retrospective EPR dosimetry. Appl. Radiat. Isot. 47(11–12), 1299–1303.

Elliott, J.C., 1994. Structure and Chemistry of the Apatites and other Calcium Orthophosphates. Elsevier, Amsterdam, ISBN: 0-444-81582-1, 387 pp.

El-Faramawy, N., Wieser, A., 2006. The use of deciduous molars in EPR dose reconstruction. Radiat. Environ. Biophys. 44, 273–277.

El-Faramawy, N.A., El-Somany, I., Mansour, A., Maghraby, A.M., Eissa, H., and Wieser, A., 2018. Camel molar tooth enamel response to gamma rays using EPR spectroscopy. Radiat. Environ. Biophys. 57, 63-68.

El-Faramawy, N.A., 2005. Comparison of g- and UV-light-induced EPR spectra of enamel from deciduous molar teeth. Appl. Radiat. Isot. 62, 191-195.

Fattibene, P., Angelone, M., De Coste, V., Pillon, M., 2004a. Dosimetric response of tooth enamel to14 MeV neutrons. Radiat. Environ. Biophys. 43(2), 85–90.

Fattibene, P., Angelone, M., Pillon, M., De Coste, V., 2004b. In phantom dosimetric response of tooth enamel to neutrons. Radiat. Prot. Dosim. 110,559–563.

Fattibene, P., Angelone, M., Pillon, M., De Coste, V., 2003. Tooth enamel dosimetric response to 2.8 MeV neutrons. Nucl. Instrum. Meth. B 201, 480–490.

Fattibene, P., Callens, F., 2010. EPR dosimetry with tooth enamel: A review. Appl. Radiat. Isot. 68, 2033-2116.

Fattibene, P., Wieser, A., Adolfsson, E., Benevides, L.A., Brai, M., Callens, F., et al., 2011. The 4th international comparison on EPR dosimetry with tooth enamel. Part 1: report on the results. Radiat. Meas. 46:765–771.

Godfrey-Smith, D.I., 2008. Towards in vivo OSL dosimetry of human tooth enamel. Radiat. Meas. 45, 854-858.

Gordy, W., Aard, W.B., Shields, H., 1955. Microwave spectroscopy of biological substances. Paramagnetic resonance in x-irradiated amino acids and proteins. Proc. Natl. Acad. Sci. USA 41, 983–996.

Guilarte, V., Trompier, F., Duval, M., 2016. Evaluating the potential of Q-band ESR spectroscopy for dose reconstruction of fossil tooth enamel. PLoS ONE 11(3): e0150346. doi: 10.1371/journal.pone.0150346.

Gualtieri, G., Colacicchi, S., Sgattoni, R., Giannoni, M., 2001. The Chernobyl accident: EPR dosimetry on dental enamel of children. Appl. Radiat. Isot. 55, 71–79.

Harshman, A., Johnson, T., 2019. Dose reconstruction using electron paramagnetic resonance dosimetry of tooth enamel from wild boar living in the Fukushima exclusion zone. Health Phys. 116 (6), 779 – 806.

Hayes, R.H., Kenner, G.H., Haskell, E.H., 1998. EPR Dosimetry of Pacific Walrus (Odonebus Rosmarus Divergens) Teeth. Radiat. Prot. Dosim. 77, 55–63.

Hayes, R.H., Haskell, E.H., Romanyukha, A.A., Kenner, G. H., 1998. A technique for increasing reproducibility in EPR dosimetry of tooth enamel. Meas. Sci. Technol. 9, 1994–2006.

Hassan, G.M., Alboelezz, E., El-Khodary, A., Eissa, H.M., 2010. Inter-comparison study between human and cow teeth enamel for low dose measurement using ESR. Nucl. Instrum. Methods Phys. Res. B. 268, 2329-2336.

Haskell, E.D., Hayes, R.B., Kenner, G.H., 1999a. An EPR dosimetry method for rapid scanning of children following a radiation accident using deciduous teeth. Health Phys. 76, 137–144.

Haskell, E.H., Hayes, R.B., Kenner, G.H., Wieser, A., Aragno, D., Fattibene, P., Onori, S., 1999b. Achievable precision and accuracy in EPR dosimetry of tooth enamel. Radiat. Prot. Dosim. 84, 527–535.

Haskell, E.H., Hayes, R.B., Kenner, G.H., 1997. Improved accuracy of EPR dosimetry using a constant rotation goniometer. Radiat. Meas.27, 325–329.

ISO, 2013. Radiological protection – Minimum criteria for electron paramagnetic resonance (EPR) spectroscopy for retrospective dosimetry of ionizing radiation – Part 1: General principles, International Standard, ISO 13304-1.

ICRP, 2003. ICRP Publication 91: A framework for assessing the impact of ionizing radiation of non-human species. Ann. ICRP 33, 201–266.

ICRU, 1977. Neutron Dosimetry for Biology and Medicine. ICRU Report 26. International Commission on Radiation Units and Measurements, Washington, ISBN: 0-913394-20-3, 128 pp.

ICRU, 2002. Retrospective Assessment of Exposures to Ionising Radiation. International Commission on Radiation Units and Measurements. International Commission on Radiation Units and Measurements, Bethesda, USA. ICRU Report 68.

Ikeya, M., Miyajima, J., Okajima, S., 1984. ESR dosimetry for atomic bomb survivors using shell buttons and tooth enamel. Jpn. J. Appl. Phys. 23, 697–699.

Ikeya, M., 1993. New Application of Electron Spin Resonance - Dating, Dosimetry and Microscopy. Word Scientific, Singapore.

Jacob, P., Goksu, Y., Meckbach, R., Wieser, A., 2002. Retrospective dosimetry for external exposures. International Congress Series. 1225, 141-148.

Jiao, L, Liu, Z.C., Ding, Y.Q., Ruan, S.Z., Wu, Q., Fan, S.J., Zhang, W.Y., 2014. Comparison study of tooth enamel ESR spectra of cows, goats and humans. J. Radiat. Res. 55, 1101-1106.

Khan, F.H., 2003. Electron paramagnetic resonance biophysical dosimetry with tooth enamel. PhD thesis, McMaster University, Hamilton, Canada.

Kinoshita, A., Guzman, C., Sandra, C., Sakamoto-Hojo, E., Camparato, M.L., Picon, C., Baffa, O., 2003. Evaluation of a high dose to a finger from a $^{60}$Co accident. Health Phys. 84, 477-482.

Kleinerman, R.A., Romanyukha, A.A., Schauer, D.A., Tucker, J.D., 2006. Retrospective assessment of radiation exposure using biological dosimetry: Chromosome painting, electron paramagnetic resonance and the glycophorin a mutation assay. Radiat. Res. 166 (1, Part 2), 287–302.

Krefft, K., Drogoszewska, B., Kaminska, J., Juniewicz, M., Wołakiewicz, G., Jakacka, I., Ciesielski, B., 2014. Application of EPR dosimetry in bone for ex vivo measurements of doses in radiotherapy patients. Radiat. Prot. Dosim. 162, 38-42.

Lund, A., Shiotani, M., Shimada, S., 2011. Principles and Applications of ESR Spectroscopy. Springer Science+Business Media B.V.

Mesterhazy, D., Osvay, M., Kova´, A., Kelemen, A., 2011. Accidental and retrospective dosimetry using TL method. Radiat. Phys. Chem. 81, 1525–1527.

Mitchell, B.S., 2004. An introduction to materials engineering and science: For chemical and materials engineers. John Wiley & Sons, Inc., Hoboken, New Jersey.

Nakamura, N., Miyazawa, C., Akiyama, M., Sawada, S., Awa, A.A., 1998. A close correlation between electron spin resonance (ESR) dosimetry from tooth enamel and cytogenetic dosimetry from lymphocytes of Hiroshima atomic- bomb survivors. Int. J. Radiat. Biol. 73, 619–627.

Pivovarov, S., Rukhin, A., Seredavina, T., Zhdanov, A., 2002. Retrospective EPR dosimetry in Semipalatinsk nuclear test site region. In: Kawamori, A., Yamauchi, J., Ohta, H. (Eds.), EPR in the 21st Century: Basics and Applications to Material, Life and Earth Sciences, Proceedings of the Third Asia Pacific EPR/ESR Symposium. Kobe, Japan, pp. 634-639.

Rudko, V.V., Vorona, I.P., Baran, N.P., Ishchenko, S.S., Zatovsky, I.V., Chumakova, L.S., 2010. The mechanism of $CO_2^-$ radical formation in biological and synthetic apatites. Health Phys. 98, 322-326.

Romanyukha, A.A., Regulla, D., Vasilenko, E., Wieser, A., 1994. South Ural nuclear workers: comparison of individual doses from retrospective EPR dosimetry and operational personal monitoring. Appl. Radiat. Isot. 45, 1195-1199.

Romanyukha, A.A., Ignatiev, E.A., Vasilenko, E.K., Drozhko, E.G., Wieser, A., Jacob, P., et al., 2000. EPR dose reconstruction for Russian nuclear workers. Health Phys. 78, 15–20.

Romanyukha, A.A., Schauer, D.A., 2002. EPR dose reconstruction in teeth: Fundamentals, applications, problems, and perspectives. In: Kawamori, A., Yamauchi, J., Ohta, H. (Eds.), EPR in the 21" Century: Basics and applications to material, life and earth sciences. Elsevier Science B.V., pp. 603-612.

Romanyukha, A., Francois Trompier, F., Reyes, R.A., 2014. Q-band electron paramagnetic resonance dosimetry in tooth enamel: biopsy procedure and determination of dose detection limit. Radiat. Environ. Biophys. 53, 305–310.

Romanyukha, A., Mitchell, C.A., Schauer, D.A., Romanyukha, L., Swartz, H.M., 2007. Q-band EPR biodosimetry in tooth enamel microsamples: feasibility and comparison with X-band. Health Phys. 93 (6), 631-635.

Salikhov, I., Hirata, H., Walczak, T., Swartz, H.M., 2003. An improved external loop resonator for in vivo L-band EPR spectroscopy. J. Magn. Reson. 64 (1), 54–59.

Schauer, D.A., Iwasaki, A., Romanyukha, A.A., Swartz, H.M., Onori, S., 2007. Electron paramagnetic resonance (EPR) in medical dosimetry. Radiat. Meas. 41, 117-123.

Schauer, D.A., Coursey, B.M., Dick, C.E., McLaughlin, W.L., Puhl, J.M., Desrosiers, M.F., et al., 1996. A radiation accident at an industrial accelerator facility. Health Phys. 65(2), 131-140.

Shishkina, E.A., Shved, V.A., Degteva, M.O., Tolstykh, E.I., Ivanov, D.V., Bayankin, S.N., et al., 2003. Issues in the validation of external dose: Background and internal dose components of cumulative dose estimated using the electron paramagnetic resonance (EPR) method. Final Report for Milestone 7, Part 1. US–Russian Joint Coordinating Committee on Radiation Effects Research. Project 1.1., 67 pp.

Skaleric, U., Ravnik, C., Cevc, P., Schara, M., 1982. Microcrystal arrangement in human deciduous dental enamel studied by electron paramagnetic resonance. Caries Res. 16, 47–50.

Sholom, S.V., Chumak, V.V., 2005. Variability of parameters in retrospective EPR dosimetry with teeth for Ukrainian population. Appl. Radiat. Isot. 62(2), 201–206.

Shishkina, E.A., Volchkova, A., Timofeev, Y.S., Fattibene, P., Wieser, A., Ivanov, D.V. et al., 2016. External dose reconstruction in tooth enamel of Techa riverside residents. Radiat. Environ. Biophys. 55:477–499.

Swartz, H.M., 1965. Long-lived electron spin resonance in rats irradiated at room temperature. Radiat. Red. 24, 579-58.

Tatsumi-Miyajima, J., Okajima, S., 1991. Physical dosimetry at Nagasaki—Eur-opium-152 of stone embankment and electron spin resonance of teeth from atomic bomb survivors. J. Radiat. Res. (Tokyo), Suppl. 83–98.

Takahashi, F., Yamaguchi, Y., Iwasaki, M., Miyazawa, C., Hamada, T., 2001. Relations between tooth enamel dose and organ doses for electron spin resonance dosimetry against external photon exposure. Radiat. Prot. Dosim. 95 (2), 101-108.

Trompier, F., Sadlo, J., Michalik, J. W., Mazal, A., Clairand, I., Rostkowska, J., et al., 2007. EPR dosimetry for actual and suspected overexposures during radiotherapy treatments in Poland. Radiat. Meas. 42, 1025-1028.

Trompier, F., Tikunov, D.D., Ivannikov, A., Clairand, I., 2006. ESR investigation of joint use of dentin and tooth enamel to estimate photon and neutron dose components of a mixed field. Radiat. Prot. Dosim. 120 (1–4), 191–196.

Toyoda, S., Tanizawa, H., Romanyukha, A.A., Miyazawa, C., Hoshi, M., Ueda, Y., et al., 2003. Gamma-ray dose response of ESR signals in tooth enamel of cows and mice in comparison with human teeth. Radiat. Meas. 37, 341-346.

Ishii, H., Ikeya, M., Okano, M., 1990. ESR dosimetry of teeth of residents close to Chernobyl reactor accident. J. Nucl. Sci. Technol. 27, 1153–1155.

Ivannikov, A.I., Zhumadilov, Zh, Gusev, B.I., Miyazawa, Ch, Jiao, L., Skvortsov, V.G., et al., 2002. Individual dose reconstruction among residents living in the vicinity of the Semipalatinsk Nuclear Test Site using EPR spectroscopy of tooth enamel. Health Phys. 83, 183-196.

Ivannikov, A.I., Skvortsov, V.G., Stepanenko, V.F., Tikunov, Tsyb, A. F., Khamidova, L.G., 2000. Tooth enamel EPR dosimetry: sources of errors and their correction. Appl. Radiat. Isot. 52, 1291-1296.

Ivannikov, A.I., Tikunov, D.D., Skvortsov, V.G., Stepanenko, V.F., Khomichyonok, V.V., Khamidova, L.G., et al., 2001. Elimination of the background signal in tooth enamel samples for EPR-dosimetry by means of physical–chemical treatment. Appl. Radiat. Isot. 55, 701–705.

Scientific Committee on the Effects of Atomic Radiation, UNSCEAR, 2012. Sources, Effects and Risks of Ionizing Radiation, Scientific Annexes A and B, United Nations.

Vugman, N.V., Rossi, A.M., Rigby, S.E., 1995. EPR dating $CO_2^-$ sites in tooth enamel apatites by ENDOR and triple resonance. Appl. Radiat. Isot. 46 (5), 311–315.

Wieser, A., Mehta, K., Amira, S., Aragno, D., Bercea, S., Brik, A., et al., 2000. The 2nd international intercomparison on EPR tooth dosimetry. Radiat. Meas. 32, 549-557.

Wieser, A., El-Faramawy, N., 2002. Dose reconstruction with electron paramagnetic resonance spectroscopy of deciduous teeth. Radiat. Prot. Dosim.101 (1–4), 545–548.

Wieser, A., Romanyukha, A., Degteva, M., Kozheurov, V., Petzoldt, G., 1996. Tooth enamel as a natural beta dosimeter for bone seeking radionuclides. Radiat. Prot. Dosim.65, 413–416.

Wieser, A., Debuyst, R., Fattibene, P., Meghzifene, A., Onori, S., Bayankin, S.N., et al., 2005. The 3rd international intercomparison on EPR tooth dosimetry: Part 1, general analysis. Appl. Radiat. Isot. 62, 163-171.

Wieser, A., Debuyst, R., Fattibene, P., Meghzifene, A., Onori, S., Bayankin, S.N., et al., 2006. The 3rd international intercomparison on EPR tooth dosimetry: part 2, final analysis. Radiat. Prot. Dosim. 120, 176-183.

Wieser, A., Fattibene, P., Shishkina, E.A., Ivanov, D.V., DeCoste, V., Guttler, A., Onori, S., 2008. Assessment of performance parameters for EPR dosimetry with tooth enamel. Radiat. Meas. 43(2–6), 731–736.

Yamaguchi, I., Sato, H., Kawamura, H., Hamano, T., Yoshii, H., Suda, M., Miyake, M., Kunugita, N., 2016. L-band EPR tooth dosimetry for heavy ion irradiation. Radiat. Prot. Dosim., 172, 81-86.

Young, R.W., Kerr, G.D. (Eds.), 2005. Reassessment of the Atomic Bomb Dosimetry for Hiroshima and Nagasaki - Dosimetry System 2002 (DS02). Radiation Effects Research Foundation, Hiroshima.

Zdravkova, M., Wieser, A., El-Faramawy, N., Ivanov, D., Gallez, B., Debuyst, R., 2003a. An in vitro L-band EPR study with whole human teeth in a surface-coil resonator. Radiat. Meas. 37, 347–353.

Zdravkova, M., Crokart, N., Trompier, F., Asselineau, B., Gallez, B., Gaillard-Lecanu, E., et al., 2003b. Retrospective dosimetry after criticality accidents using low frequency EPR: a study on whole human teeth irradiated in a mixed neutron and gamma radiation field. Radiat. Res. 160, 168–173.

Zhumadilov, K., Ivannikov, A., Apsalikov, K., Zhumadilov, Zh, Zharlyganova, D., Stepanenko, et al., 2007. Results of tooth enamel EPR dosimetry for population living in the vicinity of the Semipalatinsk nuclear test site. Radiat. Meas. 42, 1049-1052.

Zhumadilov, K., Ivannikov, A., Stepanenko, V., Zharlyganova, D., Toyoda, S., Zhumadilov, Z., et al., 2013. ESR dosimetry study of population in the vicinity of the Semipalatinsk Nuclear Test Site. J. Rad. Res. 54, 775-779.

Zhumadilov, K., Ivannikov, A., Apsalikov, K.N., Zhumadilov, Zh, Toyoda, S., Zharlyganova, D., et al., 2006. Radiation dose estimation by tooth enamel EPR dosimetry for residents of Dolon and Bodene. J. Radiat. Res. 47, A47-A53.

Zdravkova, M., Wieser, A., El-Faramawy, N., Ivanov, D., Gallez, B., Debuyst, R., 2003. An in vitro L-band EPR study with whole human teeth in a surface-coil resonator. Radiat. Meas. 37, 347–353.

# Chapter 3

# Methodology and Instrumentation for EPR Dosimetry with Tooth Enamel

## 3.1 Collection and preparation of pure enamel samples

### 3.1.1 Confidentiality and ethical considerations for collecting tooth samples

The research that involves the human tissue (i.e., teeth) must obtain the research ethics approval from the university's Research Ethics Board (REB). This research got ethics approval from the Ontario Tech University Research Ethics Board (REB) to collect the extracted tooth samples from Durham Region, Ontario. The local dentists and residents were invited to participate in this research. The extracted teeth were collected anonymously using a code number for each sample. The collected samples were kept in a special locked container. The container was transported to Ontario Tech University and was kept in a cabinet in the lab at Ontario Tech (ERC Lab # 3092).

### 3.1.2 Laboratory safety requirements

During the sample preparation and experiment, the safety precautions must be taken from the magnetic field, electromagnetic frequency, and biohazards from the samples. The conventional X-band CW EPR spectrometer with a g-factor near 2.0 and the magnetic field 350 mT and the Q-band 1200 mT have no biological hazards; however, it can affect watches, credit cards, and pacemakers if they are brought very close to the magnetic field. In terms of the electromagnetic frequency, in vitro measurement, the microwave cavity is fully enclosed, so there is no possibility of leaking microwave radiation in significant amounts to harm the operators. However, the samples

collected from the dental clinics may be contaminated with bacteria and viruses, so these samples must be thoroughly decontaminated before preparing samples for analyses (ISO, 2013).

### 3.1.3 **Tooth sample collection, transportation, sterilization, and storage**

All samples were collected uniformly, and the circumstances of the collection, such as a sample holder, integrity of the samples, sample temperature and UV light, etc., were noted, and the sample location was recorded. All samples were given a unique code to maintain strict confidentiality and anonymity. The collected samples were transported and stored correctly as the transportation and storage may affect the integrity of the samples and change the concentration of the paramagnetic species in the samples (ISO, 2013). Other factors such as UV, X-rays, gamma rays, temperature, humidity, oxygen, sample moisture, disinfectant solution, and dust may affect the quality and quantity of free radicals in tooth enamel. Therefore, special attention was given to avoiding the possible impact of these environmental parameters on the collected tooth samples (ISO, 2013).

Tooth sample location in the mouth, health, and age are critical points to consider for collecting tooth samples for EPR dosimetry. Not all collected tooth samples from the dental clinics are equally suitable for retrospective dosimetry. The unhealthy teeth (i.e., carious teeth) with a minimal amount of sound enamel are unsuitable for dose reconstruction (Fattibene and Callens, 2010). Therefore, only healthy teeth with sufficient enamel were collected from the dental clinics for analysis. Furthermore, if available, only teeth from the inner mouth (i.e., molars and premolars) were collected and analyzed due to UV exposures in the front teeth.

### 3.1.4 **Processing the material**

Extracted teeth were considered infectious; therefore, gloves and safety glasses were worn when touching the samples. The dental material was sterilized by keeping teeth samples in about

5% sodium hypochlorite (NaOCl) for 24 hours. The safe handling of extracted teeth requires methods for antimicrobial and antiviral control. That is why the tooth sample was placed in formalin ($CH_2O$) for infection (bacterial and viral) control purposes, and then the teeth samples were rinsed and stored in a sealed glass vial (in a dark room) until further preparation. All sample preparation and processing were done in a fume-hood in the ERC 3092 lab to minimize inhalation exposures to hazardous chemicals or biological agents (IAEA, 2002; Fattibene and Callens, 2010).

### 3.1.5 **Separation of the crown from a root**

A thin layer of enamel covers the tooth crown, the root part is covered by cementum, and the internal parts of a tooth are dentin and pulp, as depicted in Figure 3.1. Since enamel is present only in the crown, as shown in Figure 3.1, the second most crucial step in sample preparation is to separate the crown from the root. The power-driven steel-wheel saw, or a mini aluminum saw as depicted in Figure 3.4c, was used. However, during the separation by using these saws, the sample was cooled with water to avoid overheating the sample due to friction between the wheel and the crown (Kirillov et al., 2002). Then a crown was cut into buccal and lingual halves, as shown in Figure 3.2; only lingual halves were used to minimize errors from UV exposures (Chumak et al., 2006; Fattibene and Callens, 2010). Before separating enamel from dentin, the crown was cleaned with a 0.1 M Ethylenediaminetetraacetic Acid Disodium Salt EDTA$Na_2$) solution to remove any metallic impurities (IAEA, 2002).

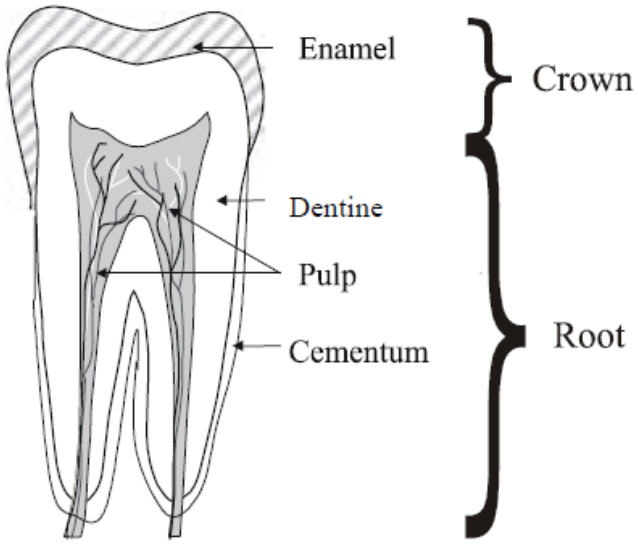


**Figure 3.1:** Anatomy of a tooth shows tooth tissue locations, enamel, dentine, pulp, and cementum. From IAEA (2002).

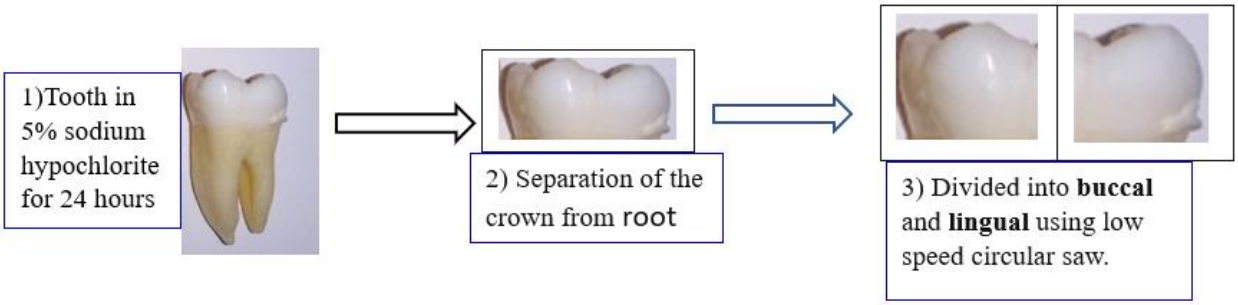


**Figure 3.2:** A tooth is divided into buccal and lingual halves.

### 3.1.4 Separation of enamel from dentin

The main goal of sample preparation is to separate the tooth enamel from the dentin. The residue of dentin and organic materials in enamel provide the BGSs and other unwanted signals (also called noises) along with the RISs, as shown in Chapter 2 (Figure 2.7). The background signals can be challenging to separate from the RIS for spectra interpretation. So, these materials need to separate from tooth enamel to get a clear signal. There are two methods to separate the enamel from dentin: (1) chemical separation; and (2) mechanical separation. In chemical separation, the whole crown is immersed into the solution of 5M potassium hydroxide (KOH) solution for 16 h in an ultrasonic bath at temperature up to 60°C, which dissolves the dentin and other organic matter, and the pure enamel is obtained (Fattibene and Callens, 2010; IAEA, 2002). As shown in Figure 3.3, the chemical separation of dentin makes the RIS clear and visible compared without a chemical treatment (Romanyukha et al., 2000a). In mechanical separation, the drill separates the enamel from the dentin. The drill should be hard alloy to avoid metal contamination in a tooth sample (IAEA, 2002). However, precautions should be taken to avoid overheating the enamel by using water cooling; heating generates new signals in the EPR spectra. However, the dental drill's speed does not affect spectra (Romanyukha et al., 2000a, 2000b, 2000c; Fattibene and Callens, 2010; IAEA, 2002). Also, the UV lamp (365 nm UV) and microscopy techniques can be used to locate any remaining dentin on tooth enamel for manual removal (IAEA, 2002). Chemical and mechanical methods have proven more effective than one technique (Ivannikov et al., 2001).

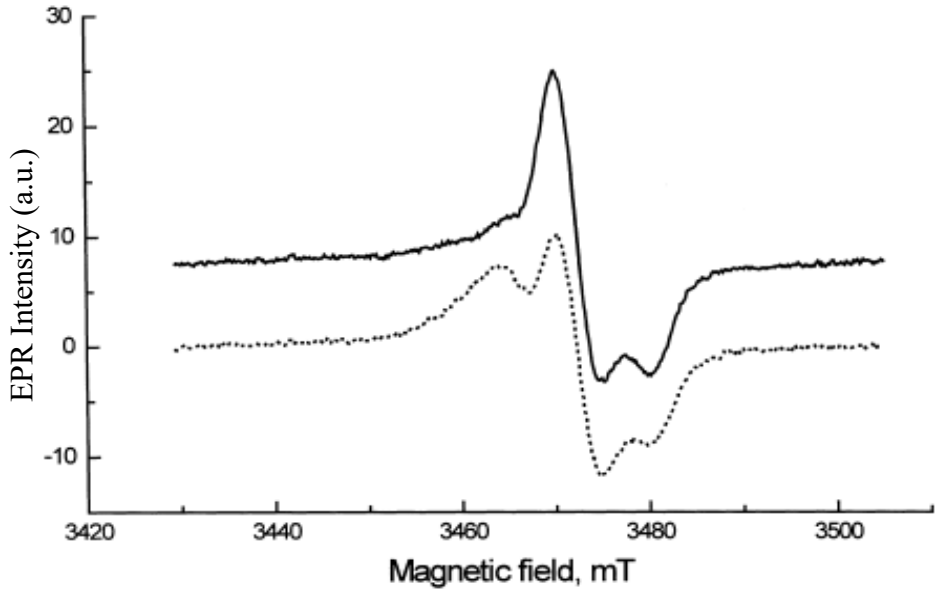


**Figure 3.3:** Effects of the organic matter on the tooth enamel EPR spectrum. The upper spectrum (solid line) in the figure is from the sample prepared by the ultrasonic treatment of tooth enamel with a 5M potassium hydroxide solution for 70 h at 60°C. The lower spectrum (dotted line) is from the sample prepared without chemical treatment. Both samples were prepared from the same tooth exposed to 2.5 Gy from a $^{60}$Co source. From Romanyukha et al. (2000a).

### 3.1.5 Tooth enamel grinding or cutting

The tooth enamel is usually ground manually by a mortar and pestle or cut into small pieces using pliers, as shown in Figures 3.4a, 3.4b, and 3.4c. (IAEA, 2002; Zhumadilov et al., 2005). Grains of different sizes are separated by sieving. However, tooth enamel powder with 0.5 – 1 mm grains is ideal for EPR dosimetry. This grain size is ideally isotropic and reduces the anisotropy of the dosimetric $^{\bullet}CO_2^-$ signal in EPR measurements (Iwasaki et al., 1993; Haskell et al., 1997; Zhumadilov et al., 2005). On the other hand, grinding down below 0.1 mm increases the native signals, decreases reproducibility, and changes the dose-response (Fattibene and Callens, 2010). Thus, the quality of an EPR spectrum is dependent on the grain size of tooth enamel. The separated and ground tooth enamel samples still may contain some impurities (i.e., dentin, organic matter,

and metals), which cause some unwanted signals like backgrounds in the EPR measurements. Those transient signals and impurities are removed using enamel purification processes: (1) routinely annealing ground tooth samples in a ventilated oven at 90°C for 2h eliminates the transient signals (Ciesielski et al., 2006; Fattibene and Callens, 2010); and (2) chemical etching is done by using alternating steps of acid etching and water rinsing which remove the unwanted stable paramagnetic centers that are located at the surface of the grains. It also shortens the lifetime of unstable surface signals. A strong acid cannot be used as it may dissolve the finely ground enamel (0.5 mm) and be lost. So, a suitable acid for chemical etching is a 20% aqueous solution of acetic acid ($CH_3COOH$). Chemical etching also removes the unwanted or parasitic signals from metal impurities in tooth enamel. At the same time, chemical etching using 42% phosphoric acid ($H_3PO_4$) in three successive 30-second etching steps can be used to remove the mechanically induced signals (Fattibene et al., 1998; IAEA, 2002). After annealing and chemical etching, the enamel samples need to be dried thoroughly to avoid the absorption of microwave radiation by water during the EPR measurements. To remove water from the sample, the enamel sample should be dried for at least 10 h at (50-60)°C (Fattibene and Callens, 2010) and stored for 3 days at room temperature and relative humidity below 60%. The ground and purified enamel sample should store for 2-8 weeks between the sample preparation, purification, and EPR measurements to decay some unstable signals formed during sample preparation (Fattibene and Callens, 2010). High-quality sample preparation techniques are vital for detecting a low dose in tooth enamel and decreasing the dose detection limit in EPR measurements (IAEA, 2002; ICRU, 2002).

**(a)**

Mortar, pestle, and sieves

**(b)**

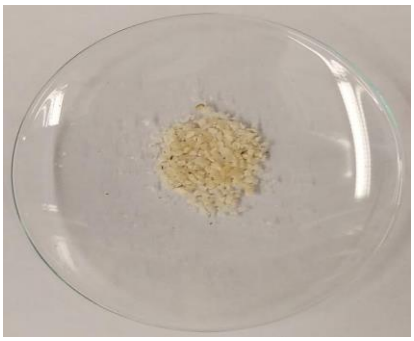

Tooth enamel powder
with 0.5-1 mm grains

**(c)**


**Figure 3.4: (a)** Mortar, pestle, and sieve to grind and filter tooth enamel powder. **(b)** Tooth enamel powder with 0.5-1 mm grains. **(c)** The mini-aluminium saw was used to separate a crown from a root, and the Mastercraft diagonal cut pliers were used to cut enamel into 0.5-1 mm grain size.

## 3.2 The fundamental principle of EPR, microwave resonator, spin relaxation, hyperfine splitting, and the background measurements

### 3.2.1 Fundamental principle of EPR spectroscopy

EPR spectroscopy is a non-destructive technique used to detect, identify, and quantify free radical centers or unpaired electrons in materials. So, the EPR quantification of free radicals or paramagnetic centers in tooth enamel makes it possible to measure the exact radiation dose an individual may have been exposed to following external exposures (Fattibene and Callens, 2010). The free radical center contains an unpaired negatively charged electron, often called the paramagnetic species, which behaves like a tiny magnet. In the absence of an external magnetic field, unpaired electrons of free radicals have spin (or magnetic moment) equal to ½ (i.e., spin quantum number, *ms*). However, the unpaired electron occupies either of two spin states ($ms = +½, -½$) if the magnetic field is applied ($B_0 \neq 0$), as shown in Figures 3.5a and 3.5b. However, in the absence of the magnetic field ($B_0 = 0$), the energy levels of these two spin states are equal (*i.e.*, $S = +½ = -½$), often called *degenerate,* as shown in Figure 3.6a. The splitting of the electron spin energy into the lower energy level ($-½$ *or* $\beta$) and the higher energy level ($+½$ *or* $\alpha$) in the magnetic field ($B_0 \neq 0$), as shown in Figure 3.6b, and equations 3.1 and 3.2 is called the *Zeeman effect*. Furthermore, the interaction of the electron's magnetic moment with the external applied magnetic field ($B_0$) is called the *electron Zeeman interaction.* According to classical physics, the electron will have the lowest energy state when the electron's magnetic moment μ is aligned with the magnetic field ($B_0$) and a state of highest energy when the magnetic moment $\mu$ is aligned against the magnetic field ($B_0$). So, the energy of the two spin states ($+½$ *and* $-½$) are different as shown in the Figure 3.5b and are given in equations 3.1 and 3.2 (Brustolon and Giamello, 2009; Fattibene and Callens, 2010; Desrosiers and Schauer, 2001; Schauer et al., 2007).

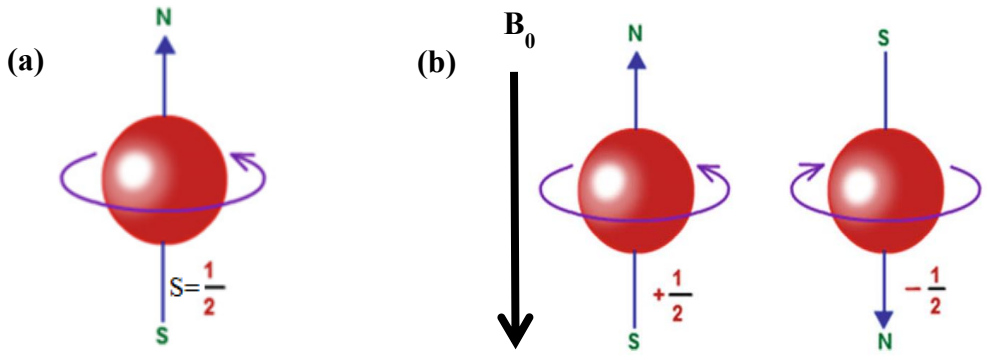


**Figure 3.5: (a)** Free or unpaired electron is a spin ½ particle. **(b)** The maximum and minimum energy of electrons, the electron will have a state of the lowest energy when the magnetic moment of the electron (μ) is aligned with the applied magnetic field. It is in the highest energy state when the moment of the electron, μ, is aligned against the magnetic field ($B_0$). From Likhtenshtein (2016).

$$E_\alpha = +(½)\, g|\mu_B|B_0 \qquad (3.1)$$

$$E_\beta = -(½)\, g|\mu_B|B_0 \qquad (3.2)$$

[Where $h$ is the Plank's constant ($h$= 6.626 × $10^{-34}$ Js), $B_0$ is the magnetic field intensity, $v$ is the radiation frequency, $g$ is the *g-factor* which is a constant (approximately equal to *2*) for a spin of ½, and $\mu_B$ is the Bohr magneton] (IAEA, 2002).

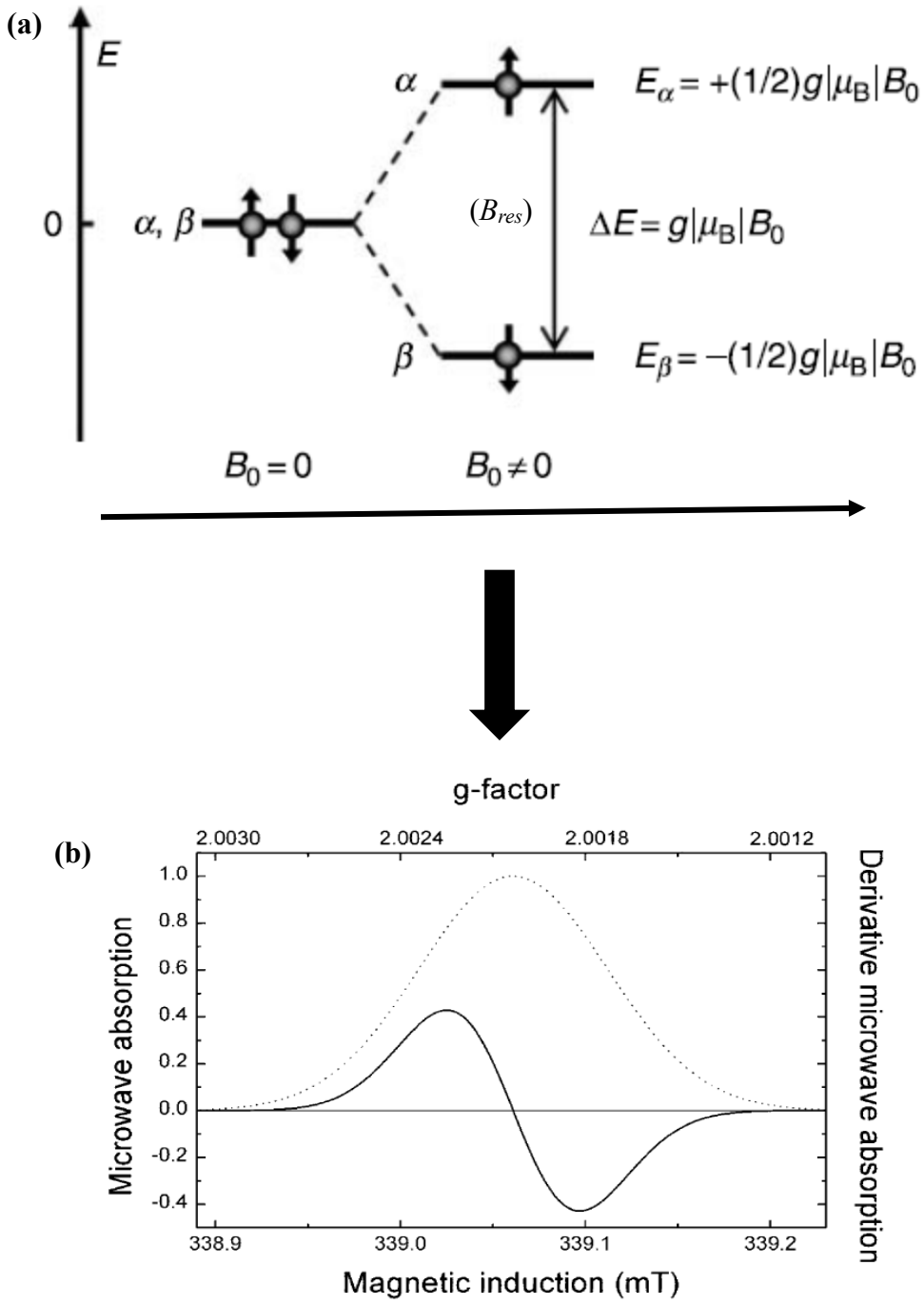


**Figure 3.6: (a)** Splitting of the energy levels in the presence of the external magnetic field ($B_0 \neq 0$), also called the *Zeeman effect*. From Brustolon and Giamello (2009). **(b)** An experimentally detected absorption (dotted line) spectrum and the first derivative of microwave absorption (EPR intensity, solid line) against the magnetic field is called an EPR spectrum. From Jacob et al. (2002).

An electron in the $\beta$ state, which is in the lower energy level, can absorb a quantum of electromagnetic radiation ($h\nu$) energy from the microwave radiation, equal to the energy difference between the $\alpha$ and $\beta$ states, as shown in equation 3.3. Consequently, the microwave energy ($h\nu$) absorbance occurs in the ***spin-flip transition***, as shown in Figure 3.6a. The intensity of these transitions is proportional to the number of unpaired electrons in tooth enamel, proportional to the absorbed dose (Brustolon and Giamello, 2009; Fattibene and Callens, 2010; Desrosiers and Schauer, 2001). The spin's absorbance of the microwave energy is called resonance ($B_{res}$). An EPR spectrometer detects the absorbance of microwave energy for this transition. After an appropriate amplification, it is experimentally displayed as a first derivative of the absorption curve with respect to the applied magnetic field (mT), as shown in Figure 3.6b (Jacob et al., 2002). To improve the signal-to-noise ratio (SNR), the modern CW EPR spectrometer uses high-frequency magnetic field modulation in combination with phase-sensitive detection, whereby the original absorbance spectrum will be changed into the first derivative EPR spectrum, as shown in Figure 3.6b (IAEA, 2002; Jacob et al., 2002; ISO, 2013). The spectrum is recorded in a digital form using a computer. In modern spectrometers, the computer also controls the operation of the spectrometer, for example, setting measurement parameters, tuning a resonator, acquiring and saving signals, and spectra processing such as the P2P amplitude height measurement, baseline correction, deconvolution, integration, etc. The main characteristics of the spectra obtained through these transitions depend on their shape, peak-to-peak linewidth ($\Delta B_{pp}$), peak to peak amplitude (R) or an EPR intensity, and the spectroscopic splitting factor (Landé g-factor) or *g – value* as shown in Figure 3.7 (IAEA, 2002; Schauer et al., 2007).

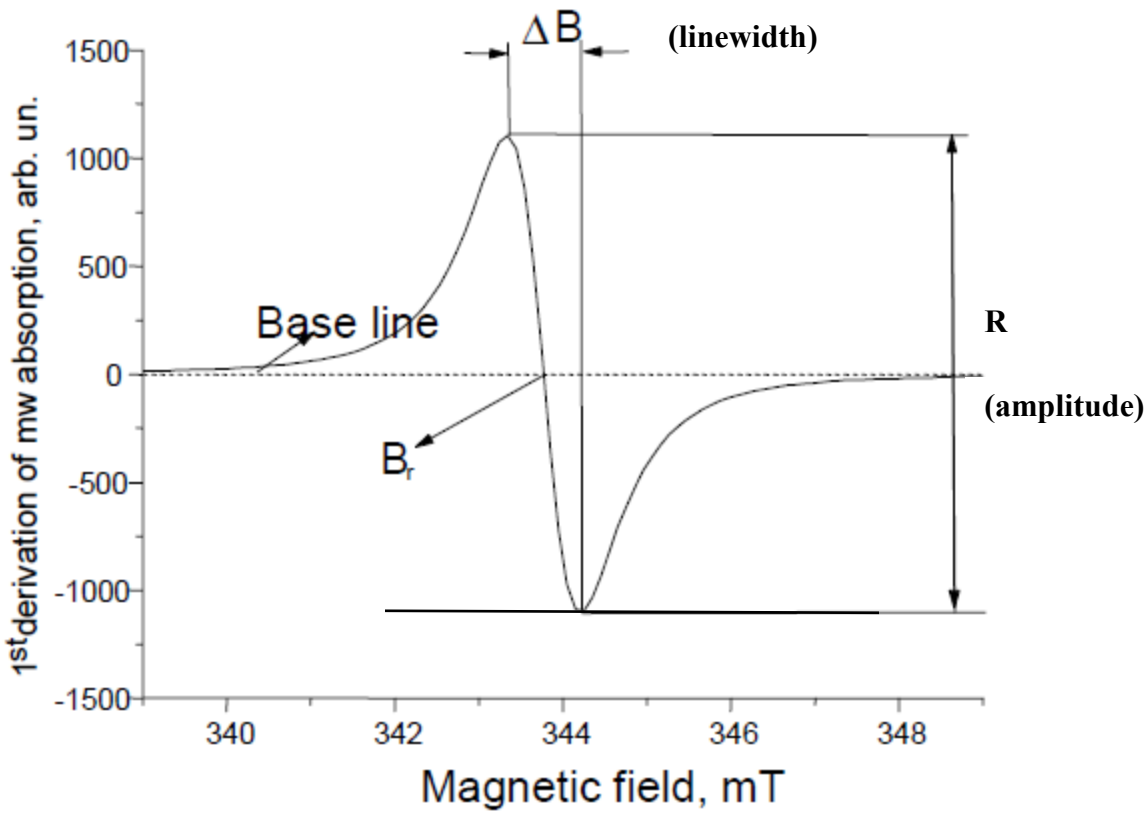


**Figure 3.7:** A typical EPR spectrum with the main characteristics such as the linewidth ($\Delta B_{pp}$), P2P height (R), baseline, and the spectroscopic splitting (g-factor). The intensity of these transitions (P2P amplitude height) depends on the number of free radicals present in tooth enamel and other samples. The highest EPR amplitude or spectrum intensity is measured using the EPR processing software (Win-EPR), which calculates the radiation dose in tooth enamel and other samples with paramagnetic properties. From IAEA (2002).

$$h\nu = E_\alpha - E_\beta = g|\mu_B|B_0 \qquad (3.3)$$

From equation (3.3), it is derived that there is a linear dependence between the applied magnetic field ($B_0 \neq 0$) and the resonance frequency ($\nu$) (Brustolon and Giamello, 2009). In a 3.5 T magnetic field, which is common in many EPR spectrometers, for g = 2.0023, equation (3.3) gives v = 9.5 GHz. This is the radiation frequency of the microwave X-band region. However, there are some EPR spectrometers with lower frequency than the X-bands like the L (1.2 GHz)

and S (3.0 GHz) bands and a higher frequency than the X-band like the Q (35 GHz) and W (94 GHz) bands, as shown in Table 3.1. However, the X-band EPR spectrometer is the most widely used because of its good sensitivity, sample size, water content, and moderate price (IAEA, 2002). However, the higher band (or frequency) EPR spectrometers are more sensitive (~20 times) and have the highest signal-to-noise ratio (SNR), requiring a minimal sample size (~2mg) than the X-band (~100 mg) EPR spectrometer (De et al., 2013; Romanyukha et al., 2014; Romanyukha et al., 2007). In all these EPR spectrometers, the EPR operates at constant microwave frequency regardless of frequencies; and the magnetic field is swept linearly due to experimental difficulty in scanning microwave frequencies in EPR (Eaton et al., 2010).

**Table 3.1:** Field for resonance for a g = 2 sample at various microwave frequencies. From Eaton et al. (2010).

| Microwave band | Microwave frequency (GHz) | $B_0$ (for g = 2) gauss |
|---|---|---|
| L | 1.2 | 390 |
| S | 3 | 1070 |
| **X** | **9.5** | **3380** |
| K | 24 | 8560 |
| Q | 35 | 12,480 |
| W | 94 | 33,600 |

### 3.2.2 Requirements for EPR spectrometers

An EPR spectrometer (EMX micro) with different components is depicted in Figure 3.8a. EPR dosimetry mainly deals with the small sample mass with a low spin concentration (i.e., low doses). In this condition, the sensitivity and stability of the EPR spectrometer are vital to solving these measurement problems. The sensitivity and stability of the spectrometer can be optimized by selecting the high sensitivity resonator (ER4119HS), as shown in Figures 3.8a and 3.8b, optimizing the acquisition parameters and minimizing the microphonic effects. For example, in

the second international intercomparison of EPR dosimetry with tooth enamel, the quality of the EPR spectrometer used highly influenced the data quality (i.e., precision and reproducibility) obtained in the dose reconstruction among many laboratories (Wieser et al., 2000).

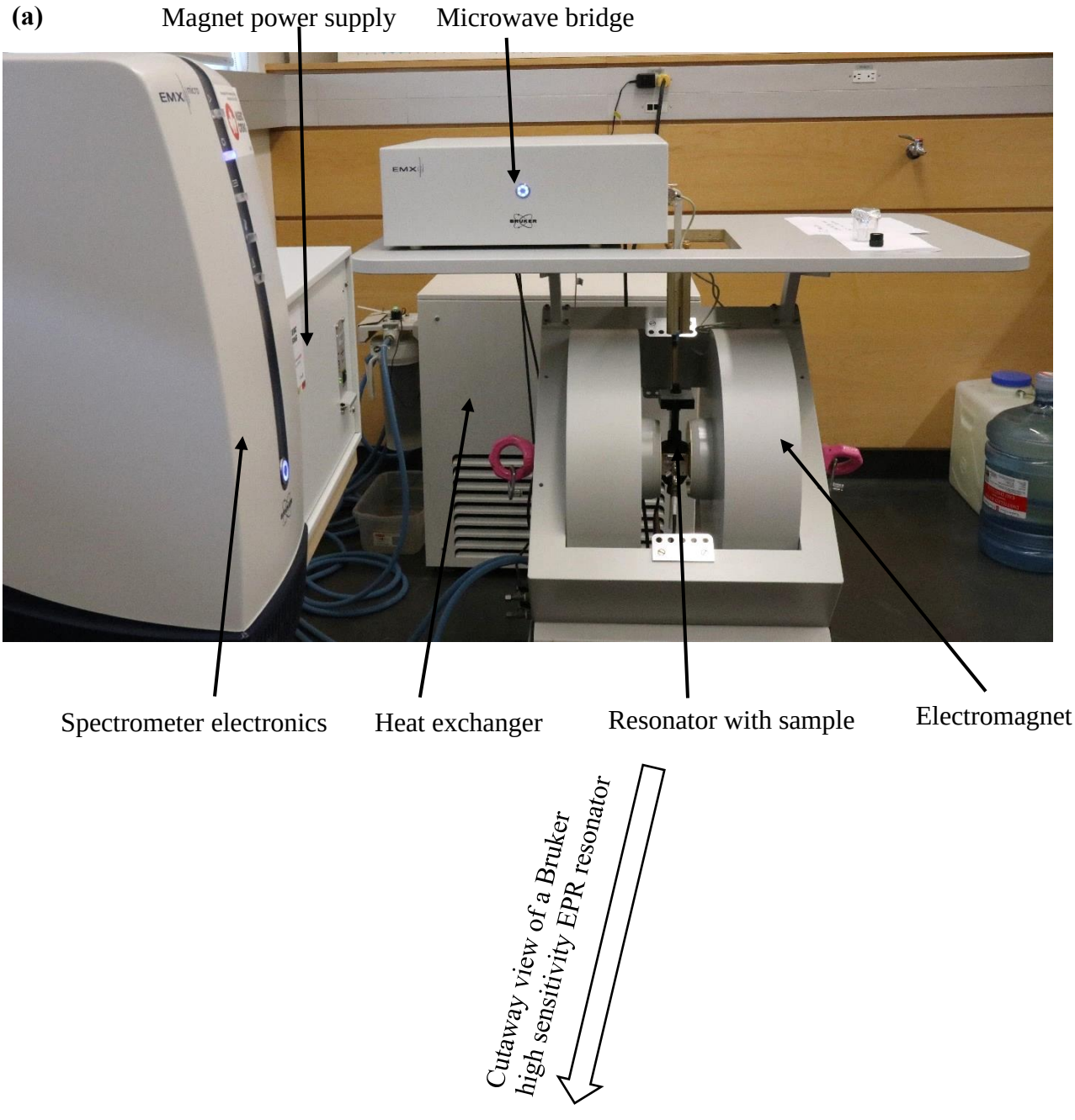

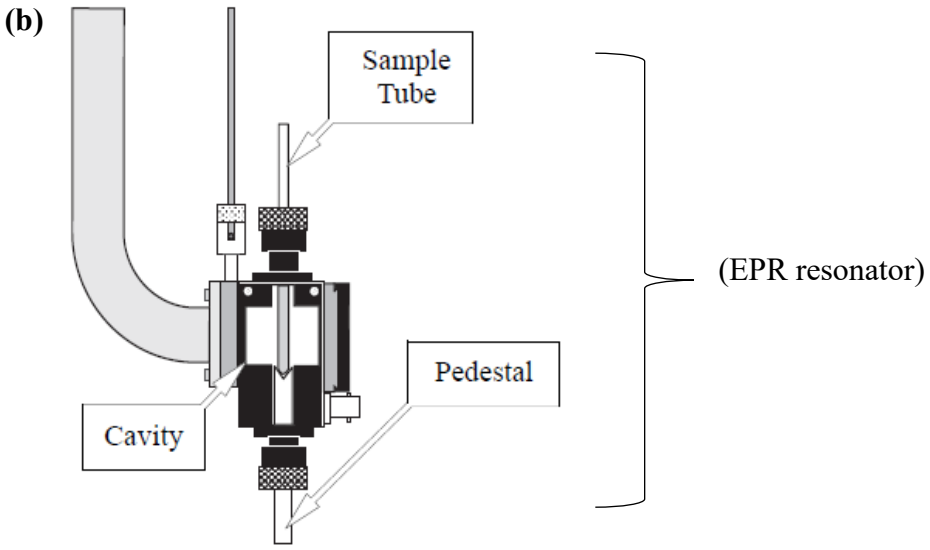


**Figure 3.8:** (**a)** The Bruker X-band CW EPR spectrometer (EMXmicro) components with a heat exchanger. **(b)** Cutaway view of the Bruker high sensitivity EPR resonator (ER4119HS). From Eaton et al. (2010).

### 3.2.3 Microwave resonator

A microwave resonator is a place in EPR where a sample is inserted for analysis, as depicted in Figure 3.8b. It has mainly two functions: (1) to generate a sufficient microwave magnetic field ($B_1$), which is required for the spin-flip transition of electrons, and (2) to convert a sample response into a detectable microwave signal.

#### 3.2.3.1 The resonator Q-factor

Both these functions depend on the Q-factor of the resonator (Brustolon and Giamello, 2009). The Q-factor also indicates how efficiently the cavity stores the microwave energy, and it is critical for the quantitative measurement in EPR spectroscopy. The Q-factor increases the spectrometer sensitivity (Eaton et al., 2010). It is defined as:

$$Q = \frac{2\pi\ (energy\ stored)}{Energy\ dissipated\ per\ cycle} \qquad \text{(Eaton et al., 2010)} \qquad (3.4)$$

Where the energy dissipated is the amount of energy lost per microwave cycle. The EPR spectrometer cavity loses energy from the sidewall of the cavity because the microwave generates electrical energy on the sidewall, which generates heat. The Q-factor of the cavity can be easily measured by using the formula as follows (Eaton et al., 2010):

$$Q = \frac{V_{res}}{\Delta V} \tag{3.5}$$

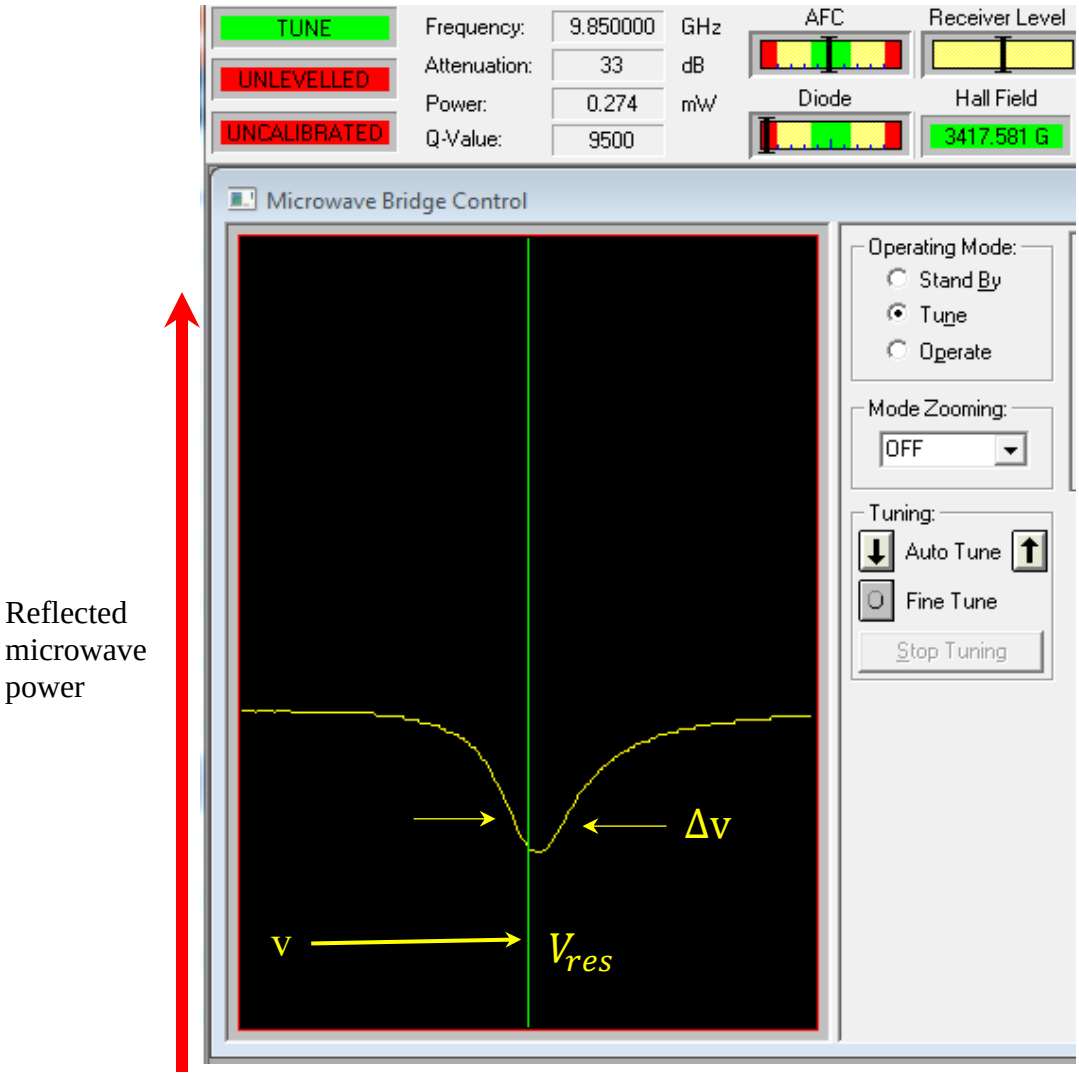


**Figure 3.9:** Reflected microwave power from the resonant cavity and its Q-value. The EPR spectrometer is in the displayed mode called "Tune," in which the microwave is swept on the horizontal axis, and the reflected microwave is detected to form data for the vertical axis.

Where *Vres* is the cavity's resonant frequency and $\Delta V$ is the width at the half-height of the resonance, as shown in Figure 3.9. There will be a standing wave inside the cavity due to resonance. The standing waves have their electric and magnetic fields out of phase, which means the magnetic field ($B_1$) is maximum, and the electric field ($E_1$) is minimum, as shown in Figure 3.10.

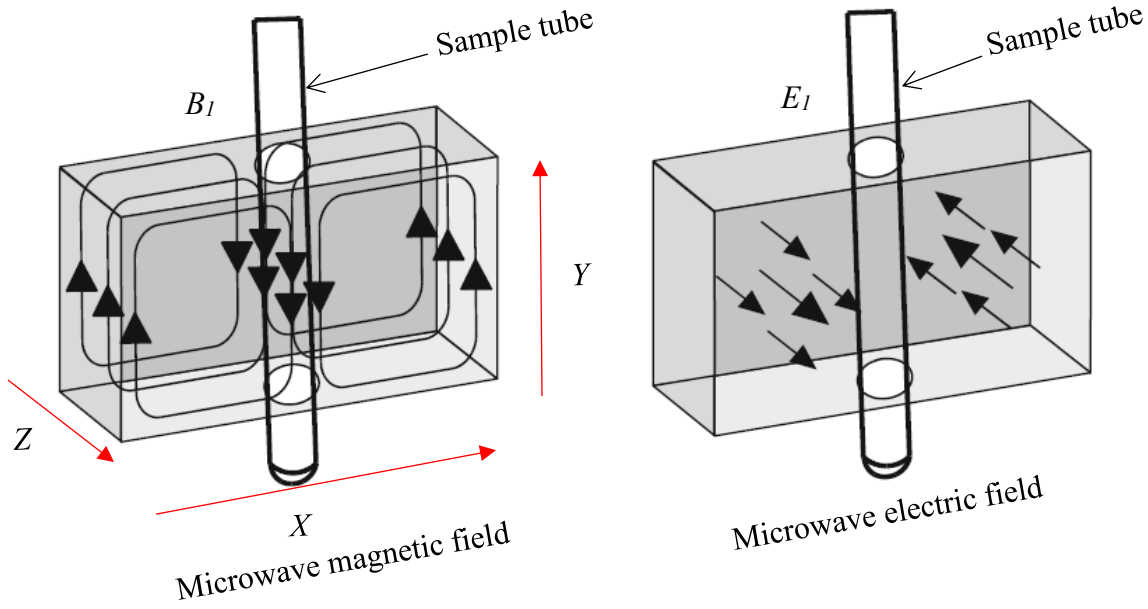


**Figure 3.10:** The distribution of the $B_1$ and $E_1$ in the EPR resonator (ER 4102ST). In a resonator, directions Y and Z correspond to the sample tube axis and magnetic field ($B_0$), respectively. From Eaton et al. (2010).

This spatial distribution of the electric and magnetic fields in the EPR cavity (Figure 3.10) has significant advantages. The magnetic field ($B_1$) causes the spin-flip transition of electrons in EPR (i.e., absorption in EPR), which eventually converts into the first derivative EPR spectrum, as shown in Figure 3.6. Suppose we place the sample in the EPR cavity with the maximum magnetic field ($B_1$) and the minimum electric field ($E_1$), as depicted in Figure 3.10. In that case,

we will get the most prominent signal with high sensitivity. Most of the modern EPR spectrometers are designed for the optimal placement of samples, as depicted in Figures 3.10 and 3.13.

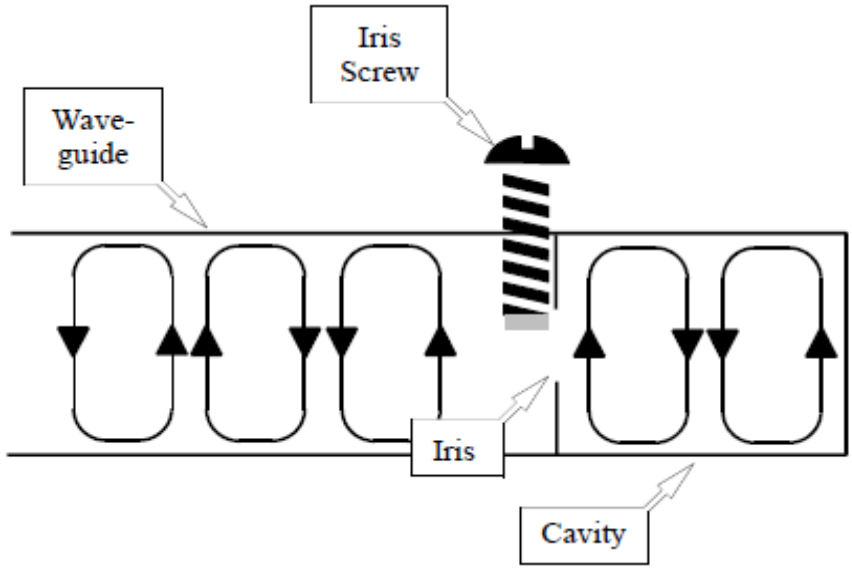


**Figure 3.11:** An iris screw to control the amount of microwave in a cavity. From Weber et al. (1998).

The size of the iris controls how much of the microwave power is reflected from the cavity and enters the cavity, as shown in Figure 3.11 (Eaton et al., 2010; Weber et al., 1998). In our experiment with tooth enamel, the cavity Q-factor with an unloaded sample was 9500, as shown in Figure 3.12a, which was a good enough sensitivity for the EPR dosimetry. Depending on the type of resonator in the X-band CW EPR spectrometer, the Q-factor values can range from 5,000 to 10,000, as depicted in Figures 3.12a and 3.12b. In an EPR dosimetry experiment, the cavity Q-factor can be measured as follows:

- Tune the resonator correctly, as described in Section 3.5 (Chapter 3);
- Then go to the tune mode;
- Adjust the attenuation to 33 dB;

- The Q-value will be displayed in the hardware information section as depicted in Figures 3.12a and 3.12b.

**(a)**

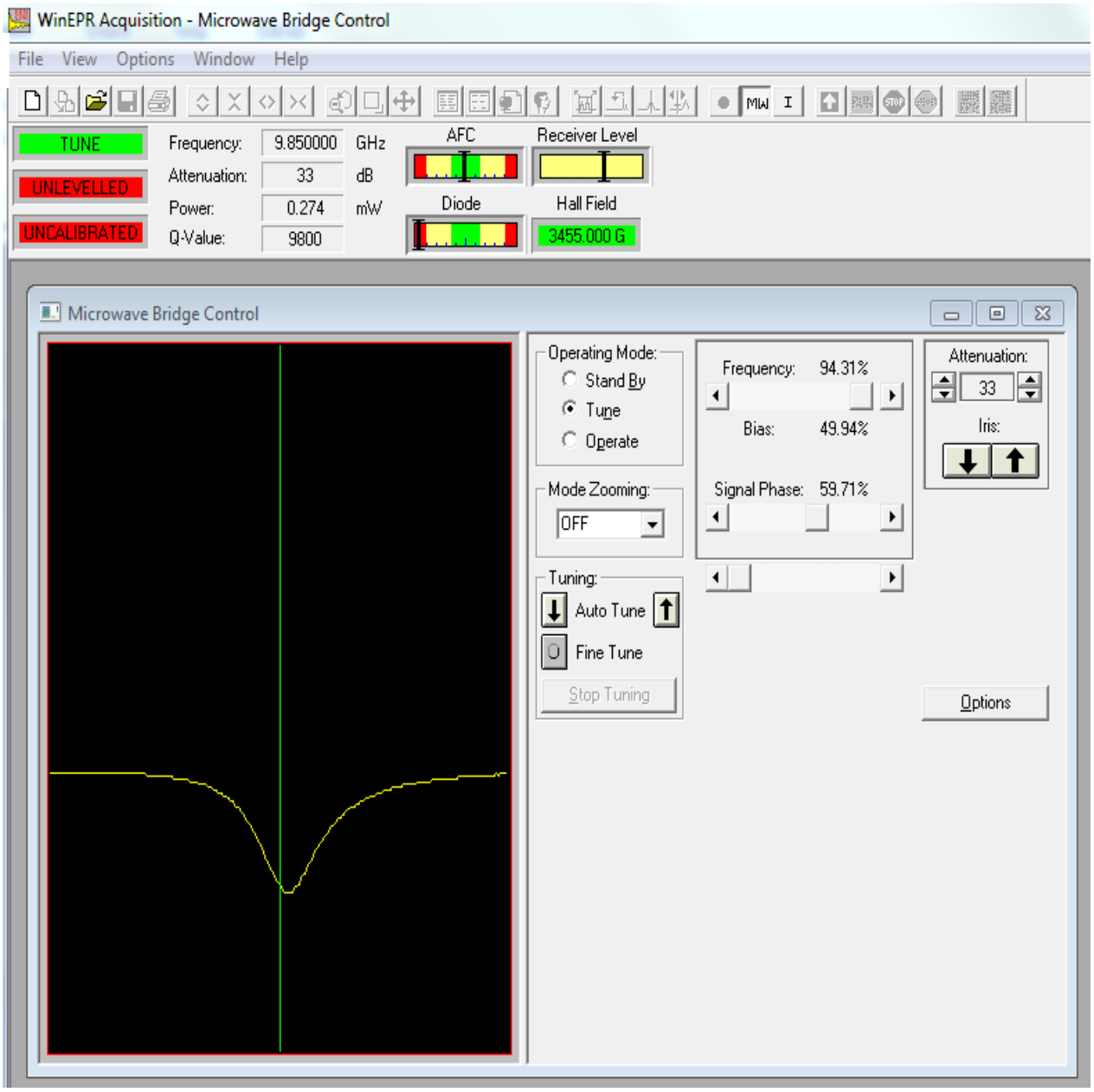

**(b)**

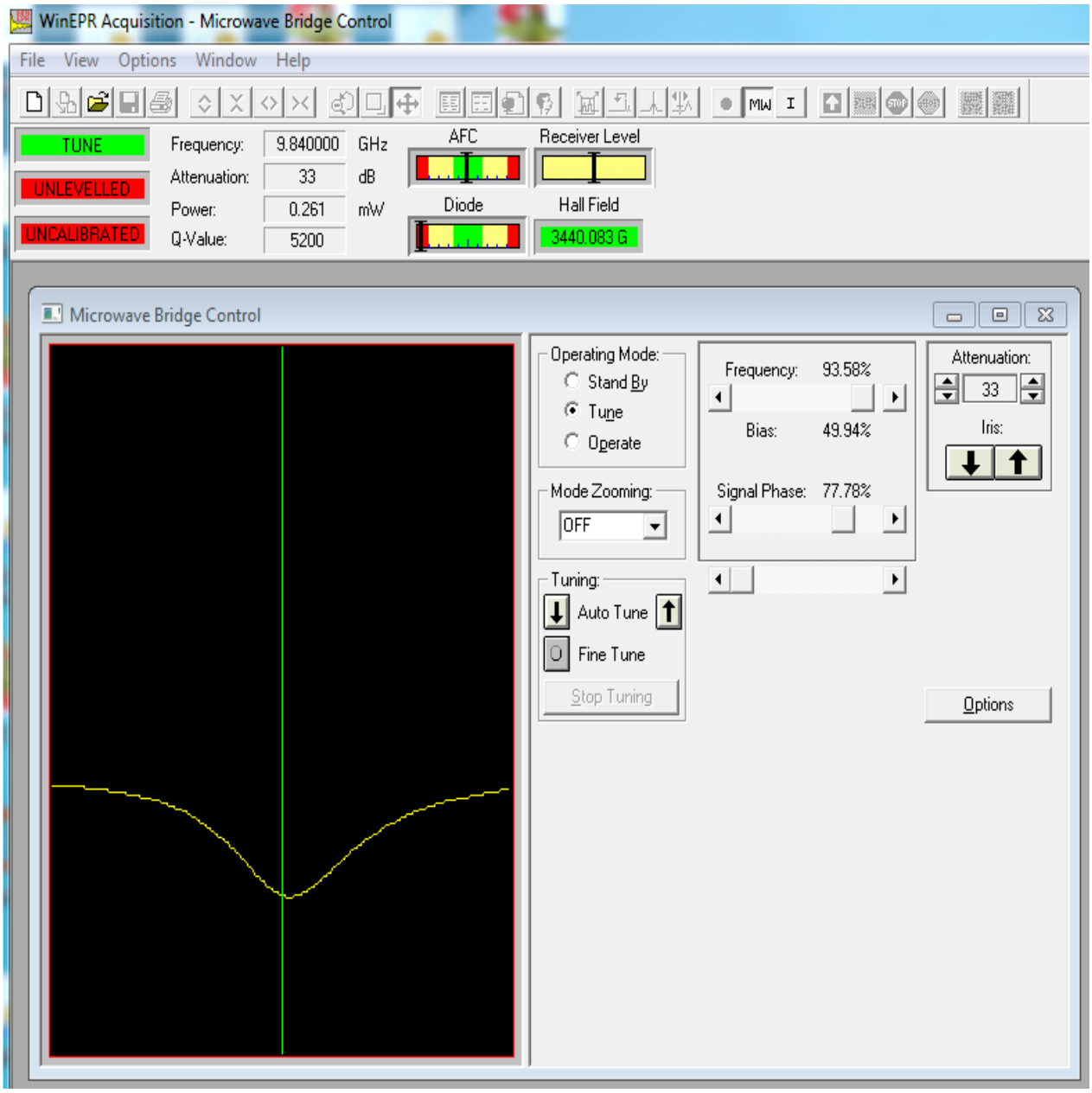


**Figure 3.12: (a)** The Q-values of the rectangular standard cavity ER 4102ST with an unloaded sample. **(b)** The Q-values after loading with a tooth enamel sample into the same resonator.

### 3.2.3.2 Filling factor (η)

The $B_1$ generated in an EPR resonator by the microwave power is given by equation 3.6 (Brustolon and Giamello, 2009; Eaton et al., 2010): $B_1 = c \times (Q \times P)^{\frac{1}{2}}$ *(3.6)*

Where c is the conversion factor, a smaller resonator has a larger conversion factor. The unit of a conversion factor is gauss/$\sqrt{W}$. The $B_1$ drives the EPR transitions. The EPR intensity increases with $B_1$ if the signal is not saturated. B1 increases proportional to the square root of the microwave power in EPR measurements (Eaton et al., 2010). Besides the Q-factor, the filling factor (η) has a linear contribution to the EPR signal, as shown in equation 3.7 (Brustolon and Giamello, 2009).

$$\Delta S_{pp} \propto \eta \times Q \qquad (3.7)$$

As the name implies, the filling factor means the extent to which the sample fills the resonator. Since it is the $B_1$ that causes the *spin-flip transition*, the sample should occupy the region of the resonator where there is a large $B_1$, as depicted in Figure 3.10. If the $B_1$ is uniform in the resonator, the filling factor will be the ratio of the sample volume to the resonator's volume. However, the $B_1$ is not uniform in the resonator, so its calculation is more complicated than merely a volume ratio. For precise results, the $B_1$ square integrated over the sample volume to the $B_1$ square integrated over the resonator volume as per equation 3.8 (Brustolon and Giamello, 2009; Eaton et al., 2010).

$$\eta = \frac{\int_{Sample} B_1^2 dV}{\int_{Cavity} B_1^2 dV} \qquad (3.8)$$

**3.2.3.3 EPR signal intensity distribution inside the resonator**

Since the resonator Q-factor (i.e., EPR sensitivity) is dependent on $B_1$, the EPR spectrum is usually recorded with a fixed microwave frequency and a variable magnetic field (Eaton et al., 2010). It is not that important at which magnetic field the resonance occurs. The choice of resonator depends on the type of sample and experiment; the conventional CW EPR uses a rectangular or cylindrical resonator. Whenever the cavity with high $B_1$ is required, pulsed EPR, transient EPR, the small-sized dielectric, and split ring resonators are used (Brustolon and Giamello, 2009).

During the EPR analysis, to achieve a high filling factor (η) for a particular sample, the sample is measured from a low to high depth in a resonator, as depicted in Figure 3.13. The optimum place (i.e., maximum $B_1$) for a particular sample is a depth where we get the highest EPR intensity. Figure 3.13 shows an EPR intensity against the distance from the center (mm) of a cavity. Details about finding an optimum place or depth inside the resonator (i.e., high filling factor) are given in Chapter 5 (Section 5.3.1).

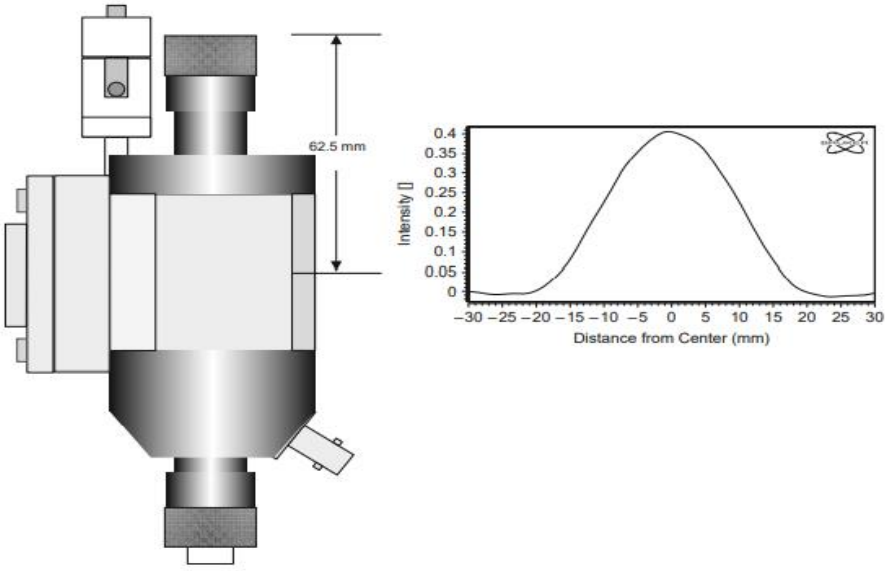


**Figure 3.13:** An EPR signal intensity distribution inside the resonator ER4119HS. From Eaton et al. (2010).

To determine the optimum sample position inside the cavity, the sample is measured from a low to high depth in a resonator. The optimum place (i.e., maximum $B_1$) for a particular sample is a depth where the highest signal intensity and the lowest electric field.

### 3.2.4 Spin relaxation and the Boltzmann distribution law

In one experiment, a sample may contain spins on the order of $10^{10}$ or higher (Brustolon and Giamello, 2009; Eaton et al., 2010). These spins interact with each other and with their

environments. However, as mentioned in section 3.2.1, the electron spin (½) splits into two spin states (i.e., high energy ½ and low energy − ½) in the presence of the external magnetic field ($B_0 \neq 0$). In thermal equilibrium with the lattice, the spins are distributed in such a way that the spins are relatively higher in the $\beta$-state (i.e., lower energy level) than in the $\alpha$-state (i.e., higher energy level), as depicted in Figure 3.14. The ratio of the spins in these two spin states depends on the temperature (T). It is expressed by the *Boltzmann distribution* law:

$$N_\alpha/N_\beta = exp(-g|\mu_B|B_0/k_BT) \qquad (3.9)$$

Where $N_\alpha$ and $N_\beta$ are the occupancy numbers of the upper and lower levels, $k_B = 1.3806 \times 10^{-23}$ $J K^{-1}$ (Boltzmann constant) and $T$ = absolute temperature of the lattice. An X-band CW EPR spectrometer operates at room temperature and 25˚C (300K). For the magnetic field on the order of 0.3 T, in this condition, $g|\mu B|B_0 << kBT$, and exponential can be expanded in series and can only retain the linear term.

$$N_\alpha/N_\beta = 1-g|\mu_B|B_0/k_BT \qquad (3.10)$$

This equation provides an excellent approximation of spins in $\beta$ and $\alpha$ states unless the system is at a higher temperature (high field) or a very low temperature. According to equation (3.10), at the X-band, in a room temperature with a sample that has 10,000 spins, on average, 5,004 spins are in a β state, and 4,996 spins are in an α state, only differing by 0.08% (Brustolon and Giamello, 2009; Eaton et al., 2010). So, the absorbance of microwave energy causes the resonance (i.e., spin states change from the low energy level state β to the higher state α, and the reverse from α to β, in a number that is proportional to the spins in the initial state as depicted in Figure 3.14. The spin couples with a lattice, so it continuously releases energy. Suppose the energy from the higher energy state (α) could not be released. In that case, the microwave energy continuously acting on the spin system (i.e., CW EPR) would eventually equalize the spin population ($N_\alpha = N_\beta$),

and absorbance of energy would stop after some time, which is called the EPR signal saturation. Also, saturation occurs if the relaxation rate is too slow (long τ) to dissipate the microwave energy or spins get higher microwave energy. The energy flow in the spin-lattice relaxation process:

***Electromagnetic field → Spin system → Lattice vibrations***

This type of energy released from the high energy level spin and returning to the lower spin state is called the ***spin-lattice relaxation process***, as shown in Figure 3.14, which avoids the signal saturation in EPR. The rate of relaxation processes is expressed by the relaxation time, τ, known as the ***spin-lattice relaxation time***, which measures how fast the higher spin returns to the lower spin state. This can be experimentally observed as the absorbance does not increase with the microwave energy (i.e., line broadening occurs at high microwave energy). This unwanted saturation can be avoided by decreasing the microwave power; usually, absorbance becomes proportional to the square root of microwave power (Lund et al., 2011). At the same time, the spins at higher energy states also decay toward zero with time ($T_1$ to $T_2$), which is called the ***spin-spin relaxation process*** (Figure 3.14). This is another process by which the high energy spins lose energy, return to the lower spin states, and prevent the EPR signal saturation (Brustolon and Giamello, 2009).

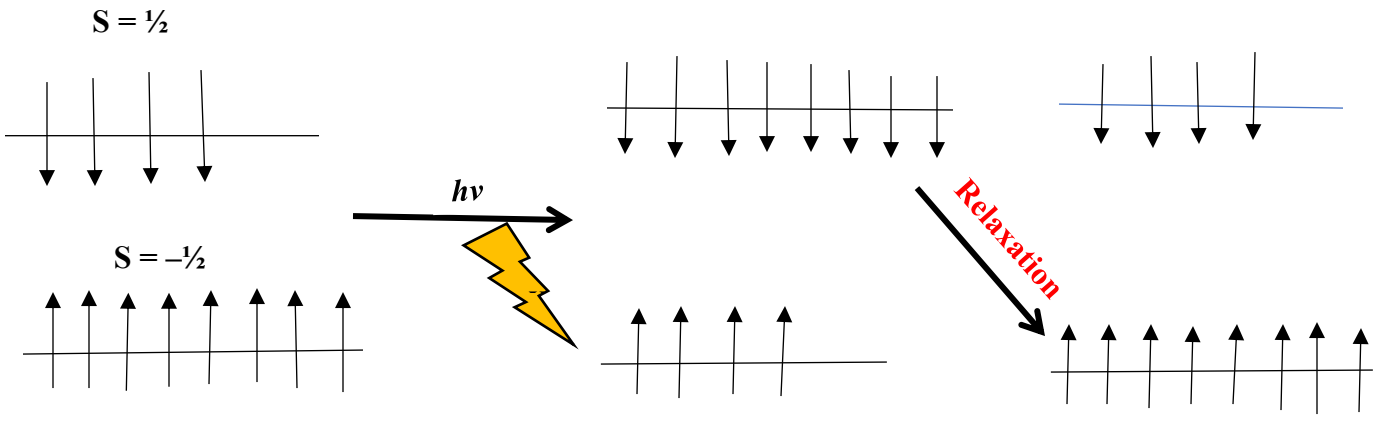


**Figure 3.14:** Spin relaxation processes during the EPR measurements.

### 3.2.5 Sensitivity

In a quantitative analysis, the concentration of samples or spins is determined by either measuring the absorption or emission (i.e., spectroscopy) of electromagnetic energy. In the case of EPR dosimetry, the absorption of microwave light by a sample is measured (called spectroscopy) to determine the spin concentration, which is proportional to the absorbed doses (Brustolon and Giamello, 2009; Eaton et al., 2010; Fattibene and Callens, 2010). In EPR, the absorption of microwave energy depends on the number of spins in the lower and higher levels. That is, the absorption intensity depends on the spin differences in these two levels (Rieger, 2007):

$$Net\ absorption = N_\beta - N_\alpha \qquad (3.11)$$

The ratio of the populations of the spins in the high and low energy levels is given by the Boltzmann equation (3.9). At ordinary temperature and the magnetic field (i.e., X-band CW EPR), the exponent is very small and can be approximated by the expression, $e^{-x} \approx 1 - x$. Thus

$$N_\alpha/N_\beta = 1 - g|\mu_B|B_0/k_BT$$

Since $N_\beta \approx N_\alpha \approx N/2$ The spin population difference can be written:

$$N_\beta - N_\alpha = N_\beta[1-(1-g|\mu_B|B_0/k_BT)] = Ng|\mu_B|B_0/2k_BT \qquad (3.12)$$

This expression shows that the EPR sensitivity (i.e., net absorption) increases with the total number of spins, N. Also, sensitivity increases with the increase in the magnetic field ($B_0$) strength and decrease in temperature (T). The field at which absorption occurs is proportional to the microwave frequency; that is why EPR with high frequencies and the magnetic field (i.e., K and Q-band EPR) are more sensitive than the X-band. However, the high frequencies EPR have smaller waveguides, which means they can only analyze small sample sizes, decreasing the Boltzmann factor, which eventually cancels the advantages of higher frequencies and the magnetic fields. Under ideal conditions, X-band can detect about $10^{12}$ spins and $10^{-12}$ moles. However, when the

EPR line is split due to hyperfine interactions, as described in Section 3.2.6, the sensitivity decreases further in EPR measurements. Nevertheless, EPR is a significantly sensitive technique than the Nuclear Magnetic Resonance (NMR) (Rieger, 2007; Weil and Bolton, 2007).

### 3.2.6 Hyperfine splitting of a resonance line

In the presence of a nuclear spin, the electron spin experiences an additional magnetic field provided by the nuclear magnetic moment (i.e., spin with a non-zero nuclear spin quantum number), as shown in Figure 3.15, which affects the EPR resonance. The hyperfine interaction is the electron-nuclear spin interaction, which splits the EPR lines into several components (Brustolon and Giamello, 2009; Eaton et al., 2010).

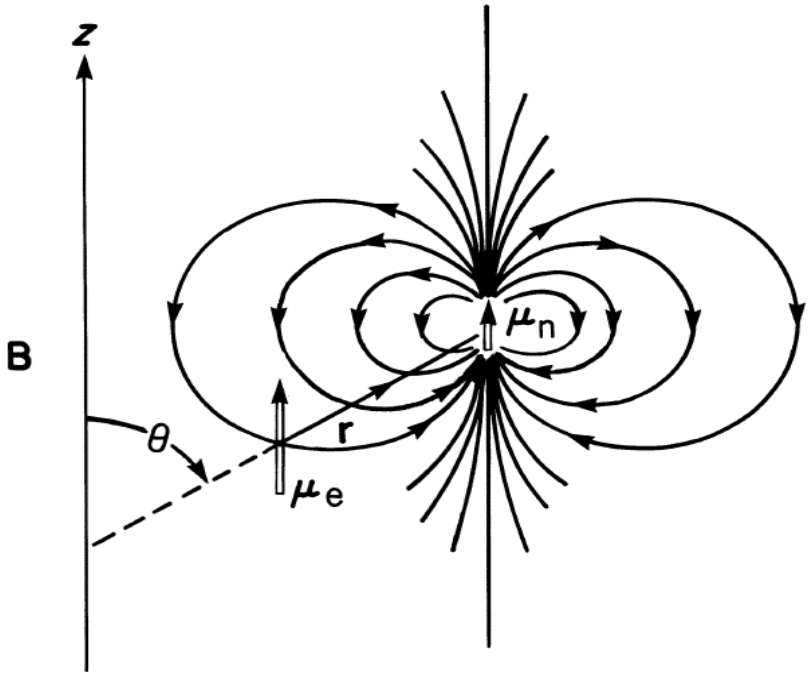


**Figure 3.15:** The electronic magnetic moment ($\mu_e$) interacts with the nuclear field ($\mu_n$) and the external applied magnetic field (B). The number of lines from the hyperfine interactions can be calculated using the formula *2nI+1*, where *n* is the number of equivalent nuclei, and *I* is the nuclear spin quantum number of a second nucleus. Angle θ is between the inter-dipole vector r and the applied field B. From Weil and Bolton (2007).

**Table 3.2:** Elements with their nuclear spins, the number of EPR lines, and their percentage natural abundances.

| Element | Isotope | Nuclear spin | No of lines | % abundance |
|---|---|---|---|---|
| Hydrogen | $^{1}H$ | ½ | 2 | 100 |
| Nitrogen | $^{14}N$ | 1 | 3 | 99.63 |
| | $^{15}N$ | ½ | 2 | 0.37 |
| **Manganese** | **$^{55}Mn$** | **5/2** | **6** | **100** |
| Iron | $^{57}Fe$ | ½ | 2 | 2.19 |
| Cobalt | $^{59}Co$ | 7/2 | 8 | 100 |
| Nickel | $^{61}Ni$ | 3/2 | 4 | 1.134 |
| Copper | $^{63}Cu$ | 3/2 | 4 | 69.1 |
| | $^{65}Cu$ | 3/2 | 4 | 30.9 |
| Vanadium | $^{51}V$ | 7/2 | 8 | 99.75 |

For example, manganese (Mn) has the nuclear spin (I) equal to 5/2, as shown in Table 3.2. The number of lines from the ***hyperfine interactions = 2nI + 1 = 2×1×5/2+1 = 6,*** which means six lines in the EPR spectrum, as depicted in Figure 3.16.

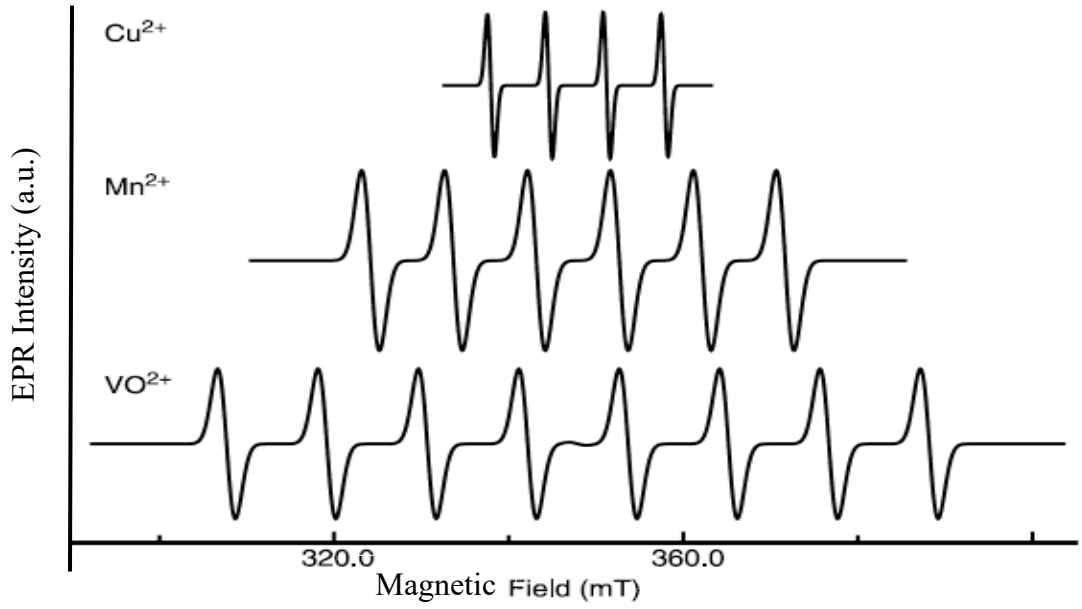


**Figure 3.16:** Hyperfine interactions split the EPR spectrum of manganese into six components using the formula *2nI+1*, where N is the number of equivalent nuclei, and I is the nuclear spin quantum number of a second nucleus. From Brustolon and Giamello (2009).

Similarly, a methyl-free radical ($^{\bullet}CH_3$) has one unpaired electron. However, it gives 4 peaks instead of one because a magnetic field of the free electron interacts with the nuclear magnetic field of three nearby hydrogens with the nuclear spins I=1/2 (same for three hydrogens). The four peaks (1:3:3:1) are due to the hyperfine splitting of the single EPR spectrum, as depicted in Figure 3.17.

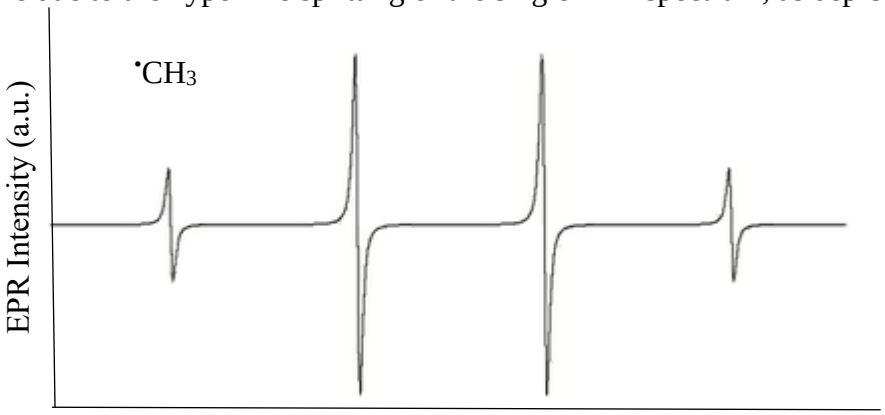


**Figure 3.17:** Hyperfine splitting of a methyl free radical ($^{\bullet}CH_3$) EPR spectrum into four components.

The splitting of EPR lines and their intensities follow Pascal's triangle if the nuclear spins of the second nucleus are ½ and 1, as discussed in Chapter 5 (Section 5.3.2). However, in the case of the transition metal ions such as manganese, the EPR intensities remain the same with a 1:1:1:1:1:1 ratio, as shown in Figure 3.16 (Brustolon and Giamello, 2009). Additionally, if $I$=1, the EPR spectrum splits using the same formula ($2nI+1$). However, the spectrum intensities will be different, as shown in Figure 3.18.

| | |
|---|---|
| | 1 |
| *n* = 1 | 1 1 1 |
| 2 | 1 2 3 2 1 |
| 3 | 1 3 6 7 6 3 1 |
| 4 | 1 4 10 16 19 16 10 4 1 |
| 5 | 1 5 15 30 45 51 45 30 15 5 1 |
| 6 | 1 6 21 50 90 126 141 126 90 50 21 6 1 |

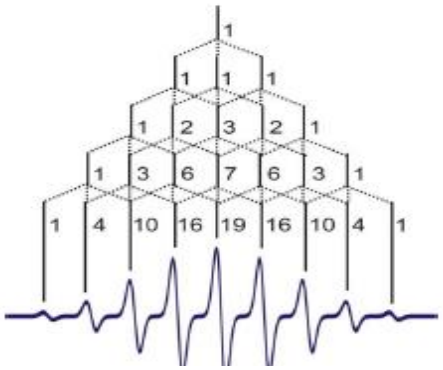


**Figure 3.18:** Pascal's triangle demonstrates the hyperfine splitting of an EPR spectrum for I = 1, where the numbers indicate the number of splitting and their relative intensities in an EPR spectrum. From Bertrand (2020); Duin (2013).

### 3.2.7 Background measurements

EPR resonators may be contaminated by paramagnetic substances such as dust, air, and samples from the previous measurements. The EPR sample tubes may have small quantities of paramagnetic species as impurities. These paramagnetic species from the resonator and EPR tubes may interfere with or mask the dosimetric signal in low dose measurements. The background subtraction can remove these unwanted signals and make the dose measurement precise, easier, and less time-consuming. That is why background subtraction is one of the essential steps to decrease the detection limit in a low dose measurement in tooth enamel and other samples (Hayes et al., 1998). The detailed background subtraction techniques and algorithms are described in Hayes et al. (1998).

### 3.2.8 Spectrometer stability and lab environmental conditions

The EPR spectrometer should reach a stable operating temperature before starting a sample analysis. The system must equilibrate under the same experimental conditions: high microwave power, high magnetic field modulation amplitude, temperature, etc. Generally, about one hour is

adequate to achieve thermal equilibrium. At the same time, lab environmental conditions such as temperature, air flow rate, and humidity must be fixed during the experiment as described in Section 5.2.4 (Chapter 5). A change in airflow may alter a cavity temperature and vibrate the sample (it causes microphonics). Temperature fluctuation reduces the spectrometer's performance by reducing the frequency stability of the cavity. Similarly, a highly humid environment increases the sample moisture, contributing to the background signals that mask the dosimetric signals. Additionally, the noise from the electromagnetic field may interfere with the magnetic field in a cavity. That is why the noise should be shielded if the source of such noise is identified. The reduction in the noise improves the quality of spectra and eventually helps decrease the detection limit in a low dose measurement (ISO, 2013).

### 3.2.9 Baseline drifts

The baseline drifts, background noises, and a low signal-to-noise (SNR) ratio will decrease the measurement accuracy, precision, and reproducibility in EPR measurements (Eaton et al., 2010). The baseline drifts can be minimized by optimizing the measurement parameters and other lab conditions (e.g., environmental and electronics). The very large modulation fields produce eddy currents on the wall of a resonator. These currents can interact with the magnetic field inside the resonator to produce a torque on the cavity, creating a resonant frequency drift, often called the linear baseline drift (Weber et al., 1998). Also, the high microwave power or large modulation fields can heat the cavity and the sample (i.e., a thermal drift). Due to thermal drifts, the cavity and sample may not achieve thermal equilibrium before performing the final tuning of the cavity, which fluctuates the baseline or slowly and randomly changes the baseline (Weber et al., 1998). The baseline drifts in alanine and tooth enamel samples are depicted in Figures 3.19a, 3.19b, and 3.19c. The baseline drifts correction on the acquired EPR spectrum can be performed during the

spectrum processing of the radiation-induced signals using the EPR processing (Win-EPR) software (Eaton et al., 2010; ISO, 2013).

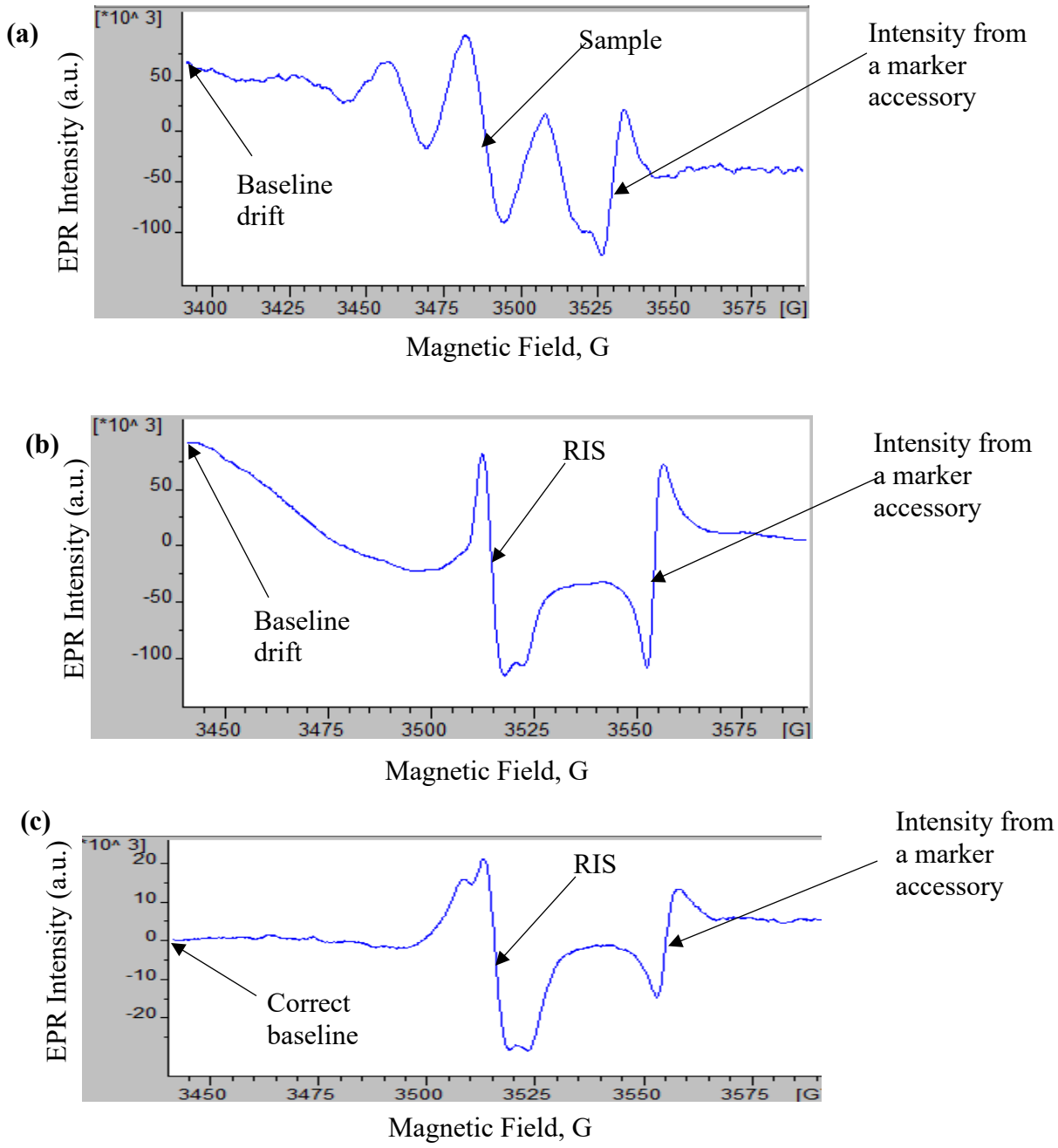


**Figure 3.19:** Baseline drifts due to change in the lab environmental conditions and microphonics in alanine **(a)**, tooth enamel **(b)**, and the correct baseline in tooth enamel irradiated to 4 Gy **(c)**.

### 3.2.10 Signal averaging and the signal to noise ratio enhancement

Very weak EPR signals can get lost in the background signals or noises. One of the ways to increase the signal-to-noise ratio and minimize the baseline drift is by increasing the recording time and signal averaging. Moreover, signal averaging can average the baseline drift problems and frequency noises (Eaton et al., 2010). The signal-to-noise ratio of the EPR spectrum is proportional to √N, where N is the number of scans in EPR measurements. The optimum spectrum recording time for tooth enamel dosimetry is 21 minutes as per the second international intercomparison on EPR tooth enamel dosimetry (Wieser et al., 2000). However, a large number of scans with a longer sweep time can be disadvantageous because of baseline drifts and an increase in noises in an EPR spectrum due to changes in lab environmental conditions and microphonics. Therefore, the spectrum recording time should not exceed 2 hours to avoid these errors (IAEA, 2002; Ivannikov et al., 2002; Eaton et al., 2010).

## 3.3 EPR spectrum acquisition

### 3.3.1 Choice and optimization of the EPR measurement parameters

To obtain high-quality spectroscopic data, the spectrometer instrumental parameters must be optimized prior to analyzing the samples. Depending on the aims of the experiment, not all parameters are equally important to optimize for the analysis, so only relevant parameters are optimized. However, a signal-to-noise ratio (SNR) should be determined as per a lab manual as it is vital for the quantitative measurements (Weber et al., 1998; Eaton et al., 2010). The derivative of the P2P amplitude of the EPR spectrum depends on the following parameters (Brustolon and Giamello, 2009).

$$\Delta S_{pp} \propto t \times B_{mod} \times \eta \times Q \times \sqrt{P} \qquad (3.13)$$

Where $p$ is the microwave power that is not saturated, $B_{mod}$ is the field modulation amplitude,

which should be smaller than P2P linewidth ($\Delta B_{pp}$), $t$ is the measurement time during which the dosimetric signal amplitude accumulates and grows linearly. The filling factor ($\eta$) and $Q$-value should be maximum as described in Section 3.2.3 (microwave resonator). Three groups of spectrometer parameters are responsible for the EPR spectrum acquisition:

(1) Magnetic field

(2) Microwave

(3) Signal channel parameters

These fundamental parameters can be seen on the basic layout of an X-band CW EPR spectrometer, as depicted in Figure 3.20. This section aims to provide the EPR acquisition parameters of the X-band CW EPR spectrometer, which is commonly used in tooth enamel retrospective dosimetry and dose reconstruction (Brustolon and Giamello, 2009; IAEA, 2002; Fattibene and Callens, 2010; ICRU, 2002).

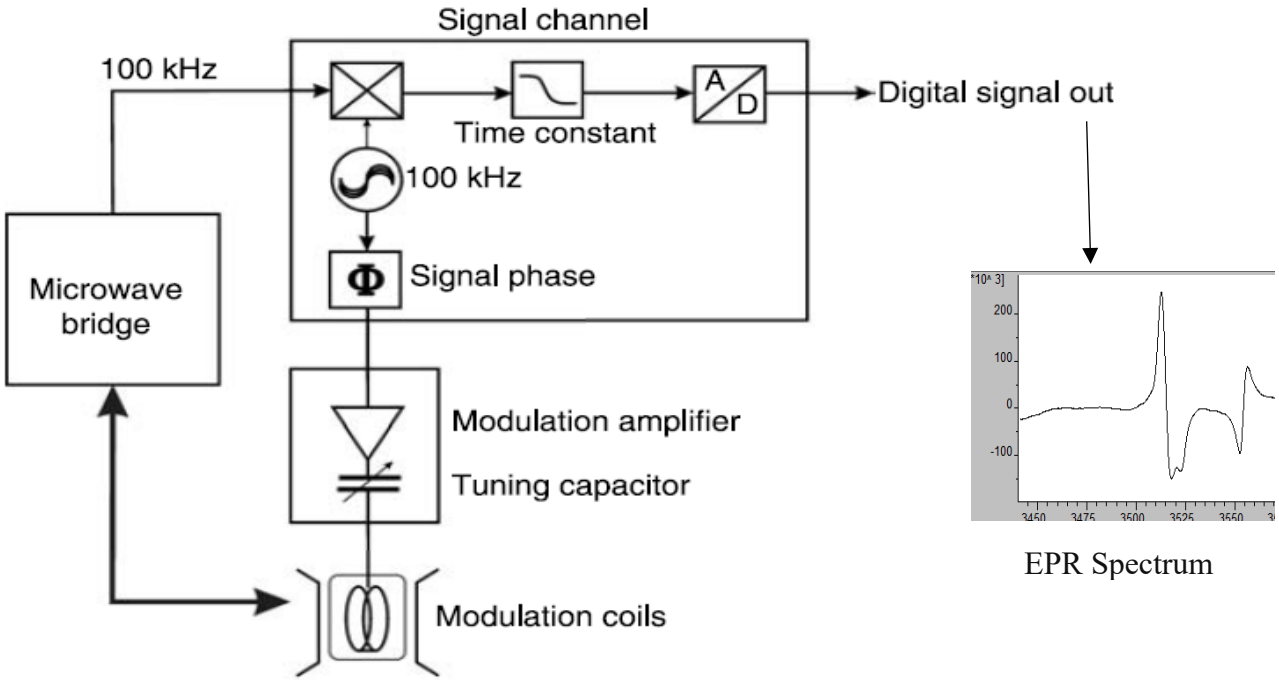


**Figure 3.20:** Block diagram of an X-band CW EPR spectrometer with the microwave bridge, signal channel, and the magnetic field parameters. From Brustolon and Giamello (2009).

3.3.1.1 **Microwave parameters**

A typical frequency of the X-band CW EPR spectrometer is close to 9.8 GHz, which means the loaded microwave cavity gets that frequency during the sample analysis (IAEA, 2002). Besides microwave frequency (*v*), another critical parameter in EPR dosimetry is microwave power (*mW*). The microwave power should adjust adequately to achieve the highest dosimetric to native signal ratios (i.e., higher spectral resolution). In other words, the microwave power should be set at a value below that at which the power saturation curve deviates from linearity, as shown in Figure 3.22 (Eaton et al., 2010; Skvortzov et al., 1995). If too much power is used, the EPR lines are broadened or distorted due to saturation, as shown in Figure 3.21, which could not provide the quantitative EPR results (particularly for measuring the spin concentrations) (Eaton et al., 2010).

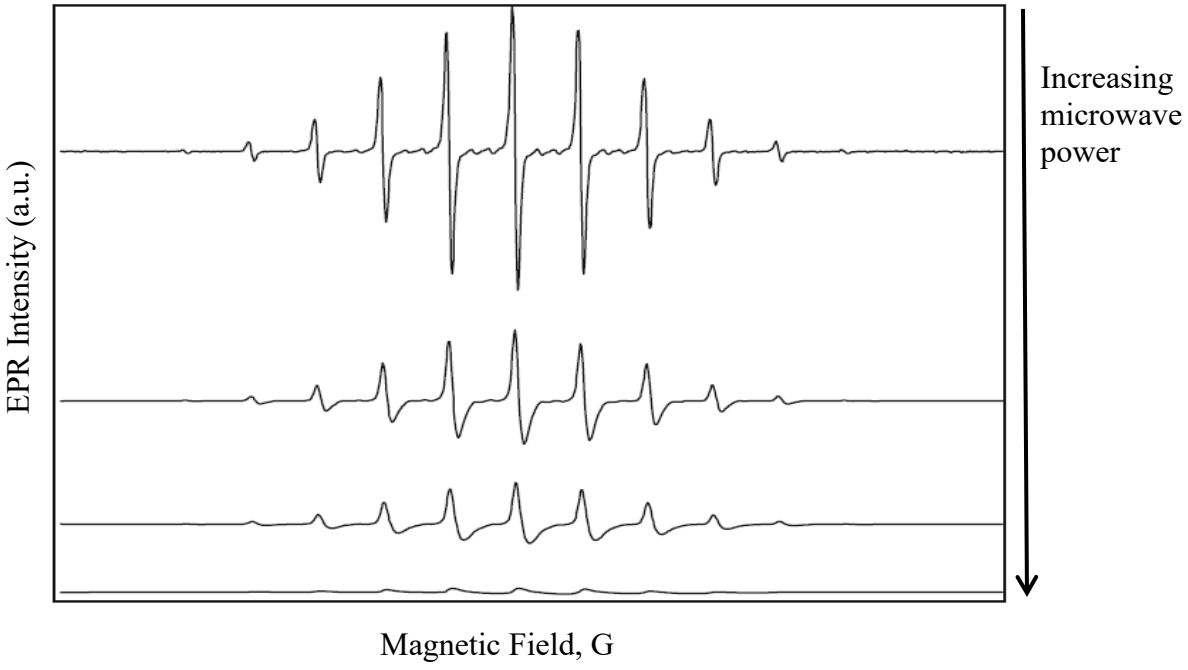


**Figure 3.21:** The microwave power increases from top to bottom, broadening or distorting the EPR lines in the EPR measurements. From Eaton et al. (2010).

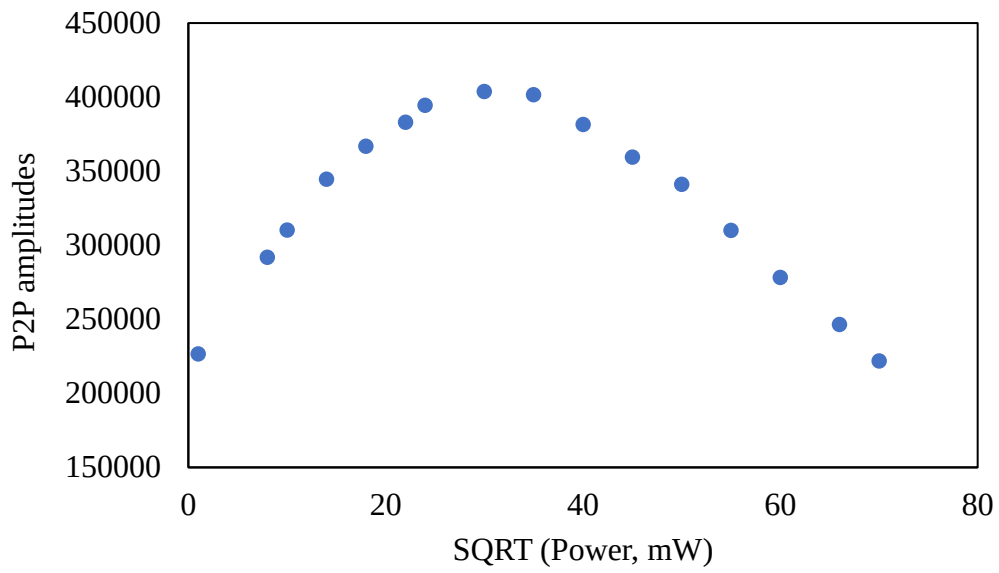


**Figure 3.22:** The power saturation curve for tooth enamel. The microwave power should be set to a value below that at which the power saturation curve deviates from linearity.

In this experiment, the saturation curve deviates at 24 mW, so the optimum power for the dosimetric analysis was 24 mW, as shown in Figure 3.22. Without appropriate power optimization, the EPR spectrum would be broadened and distorted, not estimating the accurate dose. Therefore, selecting the proper microwave power for a better spectral resolution is crucial for the accuracy and reproducibility of the results. The EPR signal intensity grows as the square root of the microwave power (mW). Generally, most power saturation curves show a linear range (non-saturating) at low microwave power and non-linear (saturation) at high power (Eaton et al., 2010). In the absence of microwave power saturation, the linear range of the EPR spectrum increases with the square root of microwave power. To check the linear range (non-saturating) for a given sample, increase the power by a factor of 4 (i.e., decrease the attenuation by 6 dB). In this condition, the EPR spectral amplitude should be increased by a factor of 2; if we do not get this value, reduce the value, and try again until we get that value, the process is called a *progressive saturation study* in EPR (Eaton et al., 2010; Barr et al., 2008). The required microwave power for better spectral

resolution depends on the microwave cavity type (Ivannikov et al., 2002; IAEA, 2002). The frequency noise and temporal drifts can be removed by analyzing samples in ambient temperature and cooling water temperature, which improve the reproducibility of the EPR measurements (IAEA, 2002; Eaton et al., 2010; Brustolon and Giamello, 2009). Also, increasing microwave power will decrease the receiver gain because the EPR lines will be broadened (Eaton et al., 2010; Barr et al., 2008). To obtain the quantitative EPR results, the receiver gain must be optimal (not too low and too high), as shown in Figure 3.23.

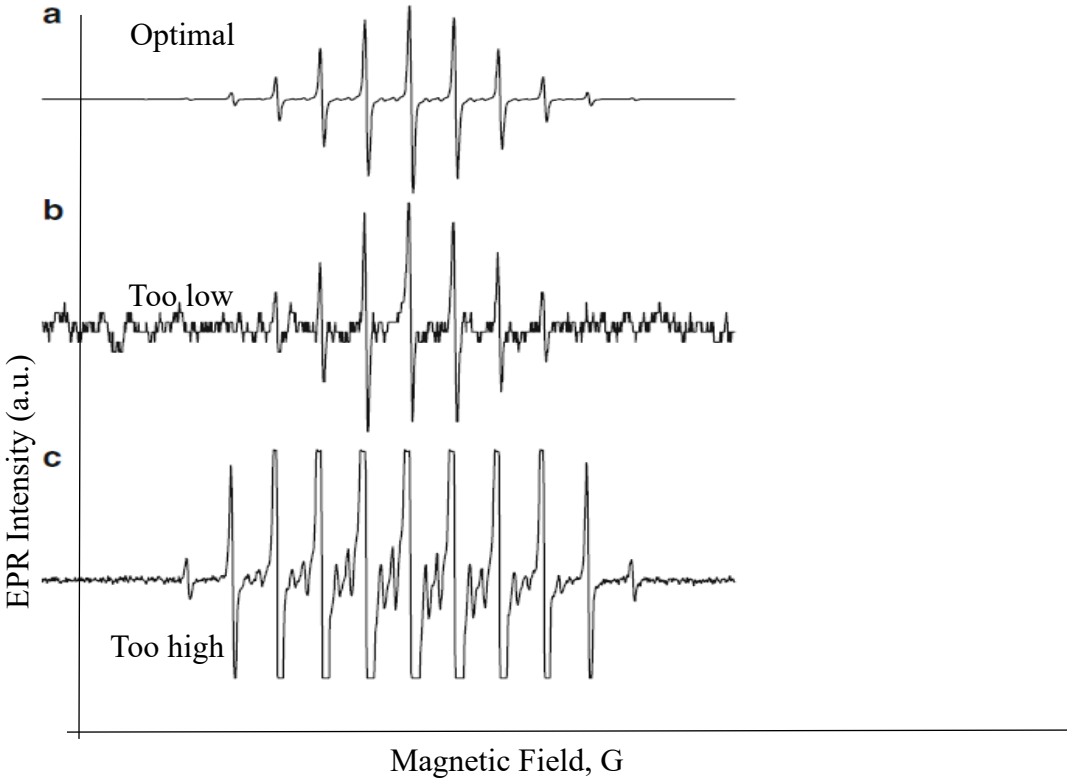


**Figure 3.23:** Effects of the receiver gain settings in the EPR spectrum. **(a)** Optimal receiver gain. **(b)** Insufficient receiver gain. **(c)** Excessive receiver gain. From Eaton et al. (2010).

### 3.3.1.2 Magnetic field parameters

The magnetic field at resonance is determined by microwave frequency. A typical value of the center of the magnetic field sweep for the X-band CW EPR spectrometer (frequency 9.8 GHz)

is 350 mT (3500 Gauss), and an EPR signal with a g-factor near 2.0. The sweep width magnetic parameter is determined by the type of post-recording spectrum and is mainly used for the dosimetric signal evaluation. (IAEA, 2002; Wieser et al., 2000; Eaton et al., 2010; ISO, 2013). Two types of magnetic field parameters, the *center field* and *sweep width* constant magnetic field, are used in the EPR spectrum acquisition. The time of sweep and resolution are related to the spectrometer signal channel parameters. However, they are included in the magnetic field parameters for practical reasons (IAEA, 2002; Eaton et al., 2010). The center field is determined by the microwave frequency ($v$) as per equation (3.3) and chosen in such a way that the dosimetric signal of tooth enamel is placed in the center of the magnetic field sweep (IAEA, 2002). The magnetic field sweep time is the number of channels used in spectrum acquisition (spectrum resolution) and the accumulation time of each channel, which is in between 20 and 80 seconds. The number of channels used by signal channels (i.e., analog-to-digital converter) for spectrum acquisition is called the resolution of the EPR spectrum. For a sweep width of 10 mT, the 1024 channel resolution is used (IAEA, 2002; Eaton et al., 2010).

#### 3.3.1.3 Signal channel parameters

For a better spectral resolution (i.e., to increase the signal-to-noise ratio), the modulation frequency should be set as high as possible; however, the highest modulation frequency in most commercial EPR spectrometers is 100 kHz. At low modulation amplitude, the height of the EPR spectrum increases; however, if the modulation amplitude is too high, the EPR signal broadens and becomes distorted (and reduces signal resolution), often called “over-modulation,” as shown in Figure 3.24b. Therefore, the optimum modulation amplitude is determined by plotting the EPR intensity versus modulation amplitude, as shown in Figure 3.24a. The highest amplitude in the graph (4 G for tooth enamel) is the optimum value for the quantitative EPR measurements (Eaton

et al., 2010). The modulation amplitude should not exceed the linewidth ($\Delta B_{pp}$) of the EPR signal (ISO, 2013). The width of the EPR signal from tooth enamel was 5 G, as described in Chapter 4 (Section 4.3.1), which was lower than the modulation amplitude (4 G).

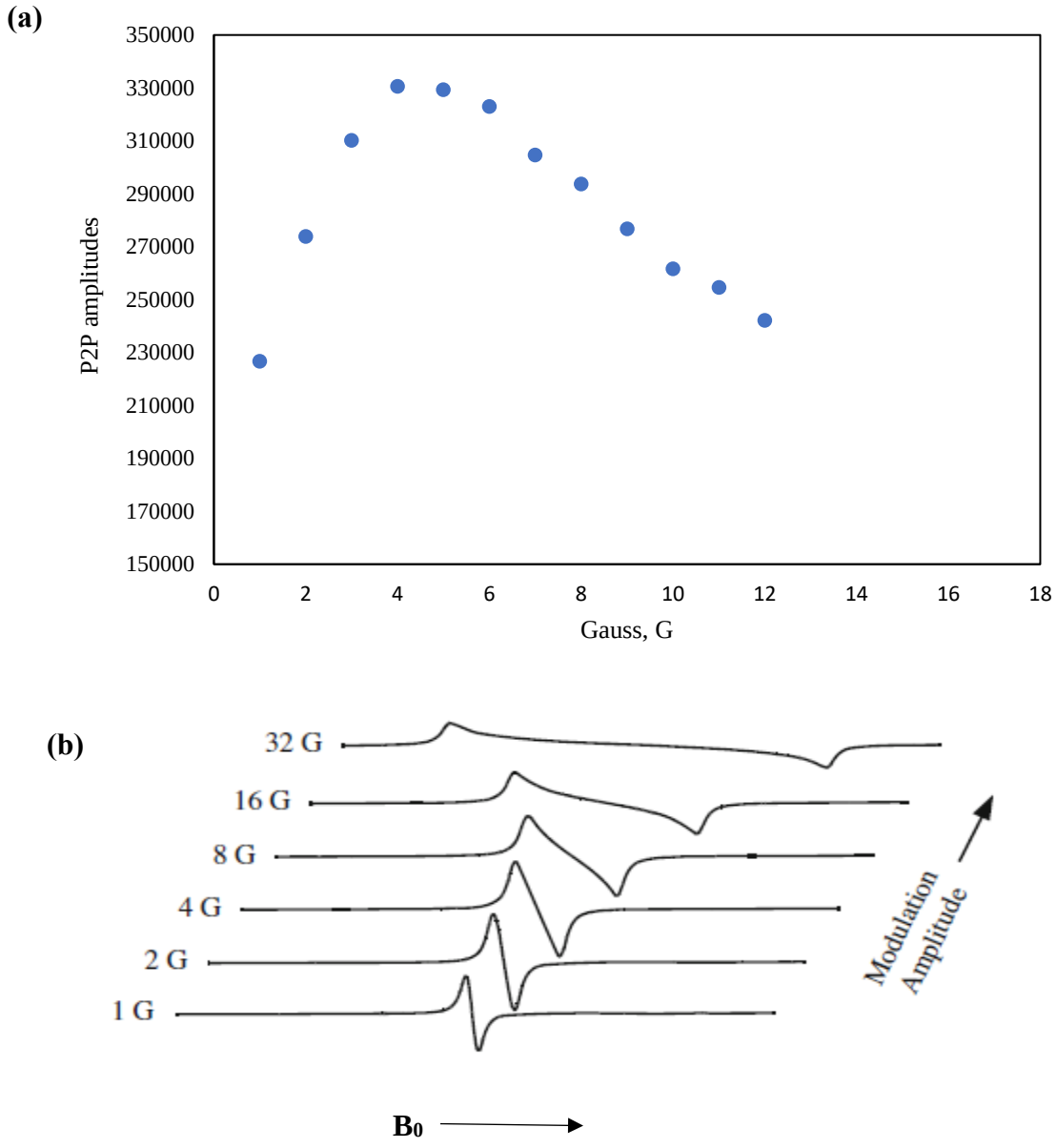


**Figure 3.24: (a)** Determination of the optimum modulation amplitude in tooth enamel. **(b)** The shape of the DPPH EPR intensity with the increase in the modulation amplitude from 1-32 G. From Eaton et al. (2010).

3.3.1.3.1 **Time constant**

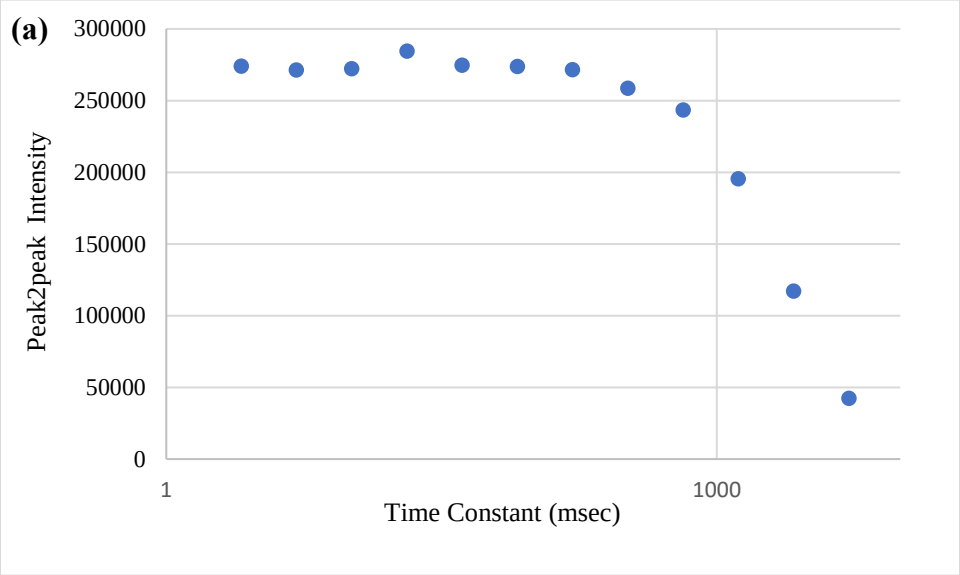


The time constant should be sufficiently long to filter out undesirable noises, yet short enough that it does not distort the EPR signal (Eaton et al., 2010). Therefore, the sample was analyzed in different time constants and measured the EPR intensity to determine the optimum time constant. The optimum EPR intensity for tooth enamel was found at a 327.68 msec time constant, as shown in Figure 3.25a. Although the signal-to-noise ratio (SNR) increases when the time constant is increased, the spectrum is distorted if the time constant is too long, as depicted in Figure 3.25b (Eaton et al., 2010; Brustolon and Giamello, 2009). If a long-time constant is used to see a weak signal, the time needed to scan a single EPR signal must be ten times higher than the time constant (Weber et al., 1998). That is why it is vital to optimizing a time constant for the quantitative low dose measurement using EPR. Additionally, the phase-sensitive detection with magnetic field modulation can significantly increase our sensitivity in the measurements; however, the appropriate modulation amplitude, frequency, and time constant must be chosen prior to the experiments (Weber et al., 1998). These variables distort the EPR signals and make the spectrum interpretation difficult.

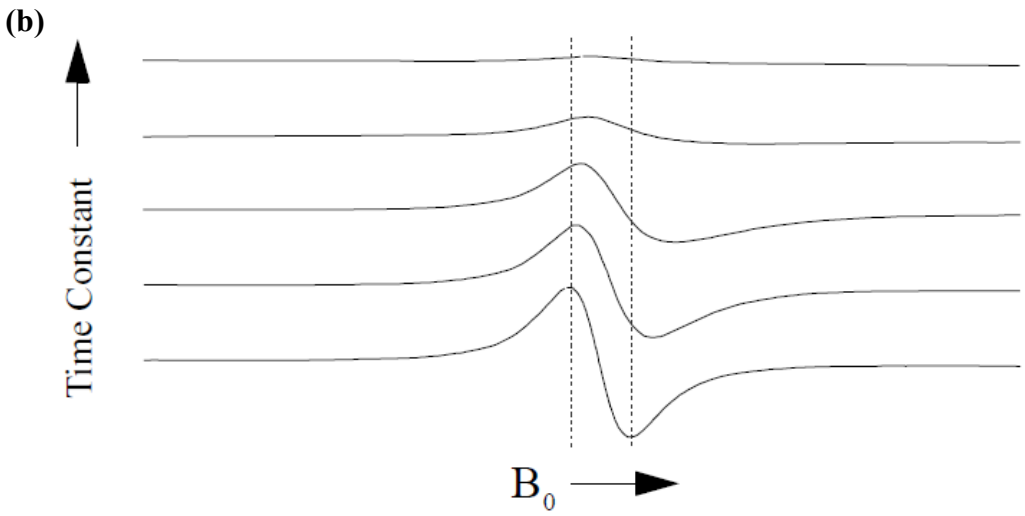


**Figure 3.25: (a)** Optimization of the time constant by plotting the EPR intensities against time constants. **(b)** Effect of using a progressively longer time constant. From Weber et al. (1998).

3.3.1.3.2 **Conversion time**

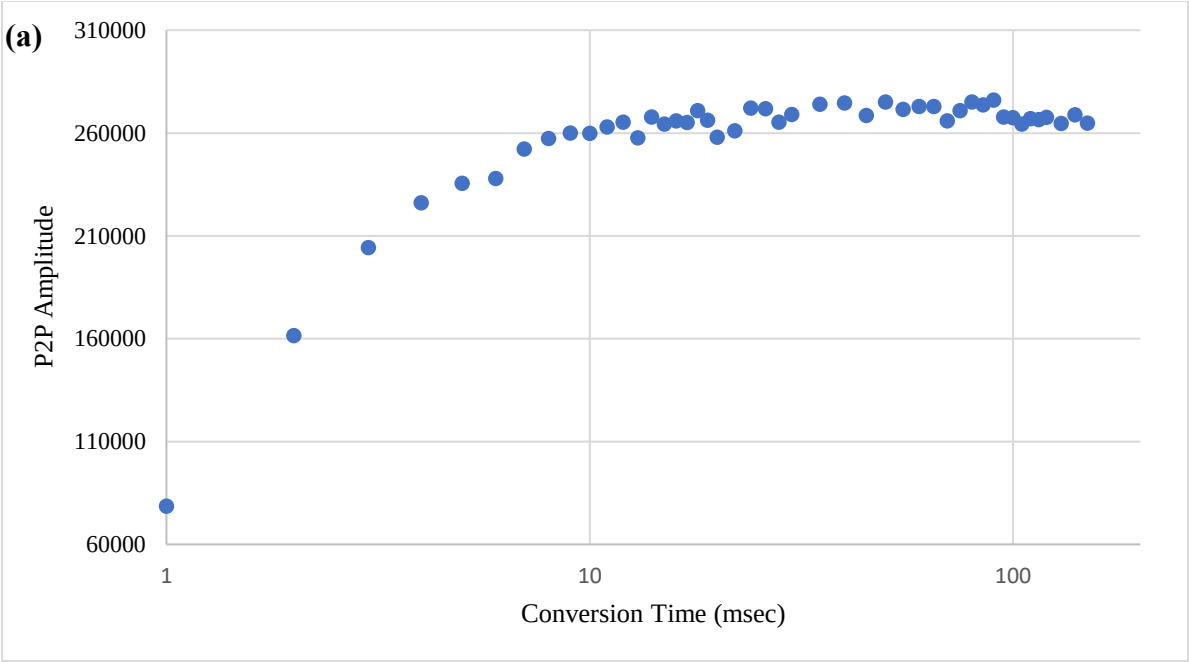

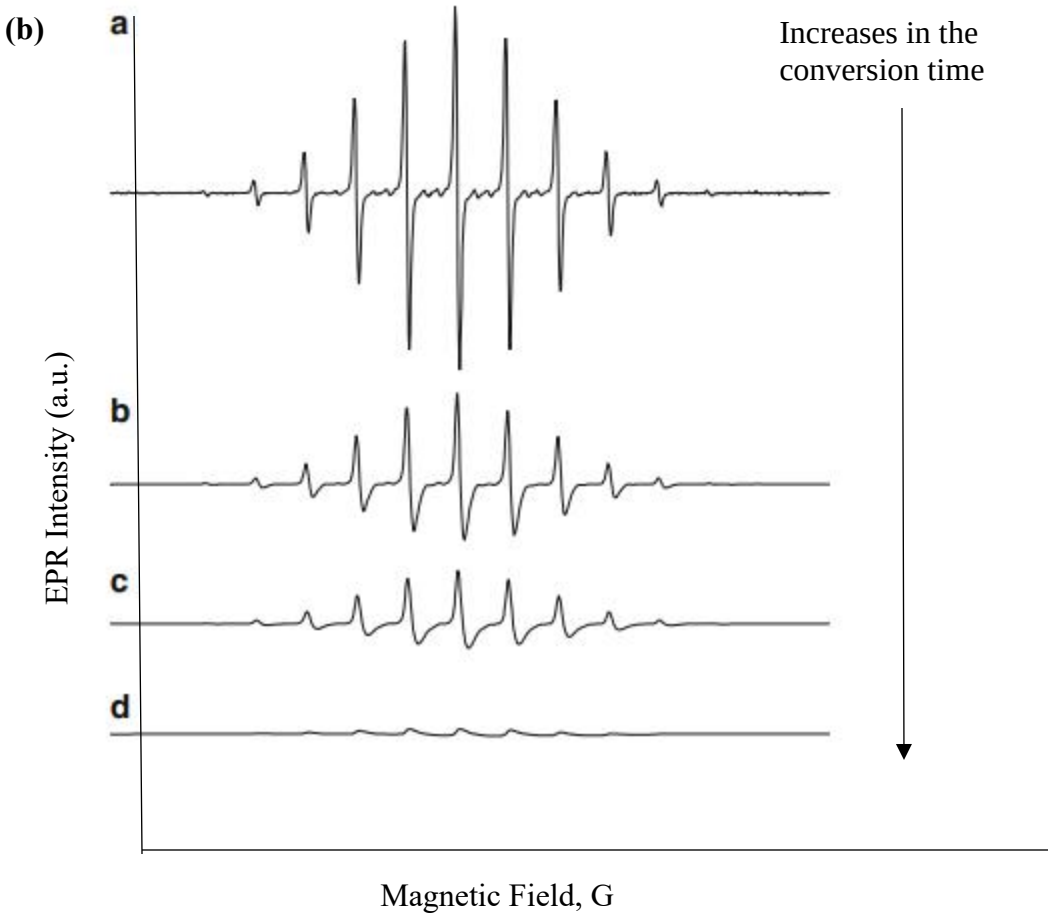


**Figure 3.26: (a**) Sweep and conversion time effects on the EPR intensity measurements. **(b)** Decrease in the resolution of an EPR spectrum due to increases in the conversion time from **(a)** to **(d)**. The spectrum nearly disappears with a longer conversion time at **(d)**. From Eaton et al. (2010).

The conversion time is when the analog to digital converter (ADC) accumulates the signals and noises at each magnetic field step of the EPR experiment (Eaton et al., 2010). The conversion time was optimized by measuring an EPR spectrum at different conversion times, as shown in Figure 3.26a, and found that the tooth enamel EPR signal was the highest at the conversion time of 41 msec, which was the optimum conversion time for this experiment (Eaton et al., 2010; Brustolon and Giamello, 2009). As seen in Figure 3.26b, the decrease in resolution of the EPR spectrum is due to an increase in the conversion time, and eventually, the spectrum nearly disappears with the long conversion time (Eaton et al., 2010).

3.4 **Optimizing sample mass and loading a tube into an EPR resonator**

Optimizing the sample mass and position in a resonator is crucial for reproducible and comparable results. Each type of EPR resonator, especially for the X-band measurements, has an optimum sample mass and a sample tube placement in the resonator for a particular sample, often called a 'working volume'. The optimum sample mass and the sample tube position depend on the inner diameter of a sample tube. Even if the sample is the same type, the mass and position need to be optimized if the tube's inner diameter changes (Eaton et al., 2010). The detailed procedure for optimizing the sample mass is described in Chapter 5 (Section 5.3.1).

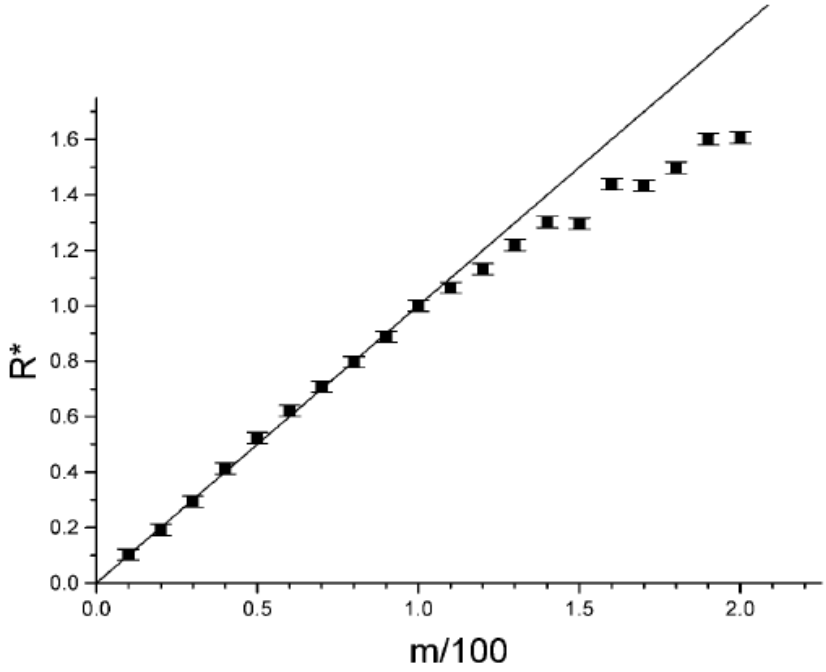


**Figure 3.27:** Dependence of a tooth enamel signal intensity on the sample mass normalized to their values at 100 mg (m/100). From Zhumadilov et al. (2005).

The dependence of the sample mass with an EPR intensity is clearly seen in Figure 3.27. In the sample mass up to 100 mg, the sample mass and intensity are linearly within 1.5%. However, at a higher sample mass (>100 mg), the linearity was deviated up to 6% at 130 mg and up to 25% at 200 mg. As the mass increases, the length of the sample inside the cavity will leave the uniform

region (i.e., high magnetic field) of the magnetic field inside the cavity (Zhumadilov et al., 2005). This clearly shows that the sample mass optimization is vital for the quantitative low dose measurement in EPR tooth enamel dosimetry.

### 3.5 Tuning the microwave bridge and cavity

The microwave bridge control parameters should be fixed as the AFC modulation to 60%, AFC AC gain to 60%, and the AFC DC Gain to 1/10, as shown in Figure 3.28a. The bridge should be tuned each time we put the samples into the cavity or move the sample or an internal standard into the cavity and start a new analysis. In modern spectrometers, the tuning process is automated. Once operators fix the microwave bridge parameters, click on the tune button (there are three modes for the microwave bridge: Stand by, Tune, and Operate), which automatically tune the bridge (Barr et al., 2008; Weber et al., 1998). At 'critical coupling' (i.e., "when the impedance is properly matched between the resonator and transmission line") (Barr et al., 2008), the microwave power incident on the resonator is completely absorbed in the resonator, and none of the power is reflected to the detector. The tuning "dip" is plotted as the microwave absorption versus frequency (GHz). Ideally, zero power is reflected at 'critical coupling,' so the 'dip' should be as deep as it will go, as depicted in Figure 3.28b (Barr et al., 2008; Eaton et al., 2010). As long as the experimental parameters, conditions of measurements, and samples are the same, reproducible tuning can be achieved through this process. It is crucial to properly tune the microwave bridges before analyzing samples for the quantitative EPR measurements (ISO, 2013).

**(a)**

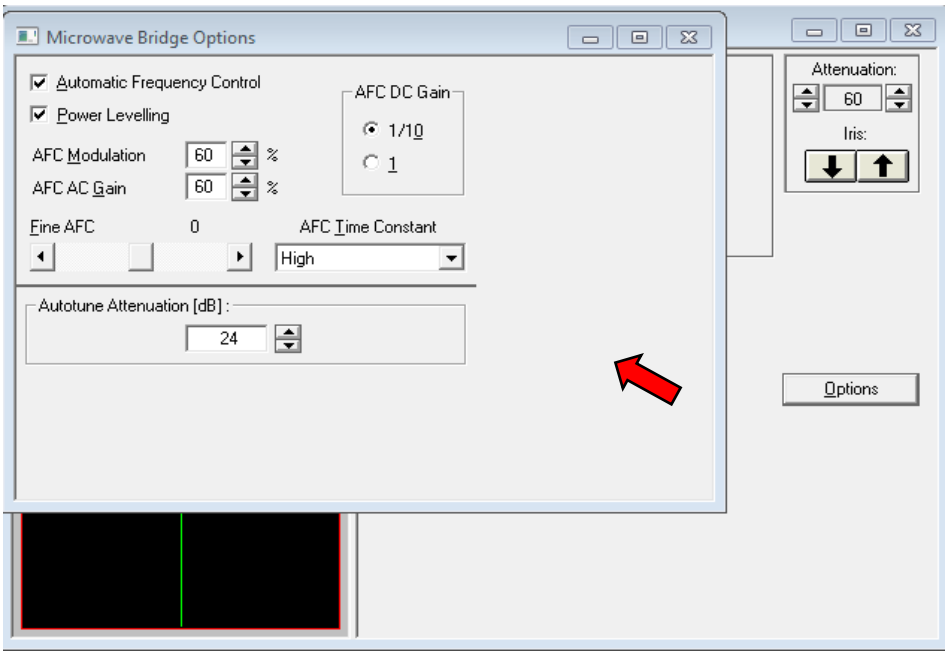


**(Resonator mode)**

**(b)**

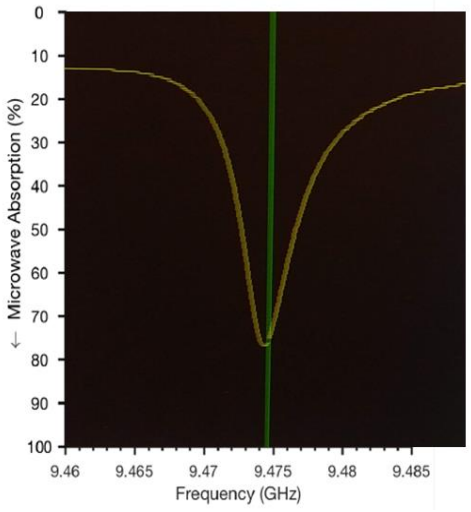


**Figure 3.28: (a)** Microwave bridge control option for solid samples, the AFC modulation and gain should be 60%, and the AFC DC Gain should be 1/10. **(b)** The microwave bridge cavity tuning and a resonator mode.

## 3.6 The Bruker ER 4119HS-2100 internal standard for normalizing an EPR spectrum

Since the Q-value of the cavity, the magnetic field/microwave frequency, and detector current vary during the EPR measurements, it is hard to get a consistent result even if the same

sample mass is used in each measurement. Using a permanently mounted internal standard, often called the marker accessory (i.e., Bruker ER 4119HS-2100 internal standard), as depicted in Figure 3.29b (also called an amplitude monitor in the cavity), one can minimize these unavoidable instrumental variances in EPR measurements. This can be done by measuring a dosimetric signal and reference standard simultaneously and using the ratio as an EPR intensity, as shown in Equation 3.14 and Figure 3.30 (Eaton et al., 2010). The position of the marker affects the intensity of the marker signal. By plotting the EPR intensities of the marker against the position (millimeter), we have to find out the best setting for our samples by ourselves. The best position for the sample was 13 mm due to the compatible P2P height amplitude (20818) with the test samples analyzed, as depicted in Figure 3.29a. Also, the position of the marker must be changed by rotating (either rotating clockwise or anticlockwise) the screw in the same direction to ensure reproducibility.

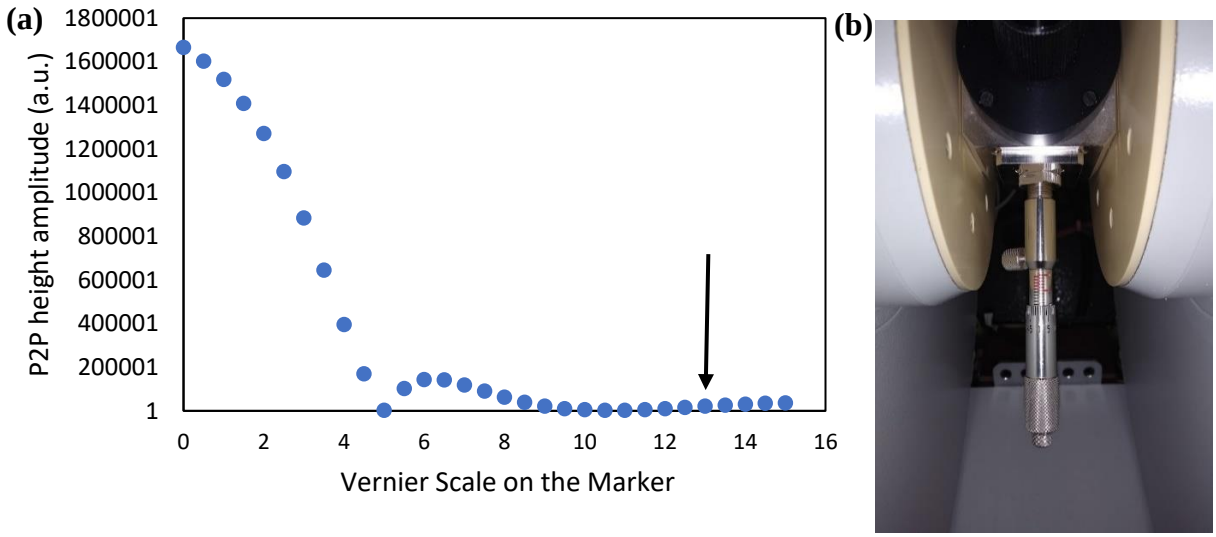


**Figure 3.29: (a)** The Bruker ER 4119HS-2100 internal standard: An intensity curve as a function of position. **(b)** Position of the marker accessory (Bruker ER 4119HS-2100 internal standard) in an EPR resonator.

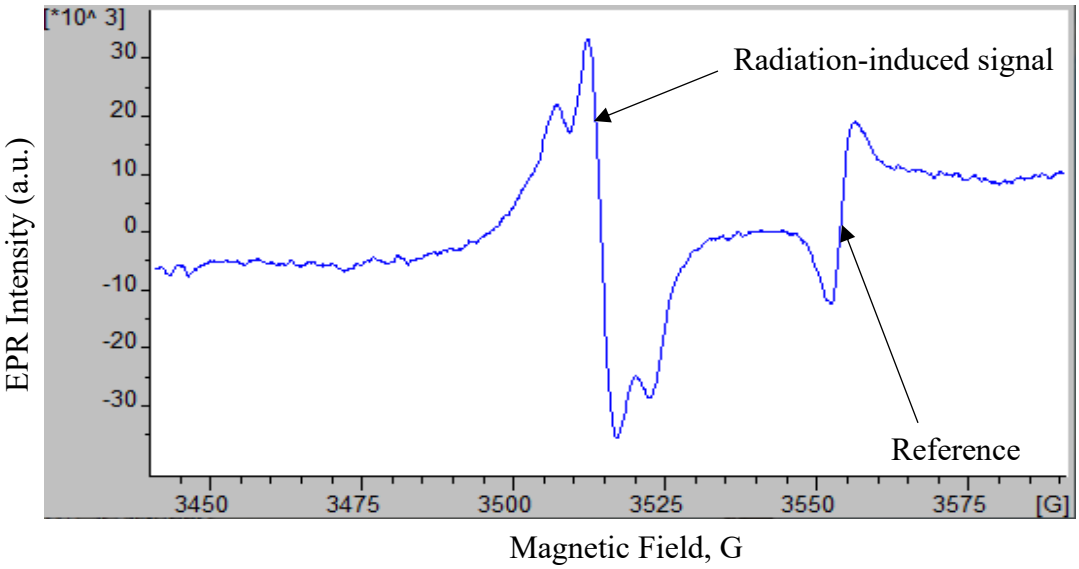


**Figure 3.30:** An EPR spectrum from tooth enamel irradiated to 5 Gy using the gamma source (Hopewell G-10), and a signal from the internal standard was used to normalize the radiation-induced signal.

$$Measured\ Value = \frac{Sample\ Intensity}{Reference\ Standard\ Intensity} \tag{3.14}$$

When a sample intensity is divided by the intensity of the reference standard, small deviations that arise from the fluctuation in temperature, humidity, and microphonics are not introduced as errors in the measurements. The dosimetric signal (sample) and the reference standard or marker accessory experience the same changes in the measurements. So, even if the sample intensity changes in the measurements, the ratio of a sample EPR intensity to the intensity of the marker accessory remains the same (Eaton et al., 2010). Similarly, a g-factor of the reference standard can be used to normalize the g-factor of a sample.

### 3.7 **Monitoring reproducibility or repeatability**

The closeness in measurement data obtained from the same quantity sample under the changed condition, such as different observers (or different labs for standardization of methodology), different instruments, times, etc., are called reproducibility or precision of the

measurements (IAEA, 2002). The periodic reproducibility check is crucial to ensure the operating conditions are expected and accurate. The frequency of measurements depends on the stability of the spectrometer and the type of measurements (ISO, 2013). For example, if we are measuring low doses quantitatively, it is always better to do more reproducibility tests than less. The reproducibility is measured in the standard deviation or relative standard deviation (RSD). In EPR tooth enamel dosimetry, the measurement reproducibility can be improved by:

(1) Making the grain sizes in the range of 0.5-1 mm as smaller grain size produces background and other unwanted signals;

(2) Since the sample positioning influences an EPR intensity in a cavity, the sample positioning must be determined at the high magnetic ($B_1$) and low electric ($E_1$) fields in the cavity;

(3) Rotating and averaging the EPR signals to eliminate the errors from the sample anisotropy as tooth enamel is a crystalline material;

(4) g-factor normalization using the Bruker ER 4119HS-2100 internal standard.

**3.8 Anisotropy correction using a goniometer**

As described in Chapter 4 (Section 4.3.2) and Chapter 5 (Section 5.3.3), crystalline materials' EPR intensities change with the rotation angle, from 0° to 360° relative to the constant magnetic field direction in a resonator. Two methods are generally used to reduce errors from the sample anisotropy: (1) use extremely small grain sizes (finely powdered sample) whereby the sample changes into amorphous form and the sample anisotropy arises from the crystalline sample can be reduced, and (2) use the larger grains (>0.5 mm) but rotate the sample during the EPR measurements using a goniometer as depicted in Figure 3.31a and 3.31b, then summed and averaged after their g-factor normalization.

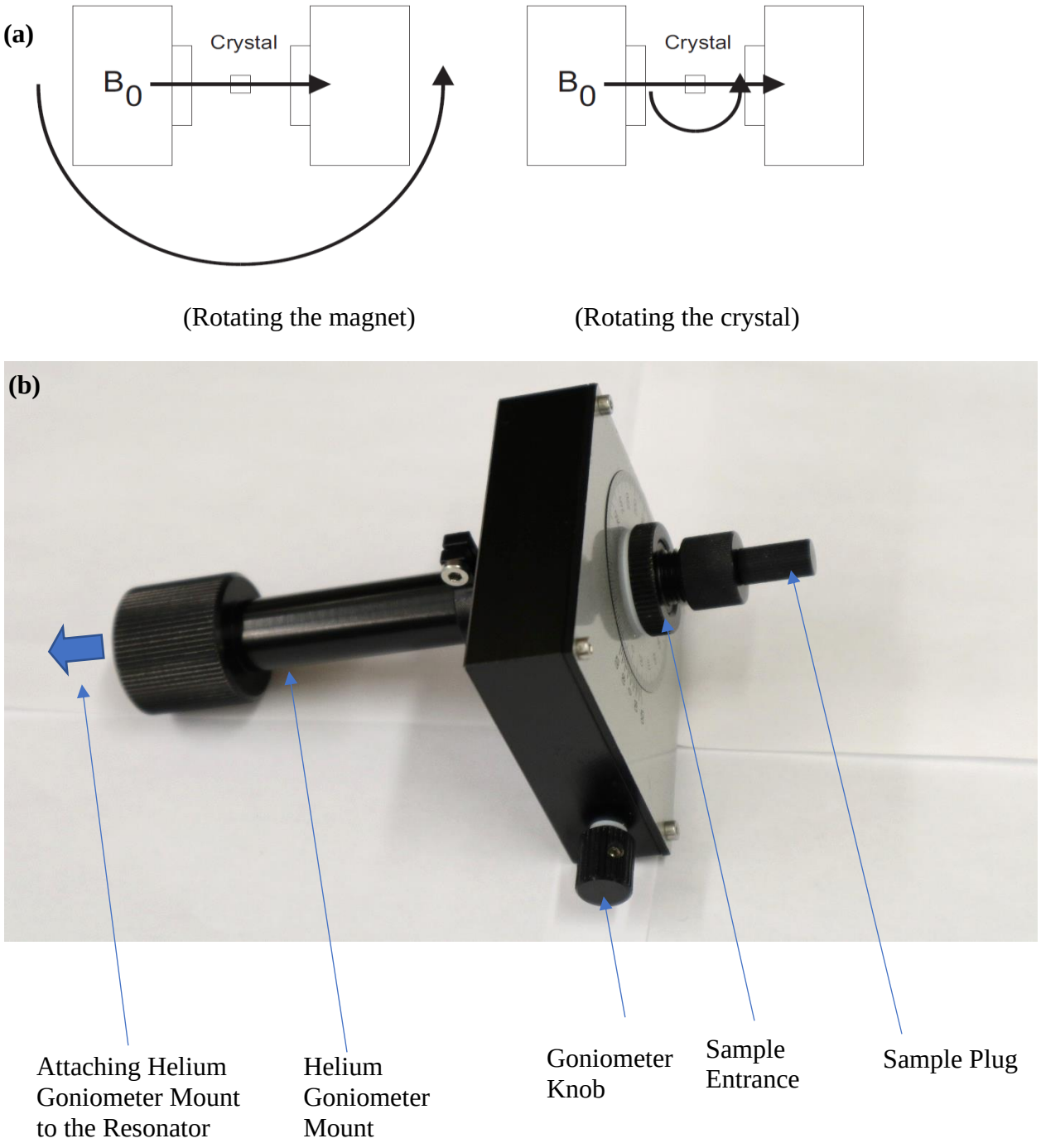


**Figure 3.31: (a)** Two means of changing the orientation of $B_0$ with respect to the crystal. The orientation of $B_0$ can be changed by rotating the magnet. A more convenient way is rotating the crystal with respect to the magnetic field ($B_0$). **(b)** The Bruker E218G1 1 axis manual goniometer. A sample is rotated by rotating the goniometer knob.

However, the first method is unworkable because the small sample size produces the background noises and mechanically induced signals (Haskell et al., 1997). Therefore, the second method is widely used for the quantitative measurement of low doses. Standard deviation or relative standard deviation is calculated to determine the errors due to the sample anisotropy as described in Chapter 5 (Section 5.3.3). Furthermore, some study has shown that due to the anisotropy of the dosimetric $^{\bullet}CO_2^-$ signal, the intensities of the g// and g⊥ signals of tooth enamel can vary by 50% (Aoba et al., 1982), contributing to errors in a low dose measurement.

Therefore, the anisotropy of the dosimetric signal can cause the main errors in the accurate low dose determination in EPR tooth enamel dosimetry. The use of a constant rotation goniometer, as shown in Figure 3.31b, reduces the effect of anisotropy by averaging the EPR spectra. Also, using a goniometer makes the measurement possible at all microwave power, where the sensitivity of the radiation-induced signal is enhanced, and accompanying anisotropies suppressed. Which eventually increases the accuracy and reproducibility of the EPR measurements in low-level dosimetry (Haskell et al., 1997; Hayes et al., 1998). The sample was inserted through the sample plug, and the helium goniometer mount was properly screwed into the EPR resonator, as depicted in Figures 3.31b and 3.32. The sample was rotated at the desired angles using the goniometer knob, as shown in Figure 3.31b. Proper handling of a goniometer and measuring an angle at each measurement is vital for the quantitative low dose measurement in EPR dosimetry.

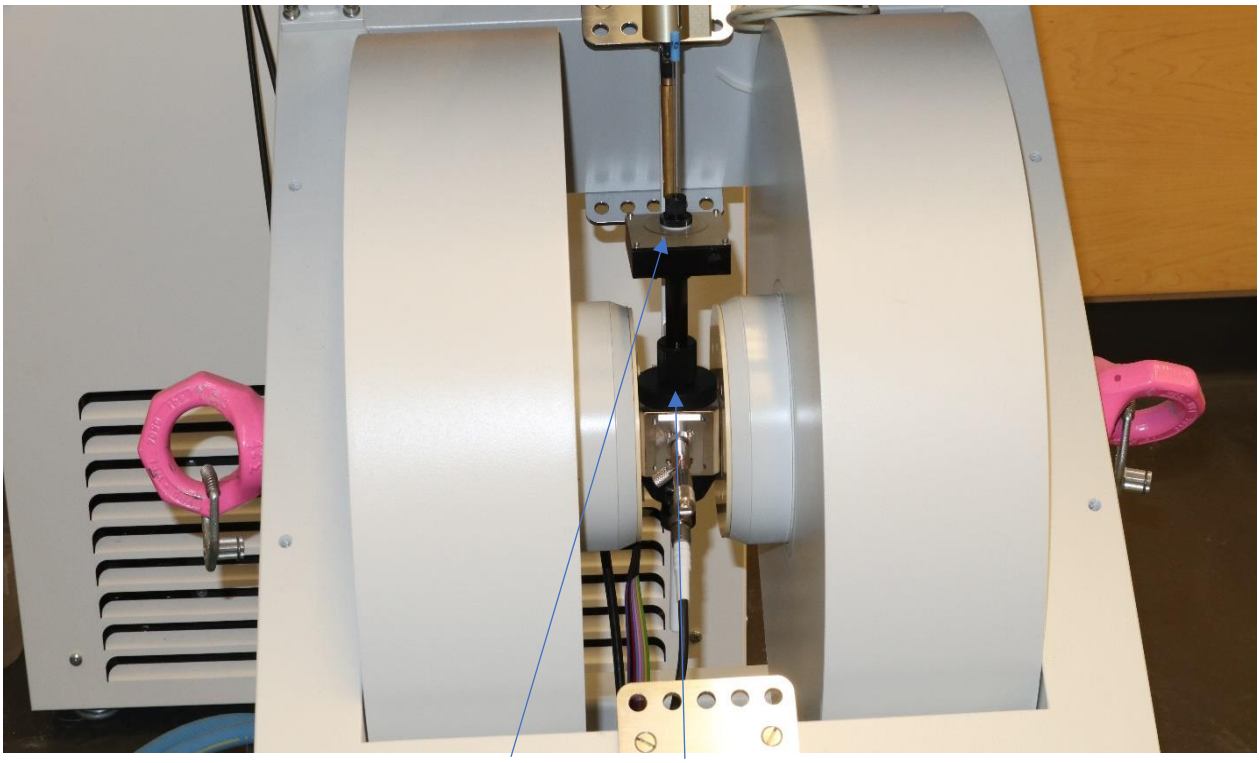


**Figure 3.32:** The Bruker E218G1 1 axis manual goniometer is mounted in the EPR resonator.

### 3.9 EPR calibration and internal standards

The routine calibration of the EPR spectrometer using the DPPH (α, α'-diphenyl-β-picryl hydrazyl) or BDAP (1,3-bisdiphenylene-2-phenylallyl), and the system performance tests (i.e., a signal to noise ratio and the cavity background tests) using the weak pitch sample are vital in order to obtain the quantitative EPR spectra (Eaton et al., 2010). Also, the in-cavity ER 4119HS-2100 marker accessory (i.e., internal standard) is used for the Landé g-factor calibration of tooth enamel EPR measurements as described in Section 3.6 (Hayes et al., 1998).

### 3.10 Determination of the absorbed dose in the samples

#### 3.10.1 Determination of a radiation-induced signal

The P2P height of an EPR spectrum is measured to estimate the absorbed dose. However, a low dose measurement is extremely challenging due to invisible dosimetric signals and the impurities' background signals, which generally mask the dosimetric signals. The dosimetric signals isolation can be done as follows:

1. Subtraction of an irradiated sample (EPR spectrum) with an unirradiated sample (EPR spectrum);
2. Complete separation of dentin from enamel using both chemical and mechanical methods;
3. The application of the dose spiking method. The low dose measurement in tooth enamel EPR dosimetry is always challenging due to the weak and overlapping dosimetric signals. However, the dosimetric signal is distinctly visible from noises at a high dose and can be measured with a high degree of precision and accuracy. That is why the dose spiking EPR technique is used to make the dosimetric signal visible, as described in Chapter 5 and the method described by Harvey (2000) and Geso et al. (2018).

#### 3.10.2 Conversion of the EPR signal into an absorbed dose

##### 3.10.2.1 Calibration curve method

As described in Chapter 1 (Section 1.1.1), the peak-to-peak (P2P) amplitude height of the major EPR line (R) was used as the dose parameter. The dose precision at low doses was significantly increased using the P2P amplitude height as it was easier to measure. The integration problems associated with the spectrum baseline and the background signals were reduced using this approach (Brustolon and Giamello, 2009). In the conventional EPR tooth enamel dosimetry,

the calibration curve converts the EPR signal into an absorbed dose. The calibration curve is expressed as $y = mx + c$ (regression line), then the original dose is expressed by

$$x = \frac{y-c}{m} \quad (3.15)$$

(Brustolon and Giamello, 2009). The actual or total dose in tooth enamel (*Dx*) is calculated by subtracting the background dose from the total measured dose ($D_T$) described in Section 3.10.3.

**3.10.2.2 Dose additive method**

In addition to the calibration curve method, the dose additive method has also been used to determine the low doses in different samples for retrospective and accident dosimetry. In this method, the same sample is irradiated multiple times and extrapolates a graph to determine the low or accident doses described in Section 1.2.1 (Chapter 1).

3.10.3 **Total dose determination**

In tooth enamel EPR dosimetry, the total dose ($D_X$) is the sum of the several components such as the natural background dose $D_{BG}$, total dose from the ultraviolet (*UV*) radiation in incisor teeth $D_{UV}$, radiation dose from diagnostic and medical dental procedures $D_{X-ray,}$ and the total radiation dose ($D_T$) measured through the EPR spectra analysis. The following equations are used to calculate the total dose ($D_X$) in tooth enamel (Bailiff et al., 2016: Ivannikov et al., 2001).

$$D_X = D_T - D_{BG} - D_{UV} \quad (3.16)$$

$$D_{BG} = A_{te}\dot{D}_{BG} \quad (3.17)$$

The background dose ($D_{BG}$) in tooth enamel is calculated using equation 3.17, where $A_{te}$ = tooth enamel age and $\dot{D}_{BGS}$ is the dose rate of the environmental exposure. The $D_{UV}$ is usually observed in the buccal parts of the front teeth (i.e., incisors) and may be unsuitable for EPR dosimetry. However, the molars, premolars, and canine teeth are recommended for the EPR tooth

enamel dose reconstruction (Ivannikov et al., 2001; IAEA, 2002). The total dose ($D_X$) determined through these EPR measurements and subsequent calculations using equation 3.16 would be an actual dose in tooth enamel. Thus, the EPR tooth enamel dosimetry will determine the total anthropogenic doses (Ivannikov et al., 2002; Bailiff et al., 2016).

### 3.11 EPR Dose reconstruction process for retrospective and accident dosimetry

The lingual dose of tooth enamel will be determined using EPR. The average lingual doses with the standard deviation will be plotted as a function of the ages. The best-fit line will be drawn, which is a trendline in an excel plot. The slope of the line will be calculated to determine the dose rate per year (mSv/year) for each age group in a population (Toyoda et al., 2011). Suppose the calculated dose rate is x mSv/year and the natural background is y mSv/year. Then the difference in the doses (equation 3.18) is from the anthropogenic sources (i.e., anthropogenic components of the total EPR dose) (Toyoda et al., 2011; Fattibene and Callens, 2010).

$$Anthropogenic\ dose\ (a) = (x - y) = b\ mGy/\text{year} \qquad (3.18)$$

People's historical dose can be calculated from this anthropogenic dose by subtracting each year's background dose; this is called the retrospective EPR dosimetry (Toyoda et al., 2011).

### 3.12 Measurement uncertainty

For meaningful results, the data obtained from EPR measurements should be accompanied by an uncertainty estimate or analysis. The measurement uncertainty can be identified as one of the two categories:

1. Type A: those evaluated by statistical methods such as standard deviation, percentage, etc.; or
2. Type B: those evaluated by other than statistical methods or non-statistical methods such as irradiation errors, low-frequency noises, etc. (ISO, 2013; IAEA, 2002).

### 3.13 Quality assurance (QA) and quality control (QC) in tooth enamel EPR dosimetry

For quality assurance in EPR tooth dosimetry, there should be a written protocol or a lab manual that describes the detailed EPR measurement procedures, including the sample preparation, parameters (microwave power, modulation amplitude, time constant, conversion time, receiver gain, etc.) optimization, dose determination, and the uncertainty analysis. The personnel or technician should have the necessary knowledge in EPR spectroscopy, run the instrument and perform the EPR spectrum analysis for dosimetry work. The lab environmental conditions such as temperature and humidity should be fixed throughout the experiments. At the same time, EPR dosimetry labs should have a program and procedure for quality control (QC). QC focuses on uncovering the failure of the testing procedure, materials, and equipment used for the dose measurement (ISO, 2013).

The QC procedures in EPR dosimetry may include the following: (1) record the dosimetric signal and internal standard at the same recording and environmental conditions and normalized the dosimetric signals by dividing the dosimetric signal to an internal standard as described in Section 3.6, which reduces the errors arise from the environmental change and microphonics; (2) a periodic assessment of the EPR spectrometer sensitivity, stability, and a signal-to-noise ratio (SNR); (3) an empty tube or unirradiated sample subtraction measured at the same experimental parameters as the investigated samples; (4) multiple measurements of the control sample (zero-dose) and a high dose sample to check the measurement variability during the analysis; (5) proper cleaning the microbalance (make sure there is no dust or a previous sample on the balance) and calibration; (6) periodic verification of the sample radiation sensitivity using a universal calibration curve; and (7) participate in the interlaboratory intercomparisons for the data reproducibility and validity of the methods as described in Chapter 1 (Section 1.1.2) (ISO, 2013; IAEA, 2002).

### 3.14 Conclusions

In the last four decades, EPR dosimetry with teeth enamel has been expanded significantly to assess doses in radiation accidents and chronic exposures. This is mainly due to the high sensitivity of EPR and a long dose retention rate of tooth enamel. Moreover, this technique is non-destructive and can repeatedly be read out (i.e., kept as documents for future inspections). The present chapter highlights the recent development in the experimental methods and instrumentation in EPR dosimetry with tooth enamel. So far, four international intercomparisons have been conducted to check the accuracy and consistency of this method for retrospective dosimetry. ISO prepared standard protocols and recommendations for retrospective dosimetry using tooth enamel using these intercomparisons and other relevant reports. A well-developed methodology, a highly sensitive EPR spectrometer, and a well-trained operator are vital for the reliable measurements of absorbed low doses in EPR dosimetry with tooth enamel.

## 3.15 References


Aoba, T., Doi, Y., Yagi, T., Okazaki, M., Takahashi, J., Moriwaki, Y., 1982. Electron spin resonance study of sound and carious enamel. Calcif. Tissue Int. 34, 88-92.

Bailiff, I.K., Sholom, S., McKeever, S.W.S., 2016. Retrospective and emergency dosimetry in response to radiological incidents and nuclear mass-casualty events: A review. Radiat. Meas. 94, 83-139.

Barr, D., Eaton, S.S., Eaton, G.R., 2008. Workshop on quantitative EPR. At the 31st annual international EPR symposium, Breckenridge, Colorado.

Bertrand, P., 2020. Electron Paramagnetic Resonance Spectroscopy Fundamentals. Springer Nature Switzerland AG 2020. https://doi.org/10.1007/978-3-030-39663-3.

Brustolon, M., Giamello, E., (Eds.). 2009. Electron paramagnetic resonance, a practitioner's toolkit. John Wiley & Sons, Inc., Hoboken, New Jersey.

Chumak, V., Ciesielski, B., Sholom, S., Schultka, K., 2006. Lessons of the third international intercomparison on EPR dosimetry with teeth: similarities and differences of two successful techniques. Radiat. Prot. Dosim.120 (1–4), 197–201.

Ciesielski, B., Schultka, K., Wolakiewicz, G., 2006. The effect of heating on background and radiation induced EPR signals in tooth enamel. Spectrochim. Acta Part A 63, 870–874.

De, T., Romanyukha, A., Trompier, F., Pass, B., Misra, P., 2013. Feasibility of Q-band EPR dosimetry in biopsy. Appl. Magn. Reson. 44, 375-387.

Desrosiers, M., Schauer, D.A., 2001. Electron paramagnetic resonance (EPR) biodosimetry. Nucl. Instr. and Meth. in Phys. Res. B. 184, 219-228.

Duin, E. (2013). Electron Paramagnetic Resonance Theory. Chemistry. Assessed at http://webhome.auburn.edu/~duinedu/epr/1_theory.pdf

Eaton, G.R., Eaton, S.S., Barr, D.P., Weber, R.T., 2010. Quantitative EPR. Springer Wien New York. DOI 10.1007/978-3-211-92948-3.

Fattibene, P., Callens, F., 2010. EPR dosimetry with tooth enamel: A review. Appl. Radiat. Isot. 68, 2033-2116.

Geso, M., Ackerly, T., Lim, S.A., Best, S.P., Gagliardi, F., Smith, C., 2018. Application of the 'Spiking' method to the measurement of low dose radiation (≤ 1Gy) using alanine dosimeters. Appl. Radiat. Isot. 133, 111-116.

Harvey, D., 2000. Modern analytical chemistry. McGraw Hill, New York.

Haskell, E.H., Hayes, R.B., Kenner, G.H., 1997. Improved accuracy of EPR dosimetry using a constant rotation goniometer. Radiat. Meas. 27, 325–329.

Hayes, R.H., Haskell, E.H., Romanyukha, A.A., Kenner, G. H., 1998. A technique for increasing reproducibility in EPR dosimetry of tooth enamel. Meas. Sci. Technol. 9,1994–2006.

IAEA, 2002. Use of electron paramagnetic resonance dosimetry with tooth enamel for retrospective dose assessment. IAEA-TECDOC-1331. International Atomic Energy Agency, Vienna, Austria, 57 pp.

ISO, 2013. Radiological protection – Minimum criteria for electron paramagnetic resonance (EPR) spectroscopy for retrospective dosimetry of ionizing radiation – Part 1: General principles, International Standard, ISO 13304-1.

Ivannikov, A.I., Tikunov, D.D., Skvortsov, V.G., Stepanenko, V.F., Khomichyonok, V.V., Khamidova, L.G., et al., 2001. Elimination of the background signal in tooth enamel

samples for EPR-dosimetry by means of physical–chemical treatment. Appl. Radiat. Isot. 55, 701–705.

Ivannikov, A.I., Zhumadilov, Zh, Gusev, B.I., Miyazawa, Ch, Jiao, L., Skvortsov, V.G., et al., 2002. Individual dose reconstruction among residents living in the vicinity of the Semipalatinsk Nuclear Test Site using EPR spectroscopy of tooth enamel. Health Phys. 83, 183-196.

Iwasaki, M., Miyazawa, C., Uesawa, T., Niva, K., 1993. Effect of sample grain size on the $CO_3^{3-}$ signal intensity in ESR dosimetry of human tooth enamel. Radioisotopes 42, 470–473.

Jacob, P., Goksu, Y., Meckbach, R., Wieser, A., 2002. Retrospective dosimetry for external exposures. International Congress Series. 1225, 141-148.

Kirillov, V., Dubovsky, S., Tolstik, S., 2002. Artefacts of electron paramagnetic resonance dosimetry caused by a mechanical effect on samples of tooth enamel. Radiat. Prot. Dosim. 102(1), 41–48.

Likhtenshtein, G., 2016. Electron Spin Interactions in Chemistry and Biology: Fundamentals, Methods, Reactions Mechanisms, Magnetic Phenomena, Structure Investigation. Springer International Publishing Switzerland.

Lund, A., Shiotani, M., Shimada, S. (Eds.), 2011. Principles and Applications of ESR Spectroscopy. Springer Science+Business Media B.V.

Rieger, P.H., 2007. Electron Spin Resonance: Analysis and Interpretation. The Royal Society of Chemistry. Thomas Graham House, Science Park, Milton Road, Cambridge CB4 0WF, UK.

Romanyukha, A.A., Desrosiers, M.F., Regulla, D.F., 2000a. Current issues on EPR dose reconstruction in tooth enamel. Appl. Radiat. Isot. 52, 1265–1273.

Romanyukha, A.A., Ignatiev, E.A., Vasilenko, E.K., Drozhko, E.G., Wieser, A., Jacob, P., et al., 2000b. EPR dose reconstruction for Russian nuclear workers. Health Phys. 78, 15–20.

Romanyukha, A., Francois Trompier, F., Reyes, R.A., 2014. Q-band electron paramagnetic resonance dosimetry in tooth enamel: biopsy procedure and determination of dose detection limit. Radiat. Environ. Biophys. 53, 305–310.

Romanyukha, A., Mitchell, C.A., Schauer, D.A., Romanyukha, L., Swartz, H.M., 2007. Q-band EPR biodosimetry in tooth enamel microsamples: feasibility and comparison with X-band. Health Phys. 93 (6), 631-635.

Romanyukha, A.A., Nagy, V., Sleptchonok, O., Desrosiers, M.F., Jiang, J., Heis, A., 2000c. Individual biodosimetry at the natural radiation background level. Health Phys. 80 (1), 71–73.

Schauer, D.A., Iwasaki, A., Romanyukha, A.A., Swartz, H.M., Onori, S., 2007. Electron paramagnetic resonance (EPR) in medical dosimetry. Radiat. Meas. 41, 117-123.

Skvortzov, V.G., Ivannikov, A.I., Eichoff, U., 1995. Assessment of individual accumulated irradiation doses using EPR spectroscopy of tooth enamel. J. Mol. Struct. 347, 321-330.

Toyoda, S., Kondo, A., Zumadilov, K., Hoshi, M., Miyazawa, C., Ivannikov, A., 2011. ESR measurements of background doses in teeth of Japanese residents. Radiat. Meas. 46, 797-800.

Weber, R.T., Jiang, J.J., Barr, D.P., 1998. EMX User's Manual. Bruker Instruments, Inc.

Weil, J.A., Bolton, J.R., 2007. Electron Paramagnetic Resonance: Elementary Theory and Practical Applications. John Wiley & Sons, Hoboken, New Jersey.

Wieser, A., Mehta, K., Amira, S., Aragno, D., Bercea, S., Brik, A., et al., 2000. The 2nd international intercomparison on EPR tooth dosimetry. Radiat. Meas. 32, 549-557.

Zhumadilov, K., Ivannikov, A., Skvortsov, V., Stepanenko, V., Zhumadilov, Z., Endo, S., et al., 2005. Tooth enamel EPR dosimetry: optimization of EPR spectra recording parameters and effect of sample mass on spectral sensitivity. J. Radiat. Res. (Tokyo) 46 (4), 435–442.

# Chapter 4

## EPR measurements of background doses in teeth of Durham Region residents, Ontario

Lekhnath Ghimire[a], Edward Waller[a]
[a] Faculty of Energy Systems and Nuclear Science
Ontario Tech University, Oshawa, ON, L1G 0C5, Canada

*(Under preparation for publication in a peer-reviewed journal)*

**Abstract**

The dose contribution of nuclear power plants in Durham Region populations was determined by analyzing environmental samples from the surrounding areas of both nuclear-generating stations (Pickering and Darlington). However, the total doses from the various sources were unknown in Durham Region populations, Ontario. Electron paramagnetic resonance (EPR) dosimetry with tooth enamel has been successfully established as an effective tool for gamma dose assessment for chronic and acute exposures in individuals, groups, or populations to reconstruct the absorbed dose down to 30 mGy. This study collected the extracted teeth from people of different ages in Durham Region, Ontario, and analyzed them using the X-band CW EPR spectrometer. The total dose rate from the natural and anthropogenic sources was 1.9721 mSv/year. The anthropogenic dose rate from the various sources was 0.6341 mSv/year, about 47.39% of the natural background dose (1.338 mSv/year) in Durham Region, Ontario. The combined anthropogenic doses from these sources were lower than the local background dose in Durham Region and lower than the regulatory annual effective dose limit of 1 mSv/year in Canada. So, based on these data, this study concluded that the anthropogenic dose contribution was lower than the regulatory limit to the local

populations, and EPR dosimetry with tooth enamel is likely to be a useful part of determining background doses in populations.

**Keywords:** Tooth Enamel; X-band CW EPR Spectroscopy; Free Radicals; Low Doses; Retrospective and Accident Dosimetry; Anthropogenic doses; Nuclear power plants.

## 4.1 Introduction

Nuclear reactors use radioactive or nuclear materials (mainly uranium and plutonium) as their fuel to generate electricity. During nuclear fuel burn-up, nuclear fission inside the reactors, different fission products are formed as a byproduct of the reactions (Martin, 2013). These fission products may release to the environment as gaseous and liquid effluents and direct radiation from the power plants, as depicted in Figure 4.1 (Soldat et al., 1974). In Canada, the typical dose to a local person who lives one year within a few km from an operating nuclear power plant was 0.001 mSv (Lane et al., 2013). On the other hand, the calculated annual dose to a person living close to the US's NGSs was less than 0.01 mSv.

In contrast, the person living far away from the NGS (within 80 km) was estimated to be less than 0.1 μSv in the US (Blevins and Andersen, 2010). Based on these data, the radiation exposures from these nuclear facilities to the local environment and the nearby residents are extremely lower than the annual regulatory limit in both the US and Canada. However, periodic environmental monitoring is essential around the nuclear facilities for ensuring the local environments and residents are safe from radiation exposures (mainly within 30 km of nuclear power plants) (Lee et al., 2019).

### 4.1.1 Pathways of exposures from nuclear facilities

The pathways of exposures from nuclear facilities to the environment and public are illustrated in Figure 4.1. Direct radiation, gaseous and liquid effluents are the main exposure pathways to humans and environments (Soldat et al., 1974). Most environmental monitoring programs at nuclear-generating stations have been done by analyzing different environmental samples from the nearby nuclear facilities (OPG, 2020). Environmental sampling and analyses can provide information about the environmental radiation doses and their impacts on the aquatic and land animals, as shown in Figure 4.1 (Soldat et al., 1974). However, it may not provide information about the doses or direct radiation exposure the general public is getting from these facilities to ensure radiological safety. Many studies have determined the environmental doses and then converted them to the human dose by numerical and computational methods (Soldat et al., 1974; OPG, 2020).

However, a direct dose measurement in humans would be the best way to estimate the radiological impact from these facilities and other anthropogenic sources. Different types of biological samples, such as blood, teeth, bones, nails, etc., have been used after the nuclear explosion or nuclear and radiological accidents to determine the directly absorbed dose in humans (IAEA, 2002; ICRU, 2002; ISO, 2013; Ainsbury et al., 2011; Trompier et al., 2014). However, due to the high radiation sensitivity of tooth enamel and its extensive dose-response linearity from low to high doses, human teeth have been used extensively to assess chronic and acute exposures, as described in Section 4.1.7.

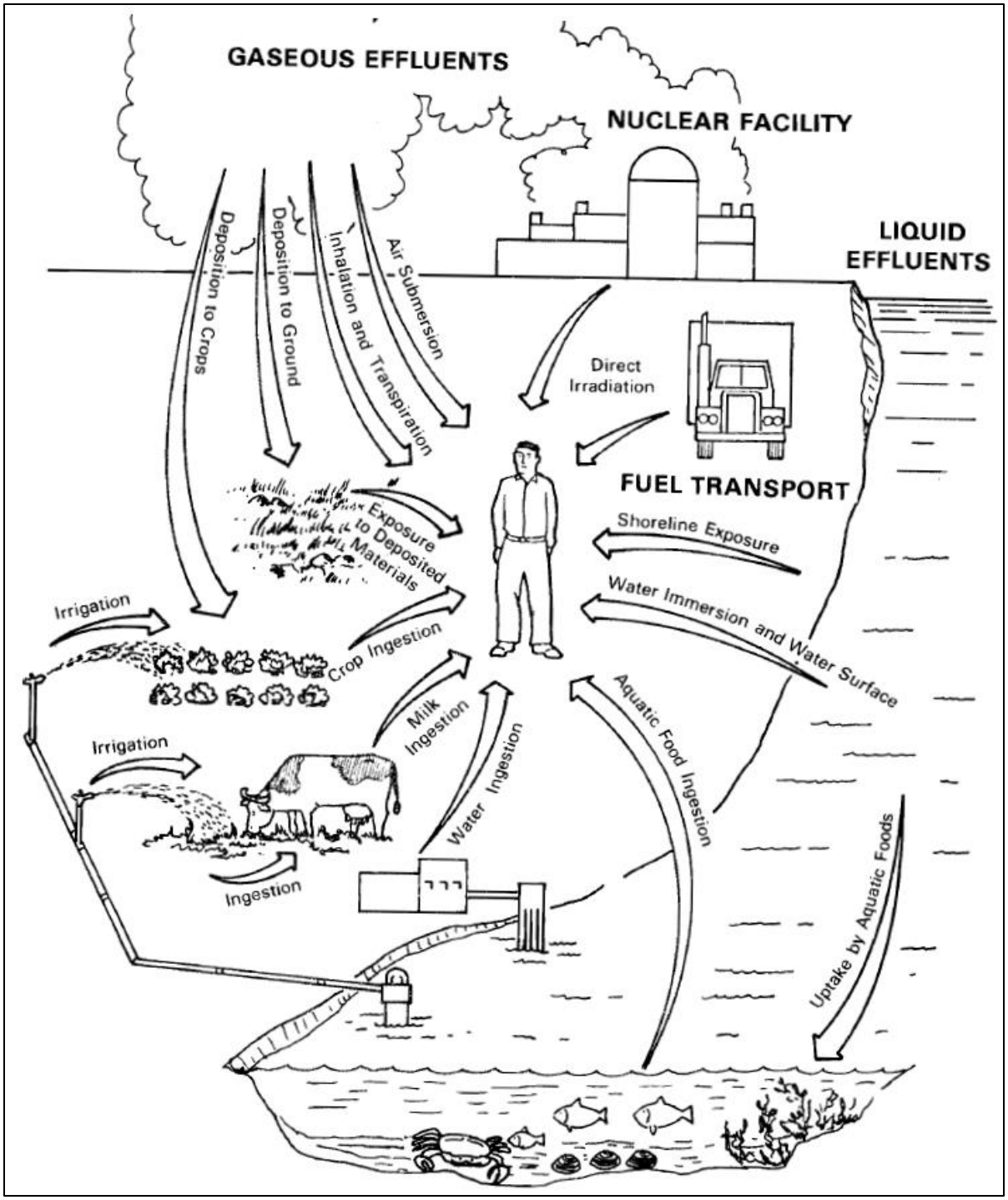


**Figure 4.1:** Potential exposure pathways from nuclear-generating stations in the events of the release of gaseous and liquid effluents and the direct radiation release from the stations to the local environments and public. From Soldat et al. (1974).

### 4.1.2 Radiation around nuclear power plants in the US and around the world

In occupational health and safety, each nuclear power plant in the US has a well-developed program for maintaining radiation levels As Low as Reasonably Achievable (ALARA) (Blevins and Andersen, 2010). Consequently, in the US, the average annual collective doses (i.e., the total radiation dose incurred by a population, also called the collective effective dose) from the operating nuclear reactors (i.e., BWR, PWR, and LWR) have been decreased from 7.74 person-Sv to 1.06 a person-Sv (i.e., a seven-fold decrease from 1973 to 2006) as depicted in Figure 4.2a. Likewise, the average annual measurable dose per worker was reduced from 6.6 mSv to 1.4 mSv, as depicted in Figure 4.2b (Blevins and Andersen, 2010). Additionally, the dose per worker was significantly lower than the annual dose limit (i.e., 50 mGy annual dose limit) from these power plants, as depicted in Figure 4.2b.

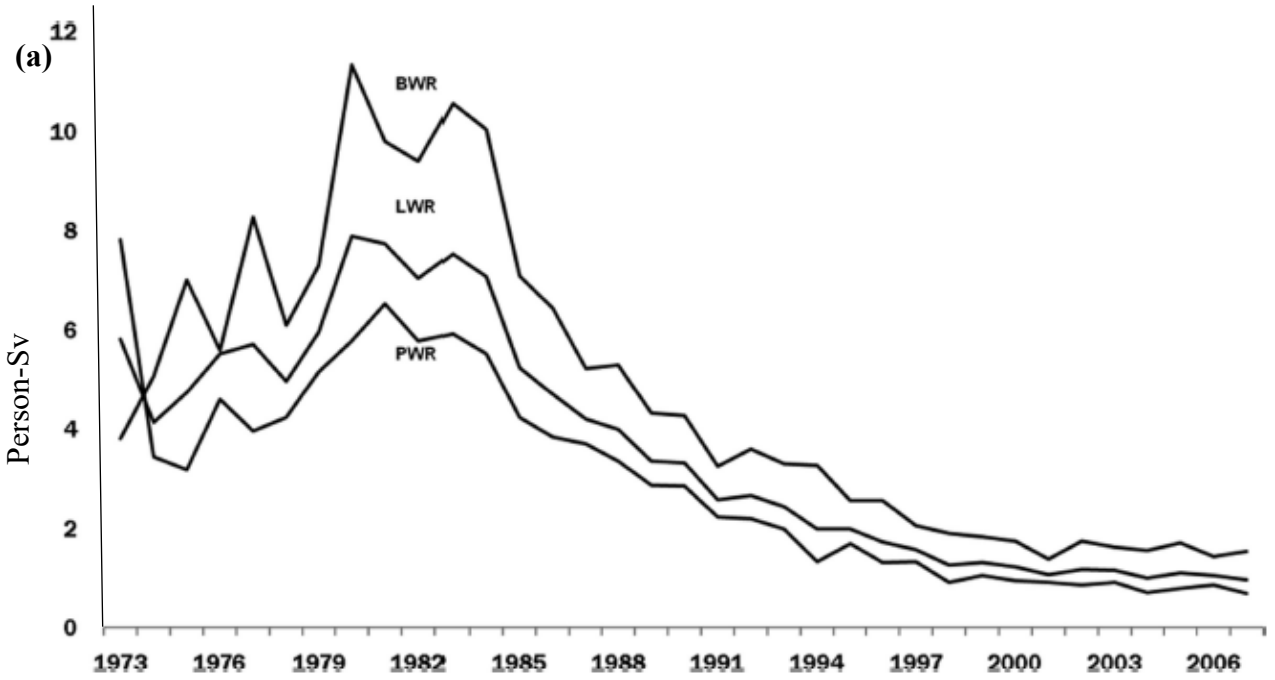

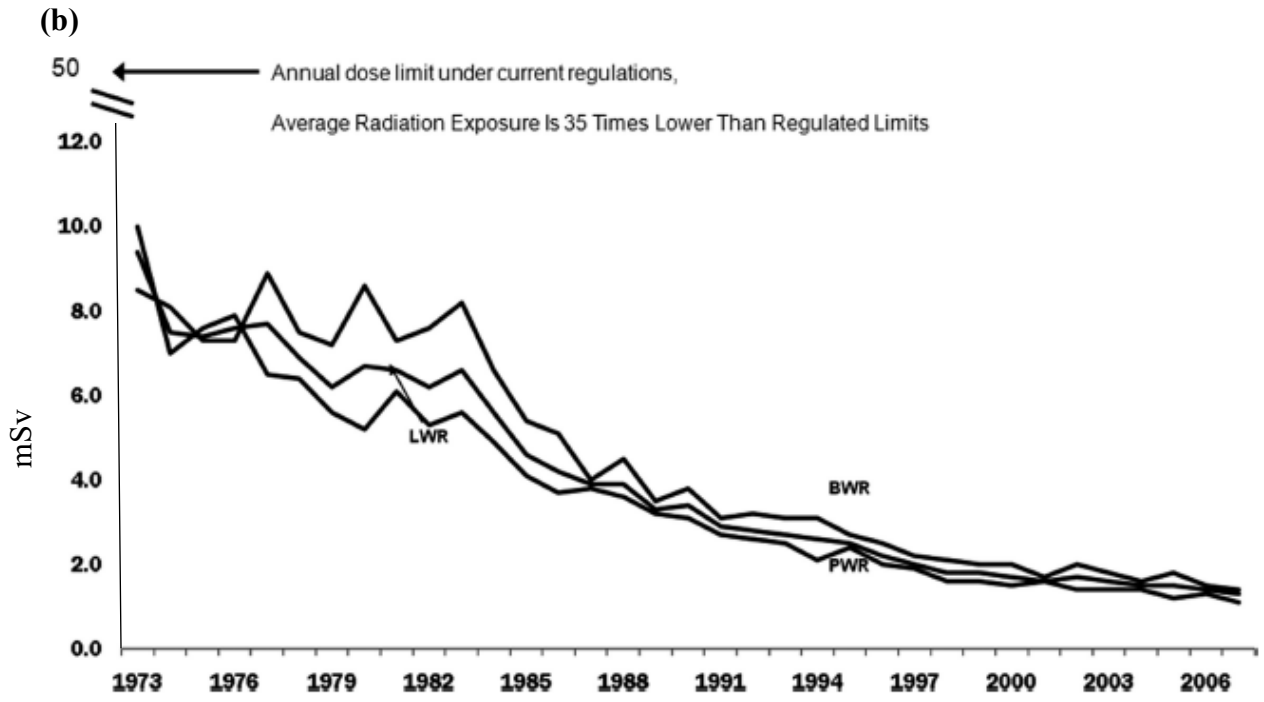


**Figure 4.2: (a)** Average annual collective dose per reactor in the US from 1973 to 2006. **(b)** Average measurable dose per worker in the US from 1973 to 2006. From Blevins and Andersen (2010).

These results demonstrated that the US nuclear power plants obtained exceptional results in regard to the radiation protection at the nuclear power plants, which ultimately protected the power plant workers, the public, and the environment (Blevins and Andersen, 2010). At the same time, the collective annual effective doses from the operation of the different types of nuclear reactors worldwide decreased from 1975 to 2002, as depicted in Figure 4.3. This demonstrated that the nuclear reactors have a well-developed policy and program to maintain the ALARA and the public and the environments are safe from the harmful effects of ionizing radiation from these facilities, not only in the US and Canada but around the world where these facilities are in operations.

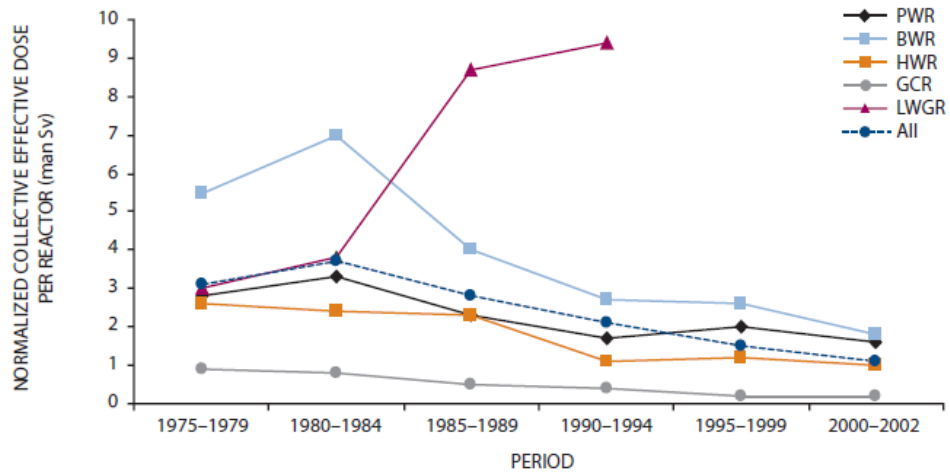


**Figure 4.3:** Worldwide trend in the annual collective effective doses per nuclear reactor operation from 1975 to 2002. From UNSCEAR (2008).

### 4.1.3 The annual effective dose from natural sources of ionizing radiation

The annual effective dose from natural sources of ionizing radiation at the Pickering and Darlington sites is 1,338 μSv (1.338 mSv), as described by the CNSC (2013) and Lane et al. (2013). The detailed procedures of determining the dose from the natural sources of ionizing radiation and the natural dose in different Canadian cities are explained by Grasty and LaMarre (2004), Grasty (2002), and Grasty et al. (1984). There are mainly four sources of public exposure to natural radiation: (1) cosmic radiation; (2) external terrestrial radiation; (3) radionuclides in the body; and (4) inhalation (Grasty and LaMarre, 2004). The natural background radiation depends on the geological environment, elevation above the sea level, and type of living accommodation. For instance, the average background dose in Canada is 1.769 mSv/year, Halifax 2.50 mSv/year, Edmonton 2.40 mSv/year, Winnipeg 4.022 mSv/year, Montreal 1.620 mSv/yr, Toronto 1.554 mSv/year, Vancouver 1.250 mSv/year; however, Kerala Coast of India has one of the highest background doses (i.e., 12.50 mSv/year) as shown in Figure 4.4a (Grasty and LaMarre, 2004; CNSC, n.d.; IAEA, 2004). The geological environment, elevation, and accommodation are almost

the same in Durham Region. That is why these nuclear-generating sites' natural background dose (1.338 mSv/year) should be equal in other parts of the Durham Region. The average radiation exposure from all sources to the world's population is 2.422 mSv/year, of which about 85% are from natural sources, as depicted in Figure 4.4b (IAEA, 2004; Grasty and LaMarre, 2004).

**(a)**

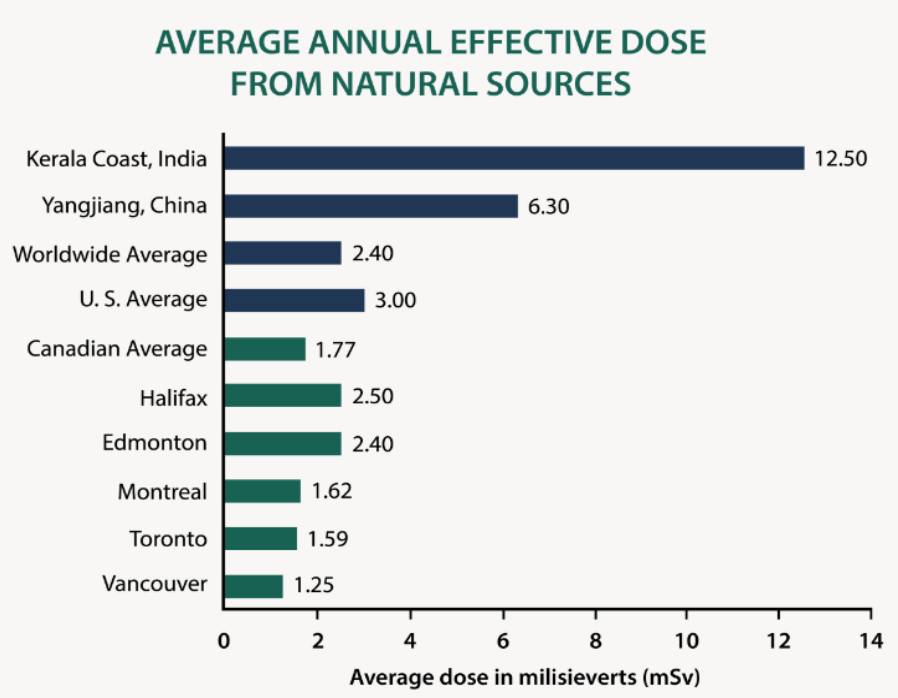


**(b)**

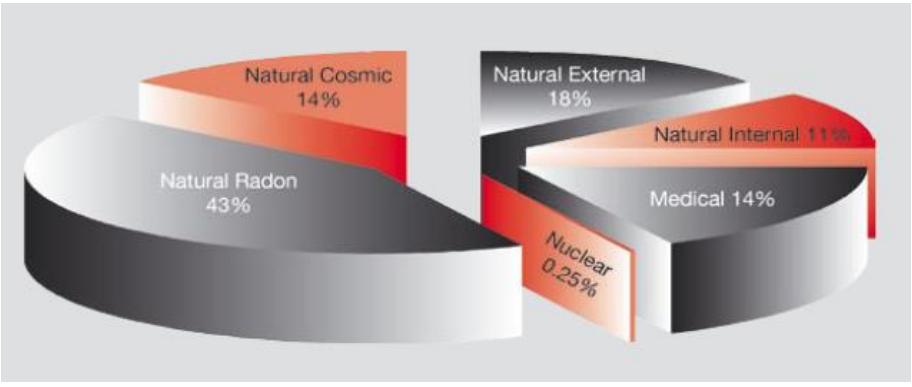


**Figure 4.4: (a)** Average annual effective dose from natural sources. **(b)** Average radiation exposures from all sources to the world's population is about 2.422 mSv/year. Over 85% of the doses are from natural sources. From CNSC (n.d.); IAEA (2004).

In the world populations' background (i.e., natural) doses, cosmic contributes about 0.39 mSv, gamma rays 0.48 mSv, internal 0.29 mSv and Radon 1.26 mSv. However, in the artificial doses, medical contributes about 0.60 mSv, atmospheric nuclear testing 0.005 mSv, Chernobyl 0.002 mSv and nuclear reactors 0.0002 mSv (UNSCEAR, 2006).

### 4.1.4 Annual public dose resulting from the operation of OPG nuclear stations

Under the Nuclear Safety and Control Act (NSCA), the licensee of each nuclear facility is required to develop, implement, and maintain the environmental monitoring programs and submit their report to the Canadian Nuclear Safety Commission (CNSC) to ensure the public and environment are protected from the radiation related to their facility's nuclear activity (CNSC, 2018). Therefore, Ontario Power Generation (OPG) environmental monitoring programs have been assessed the radiation dose from the Darlington (DN) and Pickering (PN) nuclear generating stations using various environmental samples such as air, fruits and vegetables, animal feed, eggs, poultry, milk, municipal drinking water, well and lake water, fish, beach sand, grass, and wild vegetation, etc. from the public areas around the facilities (OPG, 2020). Nine hundred sixteen of these samples were analyzed in the OPG health physics laboratory accredited by the Canadian Association for Laboratory Accreditation (CALA). Both sites' radiological emissions were identified to be lower than their licensed Derived Release Limits (DRLs) (OPG, 2020). As can be seen in Tables 4.1 and 4.2, the critical group doses due to the operation of the DN and PN are lower than the annual legal limit of 1,000 μSv/year for the Canadian public and the estimated natural background dose (i.e., naturally occurring annual public effective dose) around the DN and PN of 1,338 μSv/year in Durham Region, Ontario.

**Table 4.1:** 2020 annual Darlington public dose (nuclear critical group) calculation. From OPG (2020).

| | Dose per Age Class (microSieverts) | | |
|---|---|---|---|
| **Potential Critical Group** | **Adult** | **Child (10-year-old)** | **Infant (One-year old)** |
| Dairy Farm Residents | 0.2 | 0.2 | 0.2 |
| West/East Beach Residents | 0.2 | 0.2 | 0.1 |
| Farm Residents | **0.4** | 0.4 | 0.3 |
| Rural Residents | 0.3 | 0.2 | 0.1 |

Additionally, the Darlington (DN) dose was essentially unchanged over the last ten years. The public dose to the farm resident (farm adult) was 0.4 μSv, which was less than 0.1% of the legal limit of 1,000 μSv/year, and the estimated background dose around DN of 1,338 μSv/year, as shown in Figures 4.5a and 4.5b. The 2020 Pickering (PN) site public dose was 1.2 μSv, which was less than 0.1% of the 1,000 μSv/year legal limit for a member of the public. Also, the PN dose for 2020 was less than 0.1% of the estimated natural background dose around PN of 1,338 μSv/year from the various sources, as shown in Figures 4.6a and 4.6b (OPG, 2020). Hence, the public dose from the operation of these nuclear facilities is very small in comparison to the public's total exposure to radiation, which indicated that the health risks due to radiological contaminants were negligible (i.e., annual doses were significantly lower than the regulatory limit) around these sites in Durham Region, Ontario, which concluded no health risks to humans as a result of radiological emission from these stations. The detailed environmental monitoring results around the DN and PN nuclear-generating stations can be found in the '2020 results of environmental monitoring programs' published by OPG's radiological environmental monitoring programs (REMP) (OPG, 2020).

**Table 4.2**: 2020 annual Pickering public dose (nuclear critical group) calculation. From OPG (2020).

| | Dose per Age Class (microSieverts) | | |
|---|---|---|---|
| **Potential Critical Group** | **Adult** | **Child (10-year-old)** | **Infant (One-year old)** |
| Dairy Farm Residents | 0.3 | 0.4 | 0.5 |
| Urban Residents | **1.2** | 0.9 | 1.0 |
| Sport Fisher | 0.3 | 0.3 | 0.2 |
| C2 Correctional Institution | 0.8 | 0.8 | - |
| Industrial Workers | 0.1 | | |

**(a)**

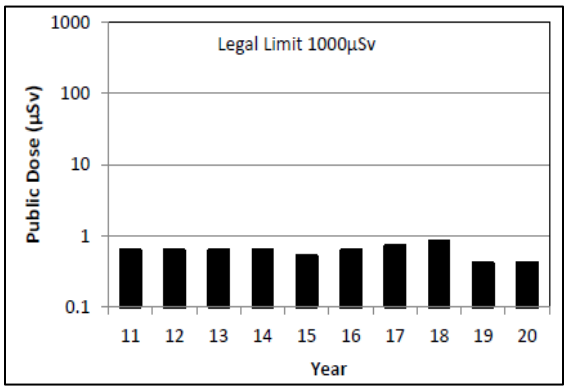


**(b)**

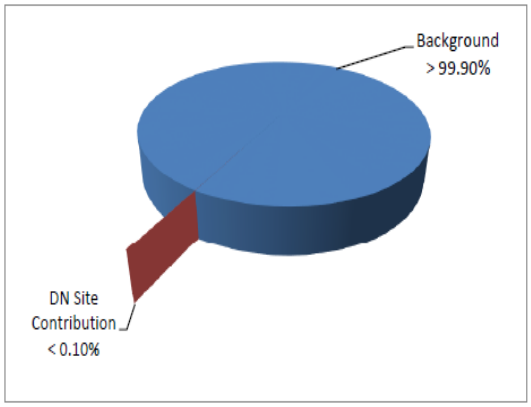


**Figure 4.5: (a)** Darlington nuclear annual public dose trends. **(b)** Comparing the 2020 Darlington nuclear public dose to the background dose. From OPG (2020).

**(a)**

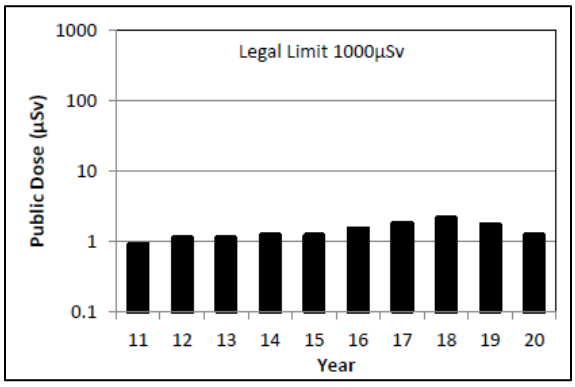


**(b)**

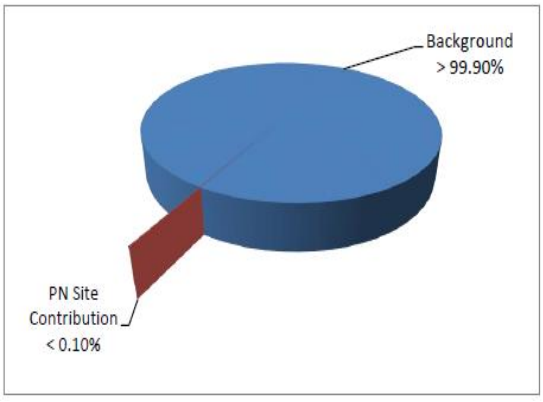


**Figure 4.6: (a)** Pickering nuclear annual public dose trends. **(b)** Comparing the 2020 Pickering nuclear public dose to the background dose. From OPG (2020).

### 4.1.5 Independent environmental monitoring program (IEMP) by the CNSC

The CNSC has implemented its Independent Environmental Monitoring Program (IEMP) to ensure the public and the environment around the licensed nuclear facilities are safe in Canada. Also, the CNSC has been using the IEMP to conduct compliance verification activities for the Canadian nuclear industries. In 2017, the CNSC staff (Figures 4.7a and 4.7b) collected samples from the nearby public areas and around the facilities, which included air, lake water, soil, sediment and sand, grass and wild vegetation, and food such as milk, fruit, and vegetables from a local farm near the Pickering site (CNSC, 2018a) and the Darlington sites (CNSC, 2018b). The collected samples were analyzed in the CNSC's laboratory. The measured radiation levels and radionuclide concentrations were below the CNSC reference levels (0.1 mSv/year), one-tenth of the CNSC's public dose limit of 1 mSv/year. More importantly, the results from the IEMP were consistent with the OPG's 2017 environmental monitoring results (CNSC, 2018a; CNSC, 2018b). These results indicated that the public and the environments around the Pickering and Darlington sites were protected. There were no adverse health impacts from these NGSs to the local people and environments.

**(a)**  **(b)** 

**Figure 4.7: (a)** A CNSC staff is collecting vegetation samples from the Pickering site. **(b)** A CNSC staff is collecting water and sediment samples at a public beach near the Pickering sites. From CNSC (2018a).

### 4.1.6 Radiation and health in Durham Region, Ontario, Canada

To determine the health effects from chronic exposures in Durham Region, the Durham Region Health Department analyzed the public radiation dose data available through the OPG's radiological environmental monitoring program (REMP), the data available in the literature, and the health data from local health centers – in part to examine the relationship, if any, between local cancer incidence and radiation exposures from these nuclear facilities. As per their analyses, the levels of radiation exposure from the Pickering and Darlington NGSs were calculated to be extremely low, and no adverse health effect to the local population from the NGSs was observed, as depicted in Figures 4.8 and 4.9 (Durham Region Health Department, 2007; Durham Region Health Department, 2017). Furthermore, the cancer incidence rates in both males and females were constant over the fourteen years and almost similar to the Ontario male and female rates. Also, the cancer incidence rates in Durham Region's children aged 0-14 were similar to those of Ontario children aged 0-14 (Lane et al., 2013). These radio-epidemiological data demonstrated no direct health impact from these NGSs' radiation exposure to the local populations in Durham Region, Ontario. However, in Durham Region, there is no direct dose (i.e., total background doses) measurement data available, and the attributed doses were allocated according to the results of the environmental sample analysis and modeling (Figures 4.5a, 4.5b, 4.6a, and 4.6b) (OPG, 2020).

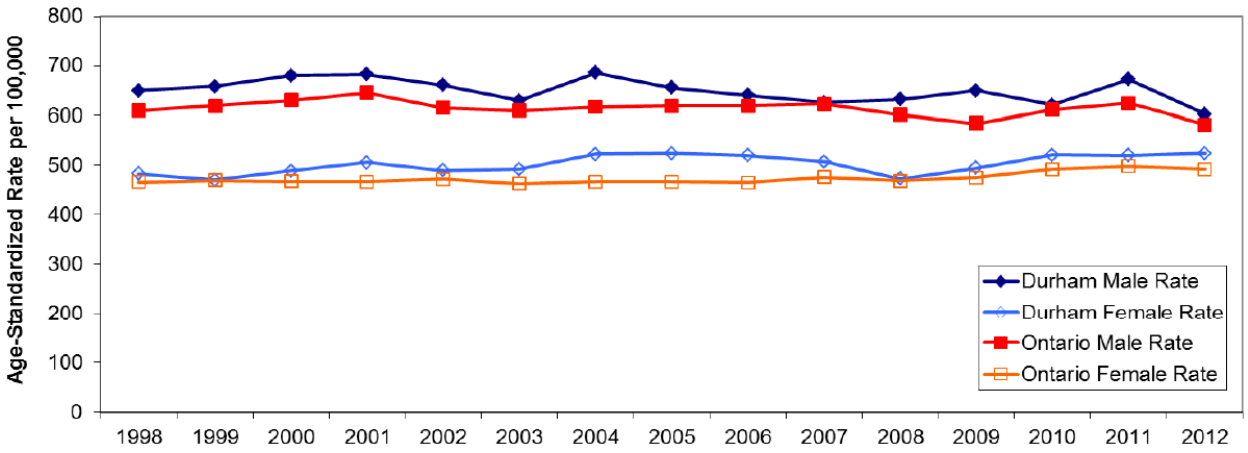


**Figure 4.8:** Age-standardized incidence of all cancers for males and females in Durham Region and Ontario, 1998 to 2012. The cancer incidence rates in both males and females were constant over the fourteen years and almost similar to the Ontario male and female rates. From Durham Region Health Department (2017).

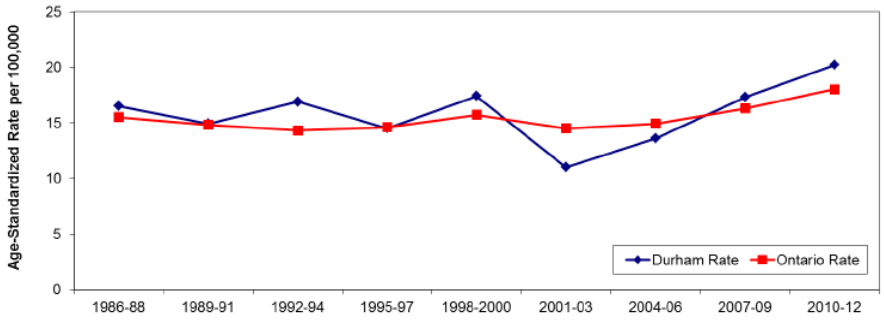


**Figure 4.9:** Age-standardized incidence of all cancers in children aged 0 to 14 years for males and females, Durham Region and Ontario, by 3-year periods, 1986 to 2012. The cancer incidence rates over the twenty-four-year period (1986-2012) in Durham and Ontario children aged 0 to 14 were almost similar. From Durham Region Health Department (2017).

The local populations would be more confident about the model predictions if direct measurements could back them. Furthermore, environmental analyses may not provide the actual doses (i.e., total doses) that the people of this region are getting from various sources such as

diagnostic radiology, nuclear medicines, radiation therapy, flights, occupational, etc. So, the chronic low dose radiation received by the local population from these different sources is uncertain. It is, therefore, essential to determine the chronic low dose radiation level received by the local population to understand its possible long-term health impacts. This is particularly important since some residents living near NGSs have expressed concern about their possible exposures (Priest, 2018) and protested against these facilities in Durham Region, Ontario, as depicted in Figures 4.10a and 4.10b. These protests demonstrated that there was a misunderstanding and a loss of public confidence in nuclear industries and their continued operations in Canada (Allison, 2006). These misunderstandings and fears may be due to the lack of direct dose measurements and proper risk communication regarding radiation exposures from the nuclear facilities and the health effects of chronic low dose radiation exposures. The direct total dose measurement in humans helped respond to questions from residents of Durham Region, Ontario. Also, it can address the public concern about the reliability and trustworthiness of existing dose estimates. Madame Marie Curie's words, "Nothing in life is to be feared, it is only to be understood". So, now, it is time to understand more about radiation, which may decrease our fear of radiation.

**(a)**


**(b)**


**Figure 4.10:** Concerns and worries regarding the exposures from the nuclear facilities in Durham Region, Ontario, Canada. **(a)** Anti-nuclear demonstration in front of the Darlington NGS in 1979.

From Gerard (1979, August 20). **(b)** Anti-nuclear demonstration at Pickering in 2018. From Streck (2018, June 26).

Thus, this study focuses on determining the direct local doses or background doses in a population using tooth enamel, also called a 'biological dosimeter', collected from Durham Region, Ontario.

### 4.1.7 Tooth enamel for EPR dose reconstruction

Experimental determination of the absorbed dose in tooth enamel using EPR dosimetry is an essential tool to reconstruct doses in individuals, groups, or populations in case of radiation accidents or chronic exposures (Zhumadilov et al., 2005; Toyoda, 2019). The usefulness of tooth enamel as an external dosimeter is due to its high radiation sensitivity and extensive dose linearity (Polyakov et al., 1995; Driessens, 1980). Additionally, tooth enamel is a highly stable component of a tooth whose composition does not change with aging as opposed to bones (Wieser et al., 2000). When tooth enamel is exposed to ionizing radiation, the carbon dioxide radical anions ($^{\bullet}CO_2^-$) are generated by ionizing radiation from a neutral carbon dioxide ($CO_2$) molecule on the surface of crystallites, and the bulk carbonate ($CO_3^{2-}$) impurities present in the hydroxyapatite crystals (Rudko et al., 2010; Moens et al., 1993). The free radicals in tooth enamel are extraordinarily stable for about ten million ($10^7$) years at normal temperature (25°C) and pressure (Hennig et al., 1981), which makes tooth enamel an 'ideal dosimeter' for both retrospective and accident dosimetry studies; it detects radiation exposures independent of the time of occurrence (Wieser et al., 2000). The concentration of these free radical centers is identified and quantified using EPR spectroscopy in the form of an EPR spectrum, as depicted in Figure 4.11 (IAEA, 2002). The highest peak-to-peak (P2P) amplitude height (R) provides the actual free radical

concentration, which is proportional to the total absorbed dose as depicted in Figure 4.11 (IAEA, 2002; ICRU, 2002).

More importantly, the intensity of the EPR signal increases proportionally with the absorbed dose from 30 mGy to 10 kGy, which is a significant dose range to reconstruct doses in both nuclear and radiological accidents and chronic exposure situations (Ikeya, 1993; Romanyukha and Schauer, 2002). Therefore, EPR tooth enamel dosimetry has been successfully established as an effective tool for gamma dose assessment for external exposures in populated areas during and after the nuclear explosion or nuclear and radiological accidents such as the radiation doses of the atomic bomb survivors (Ikeya et al., 1984; Nakamura et al., 1998), the population exposed to the Chernobyl accident (Chumak, 2013; Chumak et al., 1999; Skvortsov et al., 2000), nuclear workers in South Ural (Romanyukha et al., 1994), Russian nuclear workers (Romanyukha et al., 2000), Mayak nuclear workers (Romanov et al., 2000), and the residents of the Techa river valley (Jacob et al., 2003). These studies demonstrated that EPR dosimetry with tooth enamel could successfully measure absorbed doses in chronic and acute exposure scenarios.

Hence, in this study, our overarching research goal is to investigate the background doses (or total anthropogenic doses) in the Durham Region population, Ontario, using EPR dosimetry with tooth enamel and study retrospective dosimetry using the EPR dose reconstruction techniques.

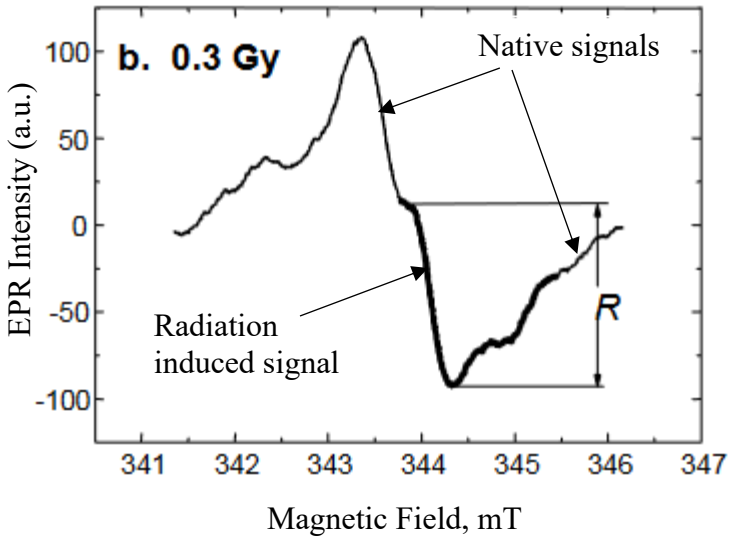


**Figure 4.11:** A dosimetric component in an EPR spectrum of tooth enamel after irradiation to 0.3 Gy. R is the P2P amplitude height of the dosimetric signal used for the EPR dose reconstruction. The native and dosimetric signals are visible in the spectrum. From IAEA (2002).

## 4.2 Materials and methods

### 4.2.1 Sampling locations

The Regional Municipality of Durham Region (Durham Region) is located in southern Ontario, Canada. It has an area of 2,523.80 square kilometers, and the total population is 645,862 (2016). The Region has two NGSs, Darlington, and Pickering, located on the shore of Lake Ontario, as shown in Figures 4.12, 4.13a, and 4.13b. The Darlington NGS started its operations from 1990 to 1999. Similarly, the Pickering NGS started its operations from 1965 to 1986. However, OPG will shut down Pickering's units 1 and 4 in 2024 and units 5 to 8 in 2025, and then eventually, a decommissioning process will be started in 2028 (OPG, n.d.-c). The stations in Durham Region generate about 30% of Ontario's electricity (Durham Region Health Department, 2007).


**Figure 4.12:** The Regional Municipality of Durham is located in southern Ontario, Canada (i.e., east of Toronto and the Regional Municipality of York). The Region has two operating nuclear-generating stations: (1) Pickering; and (2) Darlington, located in the southern part of the Region besides Lake Ontario. From Durham Region Health Department (2007).

**(a)**

**(b)**

**Figure 4.13:** An aerial view of the Pickering (a) and Darlington (b) nuclear generating stations in Durham Region, Ontario, Canada. From (OPG, n.d.-a); OPG (n.d.-b), The Pickering electrical generation capacity is 3,100 MWe, and the Darlington electrical generation capacity, is 3,500 MWe. From OPG (n.d.-a); OPG (n.d.-b).

### 4.2.2. Sampling disruption and donors' information

The COVID-19 pandemic was occurring throughout the research project, which delayed the sample collection and analysis to complete the project. Despite these challenges, the samples were collected and analyzed following the local health department guidelines and the university's lab

protocol, respectively. The information about donors/participants could not be collected due to health restrictions. However, as per the standard EPR dosimetry technique (ISO protocol 13304-1 for EPR retrospective dosimetry), the donors' information is not mandatory to determine the background doses in populations (ISO, 2013). Toyoda et al. (2011) determined the background doses in teeth of Japanese residents without collecting donors' information. The authors collected forty-six extracted wisdom teeth obtained from the Department of Dentistry, Ohu University, Japan, and analyzed the background doses in Japanese populations. Similarly, Zhumadilov et al. (2006) reconstructed the absorbed doses to the population of Dolon and Bodene (i.e., former nuclear test sites in Russia) using 35 teeth samples without sample information. Ivannikov et al. (2002) estimated absorbed doses in the Northeastern part of Kazakhstan near the Semipalatinsk Nuclear Test Site (SNTS) using 36 extracted teeth samples without collecting donors' information. If one only needs population averages or background doses in populations, teeth may be collected at random with only minimal information such as participant's age and place of residence (ICRU, 2002).

### 4.2.3 Sample preparation

As mentioned in Section 4.1.7, the extracted human teeth are used to reconstruct the background doses in Durham Region, Ontario. The research that involves the human tissue (i.e., teeth) must obtain the research ethics approval from the university's Research Ethics Board (REB). This study has been reviewed and received ethics clearance through the University's Research Ethics Board (REB # 14870) on January 05, 2019. The local dentists/dental clinics and residents were invited to participate in this study. After agreeing to participate, 64 tooth samples covering different age ranges were collected from the dental clinics as extracted during an ordinary dental practice. The samples were collected and analyzed in 2021. Teeth were sterilized by keeping in

about 5% sodium hypochlorite (NaOCl) for 24 hours. Then, the tooth samples were placed in formalin ($CH_2O$) for infection (bacterial and viral) control purposes. Finally, teeth samples were rinsed and stored in sealed glass vials (Figure 4.15) and kept in the darkroom until further preparation. The sample preparation and processing were done inside a fume-hood in the ERC 3092 lab at Ontario Tech University to minimize inhalation exposures to hazardous chemicals or biological agents (IAEA, 2002; Fattibene and Callens, 2010). The details of the sample collection and preparation techniques are described in Chapter 3 of this thesis.

Sample preparation was carried out through combined chemical and mechanical methods (Ivannikov et al., 2001). Dental fillings were removed using drilling. The crown was separated from the root using a Mastercraft mini aluminum saw, as depicted in Figure 4.14, inside a bath with cold water. The separated crowns were stored in glass vials sealed with moisture as depicted in Figure 4.15 and kept in the dark vacuum container until further sample processing.

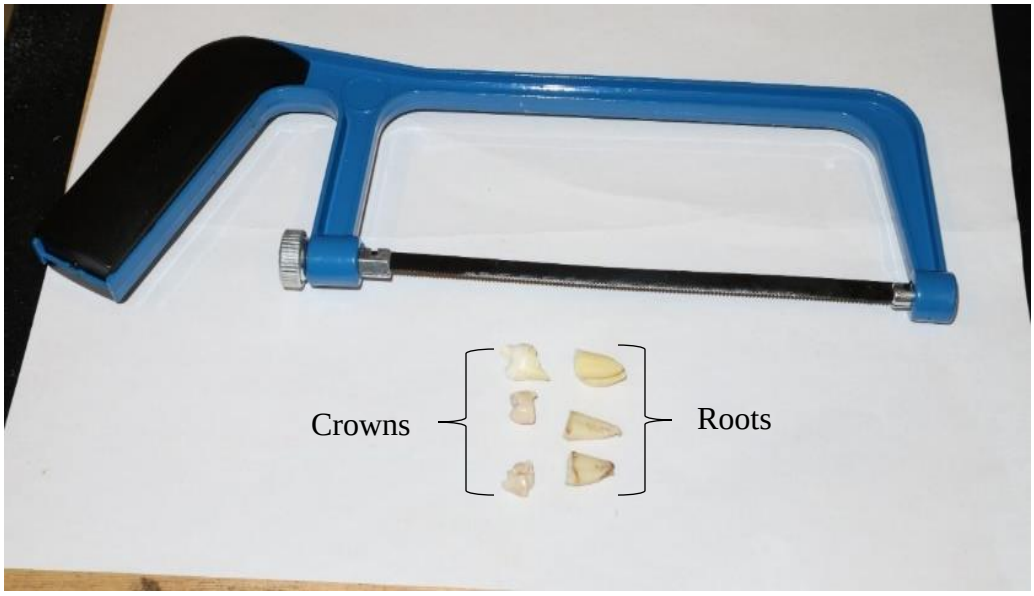


**Figure 4.14:** Mastercraft mini aluminum saw (blade material: steel and thickness = 0.06 mm) was used to separate the teeth crowns from roots.

**Figure 4.15:** The crowns were separated from the collected teeth from Durham Region, stored in glass vials, and kept in the dark vacuum container at room temperature until further processing.

The crown was divided into the buccal and lingual parts, and the enamel samples were prepared separately from them (IAEA, 2002). The metallic impurities were removed by cleaning the enamel with a 0.1 M Ethylenediaminetetraacetic Acid Disodium Salt (EDTA $Na_2$) solution. The adequately cleaned enamel was put into a 5M KOH solution for 16 h in an ultrasonic bath to separate dentin from enamel. The remaining dentin residue was identified using a 365 nm UV lamp and removed using a dental drill. As a result of this processing, the dentin impurity was completely removed from dental enamel. Then, the sample was dried at 45°C for about 1 hour and was cut by pliers (Figure 4.16a) into grains of about 0.5 - 1 mm in size (Figure 4.16b) as described by Zhumadilov et al. (2005). Using pliers instead of a mortar and pestle to grind tooth enamel has advantages. It minimizes the small grain sizes (<0.5 mm) powder fraction in grind enamel. Crushing manually in a mortar and pestle constitutes up to 30% of the sample grain sizes below 0.5 mm, which should be removed by sieving (Ivannikov et al., 2002). The 0.5 – 1 mm particle

size was chosen because the enamel sensitivity decreases, and the mechanically induced signals increase with the grain size below 0.3 mm. The reproducibility markedly decreases in the grain size higher than 1.5 mm due to increased sample anisotropy with the increase in enamel grain sizes (Iwasaki et al., 1993; Haskell et al., 1997; Zhumadilov et al., 2005). The grind samples were stored in a desiccator with silica gel beads and kept in the dark container (i.e., UV protected) at room temperature until EPR analysis, as depicted in Figure 4.16c.

**(a)**

**(b)**

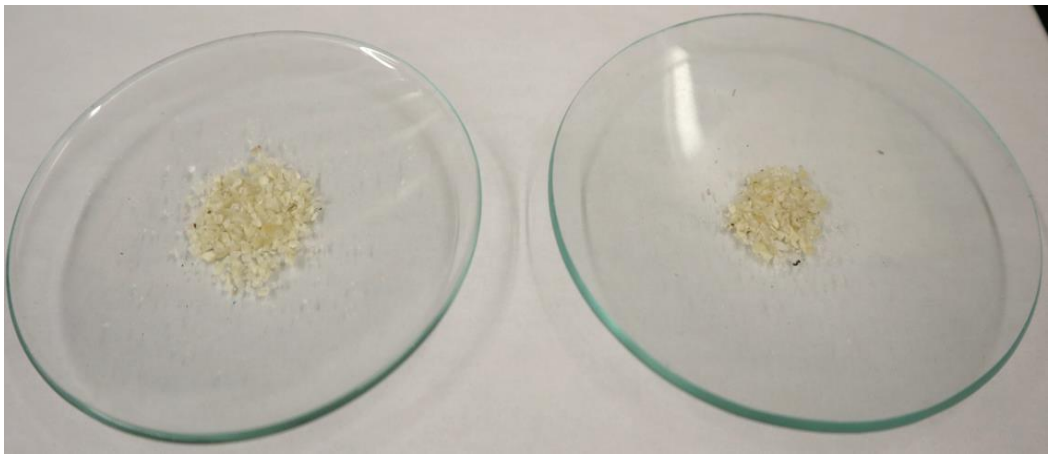

**(c)**

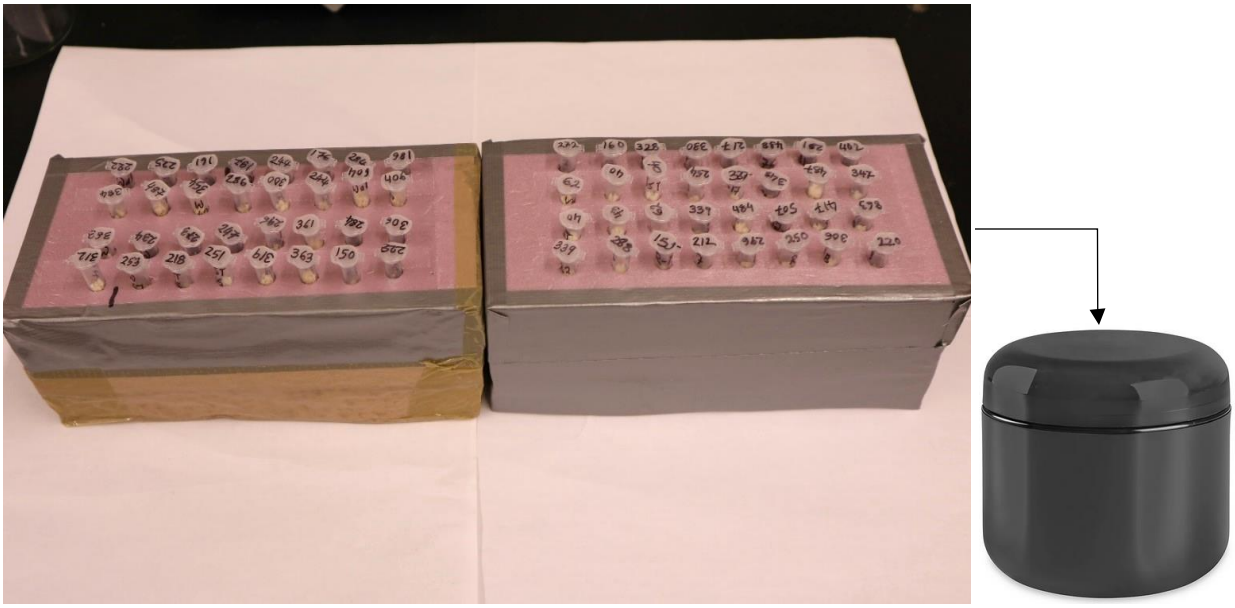

**Figure 4.16: (a)** Mastercraft diagonal cut pliers were used to cut tooth enamel into the grain sizes of about 0.5 - 1 mm **(b)**, which was ideal for the dose estimation. **(c)** The tooth enamel samples (grain sizes 0.5-1 mm) were stored in the microcentrifuge tubes and then stored with silica gel beads in a desiccator. The desiccator was kept in the dark vacuum container until EPR analyses for dose estimation.

### 4.2.4 **Sample irradiation**

The calibration curve method was used to estimate the absorbed doses in tooth enamel samples collected from Durham Region, Ontario. As described in Chapter 1 (Section 1.2.1), one of the calibration curve method's major limitations is finding a large number of samples for constructing a statistically valid calibration curve (Fattibene and Callens, 2010). So, different age group samples were mixed and divided into eight aliquots of the same mass (105 mg) (Ivannikov et al., 2002). Each sample aliquot was put into the microcentrifuge tube and housed in the 3D printed sample holder, as depicted in Figures 4.16c and 4.17b. The sample holder was aligned to

the center of the gamma source (Hopewell G-10), as shown in Figure 4.17b, using a laser alignment system. The samples were exposed to absorbed doses of 0, 30, 60, 100, 200, 500, 1000, and 1500 mGy from the $^{137}$Cs (gamma-ray) source (i.e., Hopewell G-10) by keeping the sample holder 34 cm from the center of the source as depicted in Figure 4.17b. Before samples irradiation, the gamma source was calibrated using the reference standard; the uncertainty in dose determination at 34 cm from the center of the source was less than 5% within a 95% confidence interval.

The $^{137}$Cs produces gamma rays with energies of 0.6617 MeV. The kinetic energy of the electrons expelled from atoms after interaction with photons per unit mass of medium at the place of interest is called the Kinetic Energy Release Per Unit Mass (KERMA), also called the exposure dose. The absorbed dose depends on the KERMA. The absorbed dose is the energy imparted to matter by ionizing radiation per unit mass of medium at the place of interest. At lower than 1.2 MeV, the difference between the KERMA and the absorbed dose is small (i.e., constant throughout the medium). Electronic equilibrium is usually assumed to exist, but they increase with γ-ray energy. As a result, the KERMA is almost equivalent to the exposure dose (a measure of the radiation dose based on its ability to produce ionization in the air) in $^{137}$Cs. As a result, the exposure and absorbed doses are closely related (Roesch, 1958). Also, mass-energy absorption coefficients of the air and the enamel are very similar at a photon energy of more than 100 keV (Ivannikov et al., 2002). Therefore, no correction for the energy dependence of enamel response was performed in this study. The irradiated samples were stored for 2 weeks in a darkened vacuum container with a silica bed to stabilize the mechanically induced signals, eventually reducing measurement errors. The radiation-induced signals in the irradiated samples were measured using EPR in the form of an EPR spectrum to construct a calibration curve that shows the dose-response of the radiation-induced signal as a function of the applied dose during irradiation (Figure 4.25). The same

calibration curve was used to estimate doses in the tooth enamel samples collected in Durham Region, Ontario, Canada.

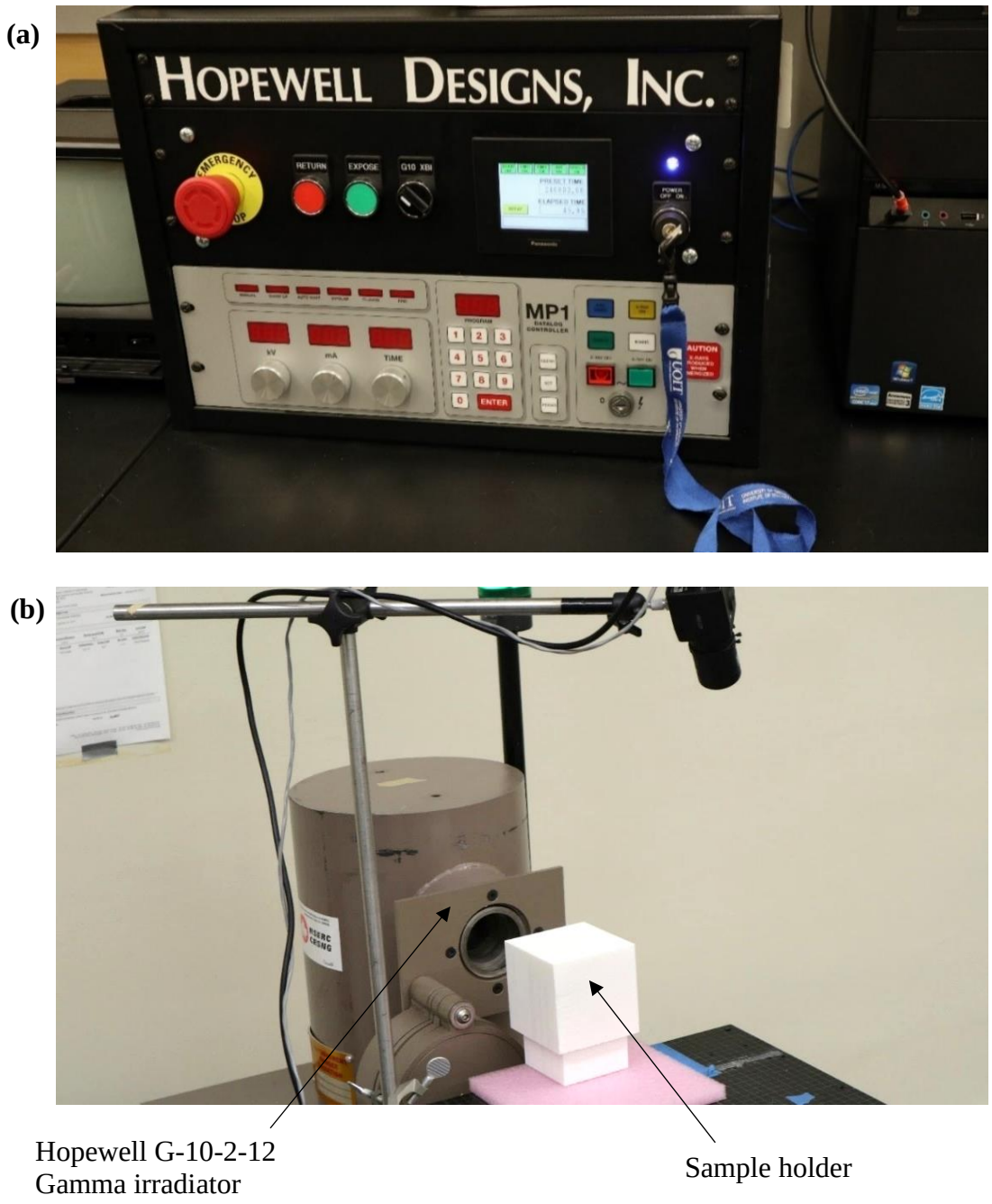


**Figure 4.17: (a)** The Hopewell G-10 $^{137}$Cs gamma source control panel. **(b)** Tooth enamel samples were exposed to gamma rays from the G-10 for constructing a calibration curve at Ontario Tech University in the ERCB058/056 radiation protection and applied radiation laboratory.

### 4.2.5 EPR measurements

The EPR spectra acquisition was performed using the X-band CW EPR spectrometer (e.g., Bruker EMX micro spectrometer), with a frequency of 9.8 GHz. The Haskris R250 – R1000 heat exchanger maintained constant magnet temperature as depicted in Figure 4.18b. The EPR spectrometer was allowed to reach a stable operating temperature before starting a sample analysis. Generally, about one hour is adequate to achieve thermal equilibrium; and all the samples were measured at a stabilized room temperature of 21˚C. The stable operating temperature is vital to avoid frequency drifting and the g-factor uncertainty during measurements (Gualtieri et al., 2001). The spectrometer was equipped with the high-quality factor (i.e., Q-factor) rectangular ER4119HS cavity. The Q-factor for the empty cavity was 10,000, and it varied from 8,300 to 5200 at loading with the EPR tube containing a tooth enamel sample, as described in Chapter 3 (Section 3.2.3.1). The following EPR spectrum acquisition parameters were optimized: microwave power 24 mW (for the high-Q cavity), the modulation frequency of 100 kHz and modulation amplitude 4 gauss, receiver time constant 327.68 msec, sweep time 41.98 sec, field sweep 150 G, number of scans 5, accumulation time 3.5 min, receiver gain $1 \times 10^3$. The Bruker ER 4119HS-2100 internal standard, which has a g factor (or a Landé g-factor) of $1.9800 \pm 0.0006$ and line width 3 G, was permanently mounted in the resonator as shown in Figure 4.18a and measured together with tooth enamel. The internal standard g-value was used to determine the g-factor values of the observed EPR signals and normalized the dosimetric signals to reduce errors due to any fluctuation in the machine response and environmental changes (Jiao et al., 2014; Eaton et al., 2010; Brustolon and Giamello, 2009). After converting data files to text files of 1024 points per spectrum, the EPR spectrum was processed using the Bruker Win-EPR software.

**(a)**

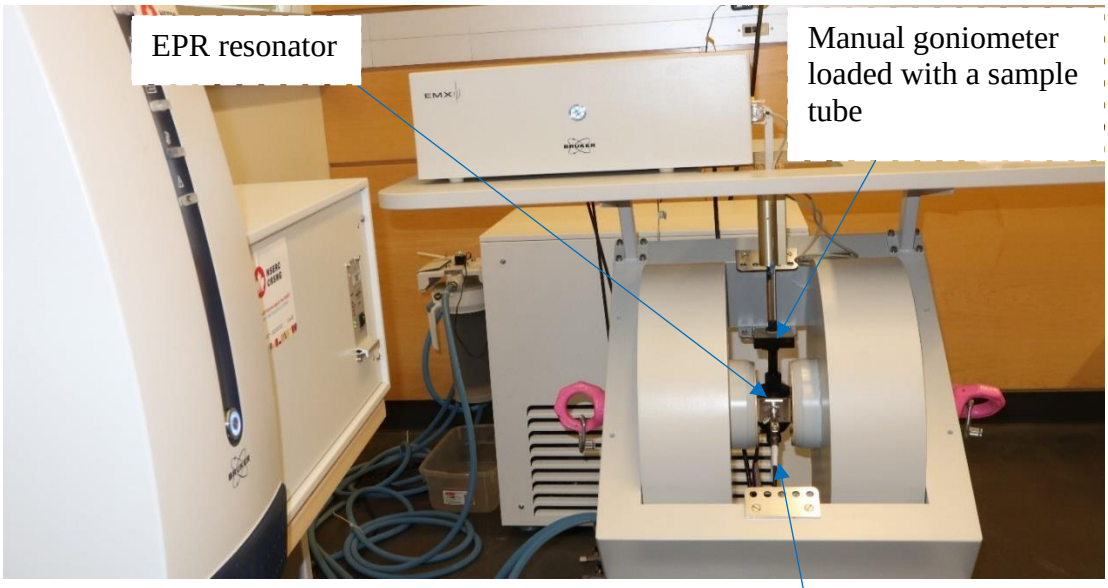


**(b)**


A Haskris R250 Heat exchanger for EPR.

**Figure 4.18**: **(a)** The Bruker X-band CW EPR spectrometer (EMX micro) equipped with a manual goniometer and the internal standard (ER 4119HS-2100) operated at room temperature at Ontario Tech University (Aerosol and radiation lab, ERC 3098). The internal standard is used to determine the g-factor values of the observed EPR signals and normalize the dosimetric signals. **(b)** The Haskris R250 – R1000 heat exchanger.

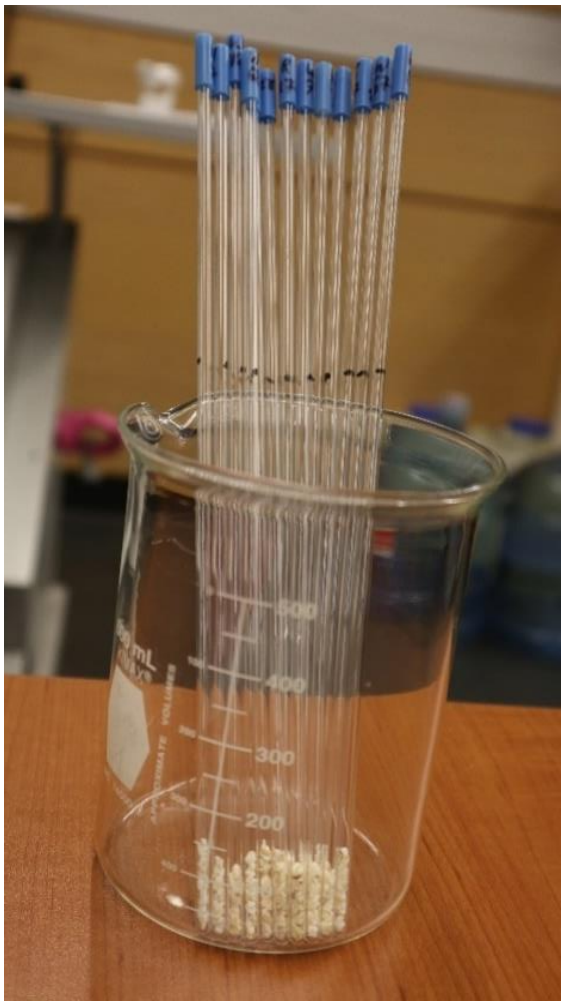


**Figure 4.19:** The 250 mm L EPR quartz tubes (4 mm thin OD) filled with a 105 mg tooth enamel (0.5 – 1 mm grain sizes) sample for the dose estimation using EPR spectroscopy.

For EPR measurements, the tooth enamel sample prepared in Section 4.2.3 was placed into the 250 mmL 4 mm thin OD wall quartz EPR sample tube, as depicted in Figure 4.19. The same size EPR sample tubes were used for all sample analyses. The EPR tube with a tooth enamel sample was taped on the clean surface gently to ensure the tube was uniformly filled with the sample. The tube position inside the cavity was determined by measuring samples at different depths. A position with a high magnetic field ($B_1$) and a low electric field ($E_1$), indicated by the

highest EPR intensity, was determined at 15 cm into the cavity. Since tooth enamel is a crystalline material, its EPR spectrum is angle-dependent because of the anisotropy of a lattice field at $g_{\perp}$= 2.0019 and $g_{\parallel}$ = 1.9988 with respect to the magnetic field position (Ikeya, 1993: Hayes et al., 1998). Therefore, the sample was measured by rotating 40 degrees clockwise up to 360 degrees (i.e., total 10 rotations including 0 degrees) using a manual goniometer, as shown in Figure 4.18a. The resulting ten EPR spectra were averaged. All recorded spectra exhibited quite visible radiation-induced signals. In order to assess the dose, the intensity of the main RIS was measured as the Peak-to-Peak (P2P) amplitude height of the signal, as depicted in Figures 4.22, 4.23, and 4.24. For cases where the P2P signal was too weak to measure directly, the center point of the signal was calculated, and the P2P amplitude height was determined using the values of the spectral width (Polyakov et al., 1995). The reproducibility was determined by measuring the same sample three times (i.e., different times) using a goniometer, and the standard deviation was calculated.

## 4.3 Results and discussion

### 4.3.1 Spectrometer sensitivity and acquisition parameters

The samples collected for the study were not irradiated prior to sample preparation and analysis. Therefore, all absorbed doses determined in this study were from both natural and anthropogenic sources. The main component in the asymmetric EPR spectrum is the radiation-induced (dosimetric) signal that arises from the radiation-induced $^{\bullet}CO_2^-$ free radicals. It has an axial shape (axial dosimetric signal) with $g_{\perp}$=2.0019 and $g_{\parallel}$=1.9988, the signal maximum at g = 2.0031, minimum at g = 1.9988, and the signal linewidth ($\Delta_{pp}$) = 0.508 mT. The dosimetric signal was separated based on its characteristic g -values and width (Polyakov et al., 1995), as depicted in Figures 4.20 and 4.24 (Polyakov et al., 1995). The P2P amplitude of the $g_{\perp}$=2.0019 was taken as a relative measure of the concentration of the radiation-induced radicals (Ignatiev et al., 1996).

The background doses in tooth enamel from the local population generally fall within the low (<100 mGy) to moderate dose region (20-500 mGy) (IAEA, 2002; ICRU, 2002; UNSCEAR, 2012). The method's accuracy in the given dose ranges depends on various factors such as the spectrometer's sensitivity and stability, sample preparation and purification, and the optimization of the EPR spectrum acquisition parameters (Zhumadilov et al., 2005).

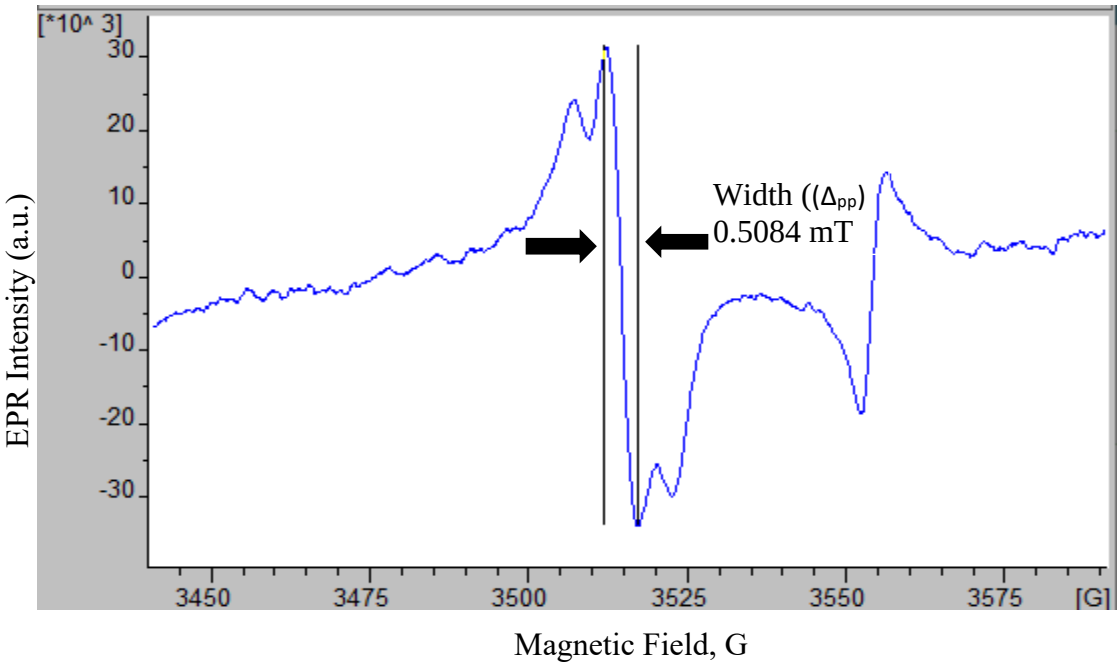


**Figure 4.20:** The linewidth ($\Delta_{pp}$) of the EPR spectrum (0.5084 mT) obtained from the tooth enamel irradiated to 5 Gy (gamma rays from the Hopewell G-10).

Additionally, the quality of the EPR spectra can be increased by using a sensitive spectrometer (Wieser et al., 2000) with a high Q-factor. This study used the EPR spectrometer with the high Q-factor (i.e., for the unloaded cavity, the Q was about 10,000, loaded was about 5,200) resonator (Bruker ER4119HS) as described in Chapter 3 (Section 3.2.3.1). Furthermore, the sample mass, position into the EPR cavity, and the EPR registration (acquisition) parameters such as microwave power, modulation amplitude, accumulation time, receiver gain, and others

were optimized as described in Section 4.2.5 to maximize the dose reconstruction accuracy (ICRU, 2002). At the same time, removal of the impurities from the tooth enamel can significantly increase the measurement precision and accuracy as it reduces the interfering signals (background or noises) from impurities (IAEA, 2002; ICRU, 2002). That is why this study used both chemical and mechanical methods to completely remove the impurities from tooth enamel, as described in Section 4.2.3. Consequently, the RISs are entirely separated from the native signals at low doses, as depicted in Figures 4.21, 4.22, 4.23, and 4.24.

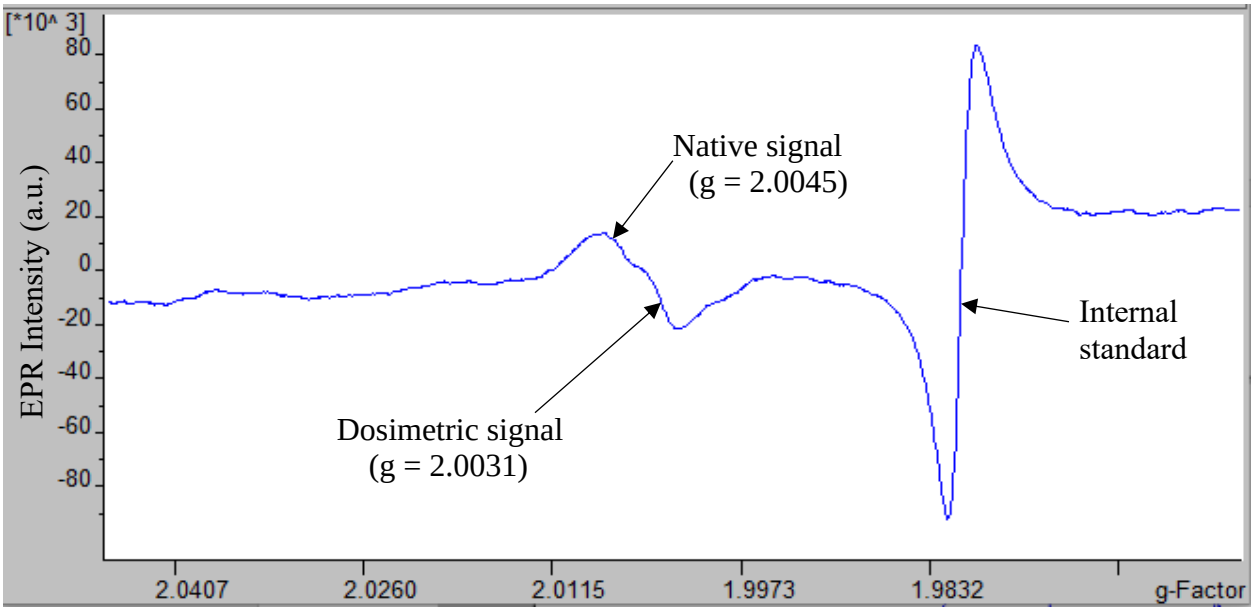


**Figure 4.21:** An EPR spectrum of human tooth enamel irradiated to 30 mGy using the G-10 gamma source at Ontario Tech University. The dosimetric and native signals are separated based on their characteristics g-values (g = 2.0045 and g = 2.0031) and a P2P linewidth.

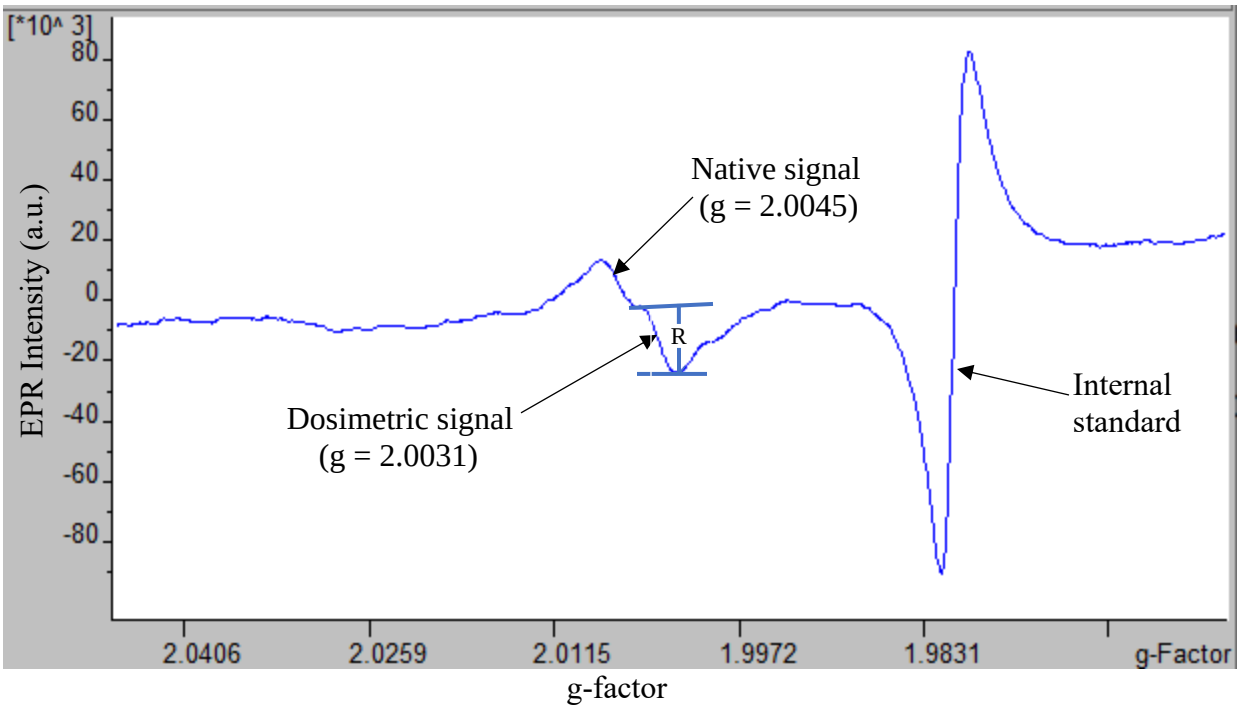


**Figure 4.22:** An EPR spectrum from tooth enamel irradiated to 60 mGy using the G-10 gamma source at Ontario Tech University. R is the P2P amplitude height of the dosimetric signal (g = 2.0031) used to calculate the absorbed dose.

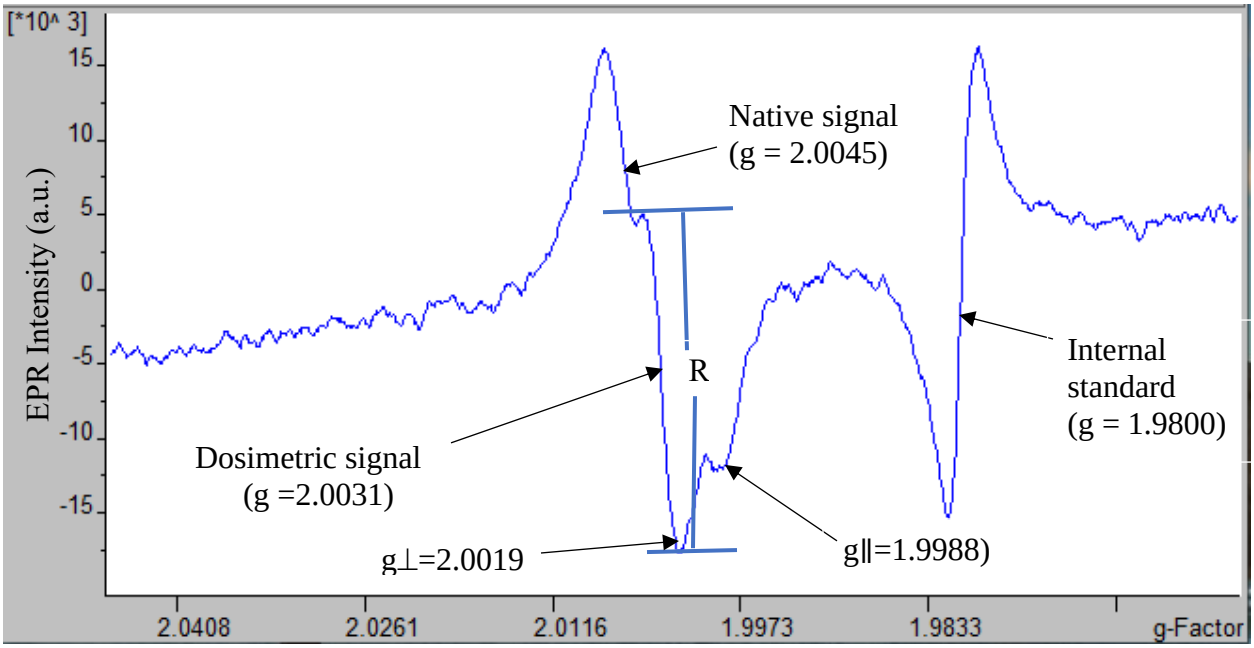


**Figure 4.23:** An EPR spectrum from tooth enamel irradiated to 300 mGy using the G-10 gamma source at Ontario Tech University. The axial dosimetric signal g-values ($g_{\perp}$=2.0019 and $g_{\parallel}$=1.9988), the signal maximum at g = 2.0031. The dosimetric signal linewidth ($\Delta_{pp}$) = 0.508 mT and the native signal at g = 2.0045. R is the P2P amplitude height used to calculate the absorbed dose in tooth enamel.

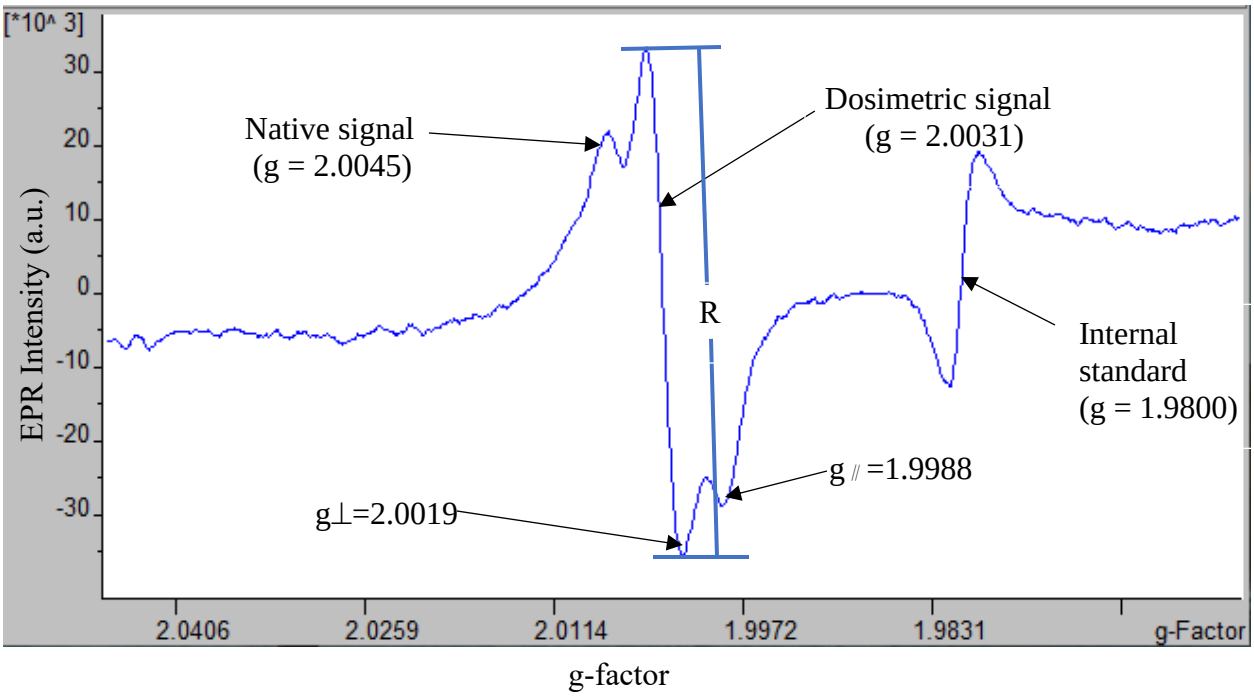


**Figure 4.24:** An EPR spectrum from human tooth enamel irradiated to 5 Gy using the G-10 gamma source at Ontario Tech University. R is the P2P amplitude height of the enamel radiation-induced signal used for EPR dose reconstruction.

The calibration curve was constructed to calculate the absorbed dose in tooth enamel as described in Section 4.2.4 and Table 4.3. The dose-response curve of the eight tooth enamel samples irradiated to 0 to 1,500 mGy is linear, as depicted in Figure 4.25. The linear regression gives dosimetric parameters and can determine the doses once the P2P amplitude height of an unknown sample is determined, as described in Chapter 3 (Sections 3.10.2 and 3.10.3).

**Table 4.3:** P2P amplitude height (normalized) in the low and moderate dose tooth enamel samples with the standard deviation of the signals.

| Dose (mGy) | P2P amplitude | Standard deviation |
|---|---|---|
| 30 | 0.22 | 0.05 |
| 60 | 0.50 | 0.08 |
| 100 | 0.81 | 0.15 |
| 200 | 1.45 | 0.23 |
| 500 | 3.20 | 0.30 |
| 1000 | 5.88 | 0.22 |
| 1500 | 8.01 | 0.28 |

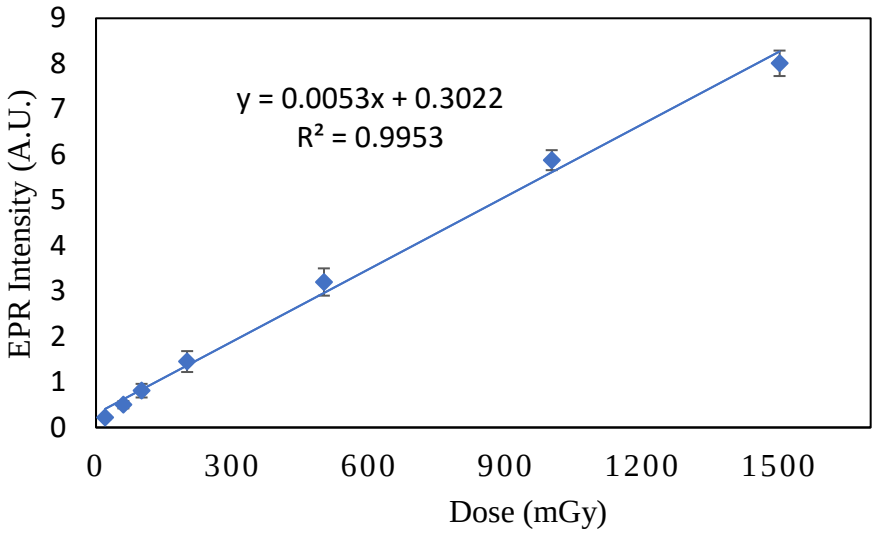


**Figure 4.25:** EPR dose-response of eight enamel samples irradiated to 0, 30, 60, 100, 200, 500, 1000, and 1500 mGy using the Hopewell G-10 gamma irradiator ($^{137}$Cs) at Ontario Tech University (ERCB058/056 Radiation Protection and Applied Radiation Laboratory).

### 4.3.2 Sample and signal anisotropy

As described in Chapter 2 (Section 2.3), a sample with a crystalline property exhibits the sample and signal anisotropy, which means an EPR spectrum depends on the different orientations of a sample into the cavity with respect to the applied magnetic field (Haskell et al., 1997). Also,

the sample and signal anisotropy depend on the grain size of the enamel. It decreases with the fine grain size; however, the fine grain sizes increase the native signals, interfering with the dosimetric signals (Iwasaki et al., 1993). The unwanted native or background signals eventually over or underestimate the absorbed doses in enamel. However, the grain sizes 0.5 – 1 mm have been proved to be optimal for minimizing the effects of sample anisotropy in tooth enamel (Iwasaki et al., 1993; Haskell et al., 1997). Still, tooth enamel is a crystalline material and can show minor anisotropy effects in this optimal grain size, which may over or underestimate the absorbed doses in enamel. The only way to minimize the measurement errors from these effects is to measure the sample multiple times at different angles and average their P2P amplitudes height for the dose calculation. As shown in Figure 4.26, despite the optimal grain size, the EPR intensities are slightly changing when the enamel sample rotates with respect to the direction of the applied magnetic field in the EPR cavity. Therefore, to minimize the errors from the sample anisotropy, each sample was rotated by 40 degrees at a time using a manual goniometer up to 360 degrees, as described in Chapter 3 (Section 3.8) and shown in Figure 4.18a. The recorded ten spectra, including a zero-degree rotation, were used to calculate the average P2P amplitude height (R) and the absorbed dose (ICRU, 2002). This technique reduces the errors that arise from the sample and signal anisotropy. Also, since the tooth enamel sample was not removed from the cavity (i.e., sample position was fixed into the cavity) at each measurement, the errors from the change in a resonant frequency and microphonics may be lower.

However, using large grain sizes, the dosimetric signal measured as P2P height can vary by about 50% due to the sample anisotropy (i.e., the contribution of axial $^{\bullet}CO_2^-$ centers to the EPR spectrum). This variation in the P2P height measurement can significantly decrease the measurement accuracy in low-dose tooth enamel EPR dosimetry (Hayes et al., 1998; Aoba et al.,

1985). Therefore, this study used the optimum sample (or grain) size (with minimal anisotropy) described in Section 4.2.3. Additionally, each sample was rotated, and the final average intensity was calculated to enhance the measurement accuracy and reproducibility.

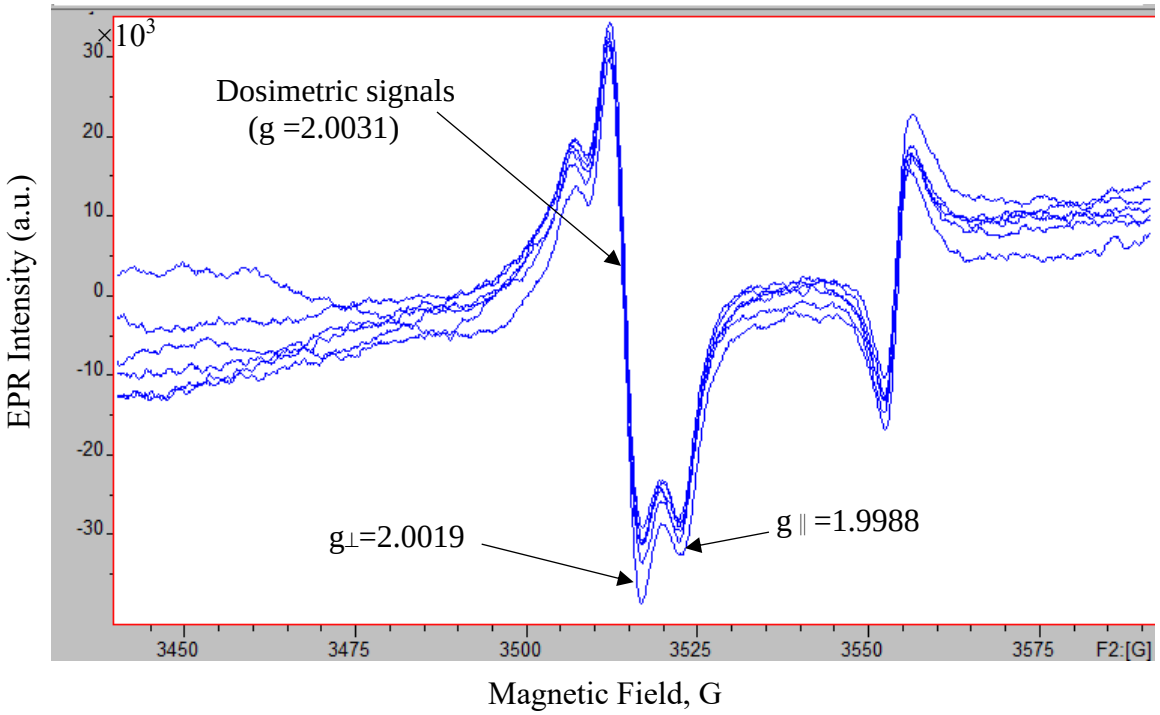


**Figure 4.26:** EPR spectra anisotropy of tooth enamel collected from Durham Region, Ontario. Tooth enamel was measured by rotating a sample 40 degrees at a time up to 360 degrees (without removing it from the cavity). The tooth enamel EPR intensity (5 Gy) changes with the rotation angle due to the sample and signal anisotropy [$g_x = g_y$ ($g\perp$) =2.0019, $g_z$ ($g\parallel$) = 1.998].

### 4.3.3 **Background doses in teeth of Durham residents**

The collection of tooth samples for EPR measurements was started in 2021. The structure of population groups and ages of the analyzed samples are presented in Table 4.4. All measured EPR spectra and participants' information were entered into a computer database, stored, and used for subsequent interpretation and statistical analysis. The tooth enamel samples were also

preserved (stored) for a future reassessment. During EPR analyses, it was found that the tooth enamel contains two types of signals: (1) the native signal (g = 2.0045) arises from dentin and other impurities, and (2) the dosimetric signal at $g_{\perp}$=2.0019, $g_{\parallel}$=1.9988, and the maximum at g = 2.0031 arises from the $^{\bullet}CO_2^-$ radical anions formed when enamel (i.e., hydroxyapatite) is exposed to ionizing radiation (e.g., gamma rays), as shown in Figures 4.27a and 4.27b. It is paramount to separate these two signals in a dose measurement, as depicted in Figures 4.27a and 4.27b. The visually distinct dosimetric signal can be measured precisely, decreasing measurement errors significantly. In addition to ionizing radiation, the UV rays also generate the free radicals on tooth enamel's outer surface, overestimating the actual dose a person gets from radiological or nuclear accidents or chronic exposures (Nilsson et al., 2001; Vorona et al., 2007). It has been shown that such exposure induces an EPR signal identical to that of the ionizing radiation exposures and can be up to 200 mGy/day (Liidja et al., 1996; Rudko et al., 2007). Front teeth were generally exposed to the UV rays, which contributed to large uncertainties (Skvortzov et al., 1995). So, this study used only the lingual part of molar tooth enamel, as described in Section 4.2.3, to reduce errors (if any) from the UV rays in a total dose measurement. However, since UV is not ionizing radiation, it produces signals with stable and unstable components. The unstable component can be removed by annealing (heating). However, the stable component can be removed by acid etching (10% HCl) since UV penetration depth is minimal (100 – 200 μm) in enamel compared with ionizing radiation. The thin outer layer affected by UV is removed by dissolving with acid (during acid etching). Therefore, the effect of UV light on the EPR signal in teeth enamel is negligible (Bailiff et al., 2016; Fattibene and Callens, 2010). So, the UV-induced signals are temporary and can be removed using proper sample preparation and storage techniques described in Section 4.2.3.

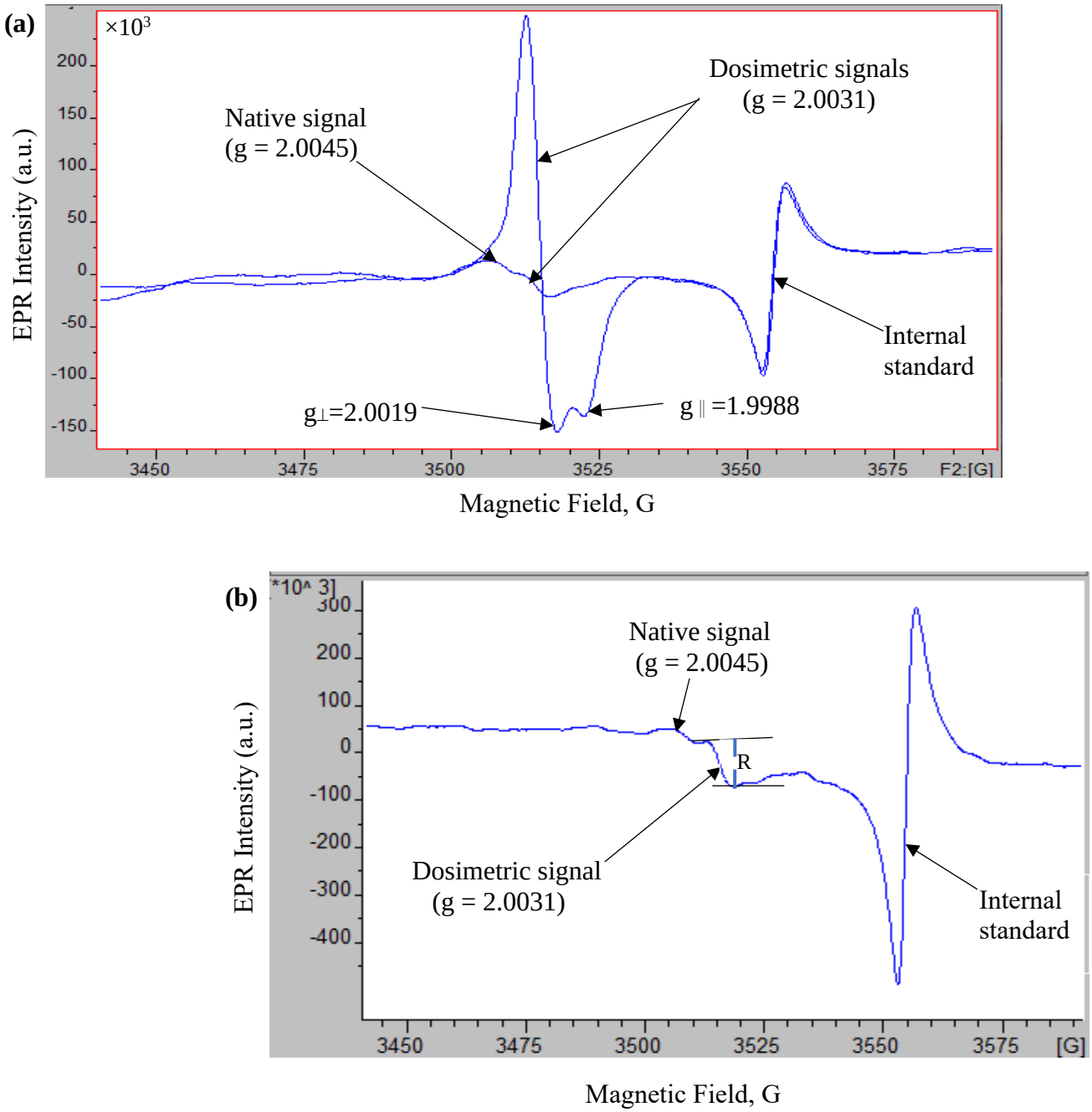


**Figure 4.27: (a)** EPR spectra of the tooth enamel samples (molar) from a 42-year-old participant before and after irradiating the sample to 5 Gy using the G-10 gamma source. The axial dosimetric signals (g⊥=2.0019 and g∥=1.9988) and the maximum value (g = 2.0031) are the characteristics of the dosimetric signals. **(b)** An EPR spectrum of the tooth enamel powder (molar) from a 78-year-old participant where the RIS was represented by R. The RIS was clear and measurable.

Each human molar tooth contains about 1,000 mg of enamel, so the enamel mass from the lingual part was enough for the complete analysis of a dose, which was optimized to be 105 mg for a single analysis. Using the X-band CW EPR spectrometer, our lowest detectable dose was 30 mGy, equal to the dose reported in the literature (29 mGy) (Romanyukha et al., 2001; Ivannikov et al., 2001). Since our absorbed dose was higher than the detection limit in tooth enamel, the dosimetric signals were visible in all age groups' teeth collected from Durham Region, Ontario. Therefore, after measuring the P2P amplitude height of each sample, the absorbed dose in tooth enamel (lingual) was determined using the calibration curve method (Figure 4.25). This also allows the samples to be used for future remeasurements. The absorbed dose (lingual) in teeth enamel at each age range was averaged, and the standard deviation was calculated. The average absorbed doses increase with the age of the people, as shown in Table 4.4 and Figure 4.28, which may be due to the accumulative effect and the stability of the absorbed doses in tooth enamel. Consequently, many of those who received higher doses were older people. The age distribution, Figure 4.28 and Table 4.4, shows that those over 70 received about four times the dose of those under 20. The radiation exposures from radioactive contamination are uniform throughout the human body in an actual situation. So, it is reasonable to guess that the dose received in enamel is close to the whole body's effective dose. To calculate the dose rate in populations, the average lingual dose from each age group with the standard deviation was plotted as a function of the ages, as depicted in Figure 4.28. The best-fit line (i.e., trendline) was drawn (Figure 4.28). The line slope was determined, which was the effective dose per year (mSv/year) to each age group in a population (Toyoda et al., 2011).

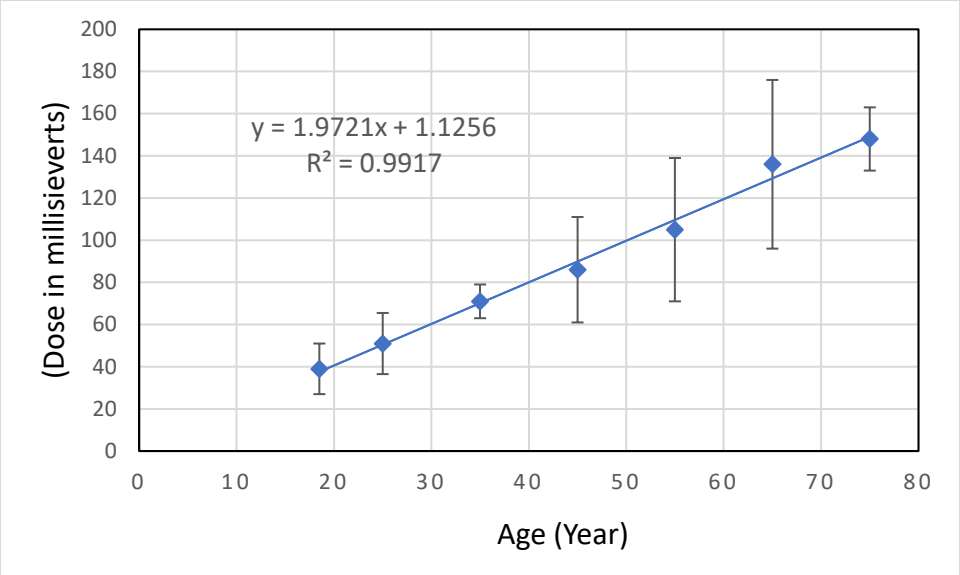


**Figure 4.28:** The average lingual doses with the standard deviation as a function of the age range of the participants. The best fit line (trendline) is used to determine the slope (i.e., dose rate per year), equal to 1.9721 mSv/year.

As shown in Figure 4.28, the calculated dose rate was 1.9721 mSv/year, and the natural background dose in Durham Region, Ontario, was 1.338 mSv/year (CNSC, 2013; Lane et al., 2013 Grasty and LaMarre, 2004; Grasty, 2002; Grasty et al., 1984). The natural background radiation dose accumulates in tooth enamel during a human lifetime. Therefore, the difference in the doses (i.e., equation 4.1) was from the anthropogenic sources (i.e., medical, industrial, nuclear power plants, and others) (Toyoda et al., 2011).

$$\text{Anthropogenic dose (a)} = (1.9721 - 1.338)\ \text{mSv} = 0.6341\ \text{mSv/year} \qquad (4.1)$$

The calculated annual dose rate of 0.6341 mSv/year was the effective dose to the public from different anthropogenic sources. Furthermore, the anthropogenic doses are combined from various artificial sources such as medical doses from external X-ray diagnostic examinations, CT and conventional, nuclear medicine, radiotherapy, smoke detectors, smoking (0.005 – 40 μSv per

cigarette), flights, weapons fallout, nuclear power, nuclear power plant accidents, etc. (UNEP, 2016; Grupen and Rodgers, 2016). The smoke alarms are provided with a weak α-source from 40 kBq $^{241}$Am. However, no radiation is detected outside the ionization chamber. This demonstrated that consumer products are not a significant source of dose (Allison, 2006). In this study, the calculated combined doses from these sources were lower than the local background doses in Durham Region, Ontario, and lower than Canada's regulatory annual effective dose limit of 1 mSv/year. Using this graph (Figure 4.28) and equation 4.1, the people's historical doses can be calculated by subtracting each year's background dose from the total calculated dose rate, which is called the retrospective dose reconstruction for exposure to ionizing radiation (Toyoda et al., 2011). Similarly, this technique can also be applied to determine the sample's age or dating in archaeology if the annual background dose is known at a particular place where a tooth is found. The total dose in the sample is divided by the local background (natural) dose rate to calculate the sample's age (Ikeya, 1993).

**Table 4.4:** Age range, average lingual doses, standard deviation, and the number of samples in each age range from Durham Region, Ontario.

| Age range (yr) | Number of samples | Averaged lingual dose (mGy) | Standard Deviation (mGy) |
|---|---|---|---|
| 16-19 | 10 | 39 | 12 |
| 20-29 | 5 | 51 | 14.5 |
| 30-39 | 6 | 71 | 8 |
| 40-49 | 8 | 86 | 25 |
| 50-59 | 10 | 105 | 34 |
| 60-69 | 18 | 136 | 40 |
| 70-79 | 7 | 148 | 15 |

From these results, one can conclude that the anthropogenic doses in the people living within 30 km of the power plants were lower than the background doses and the annual regulatory limit for the public. So, there may be no adverse health effects from the anthropogenic doses to

the local populations. The dose contribution of the nuclear-generating stations is small (i.e., <0.1% of the regulatory limit of 1 mSv/year) in Durham Region, Ontario, and it was consistent with the results from the CNSC (OPG, 2017; CNSC, 2018a; 2018b). Furthermore, the radio epidemiology of cancer incidence in the Durham Region did not change the cancer incidence rates over the fifteen years (Durham Region Health Department, 2007; Durham Region Health Department, 2017). Both male and female combined cancer incidence rates were the same as the Ontario populations (Durham Region Health Department, 2007; Durham Region Health Department, 2017). These data and the radio-epidemiology of the Durham Region further demonstrated that there was minimal dose contribution from the nearby NGSs. Therefore, most of the anthropogenic dose (0.6341 mSv/year) determined in this study could be from other artificial sources such as diagnostic radiology, nuclear medicines, radiation therapy, industrial and occupational use of radioactive materials. However, more samples (i.e., wide-scale sample collection and measurements) with donors' history could provide more detailed information about the background doses in this Region.

The calculated excess dose is about 47.39% of the natural background dose (1.338 mSv/year) in Durham Region, Ontario (i.e., lower than the general public's annual effective dose limit). As mentioned above, diagnostic radiology, nuclear medicines, radiation therapy, industrial and occupational exposures could be the possible sources of the doses, but further study would be needed to identify the artificial sources. Many studies have identified radiology (dental X-rays), nuclear medicine, radiation therapy, and occupational exposures as the largest sources for the anthropogenic doses, which sometimes exceed the dose received from the natural background radiation (Gonzalez and Anderer, 1989; IAEA, 2004; Allison, 2006). Moreover, as nuclear medicine is increasing to treat and diagnose different kinds of diseases in industrialized countries,

the dose contribution from the medical use of radiation is also increasing in the general public (UNEP, 2016). On average, medical procedures contribute about 98 percent of the radiation exposure from all artificial sources and, after natural sources, are the second largest contributor to the population exposure worldwide (UNEP, 2016). Overall, the annual effective dose to a person in a year (world average) from artificial sources is 0.65 mSv; however, this value varies considerably by region, country, and health-care system (UNEP, 2016; Grupen and Rodgers, 2016). The industrialized country Japan has about 0.5 mGy/y as the dose from the artificial sources (Toyoda et al., 2011). These data demonstrated that we need a periodic assessment of artificial doses in populations to ensure the annual effective dose to an individual does not exceed a regulatory limit.

This study estimated the total anthropogenic doses in tooth enamel to the public from various sources. However, if we are interested in finding the dose contribution from the nuclear power only, in that case, the exact dose contribution from the other sources except nuclear must be determined using questionnaires during the sample collection. Still, patients (participants) may not remember the times of medical procedures they performed, the dose limit of each procedure, their personal histories of occupations, residence, diet, and lifestyle (often called recall bias). So, these data can be subject to both random and systematic errors (UNSCEAR, 2012). So, estimating an exact dose contribution from a single source is very challenging, and it may sometimes over or underestimate the total absorbed doses from those sources.

Nonetheless, EPR dosimetry with tooth enamel is undoubtedly an attractive method of retrospective dosimetry. It is also helpful in assessing the accident doses in individuals after a nuclear or radiological accident. In such a situation, the background doses from the victims, such as medical procedures, dental X-rays, etc., must be subtracted to get the actual accident doses. So,

retrospective dose reconstruction using EPR dosimetry with tooth enamel is essential for estimating the absorbed doses in chronic and acute exposure scenarios.

### 4.3.4 **Sources of uncertainties in the measured doses**

There could be dose measurement errors from the various sources, such as **(1) Participants' residency:** Teeth were collected only from the permanent residents from Durham Region, Ontario. However, if the participants are temporary residents or visitors from other provinces, this can increase the measurement uncertainty in the annual anthropogenic dose rate. However, the uncertainty will be negligible. **(2) Number of samples:** A large number of samples from different age groups can provide a more accurate anthropogenic dose in populations than a small number of samples. Nevertheless, Toyoda et al. (2011) estimated the total doses in the teeth of Japanese residents using forty-six extracted wisdom teeth obtained from the Department of Dentistry, Ohu University. Similarly, Zhumadilov et al. (2006) reconstructed the absorbed doses to the population of Dolon and Bodene (i.e., former nuclear test sites in Russia) using 35 teeth samples. Ivannikov et al. (2002) estimated absorbed doses in the Northeastern part of Kazakhstan near the Semipalatinsk Nuclear Test site using 36 extracted teeth samples. So, the sample size of this study is larger than similar previous studies. **(3) Parameter optimization:** EPR acquisition parameters depend on the type of an EPR spectrometer, its cavity, and the types of samples. The EPR acquisition parameters, including the optimal mass and sample position into the cavity, were optimized as described in Section 4.2.5, significantly reducing the measurement errors. **(4) Calibration curve:** To construct the calibration curve, tooth enamel from different age groups was mixed to make the heterogeneous samples, which can average the tooth enamel radiation sensitivity from the different age groups as described in Section 4.2.4 and Table 4.4, and eventually decrease the measurement errors (type B errors). Also, standard statistical techniques were used to

calculate the standard deviation, percentage errors, etc., to reduce type A errors in the overall dose calculations. **(5) Sample anisotropy:** Since enamel is a crystalline material (i.e., hydroxyapatite), its EPR intensity depends on the sample orientations with respect to the applied magnetic field in the EPR cavity and the tooth enamel grain sizes described in Section 4.3.2. However, this study reduced the measurement errors arising from the sample anisotropy as described in Section 4.3.2. Also, using a goniometer allows higher microwave power, which increases the sensitivity of the radiation-induced signals and suppresses anisotropies. **(6) UV exposure:** UV irradiation could contribute a significant amount of dose if teeth are exposed to UV radiation (Nilsson et al., 2001; Vorona et al., 2007; Jiao et al., 2007). However, this study removed a thin outer layer of enamel using acid etching and used only a lingual part of teeth for analyses, with negligible exposure to UV. Consequently, the errors from the UV sources were minimized in the total dose measurements. **(7) A human tooth bank:** One of the important limitations identified in this research was to obtain the extracted teeth covering different age groups on time, so it would be convenient if a human tooth bank was established in Durham Region, Ontario. Many cities close to nuclear power plants have their tooth banks for a periodic dose evaluation (ICRU, 2002; Skvortsov et al., 2000; Ivannikov et al., 2004).

## 4.4 **Conclusions**

Though nuclear is a clean and reliable source of energy, there is a constant fear in the general public about the possible exposure from nuclear facilities. However, most nuclear facilities have well-developed radiation protection plans for maintaining As Low as Reasonably Achievable (ALARA) doses. That is why the annual average collective doses from the US nuclear power plants have decreased from 7.74 person-Sv to 1.06 a person-Sv (i.e., a seven-fold decrease from 1973 to 2006). Also, the average annual measurable dose per worker was reduced from 6.6 mSv

to 1.4 mSv in the US. Consequently, the average annual dose to a person in the US living within 30 km of a nuclear-generating station was 0.01 mSv/year.

Similarly, in Canada, a person living close to nuclear-generating stations gets 0.001 mSv/year. Based on these data, there are extremely low exposures from nuclear power stations to the environment and the general public, and no adverse health effects were observed. In Durham Region, Ontario, as per the recent OPG environmental monitoring report, both Pickering and Darlington nuclear power stations are emitting less than 0.1% dose of the annual regulatory limit of 1 mSv/year and the background dose of 1.338 mSv/year for Durham Region, Ontario. So, the public and the environment are safe from any harmful effects of radiation exposures from these nuclear stations. However, there are worries and concerns from the local people in Durham Region, Ontario, regarding their total doses from the various sources, including nearby nuclear-generating stations. The direct dose measurement from the human tissues can provide the actual doses that humans are getting from the various sources, which may lessen their worries and concerns. Since human tooth enamel is a 'biological dosimeter' (i.e., a highly radiation-sensitive tissue) that can record a dose longer than the human life span, this study used tooth enamel collected from Durham Region, Ontario, to determine the total background doses from the various sources in the Region. Another advantage of tooth enamel is that it is the only human tissue that can record the low doses and can be measured down to 30 mGy. Additionally, the dose retention rate of tooth enamel is very high compared to the other tissues like blood, skin, and environmental samples. So, the tooth samples covering various age groups were collected from Durham Region with the help of the local dentists/dental clinics and residents. The samples were prepared following the ISO protocol and analyzed using the X-band CW EPR spectrometer. The measurement errors (both types A and B) were reduced by optimizing the EPR acquisition parameters, optimal sample size, constructing

the calibration curve using heterogeneous samples (to average the radiation sensitivity of different age groups), and reducing errors from the sample anisotropy. The calculated anthropogenic dose rate was 0.6341 mSv/year. Since radiation exposure from the nuclear-generating stations in Durham Region is extremely low, as described in Sections 4.1.4, 4.1.5, and 4.1.6, a large part of the calculated anthropogenic dose could be from medical applications (i.e., radiology, nuclear medicine, and radiotherapy), on average, it accounts for 98 percent of the radiation exposure from all artificial sources (UNEP, 2016). However, the estimated anthropogenic dose was lower than the effective dose limit for the general public in Canada (i.e., 1 mSv/year). Therefore, as per this study, the anthropogenic doses are lower than the regulatory limit and the background dose in Durham Region, Ontario. However, further investigation would be needed to identify the sources of anthropogenic radiation and conclude this Region's situation.

**Acknowledgements**

We would like to thank all the dentists/dental clinics and the residents who provided the extracted teeth for the study. The work described was undertaken as part of the independent, low-dose research program "Addressing Public Concerns about Their Exposure to Low Doses of Anthropogenic Radiation," funded by the CANDU Owners Group Inc. Funding was also received from the Natural Sciences and Engineering Research Council (NSERC) of Canada. Also, the authors would like to thank Dr. Nicholas Priest for his suggestion for this project.

**Compliance with ethical standards:** This study has been reviewed the ethics clearance through Ontario Tech University’s Research Ethics Committee (REB # 14870) on January 05, 2019.

**Conflict of interest:** The authors declare that they have no conflict of interest.

## 4.5 References


Aoba, T., Doi, Y., Yagi, T., Okazaki, M., Takahashi, J., Moriwaki, Y., 1982. Electron spin resonance study of sound and carious enamel. Calcif. Tissue Int. 34, 88-92.

Allison, W., 2006. Fundamental physics for probing and imaging. Oxford University Press Inc., New York.

Ainsbury, E.A., Bakhanova, E., Barquinero, J.F., Brai, M., Chumak, V., Correcher, V. et al. 2011. Review of retrospective dosimetry techniques for external ionising radiation exposures. Radiat. Prot. Dosim. 147 (4), 573-592.

Bhat, M., 2005. EPR tooth enamel as a tool for validation of retrospective doses: an end-user perspective. Appl. Radiat. Isot. 62,155-161.

Bailiff, I.K., Sholom, S., McKeever, S.W.S., 2016. Retrospective and emergency dosimetry in response to radiological incidents and nuclear mass-casualty events: A review. Radiat. Meas. 94, 83-139.

Blevins, M.R., Andersen, R.L., 2010. Radiation protection at U.S. nuclear power plants—today and tomorrow. Health Phys, 100, 1, 35-38.

Brustolon, M., Giamello, E., (Eds.). 2009. Electron paramagnetic resonance, a practitioner's toolkit. John Wiley & Sons, Inc., Hoboken, New Jersey.

Canadian Nuclear Safety Commission (CNSC), 2013. Radiation and incidence of cancer around Ontario nuclear power plants from 1990 to 2008 (The RADICON Study) - Summary Report. Retrieved October 20, 2021, from https://www.scirp.org/pdf/JEP_2013082813431470.pdf

Canadian Nuclear Safety Commission (CNSC), 2018a. Independent Environmental Monitoring Program: Pickering Nuclear Power Generating Site. Retrieved October 20, 2021, from https://nuclearsafety.gc.ca/eng/resources/maps-of-nuclear-facilities/iemp/pickering.cfm#r2017

Canadian Nuclear Safety Commission (CNSC), 2018b. Independent Environmental Monitoring Program: Darlington nuclear generating site. Retrieved October 20, 2021, from https://nuclearsafety.gc.ca/eng/resources/maps-of-nuclear-facilities/iemp/darlington.cfm#current

Canadian Nuclear Safety Commission (CNSC), n.d. Radiation doses. Retrieved October 20, 2021, from http://nuclearsafety.gc.ca/eng/resources/radiation/introduction-to-radiation/radiation-doses.cfm

Chumak, V.V., 2013. Retrospective dosimetry of populations exposed to reactor accident: Chernobyl example, lesson for Fukushima. Radiat. Meas. 55, 3-11.

Chumak, V., Sholom, S., Pasalkaya, L., 1999. Application of high precision EPR dosimetry with teeth for reconstruction of doses to Chernobyl populations. Radiat. Prot. Dosim. 84, 515–520.

Desrosiers, M., Schauer, D.A., 2001. Electron paramagnetic resonance (EPR) biodosimetry. Nucl. Instr. and Meth. in Phys. Res. B. 184, 219-228.

Driessens, F.C.M., 1980. The mineral in bone, dentine and tooth enamel. Bull. Soc. Chim. Belg. 89, 663-689.

Durham Region Health Department, 2007. Radiation and Health in Durham Region 2007. Whitby, Ontario: The Regional Municipality of Durham. Retrieved January 21, 2021, from

https://healthdocbox.com/67784217-Cancer/Radiation-health-in-durham-region-report-2007.html

Durham Region Health Department, 2017. Cancer at a Glance in Durham Region. Whitby, Ontario: The Regional Municipality of Durham. Retrieved January 21, 2021, from https://www.durham.ca/en/health-and-wellness/resources/Documents/HealthInformationServices/HealthStatisticsReports/Cancer-at-a-Glance.pdf

Eaton, G.R., Eaton, S.S., Barr, D.P., Weber, R.T., 2010. Quantitative EPR. Springer Wien New York. DOI 10.1007/978-3-211-92948-3.

Fattibene, P., Callens, F., 2010. EPR dosimetry with tooth enamel: A review. Appl. Radiat. Isot. 68, 2033-2116.

Gerard, W., 1979. August 20. Nuclear power: debate for the'80s. Maclean's. Retrieved October 10, 2021, from https://archive.macleans.ca/article/1979/8/20/nuclear-power-debate-for-the80s

Gonzalez, A.J., Anderer, J., 1989. Radiation versus radiation: Nuclear energy in perspective, a comparative analysis of radiation in the living environment. IAEA Bulletin 2; Retrieved October 10, 2020, from https://www.iaea.org/sites/default/files/publications/magazines/bulletin/bull31-2/31205642131.pdf

Grasty, R.L., Carson, J.M., Charbonneau, B.W., Holman, P.B., 1984. Natural background radiation in Canada. Geol. Surv. Can. Bull. 360.

Grasty, R.L., 2002. The Annual Effective Dose from Natural Sources of Ionizing Radiation in Canada, Gamma-Bob Report 02-6.

Grasty, R.L., LaMarre, J.R., 2004. The annual effective dose from natural sources of ionising radiation in Canada. Radiat. Prot. Dosim. 108 (3): 215-26.

Grupen, C., Rodgers, M., 2016. Radioactivity and Radiation: What They Are, What They Do, and How to Harness Them. Springer International Publishing Switzerland. DOI 10.1007/978-3-319-42330-2

Gualtieri, G., Colacicchi, S., Sgattoni, R., Giannoni, M., 2001. The Chernobyl accident: EPR dosimetry on dental enamel of children. Appl. Radiat. Isot. 55, 71–79.

Haskell, E.H., Hayes, R.B., Kenner, G.H., 1997. Improved accuracy of EPR dosimetry using a constant rotation goniometer. Radiat. Meas. 27, 325–329.

Hayes, R.H., Haskell, E.H., Romanyukha, A.A., Kenner, G.H., 1998. A technique for increasing reproducibility in EPR dosimetry of tooth enamel. Meas. Sci. Technol. 9, 1994–2006.

Hennig, G.J., Herr, W., Weber, E., Xirotiris, N.I., 1981. ESR-dating of the fossil hominid cranium from Petralona Cave, Greece. Nature. 292 : 533-536.

ICRU, 2002. Retrospective Assessment of Exposures to Ionising Radiation. International Commission on Radiation Units and Measurements. International Commission on Radiation Units and Measurements, Bethesda, USA. ICRU Report 68.

Ignatiev, E.A, Romanyukha, A., Koshta, A.A., Wieser, A., 1996. Selective saturation method for EPR dosimetry with tooth enamel. Appl. Radiat. Isotop. 47, 333–7.

ISO, 2013. Radiological protection – Minimum criteria for electron paramagnetic resonance (EPR) spectroscopy for retrospective dosimetry of ionizing radiation – Part 1: General principles, International Standard, ISO 13304-1.

IAEA, 2002. Use of electron paramagnetic resonance dosimetry with tooth enamel for retrospective dose assessment. IAEA-TECDOC-1331. International Atomic Energy Agency, Vienna, Austria, 57 pp.

IAEA, 2004. Radiation, people and the environment. IAEA/PI/A.75 / 04-00391. International Atomic Energy Agency, Vienna, Austria, 85 pp.

Ikeya, M., 1993. New Application of Electron Spin Resonance - Dating, Dosimetry and Microscopy. Word Scientific, Singapore.

Ikeya, M., Miyajima, J., Okajima, S., 1984. ESR dosimetry for atomic bomb survivors using shell buttons and tooth enamel. Jpn. J. Appl. Phys. 23, 697–699.

Ishii, H., Ikeya, M., Okano, M., 1990. ESR dosimetry of teeth of residents close to Chernobyl reactor accident. J. Nucl. Sci. Technol. 27, 1153–1155.

Ivannikov, A.I., Gaillard-Lecanu, E., Trompier, F., Stepanenko, V.F., Skvortsov, V.G., Borysheva, N. B., et al., 2004. Dose reconstruction by EPR spectroscopy of tooth enamel: Application to the population of Zaborie village exposed to high radioactive contamination after the Chernobyl accident. Health Phys. 86(2), 121–134.

Ivannikov, A.I., Tikunov, D.D., Skvortsov, V.G., Stepanenko, V.F., Khomichyonok, V.V., Khamidova, L.G., et al., 2001. Elimination of the background signal in tooth enamel samples for EPR-dosimetry by means of physical–chemical treatment. Appl. Radiat. Isot. 55, 701–705.

Ivannikov, A.I., Zhumadilov, Zh, Gusev, B.I., Miyazawa, Ch, Jiao, L., Skvortsov, V.G., et al., 2002. Individual dose reconstruction among residents living in the vicinity of the Semipalatinsk Nuclear Test Site using EPR spectroscopy of tooth enamel. Health Phys. 83, 183-196.

Iwasaki, M., Miyazawa, C., Uesawa, T., Niva, K., 1993. Effect of sample grain size on the $CO_3^{3-}$ signal intensity in ESR dosimetry of human tooth enamel. Radioisotopes 42, 470–473.

Jacob, P., Goksu, Y., Taranenko, V., Meckbach, R., Bougrov, N.G., Degteva, M.O., et al., 2003. On an evaluation of external dose values in the Techa River Dosimetry System (TRDS) 2000. Radiat. Environ. Biophys. 42, 169–174.

Jiao, L, Takada, J., Endo, S., Tanaka, K., Zhang, W., Ivannikov, A., et al., 2007. Effects of sunlight exposure on the human tooth enamel ESR spectra used for dose reconstruction. J. Radiat. Res. (Tokyo) 48(1), 21–29.

Jiao, L., Liu, Z.C., Ding, Y.Q., Ruan, S.Z., Wu, Q., Fan, S.J., et al., 2014. Comparison study of tooth enamel ESR spectra of cows, goats and humans. J. Radiat. Res. 55, 1101-1106.

Lane, R., Dagher, E., Burtt, J., Thompson, P.A., 2013. Radiation Exposure and Cancer Incidence (1990 to 2008) around Nuclear Power Plants in Ontario, Canada. J. Environ. Prot. 4, 888-913. http://dx.doi.org/10.4236/jep.2013.49104

Lee, U., Lee, C., Kim, M., Kim, H.R., 2019. Analysis of the influence of nuclear facilities on environmental radiation by monitoring the highest nuclear power plant density region. Nucl. Eng. Technol. 51, 1626-1632.

Liidja, G., Past, J., Puskar, J., Lippmaa, E., 1996. Paramagnetic resonance in tooth enamel created by ultra-violet light. Appl. Radiat. Isot. 47, 785–788.

Martin, J.M., 2013. Physics for Radiation Protection. Wiley-VCH.

Moens, P.D.W., Callens, F.J., Verbeeck, R.M.H., Naessens, D.E., 1993. An EPR spectrum decomposition study of precipitated carbonated apatites (NCAP) dried at 258ºC: absorption of molecules from the atmosphere on the apatite powders. Appl. Radiat. Isot. 44, 279-285.

Nakamura, N., Miyazawa, C., Akiyama, M., Sawada, S., Awa, A.A., 1998. A close correlation between electron spin resonance (ESR) dosimetry from tooth enamel and cytogenetic dosimetry from lymphocytes of Hiroshima atomic-bomb survivors. Int. J. Radiat. Biol. 73, 619–627.

Nilsson, J., Lund, E., Lund, A., 2001. The effects of UV-irradiation on the ESR-dosimetry of tooth enamel. Appl. Radiat. Isot. 54,131–139.

Ontario Power Generation (OPG), 2017. Results of the environmental monitoring programs. Retrieved from www.opg.com › environmental-monitoring-program-2017-report

Ontario Power Generation (OPG), 2020. Results of environmental monitoring programs. N-REP-03443-10026. Retrieved October 10, 2021, from https://www.opg.com/documents/environmental-monitoring-program-2020-report/

Ontario Power Generation (OPG), n.d.-a. Darlington Nuclear Generating Station. Retrieved October 10, 2021, from https://www.opg.com/powering-ontario/our-generation/nuclear/darlington-nuclear/

Ontario Power Generation (OPG), n.d.-b. Pickering Nuclear Generating Station. Retrieved October 10, 2021, from https://www.opg.com/powering-ontario/our-generation/nuclear/pickering-nuclear-generation-station/

Ontario Power Generation (OPG), n.d.-c. The future of Pickering Generating Station. Retrieved October 20, 2021, from https://www.opg.com/powering-ontario/our-generation/nuclear/pickering-nuclear-generation-station/future-of-pickering/

Polyakov, V., Haskell, E., Kenner, G., Huett, G., Hayes, R., 1995. Effect of mechanically induced background signal on EPR dosimetry of tooth enamel. Radiat. Meas. 24(3), 249–254.

Priest, N., 2018. Roadmap: Addressing public concerns about their exposure to low doses of anthropogenic radiation. CANDU Owner Group Inc. Saskatoon Meeting, University of Saskatchewan, SK, Canada.

Romanov, S.A., Vasilenko, E.K., Khokhryakov, V.F., Jacob, P., 2002. Studies on the Mayak nuclear workers: dosimetry. Radiat. Environ. Biophys. 41, 23–28.

Romanyukha, A.A., Nagy,V., Sleptchonok, O., Desrosiers, M.F., Jiang, J., Heis, A., 2001. Individual biodosimetry at the natural radiation background level. Health Phys. 80(1), 71–73.

Romanyukha, A.A., Schauer, D.A., 2002. EPR dose reconstruction in teeth: Fundamentals, applications, problems, and perspectives. In: Kawamori, A., Yamauchi, J., Ohta, H. (Eds.), EPR in the 21" Century: Basics and applications to material, life and earth sciences. Elsevier Science B.V., pp. 603-612.

Roesch, W.C., 1958. Dose for nonelectronic equilibrium conditions. Radiat. Res. 9, 399-410.

Romanyukha, A.A., Ignatiev, E.A., Vasilenko, E.K., Drozhko, E.G., Wieser, A., Jacob, P., et al., 2000. EPR dose reconstruction for Russian nuclear workers. Health Phys. 78, 15 – 20.

Romanyukha, A.A., Regulla, D., Vasilenko, E., Wieser, A., 1994. South Ural nuclear workers—comparison of individual doses from retrospective EPR dosimetry and operational personal monitoring. Appl. Radiat. Isot. 45(12), 1195–1199.

Rudko, V.V., Vorona, I.P., Baran, N.P., Ishchenko, S.S., 2007. γ- and UV-induced $CO_2^-$ radicals in tooth enamel. Radiat. Meas. 42, 1181-1184.

Rudko, V.V., Vorona, I.P., Baran, N.P., Ishchenko, S.S., Zatovsky, I.V., Chumakova, L.S., 2010. The mechanism of $CO_2^-$ radical formation in biological and synthetic apatites. Health Phys. 98, 322 – 326.

Scientific Committee on the Effects of Atomic Radiation, UNSCEAR, 2006. Effects of Ionizing Radiation. Volume I. Report to the General Assembly with Scientific Annexes A and B. United Nations sales publications E.08.Ix.6. united Nations, New York.

Scientific Committee on the Effects of Atomic Radiation, UNSCEAR, 2012. Sources, Effects and Risks of Ionizing Radiation, Scientific Annexes A and B, United Nations.

Shishkina, E.A., Shved, V.A., Degteva, M.O., Tolstykh, E.I., Ivanov, D.V., Bayankin, S.N., et al., 2003. Issues in the validation of external dose: Background and internal dose components of cumulative dose estimated using the electron paramagnetic resonance (EPR) method. Final Report for Milestone 7, Part 1. US–Russian Joint Coordinating Committee on Radiation Effects Research. Project 1.1., 67 pp.

Skvortzov, V.G., Ivannikov, A.I., Eichoff, U., 1995. Assessment of individual accumulated irradiation doses using EPR spectroscopy of tooth enamel. J. Mol. Struct. 347, 321-330.

Skvortsov, V.G., Ivannikov, A.I., Stepanenko, V.F., Tsyb, A.F., Khamidova, L.G., Kondrashov, A.E., et al., 2000. Application of EPR retrospetive dosimetry for large-scale accidental situation. Appl. Radiat. Isot. 52, 1275–1282.

Soldat, J.K., Robinson, N.M., Baker. D.A., 1974. Models and Computer Codes for Evaluating Environmental Radiation Doses. BNWL-1754, Pacific Northwest Laboratories, Richland, Washington.

Streck, A., 2018, June 26. Protesters rally in Pickering to decommission the nuclear power plant. Global News. Retrieved October 10, 2021, from https://globalnews.ca/news/4298298/protesters-rally-pickering-decommission-nuclear-power-plant/

Toyoda, S., 2019. Recent Issues in X-Band ESR Tooth Enamel Dosimetry. In: Shukla, A. K. (Eds.), Electron Spin Resonance Spectroscopy in Medicine. Springer Nature Singapore, pp. 135 – 151. Pte Ltd. https://doi.org/10.1007/978-981-13-2230-3.

Toyoda, S., Kondo, A., Zumadilov, K., Hoshi, M., Miyazawa, C., Ivannikov, A., 2011. ESR measurements of background doses in teeth of Japanese residents. Radiat. Meas. 46, 797–800.

Trompier, F., Romanyukha, A., Reyes, R., and Vezin, H., Queinnec, F., Gourier, D., 2014. State of the art in nail dosimetry: free radicals identification and reaction mechanisms. Radiat. Environ. Bioph. 53, 291-303.

United Nations Environment Programme (UNEP), 2016. What is radiation? What does radiation do to us? Where does radiation come from? United Nations Environment Programme.

Vorona, I.P., Baran, N.P., Ishchenko, S.S., Rudko, V.V., 2007. Separation of the contributions from gamma-and UV-radiation to the EPR spectra of tooth enamel plates. Appl. Radiat. Isot. 65(5), 553 – 556.

Wieser, A., Mehta, K., Amira, S., Aragno, D., Bercea, S., Brik, A., et al., 2000. The 2nd international intercomparison on EPR tooth dosimetry. Radiat. Meas. 32, 549 – 557.

Zhumadilov, K., Ivannikov, A., Apsalikov, K.N., Zhumadilov, Zh, Toyoda, S., Zharlyganova, D., et al., 2006. Radiation dose estimation by tooth enamel EPR dosimetry for residents of Dolon and Bodene. J. Radiat. Res. 47, A47 – A53.

Zhumadilov, K., Ivannikov, A., Skvortsov, V., Stepanenko, V., Zhumadilov, Z., Endo, S., et al., 2005. Tooth enamel EPR dosimetry: optimization of EPR spectra recording parameters and effect of sample mass on spectral sensitivity. J. Radiat. Res. (Tokyo) 46 (4), 435 – 442.

# Connecting statement I

As described in Chapter 4, our lowest detection limit using the X-band CW EPR spectrometer was 30 mGy, equal to the lowest detection limit reported in the literature. However, as per the UNSCEAR (2012) report, the 10-100 mGy are in the low dose bands. These dose bands are of interest in radio-epidemiology due to the possible health effects but have not been observed until now. Since the conventional EPR methods were unable to measure the low doses (<30 mGy) with reasonable accuracy, this study explores the feasibility of using the dose spiking EPR technique to measure low doses in alanine. Since alanine is tissue equivalent, it has been used as a secondary standard in various metrology institutions. So, first, this technique was used in alanine to study its applicability in the standard samples (Chapter 5) and then applied the same technique to measure the low doses in tooth enamel (Chapter 6).

Additionally, alanine has been used in radiotherapy to measure the delivery dose accuracy to patients; however, the measurement accuracy at low doses is very low due to the invisible dosimetric signals and the background interferences. Consequently, alanine does not help measure the low doses. Several attempts have been made to decrease the detection limits by adding metal nanoparticles. The addition of metal nanoparticles increases the radiation sensitivity of alanine and significantly decreases the detection limit. However, it loses its property of tissue equivalence, which makes it unsuitable for use in radiotherapy. So, this chapter describes the applicability of the dose spiking technique to measure low doses with high measurement accuracy.

# Chapter 5

## Applicability of the dose spiking EPR method for the quantitative measurements of low doses in EPR alanine dosimetry

Lekhnath Ghimire[a], Edward Waller[a]
[a] Faculty of Energy Systems and Nuclear Science
Ontario Tech University, Oshawa, ON, L1G 0C5, Canada

*Journal of Nuclear Engineering and Radiation Science (Under review)*

**Abstract**

Ionizing radiation generates unpaired electrons or free radical centers in alanine. The Electron Paramagnetic Resonance (EPR) detects, identifies, and quantifies these free radicals, proportional to the absorbed dose. The accurate measurements of low doses using EPR dosimetry with alanine are highly challenging due to (1) the weak EPR dosimetric signal from low dose alanine and measurement errors, (2) the sample anisotropy in crystalline alanine, and (3) the background signals from sample impurities. This study explores the feasibility of using the dose spiking EPR technique to overcome these challenges and decrease the detection limit up to 20 mGy in a low dose measurement using EPR. The measurement errors from the sample anisotropy were reduced by rotating the samples relative to the constant magnetic field direction using a goniometer and averaging the resulting EPR spectra. This technique decreased the measurement errors at high doses; however, it was insufficient to decrease the detection limit and increase the measurement accuracy at low doses (<0.5 Gy). As a result, the high measurement accuracy at the high doses (>4 Gy) was exploited to increase the accuracy at the low doses using the dose spiking EPR technique. To this end, the low-dose alanine sample, undetectable and not reliably measurable in the X-band CW EPR spectrometer, spikes with a high dose (4 Gy). Then, the total dose was measured and

subtracted from a spike dose to get the initial low dose. This technique detected and measured the low doses with reliable accuracy (± 10%). As a result, we concluded that this method has great potential to solve the low dose measurement problems in alanine.

**Keywords:** DL-α-alanine; Ionizing radiation; X-band CW EPR spectrometer; Dosimetry; Dose spiking technique; Sample anisotropy; Dose-response curve.

## 5.1 Introduction

With its molecular formula $CH_3CH(NH_2)COOH$, alanine is one of the twenty amino acids that occur naturally. It exists in two isomeric forms: D- and L-α-alanine stereoisomers (enantiomers), as depicted in Figure 5.1a, and a racemic mixture of these isomers is the DL-α-alanine. The L- and DL-α-alanine are the most commonly used in radiation dosimetry and have attained considerable interest for use in the high dose (> 5Gy) radiation dosimetry (Baffa et al., 2002; Regulla and Deffner, 1982; Anton, 2006). The interaction of ionizing radiation (e.g., gamma rays) with alanine [$H_3N^+CH(CH_3)COO^-$], stable in a zwitterion form, produces stable free radicals, often called the Stable Alanine Radicals (SARs), as shown in equation 5.1(R1) (Anton, 2006; Heydari et al., 2002). The presence of unpaired electrons with the central carbon atom of the SAR assigns paramagnetic properties. It is responsible for the central line in the alanine EPR spectrum, as depicted in Figure 5.2. The alanine EPR spectrum is mainly due to the formation of the free radical $^{\bullet}$**CH(CH$_3$)COOH**, often called **R1**, formed by breaking the weakest C-N bond (3 eV) as shown in Figure 5.1b and Table 5.1, and produces the SAR species. However, single-crystal Electron-Nuclear Double Resonance (ENDOR) spectroscopy studies conducted by Sagstuen et al. (1997) revealed the two major free radicals (R1 and R2) formed in the irradiation of alanine samples. **R2** has been assigned to the free radical $^{+}H_3NC^{\bullet}(CH_3)COO^-$, and **R3** to $H_2NC^{\bullet}(CH_3)COOH$. The alanine EPR spectrum can be reconstructed with R1: 0.589; R2: 0.335;

R3: 0.076 (Lund et al., 2011). The R2 and R3 probably formed from unstable radicals referred to as oxidation and reduction products. However, the R1 radical is stable at room temperature, which is assumed to be formed by the deamination of the protonated radical anion as depicted in equation 5.1 (Heydari et al., 2002; Sagstuen et al., 2004).

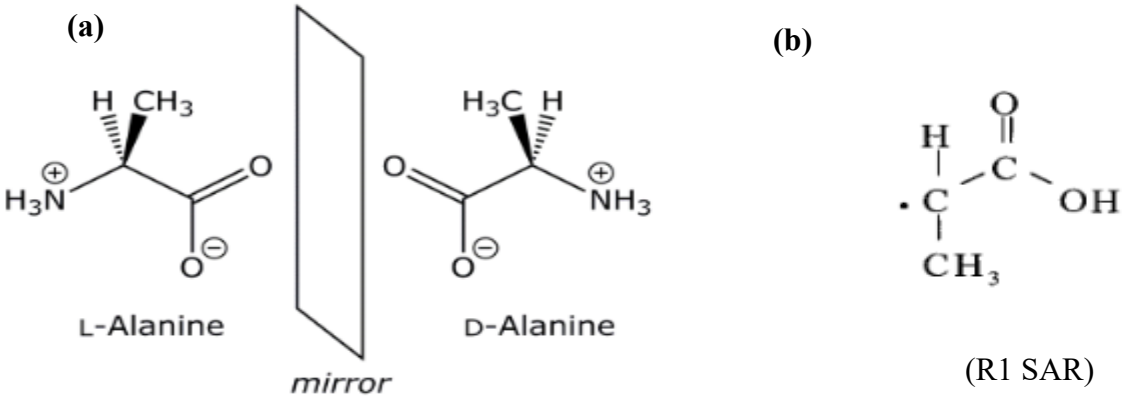


**Figure 5.1: (a)** Molecular structure of L-α-alanine and D-α-alanine. They are mirror images of each other and are called stereoisomers (enantiomers). From Eren et al. (2017). **(b)** R1 stable alanine free radical. From Sagstuen et al. (1997).

$H_3N^+CH(CH_3)COO^-$ $\xrightarrow{\gamma \text{ rays}}$ $^{\bullet}CH(CH_3)COOH + NH_3$ ……(5.1)

(Unirradiated alanine) (R1)

The amounts of ionizing radiation can be quantified in terms of the total absorbed dose by measuring the peak-to-peak (P2P) amplitude height of the central line of the EPR spectrum, as depicted in Figure 5.2 (Baffa and Kinoshita, 2014; Heydari et al., 2002; Anton, 2006). Several national metrology institutions have used EPR dosimetry with alanine as a secondary standard for radiation dosimetry. (Keizer et al., 1991; Gancheva et al., 2008; Anton, 2005). Alanine dosimeters are ideal for high dose applications because (1) its peak to peak amplitude is clear and measurable with high accuracy; (2) the alanine dosimetric signal is stable during a very long period (~1 year) and can repeatedly be read out; (3) it has the wide dose detection range (1Gy to 100 kGy); (4) it

has linear signal-to-dose dependence (≤ 10 kGy); (5) its dosimetric signal is energy and dose rate independent; (6) it is a non-destructive and fast detection method with high accuracy and low temperature of coefficient of irradiation; and (7) it has good signal stability post-irradiation (i.e., 5% signal fading per year when stored correctly) (Yordanov et al., 2013; Stuglik, 2007).

**Table 5.1:** Chemical bonds of DL-α-alanine and their strength. From Stuglik (2007).

| Chemical bond | Energy (eV) |
|---|---|
| C-H | 4.3 |
| N-H | 4 |
| C-O | 3.6 |
| C-C | 3.5 |
| C-N | 3 |

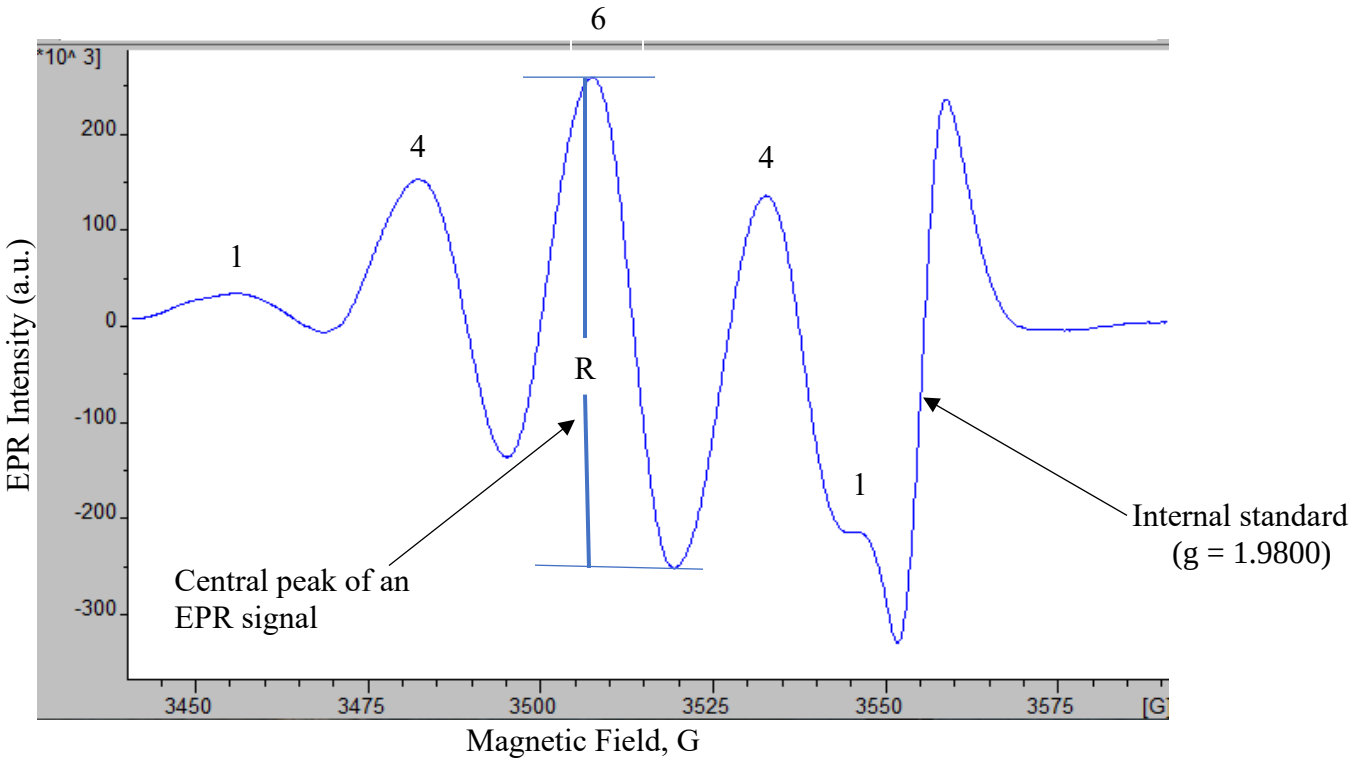


**Figure 5.2:** An EPR spectrum of an alanine powder sample exposed to 4 Gy gamma rays using the Hopewell G-10 irradiator at Ontario Tech University. R represents the P2P amplitude height used to determine the absorbed dose in alanine.

Although the chemical composition of alanine is similar to the composition of human tissue (i.e., tissue equivalent), it is not applicable to measure a low dose in radiotherapy due to high errors in the EPR measurements (IAEA, 2000). Modern radiotherapy requires less than ±5% accuracy in delivering an absorbed dose to the target tissue or tumor (IAEA, 2000; ICRU, 1976). However, it is practically impossible to achieve such a standard using the conventional alanine EPR dosimetry system, which is the main limitation of using the alanine dosimeter in low dose measurements and radiotherapy (Anton, 2006; ICRU, 1976). Several studies have been performed to increase the sensitivity of alanine in a low dose by adding different types of metal nanoparticles such as gold nanoparticles, gadolinium, potassium iodide, etc. The inclusion of metal nanoparticles significantly increased the alanine radiation sensitivity to a low dose due to the formation of many secondary electrons. However, its application was limited due to a loss of tissue equivalence (Chen et al., 2008; Guidelli and Baffa, 2014; Marrale et al., 2011). Thus, it is clear that the conventional alanine EPR dosimetry cannot measure a low dose in radiotherapy and other environmental samples (ICRU, 1976). Different studies have been conducted to decrease the detection limit in alanine EPR dosimetry. Hayes et al. (2000) lowest detection limit in alanine was 100 mGy using multistep sample analysis procedures. Goodman et al. (2017) measured the low doses in alanine, 100 – 200 mGy, using EPR. Geso et al. (2018) used the alanine pellets and initially spiked by delivering 30 Gy and the second low dose (0.5-10 Gy). They reliably measured the doses below 2 Gy by subtracting the spike signal. However, in the low dose region (less than 0.5 Gy), which is of interest in radiation epidemiology, a more extensive investigation is needed to increase the measurement accuracy and reproducibility. Therefore, the present study aims are (1) to study the effects of sample anisotropy in the low dose measurements using EPR; and (2) to use the dose spiking EPR technique to decrease the detection limit up to 20 mGy in alanine using EPR

measurements. The scope of this work is also to find the influence of the sample mass and position on the sensitivity of the X-band CW EPR spectrometer to find the optimum sample mass for the high-quality factor (Q) and filling factor (η) of the cavity.

## 5.2 Materials and methods

### 5.2.1 Alanine sample preparation

The commercial alanine powder, the DL-α-alanine, was used for this study. The powder was purchased from Sigma-Aldrich, ≥99% (HPLC) pure. The crystalline alanine sample was first dried in the oven (Heratherm General Protocol Oven OMS180 6.3 cu ft) as shown in Figure 5.3a at 42°± 1°C for 24 hours (i.e., until the sample weight became constant in the repeated measurements). Then the alanine samples were stored at room temperature in the vacuum-sealed container (i.e., desiccator) with silica beds to remove air moisture, as shown in Figure 5.3c (Bradshaw and Cadena, 1962). The weight loss of 6.4949 gm of alanine was 0.007 gm or 0.10%, attributed to the sample's loss of water or moisture. The moisture content in alanine contributes to the background signals, which may mask the dosimetric signals at low doses (Bradshaw and Cadena, 1962), consequently increasing measurement errors. Removing water moisture decreases the interferences (i.e., unwanted EPR spectra) that arise from water, eventually decreasing the detection limit and increasing measurement accuracy and reproducibility. The moisture content was not found to change by a detectable amount during irradiation and handling of the sample. The sample preparation is one of the most crucial steps for the low dose measurement in alanine as it helps reduce the alanine sample's impurities and water moisture.

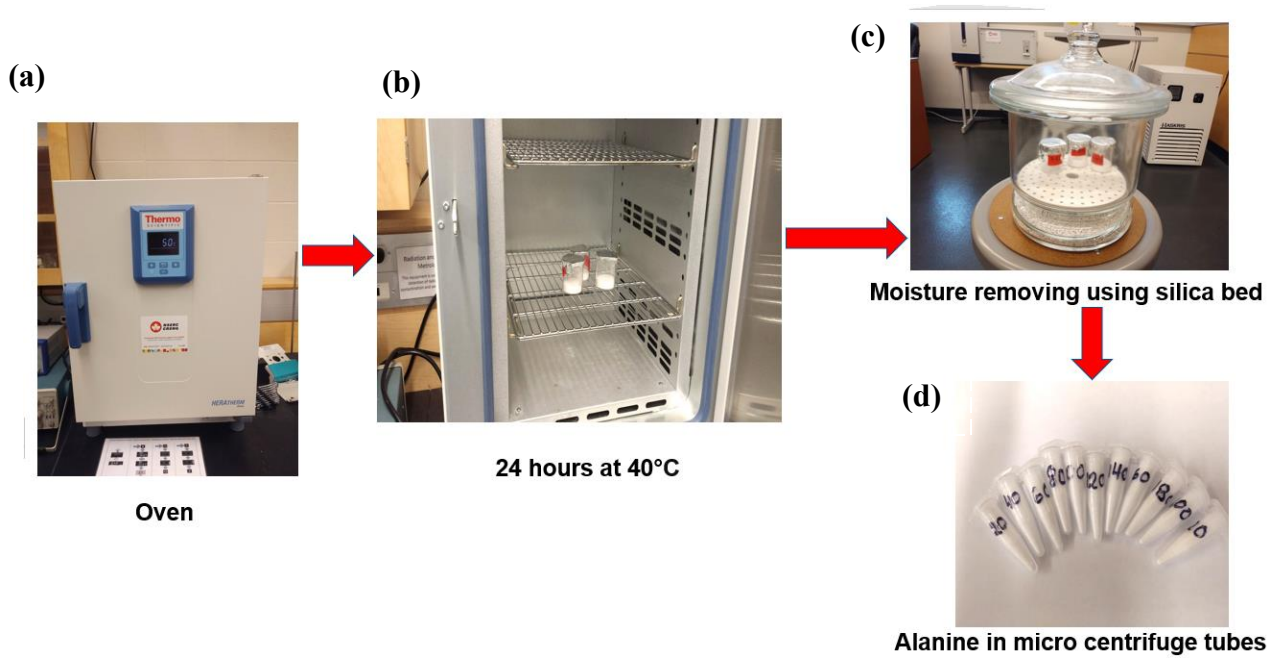


**Figure 5.3:** Alanine sample preparation by drying and removing air moisture using an oven **(a)**, sample drying in an oven **(b)**, a vacuum-sealed container (i.e., desiccator) with the silica beds **(c)**, and alanine in the microcentrifuge tubes **(d)**.

### 5.2.2 Sample irradiation

Sample irradiation was completed at Ontario Tech University (Radiation laboratory, ERC B058) using the gamma irradiator (Hopewell Designs G-10-2-12) with $^{137}$Cs activity (A) = 6.4598 Ci and photon energy 0.6618 MeV. The gamma source (G-10) was calibrated using a reference sample, and the uncertainty of a dose measurement was less than 5% at a 95% confidence interval. In the ISO series 4037-1, 4037-2, 4037-3, and 4037-4, photon reference radiation fields to calibrate dosemeters are defined. At lower than 1.2 MeV, the difference between the exposure (collision KERMA) and the absorbed dose is small (i.e., constant throughout the medium). Electronic equilibrium is usually assumed to exist due to the photoelectric effect and the detector size. Secondary charged particle equilibrium exists if the energy 'brought into' the detector is equivalent

to the energy brought ‘out of the detector’, both by secondary electrons (Behrens et al., 2009). As a result, the exposure dose is almost equivalent to the absorbed dose at lower photon energy. However, for higher energy radiation, ISO 4037-3 recommends placing a build-up plate (BUP) made of polymethyl methacrylate (PMMA) of 0.4 cm thickness to ensure secondary charged equilibrium at the detectors. Once the gamma source was calibrated, the alanine was placed in the microcentrifuge tube, as depicted in Figure 5.3d. The correctly filled centrifuge tubes were housed within the 3D printed sample holder. The sample cavities of the exact dimensions and equal distance between each sample were used to reduce the positioning errors in irradiation, as depicted in Figure 5.4a. Third, the radiation beam was aligned to the center of the sample holder using a laser alignment system, as shown in Figure 5.4b. Fourth, the samples were placed at 34 cm from the center of the G-10 source (Figure 5.4c). The dose rate (0.15788 Sv/hr) at 34 cm was calculated, then the samples were irradiated to the low gamma doses (20, 40, 60, 80, 100, 120, 140, 160, 180, 200, 220 mGy). After irradiation, the alanine-containing centrifuge tubes were removed from the sample holder and stored in the darkened container for 24 hours. After 24 hours of storing the samples, each low dose sample was paired with the unirradiated alanine (0 Gy) sample, often called a spike (i.e., reference sample). Then a spike dose of 4 Gy was delivered simultaneously to the low dose alanine samples and spiked the samples. Then the spike and the total dose samples were stored in a dark vacuum container and analyzed after 24 h of irradiation. Each sample was measured three times and averaged the EPR spectra to calculate the standard deviation. The total dose (low dose plus spike) and the spike dose (4 Gy) were analyzed using the X-band CW EPR spectrometer described in Section 5.2.4.

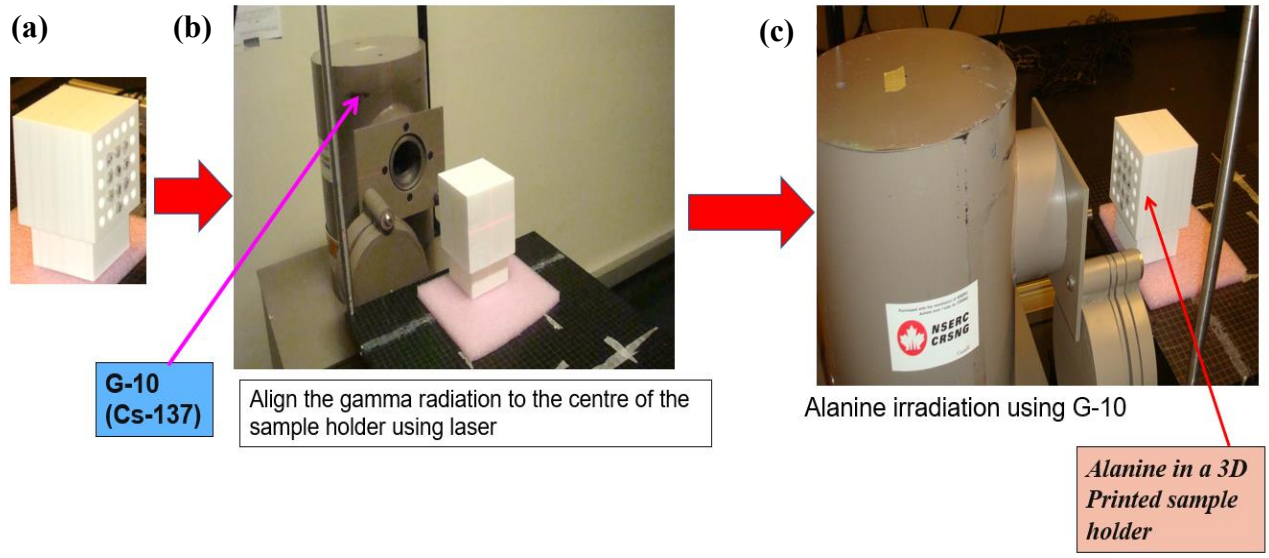


**Figure 5.4: (a)** Microcentrifuge tubes with alanine were housed within the 3D printed sample holder. **(b)** The radiation beam was aligned to the center of the sample holder using a laser alignment system. **(c)** Alanine samples were irradiated using the Hopewell G-10 ($^{137}$Cs) gamma source.

The reason behind delivering the 4 Gy spike dose to the low dose alanine samples was due to a clear dosimetric signal in the EPR measurements and the high measurement accuracy and reproducibility at that dose range as described in Section 5.3.3.

### 5.2.3 Principle of the dose spiking EPR technique

The dose spiking technique has been used in analytical chemistry to measure extremely low concentrations (i.e., μM/L) of an analyte in a solution using various spectroscopic techniques such as the inductively coupled plasma mass spectrometry (ICP-MS), mass spectroscopy, and chromatography such as gas, HPLC, etc. (Heumann et al., 1998; Weyer et al., 2002; Meisel et al., 2001; Harvey, 2000). The method involves the addition of an analyte with a known large concentration (y), called a spike, to an analyte with an unknown low concentration (x), which can

not be detected or measured using these analytical techniques. The spike increases the unknown concentration (i.e., low dose) up to 50 times, making the instrument's signal distinctly visible and reliably measurable with less errors. The combined signal (x+y) will be subtracted from the spike signal (y) to get the unknown low dose concentration (x), as shown in Figure 5.5 (Harvey, 2000; Heumann et al., 1998; Weyer et al., 2002; Meisel et al., 2001; Geso et al., 2018). The same robust analytical technique was used to make the low-dose radiation signal visible to the EPR spectrometer by adding the large dose (i.e., spike) to the low dose in alanine, which overcomes the current challenges of measuring the low doses in the X-band CW EPR spectrometer due to the low sensitivity and the background noises from impurities.

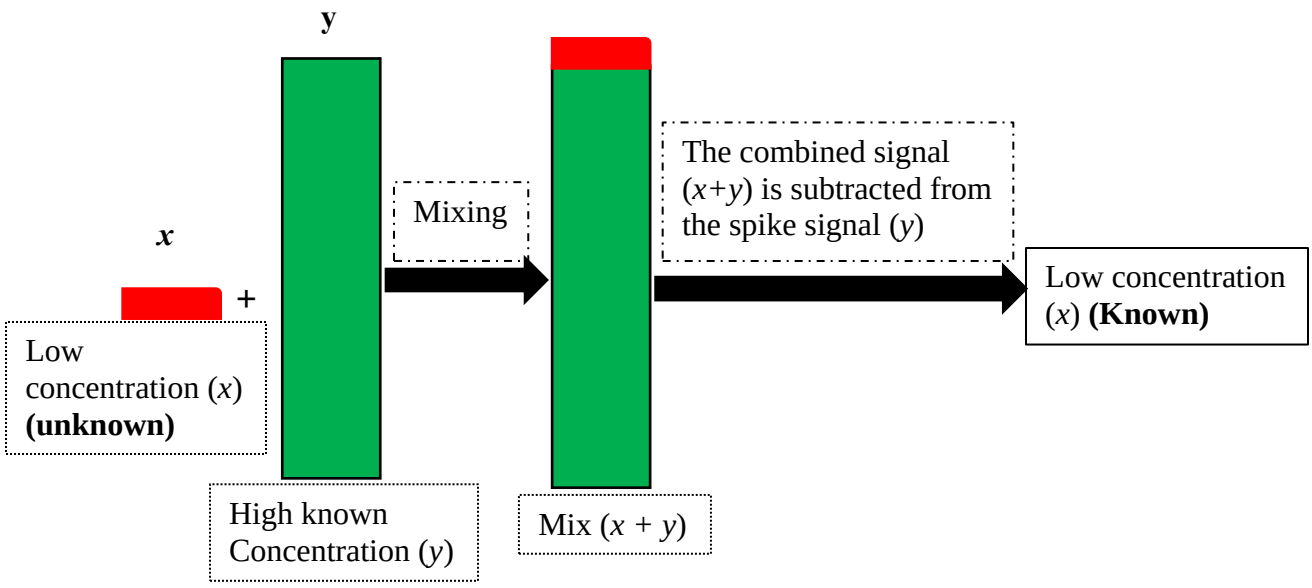


**Figure 5.5:** A schematic representation of a dose spiking technique for the low dose measurements. An unknown low concentration **(x)** is mixed with a known high concentration **(y)** to make a visible and measurable signal.

### 5.2.4 EPR measurements

The experiments were conducted at Ontario Tech University using the X-band CW EPR spectrometer (e.g., Bruker EMX micro) with a 6″ magnet, as shown in Figure 5.6. The microwave bridge of the spectrometer operates in X-band (9.8GHz) and is equipped with a frequency counter of 1 kHz resolution. The EPR spectrometer reached a stable operating temperature before starting sample analysis. All experiments were conducted at stabilized room temperature of 21˚C and relative humidity of 25%. The high sensitivity resonator (ER4119HS) was used in this experiment (Eaton et al., 2010; Anton, 2006). The optimized parameters were as follows: central field, 3480G; g = 2 with sweep width, 150 G; microwave power, 12 mW; receiver gain, $1\times10^3$; modulation amplitude, 6 G; number of scans, 10; time constant, 655.36 msec; sweep time, 41.98 sec; and conversion time, 41 msec; harmonic, first; resolution, 1024 channels. The Bruker ER 4119HS-2100 internal standard with a g factor of 1.9800 ± 0.0006 and line width 3 G was permanently mounted in the resonator as shown in Figure 5.11. The internal standard g-value was used to determine the g-factor values of the observed EPR signals and normalized the dosimetric signals to reduce errors due to any fluctuation in the machine response and environmental changes (Jiao et al., 2014; Eaton et al., 2010; Brustolon and Giamello, 2009). The EPR sample tube (thin wall quartz) with an outer diameter (OD) of 4 mm and 250 mm length was used in all the experiments. Since alanine is a crystalline material, as described in Section 5.3.3, its EPR spectrum is angle-dependent because of the anisotropy of the lattice field with respect to the position of the magnetic field. Therefore, the sample was measured by rotating 20 degrees up to 360 degrees (i.e., 19 rotations) using a manual goniometer (i.e., Bruker E218G1 1 manual axis goniometer), resulting in nineteen spectra were averaged. The reproducibility was determined by measuring the same sample three times and calculating the standard deviation.

**Figure 5.6:** The X-band CW EPR spectrometer (EMXmicro) at Ontario Tech University with a manual goniometer mounted in a resonator.

## 5.3 **Results and discussion**

### 5.3.1 **Sample positioning and mass in the EPR resonator**

Three fundamental problems influence the quantitative measurement of low doses in EPR spectroscopy (Goodman et al., 2017; Eaton et al., 2010; Brustolon and Giamello, 2009):

1. The selection of the acquisition parameters (i.e., microwave power, modulation amplitude, time constant, conversion time, receiver gain, etc.);
2. Sample positioning and mass in the EPR resonator;
3. Measurement, processing, and interpretation of the acquired EPR spectrum.

Furthermore, the detection limit can be decreased further by improved sample preparation; reducing errors due to the sample anisotropy; and using the internal standard or reference to normalize the dosimetric signals (Brustolon and Giamello, 2009; Eaton et al., 2010). This paper

focuses on optimizing these parameters and reducing errors from the sample anisotropy for the quantitative low dose measurements using EPR.

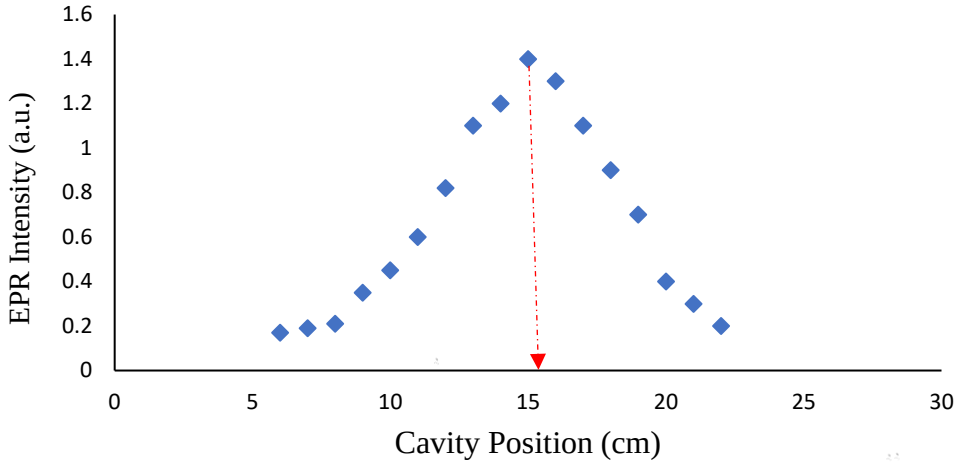


**Figure 5.7:** Signal intensity of the sample (4 Gy) at different heights in the cavity. The highest signal intensity is at 15 cm into the EPR resonator, representing the highest sensitivity for the sample.

The proper position of the sample into the EPR resonator is vital for the quantitative low-dose EPR measurements. The component of the microwave field is the main driver for the electron-flip transition in EPR spectroscopy. Therefore, the sample must be placed in the microwave magnetic field ($B_1$) maximum and the electric field ($E_1$) minimum, where the highest signal and sensitivity are achieved (Eaton et al., 2010). To determine the optimum sample position into the EPR resonator, the alanine sample's EPR intensity was measured at different depths into the cavity and found the highest EPR intensity at 15 cm into the resonator mounted with a goniometer as shown in Figures 5.7 and 5.11, which represents the highest sensitivity and the optimum position for the sample analysis (Eaton et al., 2010; Brustolon and Giamello, 2009). At the same time, the mass of the sample affects the cavity quality factor (Q) and the sensitivity of the measurement. That is why the sample mass was optimized by measuring the low to high masses as depicted in Figure 5.8 and found a linear relationship up to 161.4 mg, which was the optimum sample mass

for the quantitative measurements. More importantly, lower or higher sample mass would provide a broadened or distorted signal and reduce the signal resolution, which would not provide the optimal dosimetric estimate (Eaton et al., 2010; Brustolon and Giamello, 2009).

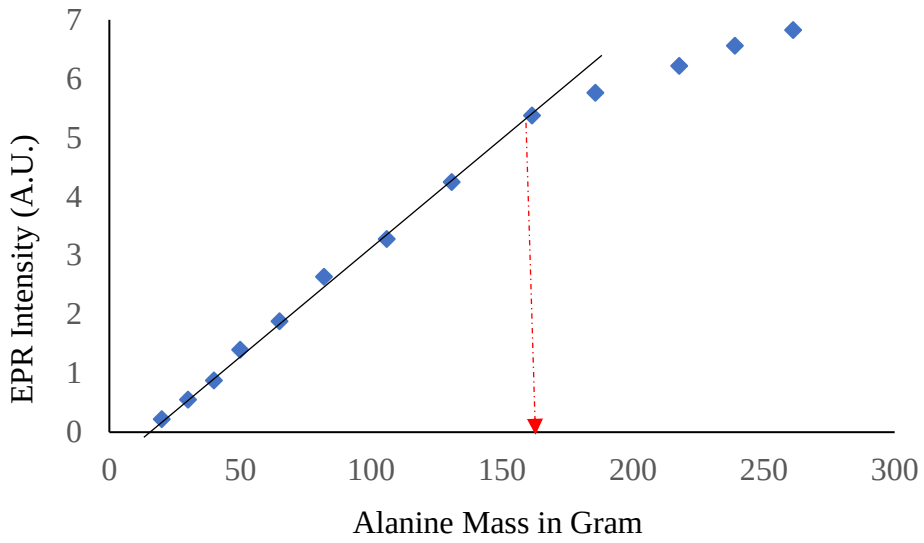


**Figure 5.8:** Microwave cavity was calibrated as a function of the sample mass and found that the optimum sample mass was 161.4 mg.

### 5.3.2 Measurement, processing, and interpretation of the acquired spectrum

The EPR spectrum of irradiated alanine consists of 5 peaks in a 1:4:6:4:1 ratio, as shown in Figures 5.2 and 5.9a and 5.9b (Weil and Bolton, 2007; Lund et al., 2011). The adjacent four peaks are due to hyperfine interactions of the unpaired electron with four hydrogen atoms present in the alanine free radical $CH_3C^{\bullet}HCOO^-$. The formula can determine the number of lines from the hyperfine interactions: 2nI + 1, where n is the number of equivalent nuclei, and I is the nuclear spin quantum number. Hydrogen has I = ½, which means five lines in the alanine EPR spectrum. Pascal's triangle gives the relative intensities (1:4:6:4:1), as shown in Figures 5.9a and 5.9b (Weil and Bolton, 2007).

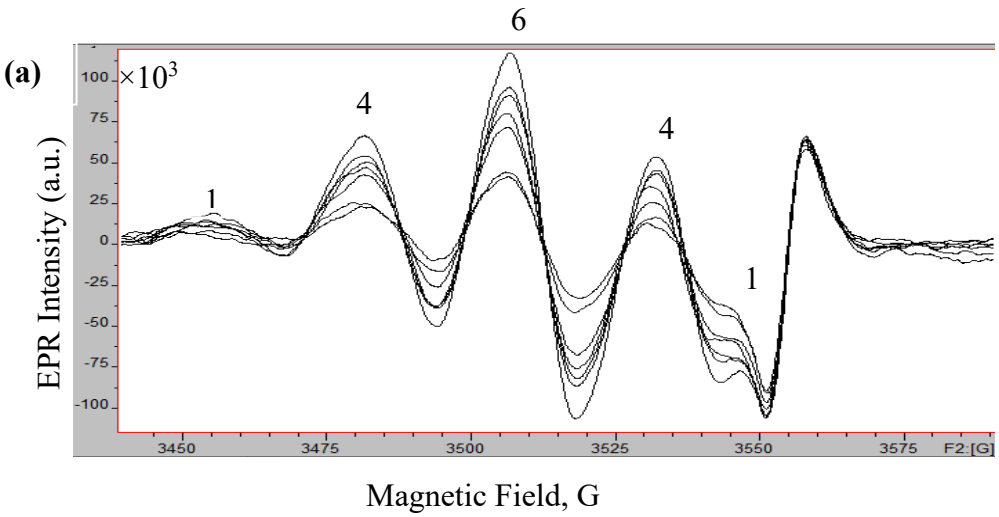


**(b)**

1

1 1

1 2 1

1 3 3 1

**1 4 6 4 1**

1 5 10 10 5 1

**Figure 5.9: (a)** EPR spectra of the alanine sample irradiated to 0.5, 1, 1.5, 2, 2.5, 3, 3.5, and 4 Gy. Microwave power, 12 mW; receiver gain, $1\times10^3$; modulation amplitude, 10 G; number of scans, 10; time constant, 655.36 msec; sweep time, 41.98 sec; and conversion time, 41 msec; harmonic, first; resolution, 1024 channels. **(b)** Pascal's triangle demonstrates the hyperfine splitting of the alanine EPR spectrum, where the numbers indicate the number of splitting and their (spectra) relative intensities in the EPR spectrum.

The amplitude (or peak-to-peak height) of the central peak (peak 6) was measured using the Bruker BioSpin WinEPR processing software. After each measurement, the dosimetric signal was normalized to the reference signal (i.e., divide the dosimetric signal intensity by the reference sample's intensity) to reduce errors due to environmental changes within the cavity or any variability in the machine response (Jiao et al., 2014; Eaton et al., 2010; Brustolon and Giamello, 2009). Furthermore, reducing errors using the internal standard can increase the data precision and

accuracy and eventually help to decrease the detection limit in the low dose measurement. However, as alanine has a crystalline property, the EPR measurement of low doses may get errors from the sample anisotropy.

### 5.3.3 Reducing measurement errors due to the sample anisotropy

Anisotropy is a fundamental property of all crystalline materials, increasing with increased crystalline properties. Sample anisotropy can cause an error in the EPR dose measurements. However, it depends on the extent of samples' crystallinity and grain sizes (Aoba et al., 1982; Iwasaki et al., 1993; Haskell et al., 1997). Alanine is a polycrystalline material with an orthorhombic crystal structure, as shown in Figure 5.10a. All three axes (a, b, and c) are unequal and perpendicular in this crystal structure, as depicted in Figures 5.10a and 5.10b. Therefore, the anisotropy occurs along with all three directions, which means the alanine's EPR spectrum will be different if the magnet ($B_0$) is aligned in these three different axes, x, y, and z (Brustolon and Giamello, 2009). That is why the EPR spectrum intensity will be changed if the direction of the magnetic field ($B_0$) is changed with respect to the crystal's axes (Figure 5.10b).

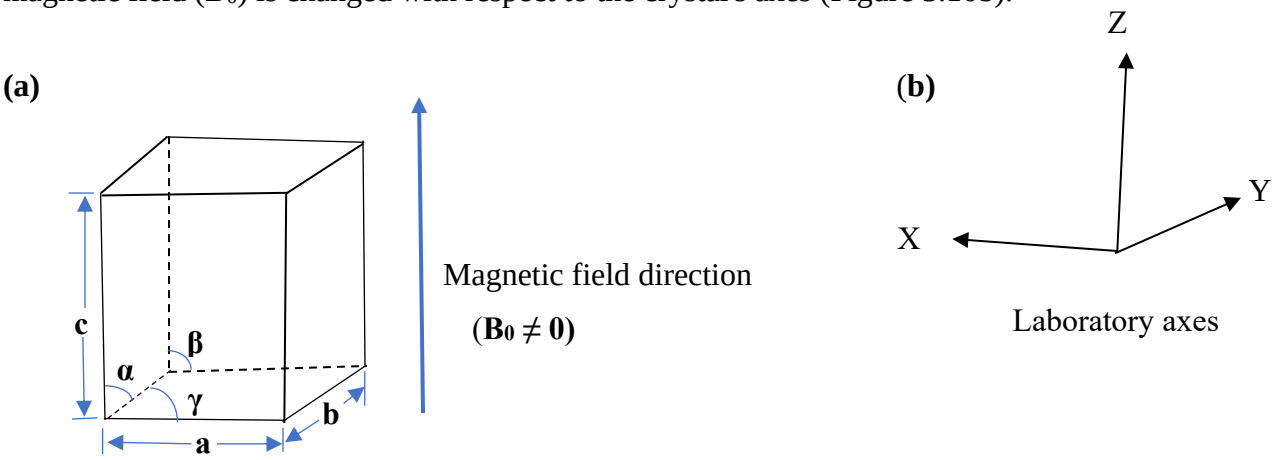


**Figure 5.10: (a)** Orthorhombic crystal structure of alanine. The vertical arrow represents the direction of the magnetic field in a single crystal. **(b)** The laboratory axes of the applied magnetic field. All crystal axes are unequal ($a \neq b \neq c$) and $\alpha = \beta = \gamma = 90^{\circ}$.

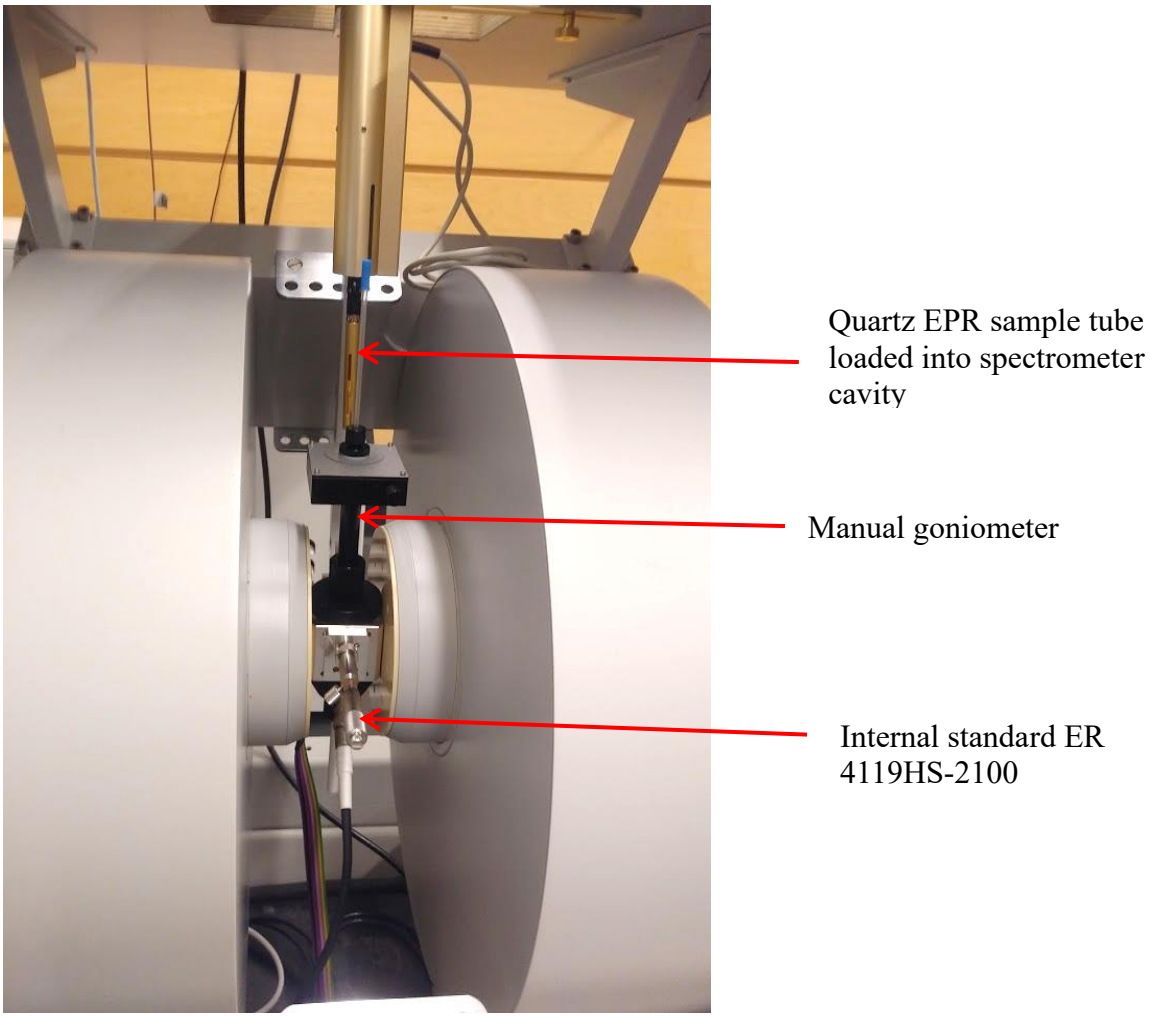


**Figure 5.11:** A goniometer (E 218G1 1 Axis manual goniometer) is mounted in an EPR resonator.

**Table 5.2:** Using a goniometer, the calculated doses in alanine samples with and without sample rotation. The uncertainty in the EPR intensity comes from the sample anisotropy and impurities.

| **No rotation of samples** | | | | **0 to 360 degrees rotation of samples** | | | |
|---|---|---|---|---|---|---|---|
| Actual dose (Gy) | Adjusted Intensity | Cal Dose (Gy) | Errors (%) | Actual dose (Gy) | Adjusted Intensity | Cal Dose (Gy) | Errors (%) |
| 0.5 | 88013 ± 3709 | 0.79 | 58.0 | 0.5 | 83137 ± 2809 | 0.73 | 46.0 |
| 1.5 | 105957 ± 4741 | 1.13 | 24.7 | 1.5 | 113023 ± 3742 | 1.30 | 13.3 |
| 2 | 138488 ± 6186 | 1.8 | 10.0 | 2 | 141788 ± 5166 | 2.16 | 8.0 |
| 2.5 | 192369 ± 8180 | 2.79 | 11.6 | 2.5 | 185053 ± 7080 | 2.67 | 6.8 |
| 3 | 219056 ± 4252 | 3.3 | 10.0 | 3 | 210337 ± 3202 | 3.15 | 5.0 |
| 3.5 | 227838 ± 5864 | 3.47 | 0.9 | 3.5 | 227811 ± 4964 | 3.48 | 0.6 |
| 4 | 254216 ± 6083 | 3.97 | 0.7 | 4 | 254968 ± 5623 | 4.00 | 0.0 |

The sample anisotropy of alanine was determined by measuring the alanine samples ranging from the low to high doses (0.5, 1.5, 2, 2.5, 3, 3.5, and 4 Gy) in the EPR spectrometer mounted with a manual goniometer (Bruker E218G1), as can be seen in Figure 5.11. The samples were measured by rotating 0 to 360 degrees (20-degree increments) and averaged 19 spectra. The EPR spectra obtained from these measurements were varied on the order of 1.5 to 5.10 percent relative standard deviation (RSD) (Figure 5.12) based on the different orientations of the samples with respect to the applied magnetic field in the EPR resonator. These data clearly show that the alanine EPR intensity is orientation-dependent due to a crystalline property of alanine.

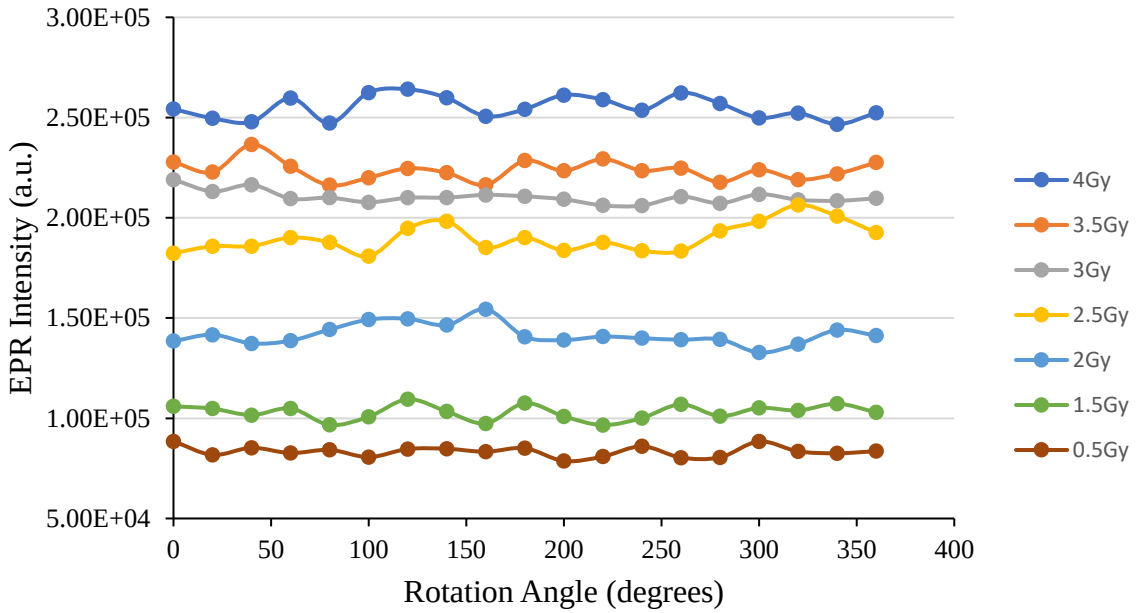


**The percent standard deviation = 1.5 to 5.1**

**Figure 5.12:** The alanine samples irradiated from 0 to 4 Gy were analyzed by rotating from 0 to 360 degrees using a manual goniometer. Each sample's EPR spectra were averaged. The average change in the percent relative standard deviation (RSD) was 1.5 to 5.1.

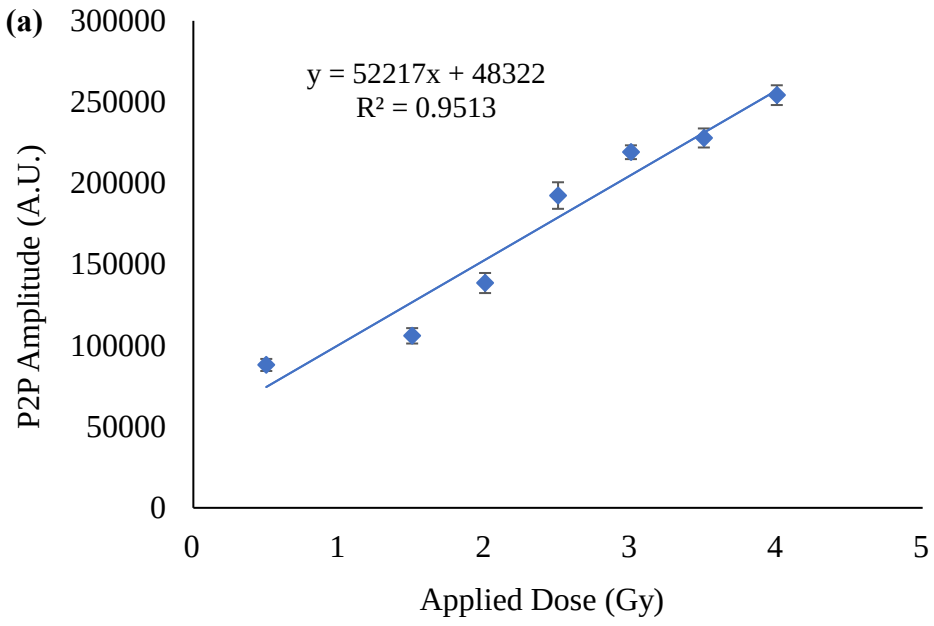

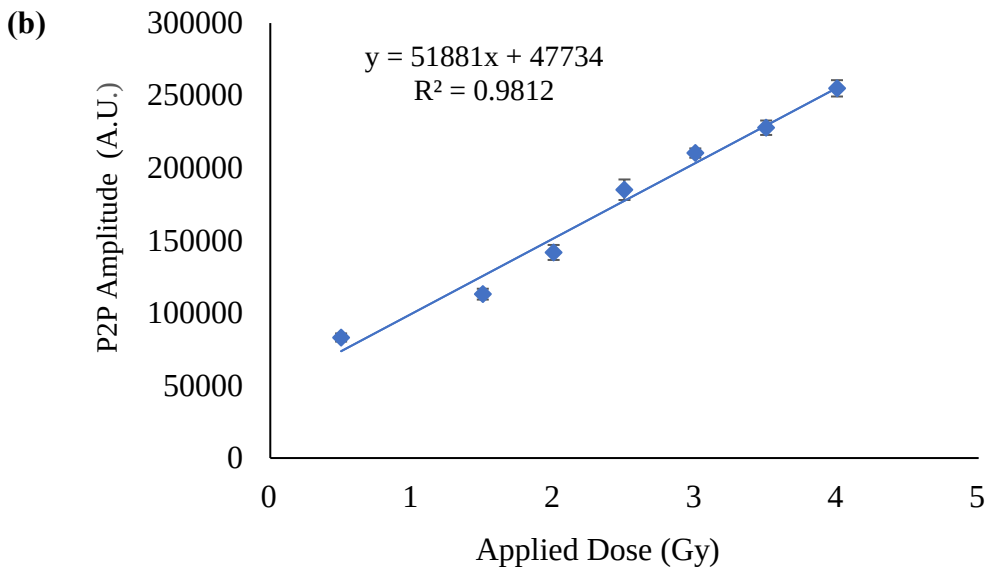


**Figure 5.13:** Dose-response curves for the alanine dosimeter irradiated with gamma-rays from the Hopewell G-10 to 0.5 – 4 Gy doses. (a) Without sample rotation. (b) Sample rotation from 0 to 360 degrees using a manual goniometer.

The irradiated alanine samples (0.5 - 4 Gy) were used to build the calibration curves (i.e., dose-response curve) using: (1) the EPR intensity obtained from no rotation (Figure 5.13a) and (2) the average EPR intensity obtained from 0-360-degrees rotation of the same samples (Figure 5.13b). The doses were calculated in both measurements. The rotating and averaging EPR spectra decreased the measurement errors by about 10% at the low doses compared to no rotation, as shown in Table 5.2. However, this decrease in measurement errors could not decrease the detection limit and precision in the measurements needed in low dose research and radiotherapy. From these results, one can conclude that reducing measurement errors from the sample anisotropy cannot decrease the measurement errors and decrease the detection limit at low doses in alanine. However, using this technique, the percentage errors were significantly reduced in the high dose measurements (the relative reproducibility on the P2P intensity was better than 0.05%), which

demonstrated that the sample rotation technique would increase the accuracy and reproducibility at the high doses in alanine. Hence, the measurement accuracy and reproducibility obtained in the high-dose measurements were exploited to increase the accuracy at the low doses in alanine using the dose spiking EPR technique described in Section 5.3.4.

### 5.3.4 **Low dose measurements in alanine using the dose spiking EPR technique**

As mentioned in Section 5.1, using alanine dosimeters (i.e., alanine pellets), the lowest dose successfully measured in alanine was 100 mGy using multistep EPR procedures and took several days (Hayes et al., 2000). Consequently, the high precision and accuracy of low dose measurements using the conventional EPR dosimetry techniques are challenging and time-consuming. A reliable and fast measurement of low doses with high precision and accuracy can overcome the current limitations of using alanine in a low dose measurement and radiotherapy. To this end, this study further explores the feasibility of using the dose spiking EPR technique to measure low doses in alanine (Harvey, 2000; Geso et al., 2018). The dose spiking technique is based on the fact that the dosimetric signal grows linearly with the added artificial dose in the alanine dosimeter (Geso et al., 2018). However, the signals from the background do not change as a function of the added dose as the impurity's concentrations are low (i.e., alanine is ≥99% HPLC pure) in comparison to the dosimetric material (i.e., alanine) (Geso et al., 2018; Harvey, 2000). Also, as we spike the low dose to the high dose and measure the EPR spectrum using EPR, we can exploit the benefit of the low measurement errors at the high doses to measure the low doses due to distinctly visible and measurable dosimetric signals at the high doses, as described in Section 5.3.3.

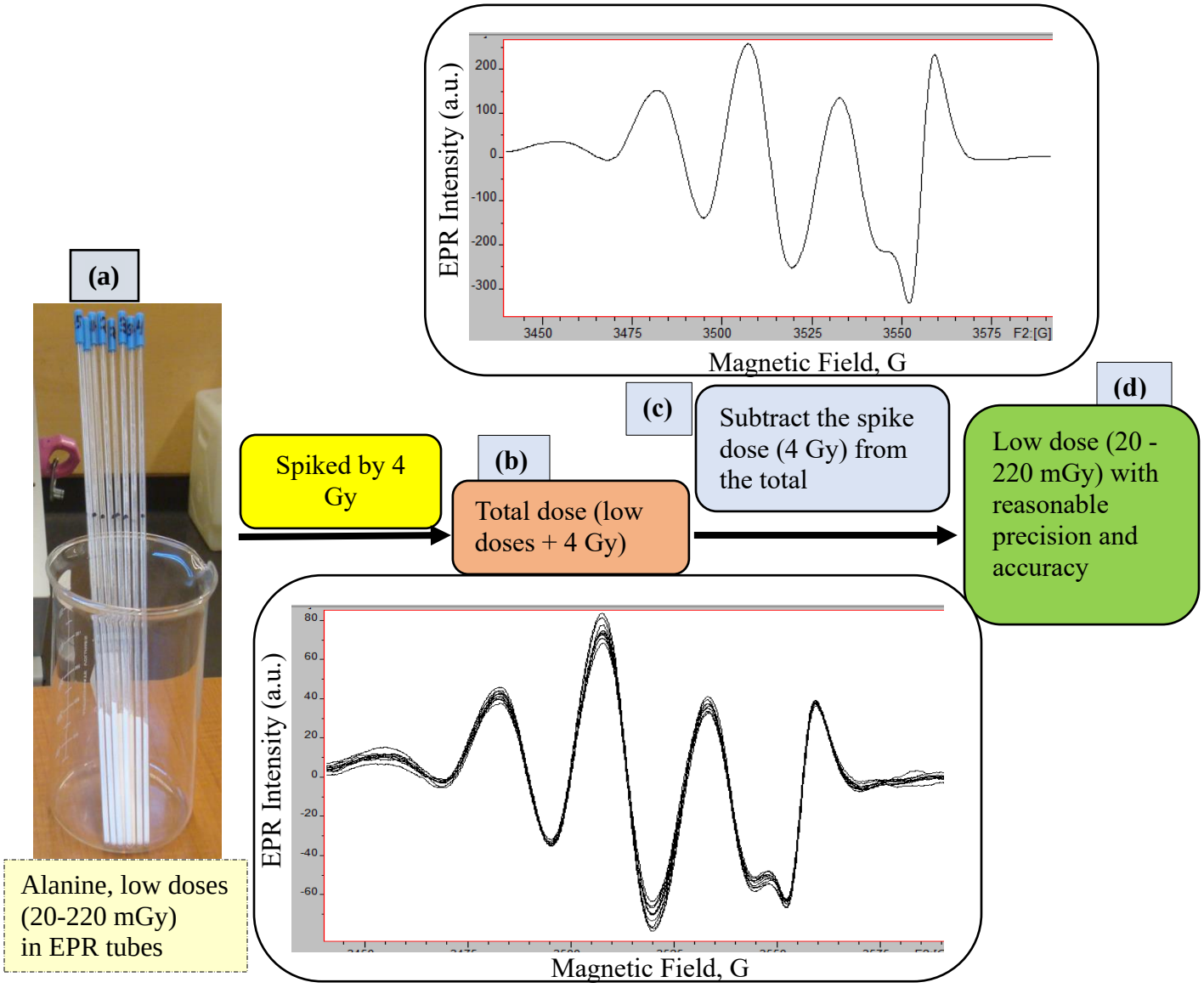


**Figure 5.14:** A schematic of the low dose spiking and subtracting techniques using EPR. **(a)** Low doses of alanine samples from 20-220 mGy in EPR tubes. **(b)** EPR spectra of the total doses (low dose plus spike). **(c)** Spike dose was subtracted from the total dose to get the low dose **(d)** in alanine.

**Table 5.3:** The low-dose alanine samples were spiked by delivering a high dose. The difference in the EPR intensities of the total and spike doses and the standard deviation were calculated.

| First dose (mGy) (Low doses) | Second dose (4 Gy) (Spike) | Total dose (low + spike) | EPR Intensity (Total dose – Spike) | σ (Total dose – Spike) |
|---|---|---|---|---|
| 20 | 4 | 4.02 | 0.16 | 0.018 |
| 40 | 4 | 4.04 | 0.25 | 0.023 |
| 60 | 4 | 4.06 | 0.34 | 0.032 |
| 80 | 4 | 4.08 | 0.44 | 0.047 |
| 100 | 4 | 4.1 | 0.54 | 0.058 |
| 120 | 4 | 4.12 | 0.64 | 0.061 |
| 140 | 4 | 4.14 | 0.74 | 0.077 |
| 160 | 4 | 4.16 | 0.83 | 0.087 |
| 180 | 4 | 4.18 | 0.92 | 0.091 |
| 200 | 4 | 4.2 | 1.03 | 0.105 |
| 220 | 4 | 4.22 | 1.12 | 0.113 |

Therefore, in this study, the low doses (20 – 220 mGy) were spiked to the high doses by delivering 4 Gy, as shown in Figure 5.14 Table 5.3. The EPR intensities of the low doses were calculated by subtracting the total doses from the spike doses, as depicted in Figure 5.14 and Table 5.3. The dose-response curve was constructed by plotting the EPR intensity (i.e., total – spike) versus the low doses in alanine. The low doses were calculated using the calibration curve as depicted in Figure 5.15. The limit of detection of this method was 20 mGy with significantly low errors (±10%) in the dose measurements than the previous similar studies (Geso et al., 2018; Hayes et al., 2000). Furthermore, as shown in Table 5.3, the standard deviation of the total dose EPR intensity minus spike was minimal, demonstrating the precision in the measurements and usefulness of the method to measure the low doses in alanine. These data demonstrated that the dose spiking EPR technique could increase the low dose measurement precision and accuracy than the conventional EPR dosimetry techniques.

However, in the conventional technique, the EPR intensity of the radiation-induced signals is minimal (and sometimes invisible in the X-band CW EPR spectrometer) and masked by the background noises at low doses (20 mGy to 200 mGy). Therefore, these signals are too small to measure accurately using EPR. Consequently, the low calculated dose could over or underestimate the total dose received. On the other hand, the EPR signal is clear at high doses in the dose spiking technique, which does not need any complicated spectrum processing techniques or special spectral deconvolution methods to obtain the dosimetric signals from the background noises or signals as used by Ivannikov et al. (2001). Furthermore, as mentioned in Section 5.3.3, the peak-to-peak (P2P) amplitude height was measured in the distinctly visible radiation-induced EPR signals. This was one of the main reasons for significantly low errors in the dose spiking EPR technique. Consequently, the standard deviation for the data obtained because of subtraction of the two large doses (i.e., spike and total dose) were much lower than the low dose measurements using the conventional techniques, as shown in Table 5.3.

Also, as described in Section 5.2.2 and Table 5.3, the sample was irradiated only a single time and subtracted from the spike dose. Due to the single irradiation of the sample with the same radiation sensitivity, the dose spiking EPR technique has lower measurement errors than other conventional EPR techniques (i.e., additive dose method). The previous study (Geso et al., 2018) reliably measured the doses below 2 Gy using a similar technique. This study focused on the low dose region (<0.5 Gy) to determine the feasibility of this technique to measure the low doses. The results from this study demonstrated that the dose spiking EPR technique has the potential to decrease the detection limit in a low dose measurement using EPR and measure the low doses in alanine with sufficient precision and accuracy. One of the drawbacks of this technique is that we

need an excellent irradiation laboratory facility, the dosemeter must be properly calibrated using an ISO protocol, as mentioned in Section 5.2.2, and the sample irradiation must be done accurately. However, further validation and inter-laboratory comparison would be needed to check this technique's accuracy and reproducibility.

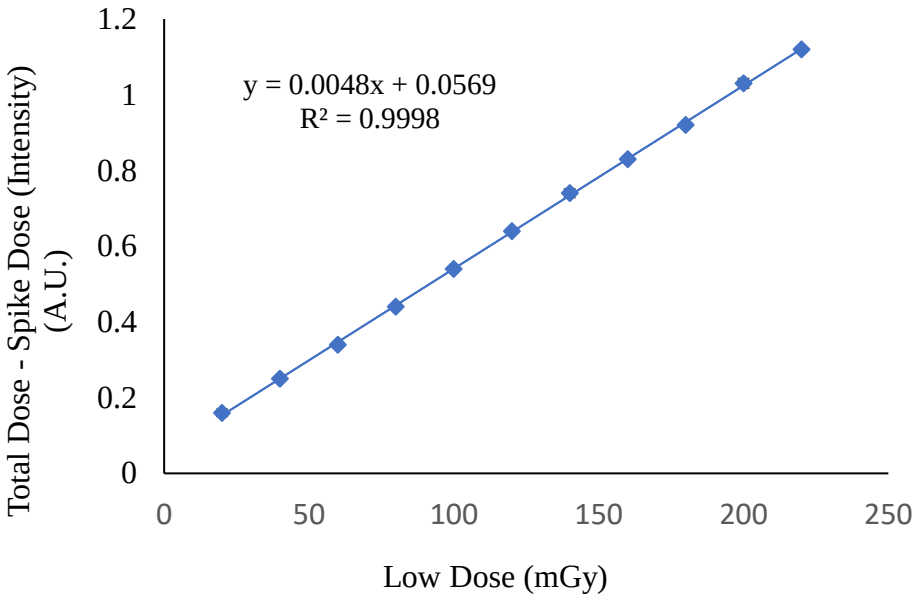


**Figure 5.15:** A dose-response of the alanine dosimeter at low doses obtained from the dose spiking EPR technique.

## 5.3 **Conclusions**

The low dose measurements in alanine using the conventional EPR dosimetry techniques are challenging due to the weak EPR dosimetric signals and a complex EPR signal analysis procedure. However, there was a high signal-to-noise ratio (SNR) at high doses and low baseline distortion, and the dosimetric signals were visible and measurable without complex spectrum processing procedures. That is why there were significantly low measurement errors in high dose measurements using EPR. Several different EPR acquisition parameters, including the sample

mass and position into an EPR cavity, which directly influence the quantitative low dose measurements in alanine, were optimized prior to analyzing the samples. Also, since alanine is a crystalline material, the measurement errors from the sample anisotropy were determined by rotating and averaging the EPR spectra. Reducing errors arising from the sample anisotropy increased the precision and accuracy of the measurement at the high doses. However, it was ineffective to decrease the low doses' measurement errors and the detection limit. Therefore, the low errors in the high dose EPR measurements as described in Section 5.3.3 were applied to measure the low doses in alanine using the dose spiking EPR technique. This technique decreased the detection limit at the low doses (20 – 220 mGy) with a high level of precision and accuracy without losing its property of tissue equivalence. Therefore, this technique would make alanine a versatile dosimeter, useful in accident dosimetry and low doses' clinical applications. Also, this technique can be applied to study the low environmental doses in tooth enamel, bones, shells, etc., with a high degree of precision and accuracy. However, further data validation and comparison would be necessary to determine its accuracy, reproducibility, and use in clinical and accident dosimetry.

**Acknowledgements**

The work described was undertaken as part of the independent, low-dose research program "Addressing Public Concerns about Their Exposure to Low Doses of Anthropogenic Radiation" funded by the CANDU Owners Group Inc. Funding was also received from the Natural Sciences and Engineering Research Council (NSERC) of Canada.

**Conflicts of Interest**

The Authors declare that there is no conflict of interest.

## 6.5 References


Anton, M., 2005. Development of a secondary standard for the absorbed dose to water based on the alanine EPR dosimetry system. Appl. Radiat. Isot. 62, 779–795.

Anton, M., 2006. Uncertainty in alanine /ESR dosimetry at the Physikalisch-Technische Bundesanstalt. Phys. Med. Biol. 51, 5419-5440.

Aoba, T., Doi, Y., Yagi, T., Okazaki, M., Takahashi, J., Moriwaki, Y., 1982. Electron spin resonance study of sound and carious enamel. Calcif. Tissue Int. 34, 88-92.

Baffa, O., Kinoshita, A., 2014. Clinical applications of alanine/electron spin resonance dosimetry. Radiat. Environ. Biophys. 53, 233-240.

Baffa, O., Kinoshita, A., Chen Abregoa, F., Silva, N.A., 2002. ESR and NMR dosimetry. In A. Kawamori, J. Yamauchi and H. Ohta (Eds). EPR in the 21" Century: Basics and applications to material, life and earth science (pp. 614-623). Elsevier Science B.V.

Behrens, R., Kowatari, M., Hupe, O., 2009. Secondary charged particle equilibrium in $^{137}$Cs and 60Co reference radiation fields. Rad. Rad. Prot. Dosim. 136, 3, 168-175.

Bradshaw, W.W., Cadena, D.G., 1962. The use of alanine as a solid dosimeter. Radiat. Res. 17, 11-21.

Brustolon, M., Giamello, E., (Eds.). 2009. Electron paramagnetic resonance, a practitioner's toolkit. John Wiley & Sons, Inc., Hoboken, New Jersey.

Chen, F., Nicolucci, P., Baffa, O., 2008. Enhanced sensitivity of alanine dosimeters to low energy X-rays: preliminary results. Radiat. Meas. 43, 467–470.

Eaton, G.R., Eaton, S.S., Barr, D.P., Weber, R.T., 2010. Quantitative EPR. Springer Wien New York. DOI 10.1007/978-3-211-92948-3.

Erena, B., Wub, F., Erena, E., Jeanb, Y.C., Van Hornb, J.D. 2017. Positron Annihilation Lifetime Analysis of Left- and Right-Handed Alanine Single Crystals. Acta Phys. Pol. 132, 5, 1456-1460.

Gancheva, V., Yordanov, N.D, Callens, F., Vanhaelewyn, G., Raffi, J., Bortolin, E. et al., 2008. An international intercomparison on ‘‘self-calibrated’ ’alanine EPR dosimeters. Radiat. Phys. Chem. 77, 357–364.

Geso, M., Ackerly, T., Lim, S.A., Best, S.P., Gagliardi, F., Smith, C., 2018. Application of the ‘Spiking’ method to the measurement of low dose radiation (≤ 1Gy) using alanine dosimeters. Appl. Radiat. Isot. 133, 111-116.

Goodman, B.A., Worasith, N., Ninlaphruk, S., Mungpayaban, H., Deng, W., 2017. Radiation dosimetry using alanine and Electron paramagnetic (EPR) spectroscopy: A new look at an old topic. Appl. Magn. Reson. 48, 155-173.

Guidelli, E.J., Baffa, O., 2014. Influence of proton beam energy on the dose enhancement factor caused by gold nanoparticles: an experimental approach. Med. Phys. 41, 032101.

Harvey, D., 2000. Modern analytical chemistry. Mc Graw Hill, New York.

Haskell, E.H., Hayes, R.B., Kenner, G.H., 1997. Improved accuracy of EPR dosimetry using a constant rotation goniometer. Radiat. Meas. 27, 325–329.

Hayes, R.B., Haskell, E.H., Wieser, A., Romanyukha, A.R., Hardy, B.L., Barrus, J.K., 2000. Assessment of an alanine EPR dosimetry technique with enhanced precision and accuracy. Nucl. Instrum. Methods Phys. 440, 453–461.

Heumann, K.G., Gallus, H.M., Radingler, G., Vogl, J., 1998. Accurate determination of element species by on-line coupling of chromatographic systems with ICP-MS using isotope dilution technique. Spectrochim. Acta B, 53(2), 273-287.

Heydari, M.Z., Malinen, E., Hole, E.O., Sagstuen, E., 2002. Alanine radicals. 2. The composite polycrystallinr alanine EPR spectrum studied by ENDOR, thermal annealing, and spectrum simulation. J. Phys. Chem. A. A 106, 8971-8977.

IAEA, 2000. Absorbed dose determination in external beam radiotherapy: An international code of practice for dosimetry based on standards of absorbed dose to water. Technical Reports Series No. 398. International Atomic Energy Agency, Vienna.

ICRU, 1976. Determination of absorbed dose in a patient irradiated by beams of x-ray or gamma rays in radiotherapy procedures ICRU Report 24 (Washington DC: International Commission on Radiation Units and Measurements).

International Organization for Standardization, 1996. X and gamma reference radiation for calibrating dosemeters and doserate meters and for determining their response as a function of photon energy—Part 1: Radiation characteristics and production methods. ISO 4037-1 (Geneva: ISO).

International Organization for Standardization, 1997. X and gamma reference radiation for calibrating dosemeters and doserate meters and for determining their response as a function of photon energy—Part 2: Dosimetry for radiation protection over the energy ranges 8 keV to 1.3 MeV and 4 MeV to 9 MeV. ISO 4037-2 (Geneva: ISO).

International Organization for Standardization. 1999, X and gamma reference radiation for calibrating dosemeters and doserate meters and for determining their response as a function of photon energy—Part 3: Calibration of area and personal dosemeters and the measurement of their response as a function of energy and angle of incidence. ISO 4037-3 (Geneva: ISO).

Iwasaki, M., Miyazawa, C., Uesawa, T., Niva, K., 1993. Effect of sample grain size on the $CO_3^{3-}$ signal intensity in ESR dosimetry of human tooth enamel. Radioisotopes 42, 470–473.

Ivannikov, A.I., Skvortsov, V.G., Stepanenko, V.F., Tikunov, D.D., Takada, J., Hoshi, M., 2001. EPR tooth enamel dosimetry: optimization of the automated spectra deconvolution routine. Health Phys. 81 (2), 124–137.

Jiao, L., Liu, Z.C., Ding, Y.Q., Ruan, S.Z., Wu, Q., Fan, S.J., Zhang, W.Y., 2014. Comparison study of tooth enamel ESR spectra of cows, goats and humans. J. Radiat. Res. 55, 1101-1106.

Lund, A., Shiotani, M., Shimada, S., 2011. Principles and Applications of ESR Spectroscopy. Springer Science+Business Media B.V.

Marrale, M., Longo, A., Spano, M., Bartolotta, A., D'Oca, M.C., Brai, M., 2011. Sensitivity of alanine dosimeters with gadolinium exposed to 6 MV photons at clinical doses. Radiat. Res. 176, 821–826.

Meisel, T., Moser, J., Fellner, N., Wegscheider W., Schoenberg, R., 2001. Simplified method for the determination of Ru, Pd, Re, Os, Ir and Pt in chromitites and other geological materials by isotope dilution ICP-MS and acid digestion. Analyst,126, 322-328.

Regulla, D.F., Deffner, U., 1982. Dosimetry by ESR spectroscopy of alanine. Appl. Radiat. Isot. 33, 1101-1114.

Sagstuen, E., Hole, E.O., Haugedal, S.R., Nelson, W.H., 1997. Alanine radicals: Structure determination by EPR and ENDOR of single crystals X-irradiated at 295 K. J. Phys. Chem. A, 101, 9763-9772.

Sagstuen, E., Sanderud, A., Hole, E.O., 2004. The solid-state radiation chemistry of simple amino acids, revisited. Radiat. Res.162(2),112-119.

Stuglik, Z., 2007. Alanine-EPR dosimetry system. why we like it? IAEA Training Course, 3-7 December 2007, Warsaw, Zofia Stuglik.

Weyer, S., Münkera, C., Rehkämper, M., Mezger, K., 2002. Determination of ultra-low Nb, Ta, Zr and Hf concentrations and the chondritic Zr/Hf and Nb/Ta ratios by isotope dilution analyses with multiple collector ICP-MS. Chem. Geol. 187(3-4), 295-31.

Yordanov, N.D., Gancheva, V., Karakirova, Y., 2013. Some Recent Developments of EPR Dosimetry. In: Lund, A., Shiotani, M. (Eds.), EPR of Free Radicals in Solids II: Trends in Methods and Applications. Springer Science+Business Media Dordrecht, pp. 311-344. DOI 10.1007/978-94-007-4887-3.

# Connecting statement II

The dose spiking technique successfully measured the low doses (20-220 mGy) in alanine with reasonable precision and accuracy, as described in Chapter 5. However, alanine and tooth enamel are different samples; their radiation sensitivities and dose-response vary. Moreover, the tooth enamel may contain more sample impurities than alanine, which may affect the dose reconstruction process in tooth enamel using EPR dosimetry. That is why this study further explores the feasibility of low dose measurements in tooth enamel using the dose spiking EPR technique.

# Chapter 6

## The dose spiking technique for measuring low doses in deciduous teeth enamel using EPR spectroscopy for retrospective and accident dosimetry

Lekhnath Ghimire[1*], Edward Waller[1]

[1]*Faculty of Energy Systems and Nuclear Science, Ontario Tech University, Oshawa, ON, L1G 0C5, Canada*
*Corresponding author's e-mail: lekhnath.ghimire@ontariotechu.net

*For this paper, the CRPA nominated me for the Young Scientists and Professionals Award for the IRPA 2022 North American Regional Congress, St. Louis, Missouri, USA.*

**Abstract**

Dose estimation by electron paramagnetic resonance (EPR) has been accomplished using the standard EPR dosimetry technique (ISO protocol 13304-1 for EPR retrospective dosimetry). However, different studies showed that these techniques have high measurement errors in measuring the low doses (10 – 100 mGy) in enamel. This work proposes a new method to make a dosimetric signal visible and measurable at low doses. The sample was purified using both chemical and mechanical processes. The pure sample mass and position and the EPR acquisition parameters were optimized to enhance the spectrometer's sensitivity for the quantitative low dose measurements. At the same time to reduce errors from the sample and spectrum anisotropy, the total doses (low plus spike) and the spike dose (4 Gy) were measured by rotating 0 to 360 degrees (i.e., 40 degrees at a time) relative to constant magnetic field direction using a goniometer. Subsequently, the spectra were averaged after their g-factor normalization. However, at low doses

(<30 mGy), the RIS was obscured by the BGS. So, the dose spiking technique was used as an alternative method. Ten low-dose deciduous tooth enamel (10 - 100 mGy) samples were spiked to the higher doses by delivering 4 Gy and measured using the X-band CW EPR (Bruker EMXmicro) spectrometer. The total dose EPR signal was distinctly visible, and the P2P amplitude height was measured. Then, the total dose was subtracted with the spike, often called a reference sample, to determine the initial low doses. The measurement errors using this method were lower than the previous methods. These results demonstrated that this method could be promising for solving low dose measurement problems in EPR dosimetry with deciduous and permanent tooth enamel.

**Keywords**: Retrospective dosimetry; Ionizing radiation; EPR spectroscopy; Deciduous Teeth enamel; Dose spiking technique; Low doses.

### 6.1 Introduction

Human teeth are often called 'biological dosimeters,' which can record a low dose for longer than human life (Hennig et al., 1981; ICRU, 2002; Ivannikov et al., 2002). Additionally, human teeth are the only human tissue that can record a low dose with a very high dose stability rate. That is why the dental enamel has been used to reconstruct doses for a long time for retrospective radiation dosimetry and radio-epidemiology (Fattibene and Callens, 2010; IAEA, 2002; ICRU, 2002; Jacob et al., 2002; Toyoda, 2019). The ionizing radiation generates high stable paramagnetic centers in dental enamel called the carbon dioxide radical anions ($^{\bullet}CO_2^-$) (IAEA, 2002; Rudko et al., 2010; Lund et al., 2011). The EPR can detect and measure the concentration of these paramagnetic centers in the enamel samples prepared from the extracted teeth. The accumulated dose can be determined by measuring the P2P amplitude height of the RIS in EPR measurements, which is proportional to the absorbed dose (Desrosiers and Schauer, 2001; IAEA, 2002). The spectrum of irradiated tooth enamel consists of two components: the RIS and the BGS. In the low

dose region, the RIS at g‖ = 1.9970 and g⊥ = 2.0027 (P2P line width of 0.4 and 0.3 mT) is very difficult to separate from the BGSs due to being obscured by the native signal g = 2.0045 (P2P line width of 0.9-1 mT), which further complicates the EPR dose reconstruction process with tooth enamel (Khan et al., 2003).

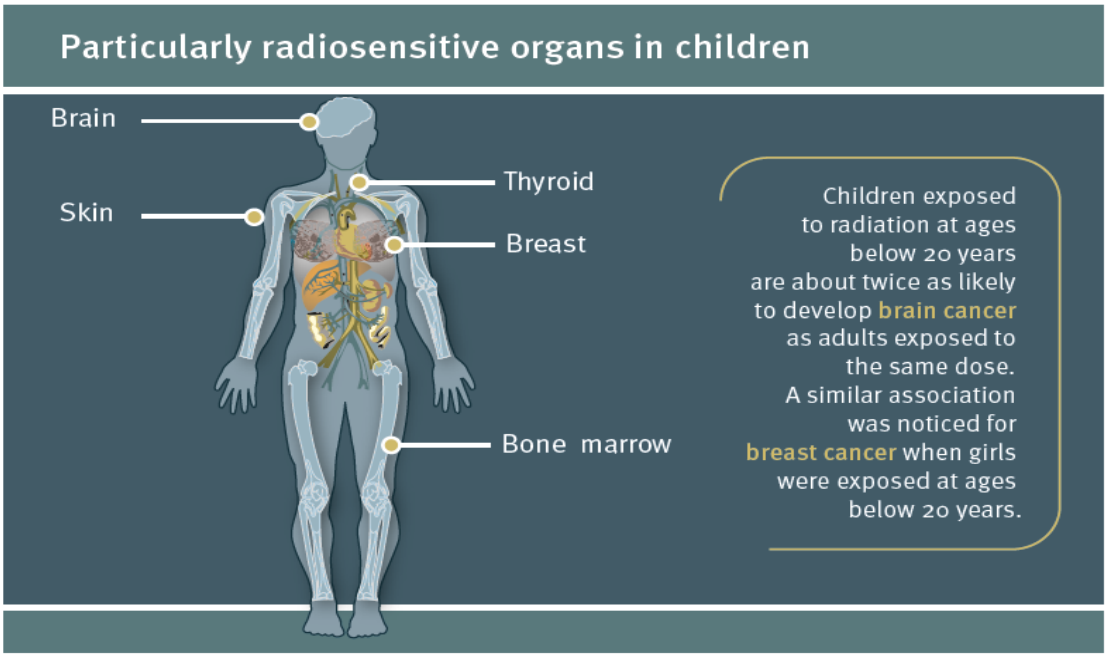


**Figure 6.1:** Radiation-sensitive organs in children. Children exposed to radiation at ages below 20 years are about twice as likely to develop brain and breast cancer as adults exposed to the same dose. From UNEP (2016).

Permanent teeth have been used to reconstruct absorbed doses in various radiation accidents using EPR dosimetry with tooth enamel (Bailiff et al., 2016; Chumak et al., 1999; Degteva et al., 2015; Ikeya et al., 1984; Zhumadilov et al., 2005). This technique has been improved, as shown in the international intercomparisons and ISO standards (ISO, 2013; Wieser et al., 2005; Wieser et al., 2006; Wieser et al., 2000). However, given their availability, there are more chances of providing deciduous teeth for dose reconstruction in the actual radiation accidents

like Fukushima Daiichi Power Plants (Murahashi et al., 2017). Moreover, it is paramount to determine the accident doses or over-exposures in children (6-12 years) because children are more susceptible than adults to ionizing radiation due to their higher radiation risk per dose as depicted in Figure 6.1 (UNEP, 2016; ICRP, 2007; Wieser and El-Faramawy, 2002). The characteristic of the EPR dosimetric signals from the deciduous teeth enamel was investigated, and it was found that their radiation sensitivities were the same as the permanent teeth (Murahashi et al., 2017). At the same time, teeth collected from children (i.e., deciduous teeth) essentially have a lower background dose than permanent teeth collected from adults, which significantly reduces the measurement errors from the background. So, deciduous teeth can be a viable alternative to permanent teeth for radiation dosimetry. Despite its advantages, only a few studies have been done to reconstruct the low absorbed doses in deciduous teeth, which were able to measure the low doses higher than 100 mGy (Gualtieri et al., 2001; Murahashi et al., 2017; Wieser and El-Faramawy, 2002). However, it is vital to measure the low doses in the range of 10 to 100 mGy in enamel, which is of interest in radiation epidemiology due to plausible health effects but not observed until now (UNSCEAR, 2012). Thus, this study uses an alternative method to measure the low doses (<100 mGy) with high precision, accuracy, and reproducibility. To this end, a simple modification in a dose reconstruction technique is performed by spiking the low dose (<100 mGy) to the high dose (4 Gy) and then subtracting the spike dose from the total dose as described in Chapter 5, often called the dose spiking technique (Geso et al., 2018). So, this study explores the feasibility of using the dose spiking EPR technique to measure the low doses in deciduous tooth enamel using the X-band CW EMX micro (EPR spectrometer) to decrease the detection limit down to 10 mGy with reliable accuracy and reproducibility. Also, this study addressed the measurement

uncertainty introduced by the EPR measurements of the enamel sample, such as the sample mass and positioning in a cavity, sample anisotropy, and g-factor normalization.

## 6.2 Materials and methods

### 6.2.1 Sample preparation

Ten deciduous molar teeth (upper and lower) samples with known history were collected from children in the range of 8-10 years of age with the help of the dental clinics/dentists and neighbors in Oshawa, Ontario. The collected tooth samples were not exposed to the medical (X-rays) and occupational radiations, as declared by the parents. The deciduous teeth sterilization, storage, and sample preparation were done as described in Chapter 3.

### 6.2.2 Sample irradiation

The sample holder with cavities of the same dimension and distance from each other, as depicted in Figure 6.2, was printed for the sample irradiation. Before irradiating the samples, the gamma source was calibrated using the reference sample. The uncertainty in dose measurements at 34 cm from the center of the G-10 gamma irradiator was less than 5% at a 95% confidence interval. The sample aliquots of 105 mg mass were placed in the sample holder and irradiated by gamma rays of the laboratory $^{137}$Cs source (Hopewell G-10, activity = 6.4598 Ci ) at Ontario Tech University in doses of 10, 20, 30, 40, 50, 60, 70, 80, 90 and 100 mGy to mimic unknown low dose exposures to individuals or groups in the case of nuclear and radiological accidents (Figure 6.2). The EPR spectra were recorded after storing the samples at room temperature not less than ten days after irradiation and sample preparation, so all the transient radiation-induced and mechanical-induced signals become stable or come to an equilibrium state. The samples were analyzed in EPR by putting the prepared samples into the 4 mm OD and 250 mm L long quartz EPR tubes, as shown in Figure 6.3a. First, the samples were analyzed using the ISO standardized

technique based on the international intercomparisons (ISO, 2013). However, the dosimetric signals were masked by the background signals at the dose range, as depicted in Figure 6.6. So, the low dose samples were re-irradiated by giving 4 Gy (i.e., spike dose) along with the control samples or reference samples with 0 Gy (i.e., blank unirradiated sample). The region behind spiking the low doses (10 – 100 mGy) by delivering 4 Gy was to make the dosimetric signal visible and measurable in enamel. This study revealed that the 4 Gy signal was distinctly separate from the native signals in the X-band CW EPR measurements, as shown in Figures 6.7 and 6.8. However, the spike dose must not be too large due to impurities present in tooth enamel.

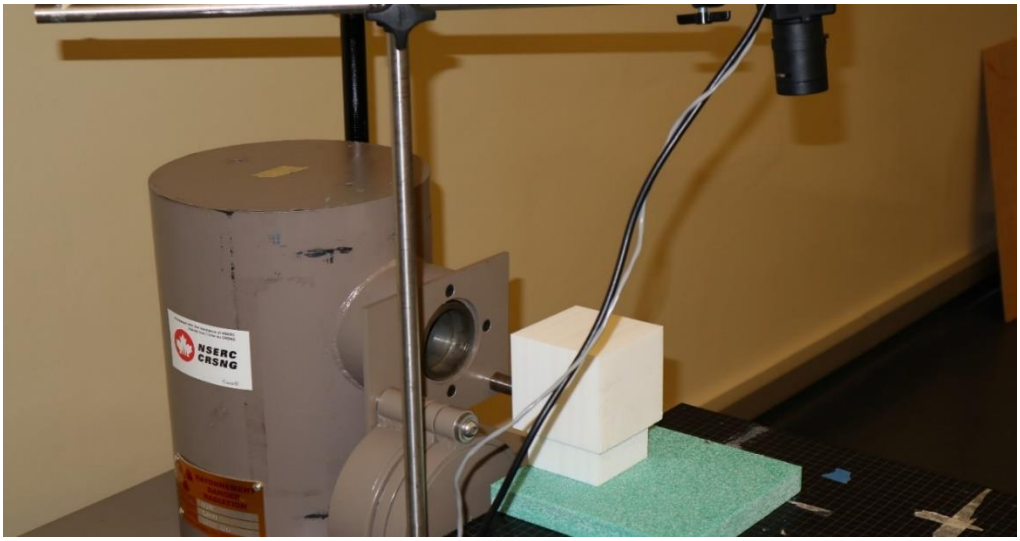


**Figure 6.2:** Tooth enamel irradiation in the 3D printed sample holder using the Cs-137 source (Hopewell G-10 gamma irradiator, activity = 6.4598 Ci) at Ontario Tech University.

### 6.2.3 EPR measurements

The EPR measurements were performed with the X-band CW EPR spectrometer (e.g., Bruker EMX micro spectrometer), with a frequency of 9.8 GHz. The following EPR spectrum acquisition parameters were optimized: microwave power 24 mW (for the high-Q cavity), the modulation frequency of 100 kHz and modulation amplitude 4 gauss, receiver time constant

327.68 msec, sweep time 41.98 sec, field sweep 150 G, number of scans 5, accumulation time 3.5 min, receiver gain $1 \times 10^3$. The Bruker marker ER 4119HS-2100 (with a g factor of 1.9800 ± 0.0006 and line width 3 G) was used as the internal reference; it was permanently mounted in the resonator as shown in Figure 6.3b and measured together with tooth enamel. The internal standard g-value was used to determine the g-factor values of the observed EPR signals and normalized the dosimetric signals to reduce the errors due to any fluctuation in the machine response and environmental changes (Bailiff et al., 2016; Fattibene and Callens, 2010, IAEA, 2002; ICRU, 2002). After converting data files to text files of 1024 points per spectrum, the spectrum was processed using the Bruker Win-EPR processing software. The essential components of the EPR spectrometer, such as the EPR sample tube loaded into a cavity, manual goniometer, internal standard, and electromagnet, are depicted in Figure 6.3b.

**(a)**

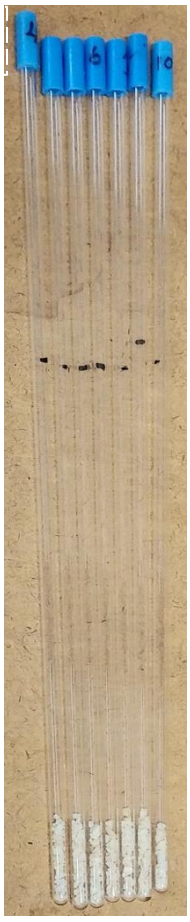

**(b)**

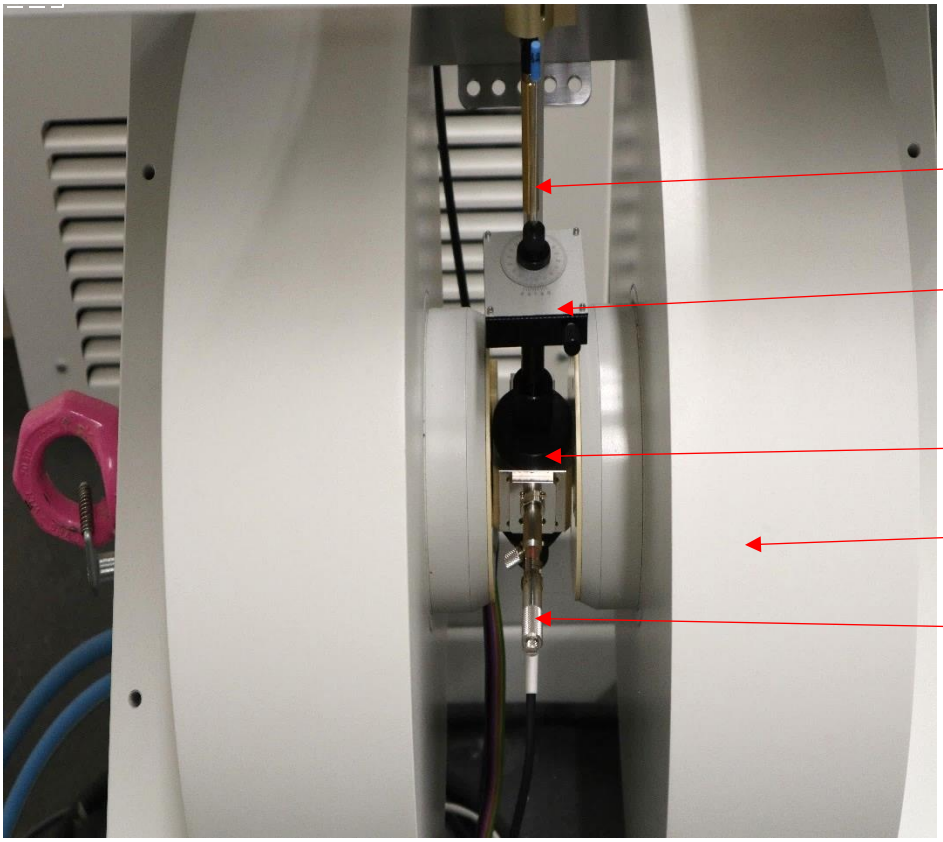


**Figure 6.3: (a)** The 250 mm L EPR tubes (4mm OD) are loaded with tooth enamel. **(b)** The Bruker ER 4119HS-2100 internal standard is mounted in a resonator to determine the g-factor values of the observed EPR signals and normalize the dosimetric signals.

## 6.3 Results and discussion

### 6.3.1 Effects of sample mass on sensitivity

The mass of the sample affects the cavity quality factor (Q) and the sensitivity of EPR measurements. That is why the sample mass was optimized by measuring the low to high mass tooth enamel samples irradiated to 4 Gy, as depicted in Figure 6.4. The RISs were normalized using the EPR signals from the internal standards, which removes errors due to environmental change and microphonics. The uncertainties of the RISs were determined by repeated measurements with rotation of samples using a goniometer, and the standard deviation was

calculated from these measurements. The 2 % variation in the dosimetric signal amplitude to the sample mass is accepted (Haskell et al., 1999; Haskell et al., 1997; Zhumadilov et al., 2005). The dependence of the dosimetric signal intensity on the sample mass is depicted in Figure 6.4. The sample mass up to 105 mg is linear within 1.4%, and declination from linearity increases as we increase the sample mass of 110 and 130 to 5% and 15%, respectively. Therefore, 105 gm with a low variation in the dosimetric signal intensity to the sample mass is the optimum sample mass for the quantitative low dose measurements in tooth enamel.

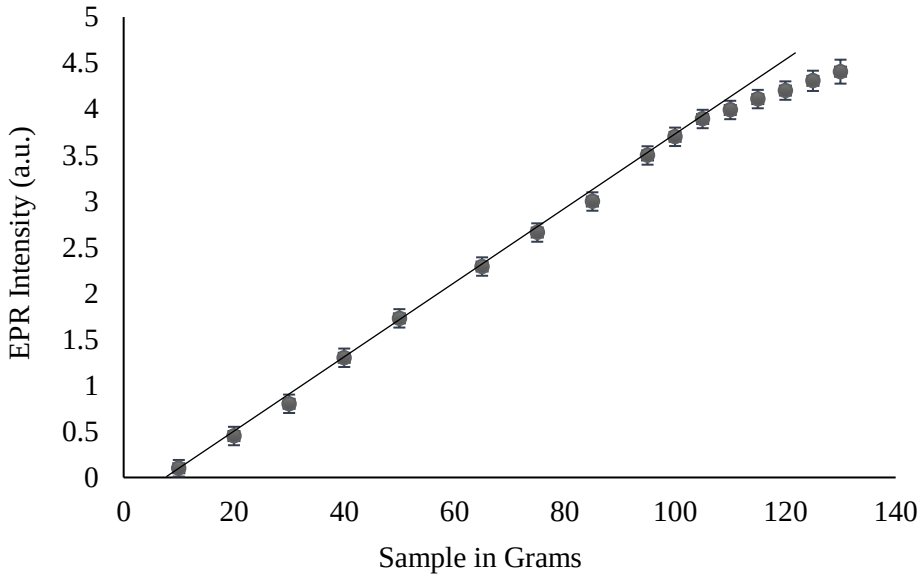


**Figure 6.4:** Microwave cavity was calibrated as a function of the sample mass and found the optimum sample mass was 105 mg for the measurements.

### 6.3.2 Standard techniques for low dose measurements

Several studies have been conducted to enhance the measurement precision, accuracy, and reproducibility; and decrease the detection limit in tooth enamel. The international intercomparisons in tooth enamel dosimetry compared the achievable precision, accuracy, and

reproducibility in the low dose region. In the second intercomparison, eighteen participants were provided tooth enamel samples irradiated from 0-1,000 mGy. Each laboratory prepared its samples by itself, determined the EPR acquisition parameters, and estimated the doses by their protocols. Six out of eighteen laboratories could reconstruct all the applied doses within ±25% and ±100 mGy below 400 mGy (Wieser et al., 2000). All participants' results concluded that besides EPR parameters and the lab conditions, the quality of the EPR spectrometer used highly influenced the data obtained in the dose reconstruction (Wieser et al., 2000). In the third international intercomparison, fourteen laboratories participated in the program. The participants' laboratories performed tooth enamel dosimetry in 79 – 704 mGy by preparing samples themselves and estimating the doses by their procedures. The relative standard deviation was better than 27% for the applied doses in 79 – 704 mGy in all these methods (Wieser et al., 2005; Wieser et al., 2006). These international intercomparisons demonstrated that the accuracy in EPR tooth enamel dosimetry at low doses was highly challenging as there was >20% variation among the participating laboratories.

Essentially, the background signal obscures the radiation-induced signal at the low dose range (Ignatiev et al., 1996). Historically, two approaches were used to decrease the detection limit: (1) computer simulation to differentiate between the RIS and BGS (Ivannikov et al., 2002; Sholom and Chumak, 2003, Zhumadilov et al., 2005); and (2) the signal-selective microwave saturation technique. In the latter approach, the same tooth enamel was analyzed at two different microwave powers. The saturation behavior of the RIS and the BGS were different (i.e., 150 mW for RIS and 2 mW for BGS), which was used to separate them, as depicted in Figure 6.5. This technique improved the EPR spectrum resolution by a factor of 10 and reduced the minimum detectable dose to about 100 mGy (Ignatiev et al., 1996). However, this method has certain

difficulties at low doses. Additionally, Wieser and El-Faramawy (2002) detection threshold for the absorbed dose in deciduous tooth enamel was 100 mGy using special software for spectrum deconvolution. Likewise, Ivannikov et al. (2002) used an automatic computer procedure (i.e., spectra deconvolution procedure) for processing spectra from 100-500 mGy by extracting the RIS from the total EPR spectrum and determining the RIS intensity. This procedure deconvolutes the total EPR spectrum of tooth enamel to the RIS and BGS by applying non-linear squares fitting of a model spectrum to the experimental one (Ivannikov et al., 2002; Wieser et al., 2002; Zhumadilov et al., 2006; Zhumadilov et al., 2005). However, these studies did not determine the spectra deconvolution procedure's ability to differentiate the RIS and BGS in the tooth enamel EPR spectrum at the low dose range (10-100 mGy). Moreover, using these techniques, there were more than 20% measurement errors in the dose range of 100-500 mGy. Therefore, it is clear that the precise low dose estimation using the standard tooth enamel EPR dosimetry is challenging. Hence, as an alternative method, the dose spiking EPR technique was used to determine its applicability to measure the low doses in EPR dosimetry with deciduous tooth enamel.

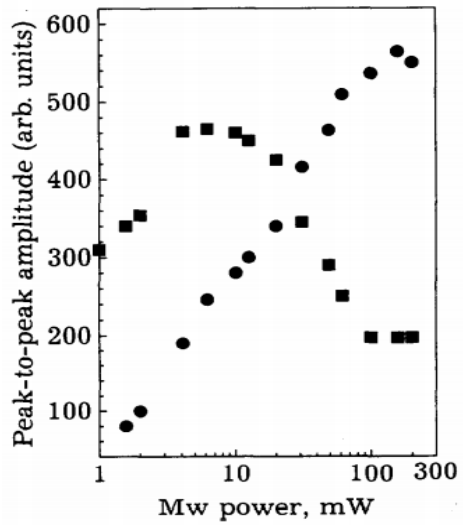


**Figure 6.5:** Signal-selective microwave saturation, (●) RIS, and (■) BGS on mW power. From Ignatiev et al. (1996).

### 6.3.3 Estimation of the low doses without spiking

The dosimetric signal is interwound with the native signal in the deciduous tooth enamel irradiated to the low doses (10-100 mGy) as shown in Figure 6.6. That is why it is very challenging to measure the RIS with reliable precision using the standard EPR dosimetry technique (ISO protocol 13304-1 for EPR retrospective dosimetry). The dose spiking EPR technique was used to make the dosimetric signal visible and measurable, as described in Chapter 5 (Section 5.3.4) (Harvey, 2000; Geso et al., 2018). Then, the dose-response curve was constructed by plotting the EPR intensities from the low doses (i.e., EPR intensities from the total doses minus the spike doses) against the laboratory-applied doses (Figure 6.11) to calculate the final low doses in the samples.

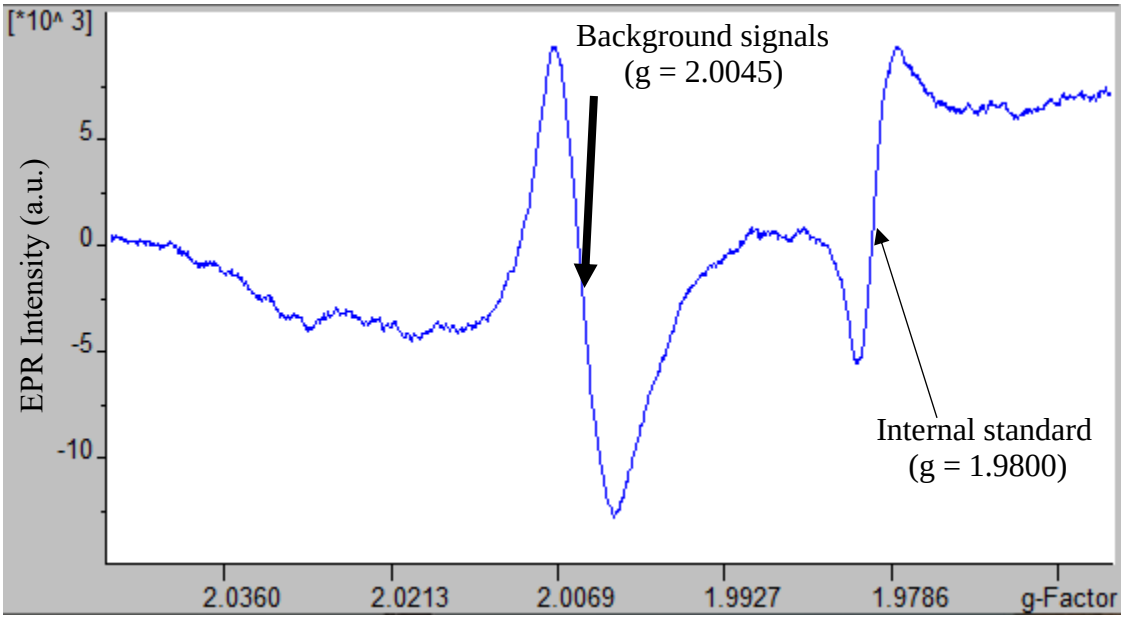


**Figure 6.6:** An EPR spectrum from the deciduous tooth enamel irradiated to 10 mGy using the gamma source (Hopewell G-10). The g value of the spectrum (g = 2.0045) is the characteristic value of the native or background signal. The radiation-induced signal is not visible in the spectrum at this dose.

### 6.3.4 The dose spiking technique for EPR dosimetry with deciduous tooth enamel

As described in Section 6.1, the RIS is the main component for EPR dosimetry with tooth enamel. At low doses, the radiation induced EPR signal in tooth enamel is always minimal compared to the organic radical at g = 2.0045. So, it is strongly masked by the background signal. That is why separating the RIS from the organic signal is very difficult, and the calculated dose could over or underestimate the total dose received. This study used dose spiking as an alternative technique to the standard EPR tooth enamel dosimetry (Geso et al., 2018; Harvey, 2000; ISO, 2013). In this technique, the spike dose (up to 5 to 50 times) was delivered to the low doses to bring the signal into the range that the X-band CW EPR spectroscopy can reliably measure. The EPR measurement of the total dose (i.e., low dose plus spike) was subtracted from the spike dose to get the low dose in tooth enamel (Geso et al., 2018; Harvey, 2000). The natural background dose was subtracted as described in Chapter 3 (Section 3.10.3). The RIS signals are mainly from the $^{\bullet}CO_2^-$ radical anions present in dental enamel, the concentration of enamel is higher than the impurities in the prepared sample. So, as we irradiate the tooth enamel sample, the free radical concentrations in organic matter and impurities do not increase in the same proportion of the $^{\bullet}CO_2^-$ radical anions in enamel. Therefore, the EPR spectrum from the $^{\bullet}CO_2^-$ radical anions at $g_{\parallel}$ = 1.9988 and $g_{\perp}$ = 2.0019 (P2P line width of 0.4 and 0.3 mT) are distinct from the background signals at g = 2.0045 as shown in Figures 6.7 and 6.9.

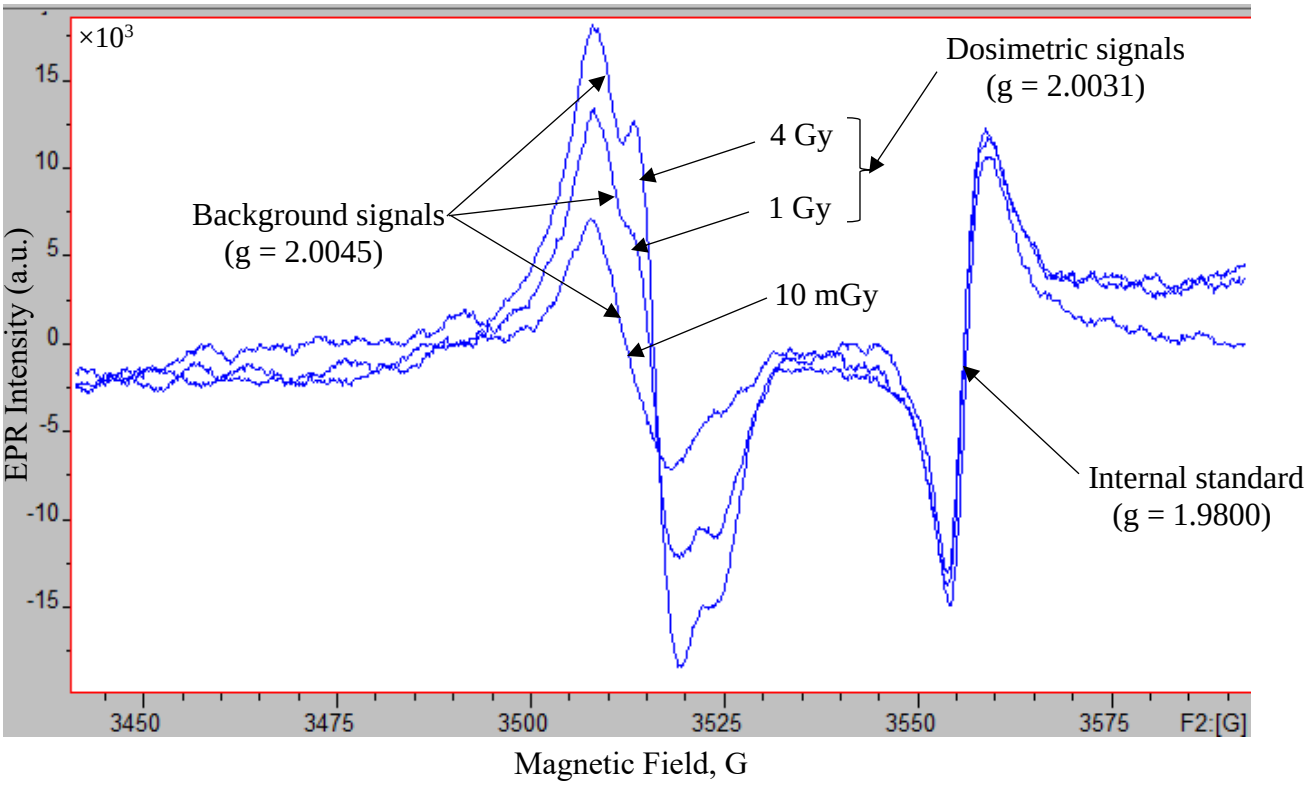


**Figure 6.7:** EPR spectra from the tooth enamel samples irradiated to 10 mGy, 1 Gy, and 4 Gy, respectively. As the tooth enamel is irradiated, the radiation-induced signals become more visible and measurable, increasing precision and accuracy in the EPR measurements.

Furthermore, as shown in Figures 6.7 and 6.9, the dosimetric signal intensity increases with the irradiation dose; however, the native signal essentially remains constant with the irradiation and can be considered independent of the irradiation dose (Gualtieri et al., 2001). Additionally, the background signal has longer electron spin relaxation times and saturates more quickly than the radiation-induced signal, as shown in Figure 6.8 (Ignatiev et al., 1996; Sato et al., 2007; Yu et al., 2015). As a result, the dose spiking method enhances the EPR signal (RIS) by adding artificial radiation at known doses. In contrast, the intensity of the BGS is almost unchanged (i.e., radiation insensitive) and left behind (Gualtieri et al., 2001; Wieser et al., 2002), as depicted in Figures 6.7,

6.8, and 6.9. Thus, the dose spiking technique exploits the benefit of the radiation insensitive native signal and the highly radiation-sensitive dosimetric signals for determining the low doses in tooth enamel using X-band CW EPR spectroscopy.

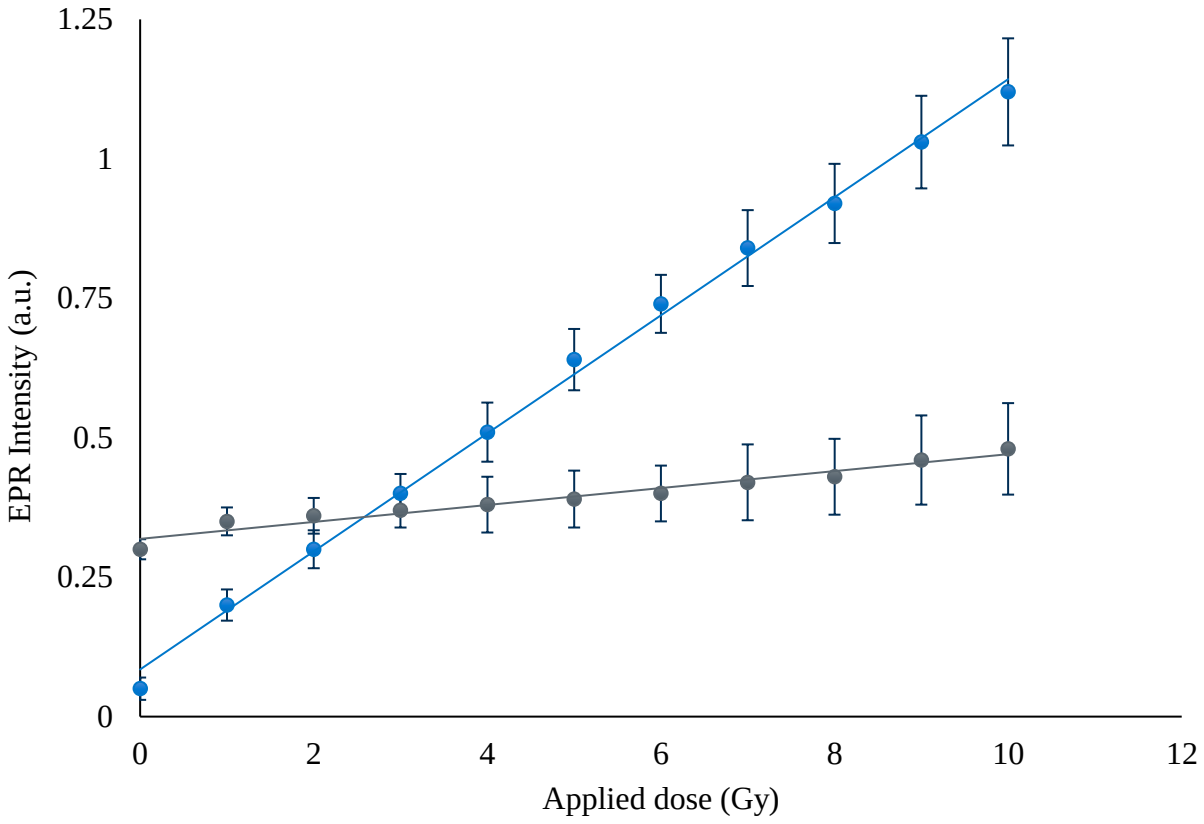


**Figure 6.8:** The EPR intensities of the dosimetric ($^{\bullet}CO_2^-$ radical anions) (●) and native signals (●) of deciduous incisors teeth against the applied irradiation doses.

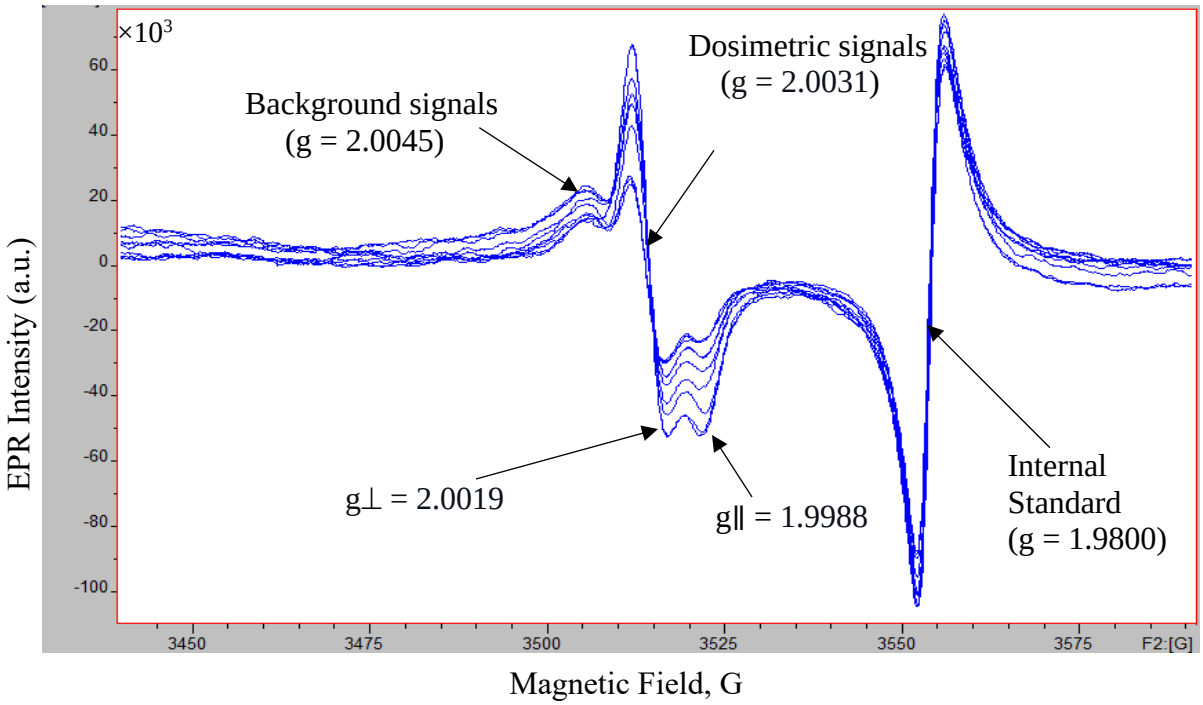


**Figure 6.9:** The total doses (low + spike) EPR intensities are distinctly visible and measurable. However, the background signals remain constant with the applied artificial doses.

As shown in Table 6.1 and Figures 6.9 and 6.10, the low doses were spiked to the high dose (4 Gy), and the total dose and the spike dose were measured using the X-band CW EPR spectrometer. However, no complicated spectra processing software was required to separate the RIS from the BGS. The EPR intensity of the total dose was subtracted from the spike dose to get the EPR intensity from the low doses and the standard deviation, as shown in Table 6.1. The low doses were determined using the dose-response curve (Figure 6.11) obtained by plotting the EPR intensities (i.e., EPR intensities of the total dose minus spike dose) against the laboratory-applied low doses. The standard deviations of the EPR intensities (i.e., total minus spike) were relatively small (±10%), as shown in Table 6.1. There was a reliable detection of low doses with lower errors than the standard method. This result demonstrated that the dose spiking technique promises to decrease the detection limit and increase the measurement precision and reproducibility in the EPR

dosimetry with tooth enamel. On the other hand, in the standard technique, the RIS may not be visualized clearly for a low dose estimation using X-band CW EPR. So, the low dose was determined by multiple irradiations and plotting a graph of the same sample. Using this technique, the high measurement errors (i.e., up to 39%) in a low dose could be from multiple irradiations of the same sample to determine a low dose (Bailiff et al., 2016; Fattibene and Callens, 2010). While using spectra deconvolution computer software, the dose measurements errors were more than 20% at the low doses (100 - 500 mGy) in tooth enamel (Ivannikov et al., 2002; Wieser et al., 2002; Zhumadilov et al., 2006; Zhumadilov et al., 2006). However, the dose spiking technique can amplify the RIS signal amplitude high enough to be seen and measured in the single irradiation dose. In this way, this technique can be instrumental in reconstructing the retrospective and accident low doses to victims of radiation accidents.

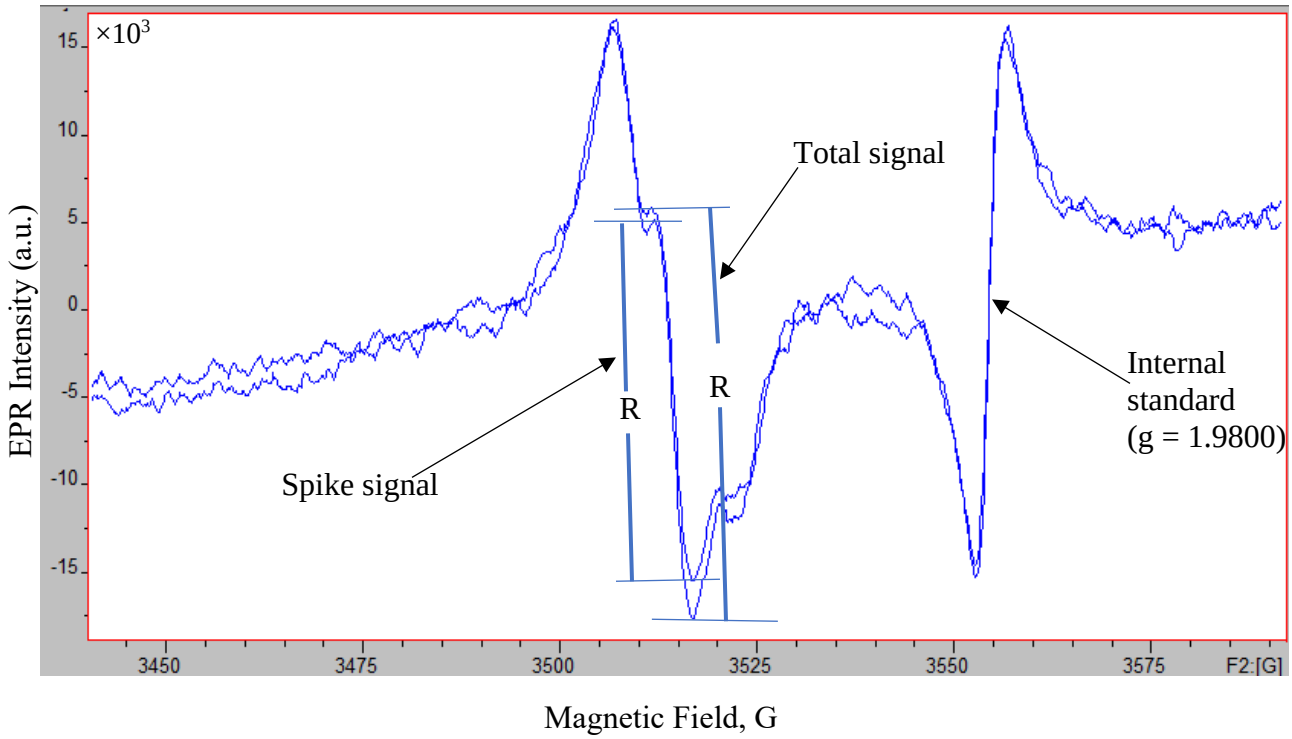


**Figure 6.10:** EPR intensities of the total (4.01 Gy) and the spike (4 Gy) doses from the irradiated (gamma) tooth enamel. The EPR intensity of the total dose was subtracted from the spike dose

(total dose – spike) to get the EPR intensity from the low dose. R is the P2P amplitude height used for determining the absorbed dose in tooth enamel.

**Table 6.1:** The low dose measurements in deciduous teeth enamel using the dose spiking EPR technique.

| Low dose (mGy) | Weight (gm) | Spike dose (4 Gy) | Total dose (low + spike) | EPR Intensity (Total dose – Spike) | σ(Total dose – Spike) |
|---|---|---|---|---|---|
| 10 | 105 | 4 | 4.01 | 0.08 | 0.0120 |
| 20 | 105 | 4 | 4.02 | 0.13 | 0.0156 |
| 30 | 105 | 4 | 4.03 | 0.17 | 0.0187 |
| 40 | 105 | 4 | 4.04 | 0.22 | 0.0197 |
| 50 | 105 | 4 | 4.05 | 0.27 | 0.0351 |
| 60 | 105 | 4 | 4.06 | 0.32 | 0.0320 |
| 70 | 105 | 4 | 4.07 | 0.37 | 0.0296 |
| 80 | 105 | 4 | 4.08 | 0.42 | 0.0315 |
| 90 | 105 | 4 | 4.09 | 0.46 | 0.0437 |
| 100 | 105 | 4 | 4.10 | 0.52 | 0.0442 |

One of the possible reasons for significantly low errors with this technique could be the single irradiation and the dose subtraction instead of the multiple irradiations and subtraction technique in the dose additive method, which has been used to reconstruct a low dose in the conventional tooth enamel EPR dosimetry technique. Using this method, the uncertainty was about ±10%, lower than the previous methods in the low dose measurements. Another advantage of this method is the single irradiation of tooth enamel, making dose reconstruction non-destructive, and the sample can be reused for future dose evaluation. The decrease in the detection limit and increase in the measurement accuracy and reproducibility could open new opportunities for epidemiological studies of the health effects of low doses of ionizing radiation. Although the dose spiking technique is a common practice in analytical chemistry to measure analytes with extremely

low concentrations (i.e., micromolar level), the novelty, in this case, is the use of this technique to measure low doses in tooth enamel using EPR dosimetry.

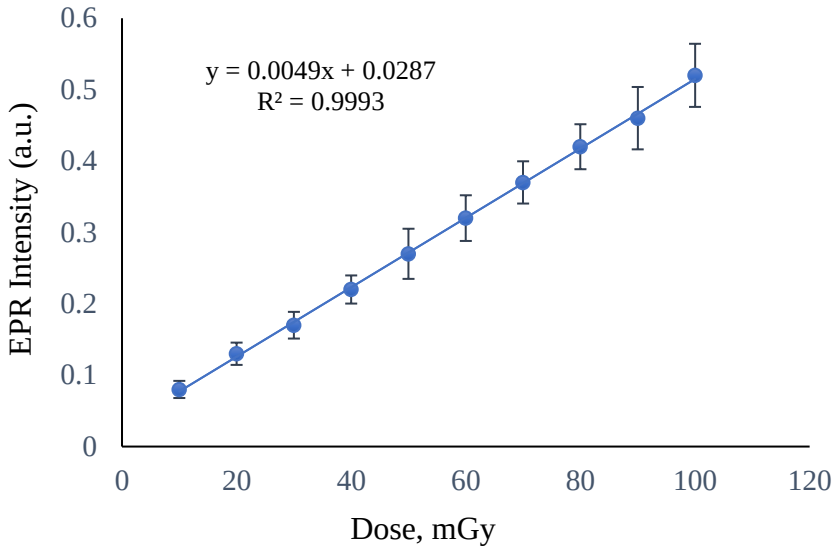


**Figure 6.11:** A dose-response of the tooth enamel at the low doses obtained from the dose spiking EPR technique.

One of the drawbacks of this technique is that we need an excellent irradiation laboratory facility, and the sample irradiation must be done accurately. To develop this technique as the standard technique for the low dose retrospective and accident dosimetry, the data obtained from this technique must be compared with other laboratories for accuracy and reproducibility.

## 6.4 Conclusions

Children's teeth (deciduous) naturally fall out from age 6 to 12 and are readily available for dose reconstruction after radiological accidents. Additionally, children are more vulnerable to radiation exposures from radiological accidents or contamination already present in their locations from past nuclear activities. So, it is vital to determine the absorbed dose in deciduous teeth to determine the possible health effects of radiation exposures on children. To this end, a new EPR

tooth enamel dosimetry technique, the dose spiking EPR technique to measure the low doses, has been used. Since the sample was irradiated at a single time and subtracted from the spike dose, it reduces the measurement errors encountered from the multiple irradiations and the complex spectra processing processes generally used in the conventional EPR tooth enamel dosimetry technique. The measurement accuracy was increased by preparing samples using the standard protocol and irradiating them in the calibrated gamma irradiator. The EPR spectrometer sensitivity was increased by optimizing the acquisition parameters, sample position, and mass into the microwave cavity. The low doses in deciduous tooth enamel samples (10-100 mGy) were determined with reliable precision (± 10%) and accuracy, as shown in Table 6.1. These results concluded that the dose spiking EPR technique could be promising to solve the low dose measurement problems in tooth enamel EPR dosimetry for the retrospective and accident dose assessment. However, further inter-lab intercomparison and data validation will be helpful to make this technique widely applicable.

**Acknowledgements**

We would like to thank those who provided us with the extracted teeth for the study. The work described was undertaken as part of the independent, low-dose research program "Addressing Public Concerns about Their Exposure to Low Doses of Anthropogenic Radiation," funded by the CANDU Owners Group Inc. Funding was also received from the Natural Sciences and Engineering Research Council (NSERC) of Canada. Also, the authors would like to thank Dr. Nicholas Priest for his suggestion for this project.

**Compliance with ethical standards:** This study has been reviewed the ethics clearance through Ontario Tech University's Research Ethics Committee (REB # 14870) on January 05, 2019.

**Conflict of interest:** The authors declare that they have no conflict of interest.

## 5.5 References


Bailiff, I.K., Sholom, S., McKeever, S.W.S., 2016. Retrospective and emergency dosimetry in response to radiological incidents and nuclear mass-casualty events: a review. Radiat. Meas. 94, 83-139.

Chumak, V., Sholom, S., Pasalkaya, L., 1999. Application of high precision EPR dosimetry with teeth for reconstruction of doses to Chernobyl populations. Radiat. Prot. Dosim. 84, 515–520.

Degteva, M.O., Shagina, N.B., Shishkina, E.A., Vozilova, A.V., Volchkova, A.Y., Vorobiova, M.I., et al., 2015. Analysis of EPR and FISH studies of radiation doses in persons who lived in the upper reaches of the Techa River. Radiat. Environ. Biophys. 54, 433-444.

Desrosiers, M., Schauer, D.A., 2001. Electron paramagnetic resonance (EPR) biodosimetry. Nucl. Instr. and Meth. in Phys. Res. B. 184, 219-228.

Fattibene, P., Callens, F., 2010. EPR dosimetry with tooth enamel: A review. Appl. Radiat. Isot. 68, 2033-2116.

Geso, M., Ackerly, T., Lim, S.A., Best, S.P., Gagliardi, F., Smith, C., 2018. Application of the 'Spiking' method to the measurement of low dose radiation (≤ 1Gy) using alanine dosimeters. Appl. Radiat. Isot. 133, 111-116.

Gualtieri, G., Colacicchi, S., Sgattoni, R., Giannoni, M., 2001. The Chernobyl accident: EPR dosimetry on dental enamel of children. Appl. Radiat. Isot. 55, 71–79.

Harvey, D., 2000. Modern analytical chemistry. McGraw Hill, New York.

Haskell, E.D., Hayes, R.B., Kenner, G.H., 1999. An EPR dosimetry method for rapid scanning of children following a radiation accident using deciduous teeth. Health Phys.76, 137–144.

Haskell, E.H., Hayes, R.B., Kenner, G.H., 1997. Improved accuracy of EPR dosimetry using a constant rotation goniometer. Radiat. Meas. 27, 325–329.

Hennig, G.J., Herr, W., Weber, E., Xirotiris, N.I., 1981. ESR-dating of the fossil hominid cranium from Petralona Cave, Greece. Nature. 292: 533-536.

IAEA, 2002. Use of electron paramagnetic resonance dosimetry with tooth enamel for retrospective dose assessment. IAEA-TECDOC-1331. International Atomic Energy Agency, Vienna, Austria, 57 pp.

ICRP, 2007. ICRP Publication 103: The 2007 recommendations of the international commission on radiological protection. Ann. ICRP 37 (2–4), 1–332.

ICRU, 2002. Retrospective Assessment of Exposures to Ionising Radiation. International Commission on Radiation Units and Measurements. International Commission on Radiation Units and Measurements, Bethesda, USA. ICRU Report 68.

Ignatiev, E.A, Romanyukha, A., Koshta, A.A., Wieser, A., 1996. Selective saturation method for EPR dosimetry with tooth enamel. Appl. Radiat. Isotop. 47:333–7.

Ikeya, M., Miyajima, J., Okajima, S., 1984. ESR dosimetry for atomic bomb survivors using shell buttons and tooth enamel. Jpn. J. Appl. Phys. 23, 697- 699.

ISO, 2013. Radiological protection – Minimum criteria for electron paramagnetic resonance (EPR) spectroscopy for retrospective dosimetry of ionizing radiation – Part 1: General principles, International Standard, ISO 13304-1.

Ivannikov, A.I., Zhumadilov, Zh, Gusev, B.I., Miyazawa, Ch, Jiao, L., Skvortsov, V.G., et al., 2002. Individual dose reconstruction among residents living in the vicinity of the Semipalatinsk Nuclear Test Site using EPR spectroscopy of tooth enamel. Health Phys. 83, 183-196.

Jacob, P., Goksu, Y., Meckbach, R., Wieser, A., 2002. Retrospective dosimetry for external exposures. International Congress Series. 1225, 141-148.

Khan, R.F.H., Boreham, D.R., Rink, W.J., 2003. Quantification of Low Amplitude Dosimetric Signal in EPR Teeth Dosimetry – A Novel Approach. Rad. Prot. Dosim. 103(4):359-362.

Lund, A., Shiotani, M., Shimada, S., 2011. Principles and Applications of ESR Spectroscopy. Springer Science+Business Media B.V.

Murahashi, M., Toyoda, S., Hoshi, M., Ohtaki, M., Endo, S., Tanaka, K., et al., 2017. The sensitivity variation of the radiation induced signal in deciduous teeth to be used in ESR tooth enamel dosimetry. Radiat. Meas. 106, 450–4.

Rudko, V.V., Vorona, I.P., Baran, N.P., Ishchenko, S.S., Zatovsky, I.V., and Chumakova, L.S., 2010. The mechanism of $CO_2^-$ radical formation in biological and synthetic apatites. Health Phys. 98, 322-326.

Sato, H., Filas, B.A., Eaton, S.S., Eaton, G.R., Romanyukha, A.A., Hayes, R., et al., 2007. Electron spin relaxation of radicals in irradiated tooth enamel and synthetic hydroxyapatite. Radiat. Meas. 42:997–1004.

Scientific Committee on the Effects of Atomic Radiation, UNSCEAR, 2012. Sources, Effects and Risks of Ionizing Radiation, Scientific Annexes A and B, United Nations.

Sholom, S.V., Chumak, V.V., 2003. Decomposition of spectra in EPR dosimetry using the matrix method. Radiat. Meas. 37 (4–5), 365–370.

Toyoda, S., 2019. Recent Issues in X-Band ESR Tooth Enamel Dosimetry. In: Shukla A. K. (Eds.), Electron Spin Resonance Spectroscopy in Medicine. Springer Nature Singapore, pp. 135-151. Pte Ltd. https://doi.org/10.1007/978-981-13-2230-3.

Wieser, A., Debuyst, R., Fattibene, P., Meghzifene, A., Onori, S., Bayankin, S.N., et al., 2005. The 3rd international intercomparison on EPR tooth dosimetry: Part 1, general analysis. Appl. Radiat. Isot. 62, 163-171.

Wieser, A., Debuyst, R., Fattibene, P., Meghzifene, A., Onori, S., Bayankin, S.N., et al., 2006. The third international intercomparison on EPR tooth dosimetry: Part 2, final analysis. Radiat. Prot. Dosim. 120 (1–4), 176–183.

Wieser, A., El-Faramawy, N., 2002. Dose reconstruction with electron paramagnetic resonance spectroscopy of deciduous teeth. Radiat. Prot. Dosim. 101 (1–4), 545–548.

Wieser, A., Mehta, K., Amira, S., Aragno, D., Bercea, S., Brik, A., et al., 2000. The 2nd international intercomparison on EPR tooth dosimetry. Radiat. Meas. 32, 549-557.

Yu, Z., Romanyukha, A., Eaton, S.A., Eaton, G.R., 2015. X-band rapid-scan electron paramagnetic resonance of radiation-induced defects in tooth enamel. Radiat. Res. 184 (2), 175–179.

Zhumadilov, K., Ivannikov, A., Apsalikov, K.N., Zhumadilov, Z., Toyoda, S., Zharlyganova, D., et al., 2006. Radiation dose estimation by tooth enamel EPR dosimetry for residents of Dolon and Bodene. J. Radiat. Res. 47 (Suppl. A), A47–A53.

Zhumadilov, K., Ivannikov, A., Skvortsov, V., Stepanenko, V., Zhumadilov, Z., Endo, S., et al., 2005. Tooth enamel EPR dosimetry: optimization of EPR spectra recording parameters and effect of sample mass on spectral sensitivity. J. Radiat. Res. (Tokyo) 46 (4), 435–442.

# Chapter 7

# Conclusions and recommendations for future work

## 7.1 Conclusions

The CNSC and OPG have been conducting environmental analyses to determine the local doses from the operation of the Pickering and Darlington NGSs in Durham Region, Ontario, Canada. Based on their results, the local public doses from these NGSs were less than 0.1% of the effective regulatory dose limit of 1 mSv/year in Canada, and the background dose near the NGSs of 1.338 mSv/year. These results indicated that the public and the environment around these facilities were protected, and there were no adverse health effects from these NGSs in Durham Region populations. By using this information and other available data, the radiation epidemiology of the Durham Region has been studied by the Durham Region health department, focusing on the cancer incidence rates and the radiation doses in public from the nearby NGSs (Durham Region Health Department, 2007; Durham Region Health Department, 2017). Based on these studies, there was essentially no change in cancer incidence rates in Durham Region over the last fourteen years; and more importantly, Durham Region's combined cancer incidence rates were the same as the Ontario average rates.

However, the OPG and CNSC were mainly focused on the environmental sample analyses and modeling to determine the absorbed doses in public from these NGSs in Durham Region. The public would be more confident if they get data from the direct dose measurement from human samples. Also, environmental samples analyses cannot provide the total background doses in public from the other sources such as radiology, nuclear medicine, radiation therapy, industrial and occupational, flights, etc. So, without knowing these potential radiation sources, it is almost

impossible to determine the possible long-term health effects of the low-dose radiation exposures in a local population and radio-epidemiology. Therefore, it is vital to determine the low total doses (including from NGSs) in a local population to understand how much anthropogenic doses the local people are getting from various sources.

Biological samples such as blood, nails, bones, and teeth have been used as the radiation dosimeters to determine the total absorbed doses for retrospective and accident dosimetry. However, some of these biological sample records absorbed doses for a short time, and their detection limits are not low enough to assess the retrospective or accident doses in populations. Fortunately, among these samples, the extracted tooth enamel has been proved to be a reliable dosimeter to assess the low doses in both acute and chronic exposure scenarios. Chemically, tooth enamel is mainly hydroxyapatite ($[Ca_{10}(PO_4)_6(OH)_2]$) (a highly radiation-sensitive crystalline material), which contains carbonate ($CO_3^{2-}$) and carbon dioxide ($CO_2$) as impurities. When enamel with these impurities is exposed to ionizing radiation, the carbonate ions change into the carbon dioxide-free radical anion ($^{\bullet}CO_2^{-}$) by capturing secondary thermalized electrons as described in Chapter 2 (Section 2.2). The free radicals formed by this process are highly stable for about 10 million years at standard temperature and pressure. Furthermore, the tooth enamel has a linear dose-response from 30 mGy to 10 kGy, a significant dose range for reconstructing the chronic or accident doses in individuals, groups, or populations.

As a result, the EPR tooth enamel dosimetry is suitable for the low-dose retrospective and accident dosimetry. Four international intercomparisons have been conducted in the last 20 years to check the tooth enamel's reliability for low dose measurements. These comparisons concluded that the EPR dosimetry with tooth enamel was a reliable technique for retrospective dosimetry. ISO published a standard for the EPR tooth enamel dosimetry, which helped make dose assessment

techniques widely available and consistent. It provided recommendations for the sample collection and data reporting (ISO, 2013). Additionally, this technique has already been used successfully to estimate acute and chronic exposures in the Chernobyl accident, the atomic bomb survivors in Hiroshima and Nagasaki, Semipalatinsk nuclear test sites, the nuclear weapons test sites in the former Soviet Union, and Russian nuclear workers as described in Chapter 2 (Section 2.6). Moreover, it is a gold standard for retrospective dosimetry and reconstructing the total lifetime accumulated radiation doses to individuals and populations. That is why this study used the extracted teeth from Durham Region, Ontario, to determine the total absorbed doses in enamel.

Since this study involved human tissue (extracted teeth), ethics clearance was obtained from the University's Research Ethics Board (REB). The COVID-19 pandemic disrupted the sampling and analysis due to limited access to the lab. However, despite those challenges, samples were collected with the help of the dental clinics/dentists and residents. The samples were processed in a laboratory at Ontario Tech University and analyzed using the X-band CW EPR spectrometer. To increase the EPR spectrometer's sensitivity and decrease the detection limits, the EPR spectrum acquisition parameters, mass, and the sample position into the EPR cavity were optimized. The absorbed dose in tooth enamel was determined by measuring the P2P amplitude height of the measured spectrum described in Chapter 3. The total dose in the teeth of 70-year-old people was about four times higher than 20 years. The dose rate in the populations was calculated by plotting the average lingual doses with the standard deviation as a function of the age range of the participants. The total (natural and artificial) calculated dose rate in Durham Region populations, Ontario, was 1.9721 mSv/year. The natural background dose of 1.338 mSv/year in the Durham Region was subtracted from the total dose rate to calculate the annual anthropogenic or artificial dose rate (0.6341 mSv/year), which was the total dose rate in enamel in the Durham

Residents from different artificial sources. The dose rate was about 47.39% of the natural background dose (1.338 mSv) in Durham Region, Ontario, and lower than the regulatory limits (1 mSv/year) for the general public in Canada, and the natural effective dose rate of 1.338 mSv/year for Durham Region, Ontario. These data demonstrated that the background doses to the public are lower than the regulatory limit in Durham Region populations. However, further study using geographically diverse samples from the Region would be necessary to conclude the amounts of artificial doses in the teeth of Durham Region residents.

While permanent teeth have been used to reconstruct the absorbed doses in nuclear or radiological accidents and chronic exposures like in Durham Region, there is a high probability of getting a deciduous tooth for retrospective and accident dosimetry. Also, it is vital to measure the low doses (10-100 mGy) in enamel, which is of interest in radiation epidemiology due to plausible health effects but has not been observed until now. Using the conventional technique, the low dose (10 - 100 mGy) measurements with high accuracy and reproducibility are extremely challenging due to the incomplete separation of the radiation-induced and native signals in the EPR measurements. Therefore, this study explored the feasibility of using the dose spiking EPR technique to measure the low doses in alanine. The low doses (20 - 220 mGy) in alanine were measured with reliable precision and accuracy. The same technique was used to measure the low doses (10 -100 mGy) in the deciduous tooth enamel. Using this method, the low dose measurement accuracy was higher (±10%) than the previous standard methods. These results concluded that the dose spiking EPR technique could be promising to solve the measurement problems at low doses in tooth enamel EPR dosimetry for the retrospective and accident dose assessment.

## 7.2 Recommendations for future work

### 7.2.1 Organ dose calculation using the MCNP radiation transport modeling

After determining the total low dose using tooth enamel EPR dosimetry, the largest challenge for dose reconstruction is the retrospective dose assessment of organ doses of individuals. It is vital to determine the organ dose to study the radio-epidemiology of a local population (ICRU, 2002). So, the organ dose conversion coefficients (depending on photon energy and geometry) should be determined using a Monte Carlo code simulating the photon transport in mathematical models (i.e., mathematical anthropomorphic phantoms) of an adult male and an adult female, respectively (Zankl et al., 1997). The organ dose will provide useful information about the absorbed dose in tooth enamel to corresponding doses in different organs and the whole body and the effective dose (Khailov et al., 2015; ICRU, 2002).

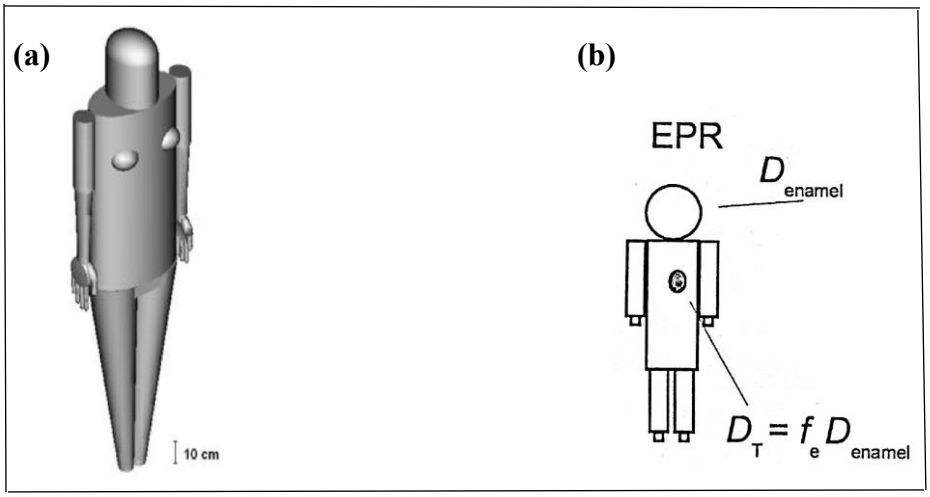


**Figure 7.1: (a)** A geometrical model of the human body created on the base of a mathematical phantom developed by Cristy and Eckerman (1997), and Khailov et al. (2015). **(b)** An Example of converting the total doses measured on tooth enamel to tissue doses, $D_{enamel}$ is the total doses in tooth enamel measured by EPR, *fe* is the dose conversion factor depending on the exposure conditions, and $D_T$ is the total organ dose. From ICRU (2002).

As shown in Figure 7.1b, the dose from tooth enamel will be multiplied by the dose conversion factor ($f_e$) to calculate the organ's dose.

### 7.2.2 Developments in EPR biodosimetry methods for triage using Q-band in mini biopsy tooth enamel samples

The X-band CW EPR with tooth enamel has been established and widely used for individuals, groups, or populations to reconstruct the absorbed doses down to 30 mGy. However, in the case of nuclear or radiological accidents, an extracted tooth sample is hard to find, which may prevent a quick accident dose assessment for a treatment plan. To overcome the challenges posed by the sample size and low sensitivity in X-band EPR spectrometers, a tooth enamel sample can be analyzed using the Q-band EPR spectrometer, which has a high SNR, high spectral resolution, and sensitivity than the X-band CW EPR spectrometer. The basic mechanism of the radiation dose measurements using both X and Q-band EPR spectrometers are the same (i.e., concentration measurement of the $^{\bullet}CO_2^-$ radical anions generated by ionizing radiation in the form of the EPR spectrum).

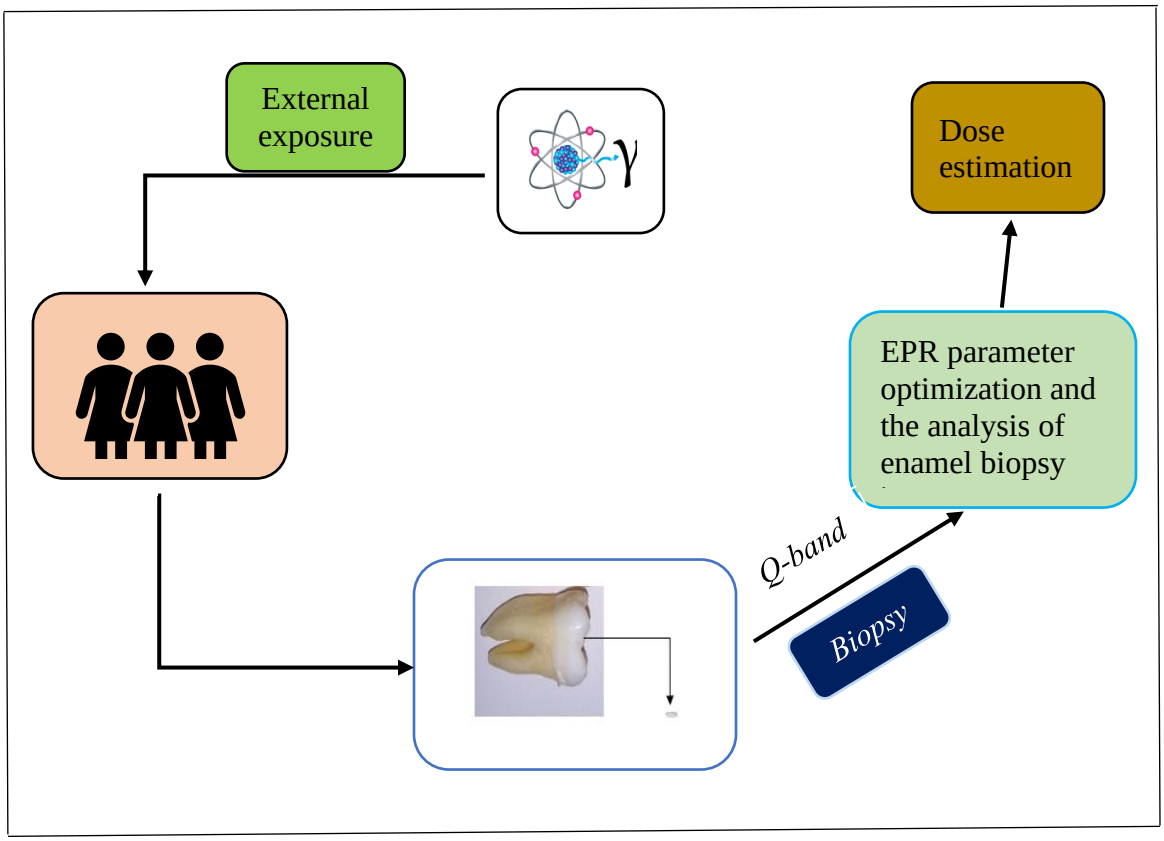


**Figure 7.2:** A conceptual model for the Q-band retrospective and accident dosimetry using mini-biopsy tooth enamel.

As mentioned in Chapters 4 and 5, different accident and retrospective dosimetry studies focused on the X-band CW EPR spectroscopy, which requires about 90 -105 mg of pure enamel for accurate dose estimation. However, this amount of tooth enamel can only be obtained from the extracted tooth without caries or diseases. Also, it is not always possible to obtain the extracted teeth for small-scale radiation accidents or to triage the population in case of large-scale nuclear or radiation accidents for accident dosimetry. Additionally, in the X-band CW EPR spectrometer, separating the RIS from the BGS in low dose measurements is very difficult. These disadvantages make the X-band CW EPR dosimetry with tooth enamel less helpful in assessing the accident doses immediately after radiation accidents and making a treatment plan for victims. Therefore,

future research should focus on determining the feasibility of using the Q-band EPR spectrometer to measure low doses in small tooth enamel biopsy to determine the accident doses (Figure 7.2) and develop this technique as a rapid, non-invasive dose estimation for accident and retrospective dosimetry.

### 7.2.3 Compare advantages and disadvantages of Q-band relative to X-band for low dose retrospective dosimetry

As described in Section 7.2.2, the Q-band EPR is highly sensitive (~ 20 times more sensitive than X-band). The high spectral resolution would be effective as it requires small samples for the complete analysis. However, the Q-band EPR dosimetry with tooth enamel is a relatively new technique, and its measurement accuracy, precision, and reproducibility at low doses are still not determined completely. So, it is vital to determine its precision and reproducibility and compare it with the X-band CW EPR dosimetry to get the full benefits from these emerging retrospective and accident dosimetry techniques and check the consistency of the X-band procedure for retrospective and accident dosimetry.

### 7.2.4 Pulsed EPR spectroscopy for determining the types of radiation

Human tooth enamel can be used for the retrospective EPR dosimetry using the X-band CW EPR spectrometer. However, this technique can not provide information about the types of radiation to which tooth enamel is exposed during a radiological accident or a chronic exposure. Different energy levels of different ionizing and non-ionizing radiation (e.g., gamma rays, X-rays, and proton and UV) can generate the free radicals ($^{\bullet}CO_2^-$) in tooth enamel with different spatial configurations (Tsvetkov et al., 2019). Since these radiations induced free radicals to remain stable for a long time ($10^9$ y at 25°C) period in fossil tooth enamel in normal conditions, a more advanced EPR spectroscopy technique such as the pulsed EPR spectroscopy can be used to determine the

differences in the spatial properties and distances between the $^{\bullet}CO_2^-$ radicals in tooth enamel produced by different types of radiation. These different spatial configurations and distances of the free radicals could be used to identify the different types of radiation (γ, X-rays, UV, n) to which the tooth enamel had been exposed (Tsvetkov et al., 2019).

### 7.2.5 The biological understanding of radiation actions at low doses

In addition to radiation epidemiology, the biological understanding (biological mechanisms) of radiation actions at low doses is necessary to determine the health effects of low dose radiation. The quantification of risks from low-dose exposures should be determined by identifying one or more early molecular markers for radiation-induced cancer. These analyses can help us understand the health effects of low-dose radiation (UNSCEAR, 2012).

### 7.2.6 A human Tooth bank in Durham Region, Ontario

The main limitation of this study is the availability of extracted teeth for the EPR analysis. Sometimes researchers may have to wait until somebody extracts a tooth for medical reasons. Also, this type of study needs different age range samples such as 20-29, 30-39, 40-49, 50-59, 60-69, and 70-79 to study the dose trends in these populations. However, gathering samples covering all age ranges may take a long time to produce statistically valid results. Therefore, every city or a residential area close to nuclear-generating stations should have a dental bank so that researchers can get teeth within a reasonable time frame to complete their research. A city can also take the initiative to establish a dental bank with the help of the local dental clinics/dentists or dental colleges and residents for a periodic dose assessment. At the same time, since the dose stability rate of tooth enamel is very high, one can also check past radiation levels by retrospective dose reconstruction techniques and support the judgment about the induction of cancer in employees due to past occupational or workplace exposures.

## 7.3 References

Cristy, M., Eckerman, F., 1997. Specific Absorbed Fraction of Energy at Various Ages from Internal Photon Sources. Appendix a. Description of the Mathematical Phantom. ORNL/TM-8381/V1, Oak Ridge. National Laboratory, Oak Ridge.

Durham Region Health Department, 2007. Radiation and Health in Durham Region 2007. Whitby, Ontario: The Regional Municipality of Durham. Retrieved January 21, 2021, from https://healthdocbox.com/67784217-Cancer/Radiation-health-in-durham-region-report-2007.html

Durham Region Health Department, 2017. Cancer at a Glance in Durham Region. Whitby, Ontario: The Regional Municipality of Durham. Retrieved January 21, 2021, from https://www.durham.ca/en/health-and-wellness/resources/Documents/HealthInformationServices/HealthStatisticsReports/Cancer-at-a-Glance.pdf

ICRU, 2002. Retrospective Assessment of Exposures to Ionising Radiation. International Commission on Radiation Units and Measurements. International Commission on Radiation Units and Measurements, Bethesda, USA. ICRU Report 68.

ISO, 2013. Radiological protection – Minimum criteria for electron paramagnetic resonance (EPR) spectroscopy for retrospective dosimetry of ionizing radiation – Part 1: General principles, International Standard, ISO 13304-1.

Khailov, A.M., Ivannikov, A.I., Skvortsov, V.G., Stepanenko, V.F., Orlenko, S.P., Flood, A.B., et al., 2015. Calculation of dose conversion factors for doses in the fingernails to organ doses at external gamma irradiation in air. Radiat. Meas. 82, 1-7.

Scientific Committee on the Effects of Atomic Radiation, UNSCEAR, 2012. Sources, Effects and Risks of Ionizing Radiation, Scientific Annexes A and B, United Nations.

Tsvetkov, Y.D., Bowman, M.K., Grishin, Y.A., 2019. Experimental Techniques—Pulsed Electron–Electron Double Resonance: Nanoscale Distance Measurement in the Biological, Materials and Chemical Sciences, Springer International Publishing: Cham, Switzerland, pp. 37–65. ISBN 978-3-030-05372-7.

Zankl, M., Drexler, G., Petoussi, N., Saito, K., 1997. The calculation of dose from external photon exposures using reference human phantoms and Monte Carlo methods, part VII: organ doses due to parallel and environmental exposure geometries, GSF-Bericht 8/97.

# Appendices

## Appendix A

### Journal Papers

### Journal Publications

1. Ghimire, L. N., Waller, E., 2021. Applicability of the dose spiking EPR method for the quantitative measurements of low doses in EPR alanine dosimetry. Journal of Nuclear Engineering and Radiation Science (Under review).

### Conference Publications

1. Ghimire, L. N., Waller, E. (June 3rd, 2018). Tooth enamel EPR dosimetry for determining anthropogenic low-dose radiation. CANDU Owners Group meeting in Saskatoon, University of Saskatchewan, SK, Canada.
2. Ghimire, L. N., Waller, E. (November 16, 2018). Estimation of lifetime doses to the public living close to NGSs using EPR measurements on extracted tooth enamel. CANDU Owners Group meeting in Ottawa, Faculty of Medicine, University of Ottawa.
3. Ghimire, L. N., Waller, E. (April 4th, 2019). Application of tooth enamel EPR retrospective dosimetry to dose reconstruction in Durham Region, Ontario. Graduate seminar, Ontario Tech University, Oshawa, ON.
4. Ghimire, L. N., Waller, E. (May 2, 2019). Application of tooth enamel EPR retrospective dosimetry to dose reconstruction in Durham Region, Ontario. Oral presentation at the 10th annual graduate research conference, Ontario Tech University, Oshawa, Canada.
5. Ghimire, L. N., Waller, E. (July 7 to 11, 2019). Estimation of lifetime doses to the public living close to NGSs using electron paramagnetic resonance (EPR) measurements on

extracted tooth enamel. Oral presentation on the Health Physics Society 64th annual meeting in Orlando, Florida, USA.

6. Ghimire, L. N., Waller, E. (September 13th, 2019). Determination of total ionizing radiation doses in human tooth enamel in Durham Region using Electron Paramagnetic Resonance (EPR) dosimetry. Durham Nuclear Health Committee meeting, Ontario Tech University, ON, Canada.
7. Ghimire, L. N., Waller, E. (December 16, 2019). Applicability of the Dose Spiking Method in Alanine EPR Dosimetry Systems to Decrease the Detection Limit in a Low Dose Measurement. UNENE R&D Workshop, Toronto, Canada.
8. Ghimire, L. N., Waller, E. (May 27 to 30, 2019). Estimate lifetime doses to the public living near nuclear power plants using electron paramagnetic resonance (EPR) measurements on extracted tooth enamel. Poster presentation on the CRPA, 2019, Ottawa, Canada.
9. Ghimire, L. N., Waller, E. (December 14, 2021). A new method for measuring low doses in deciduous teeth enamel using EPR spectroscopy for retrospective and accident dosimetry. UNENE R&D Workshop, Virtual presentation.
10. Ghimire, L. N., Waller, E. (February 23, 2022). A New Method for Measuring Low Doses in Deciduous Teeth Enamel Using EPR Spectroscopy for Retrospective and Accident Dosimetry. 2022 IRPA North American Regional Congress, St. Louis, Missouri, USA (Virtual Presentation).